

Modelling hydrological responses to climate change in a data-scarce semiarid basin in the Tianshan Mountains



**FRIEDRICH-SCHILLER-
UNIVERSITÄT
JENA**

**Dissertation
(kumulativ)**

Zur Erlangung des akademischen Grades doctor rerum naturalium
(Dr. rer. nat.)

Vorgelegt dem Rat der Chemisch-Geowissenschaftlichen Fakultät der
Friedrich-Schiller-University Jena

von MSc. Yanjun Shen
geboren am 17. May 1986 in China

Gutachter:

1. ... Prof. Dr. Alexander Brenning... ..

2. ... Prof. Dr. Wolfgang Albert Flügel... ..

(3.)

Tag der Verteidigung: 26.02.2018... ..

Erklärung zu den Eigenanteilen des Promovenden/der Promovendin sowie der weiteren Doktoranden/Doktorandinnen als Koautoren an den Publikationen und zweitpublikationsrechten bei einer kumulativen Dissertation (in die kumulative Dissertation aufzunehmen)

Für alle in dieser kumulativen Dissertation verwendeten Manuskripte liegen die notwendigen Genehmigungen der Verlage(„ Reprint permissions“) für die Zweitpublikation vor.

Die Co-Autoren der in dieser kumulativen Dissertation verwendeten Manuskripte sind sowohl über die Nutzung, als auch über die oben angegebenen Eigenanteile der weiteren Doktoranden/Doktorandinnen als Koautoren an den Publikationen und Zweitpublikationsrechten bei einer kumulativen Dissertation informiert und stimmen dem zu (es wird empfohlen, diese grundsätzliche Zustimmung bereits mit Einreichung der Veröffentlichung einzuholen bzw. die Gewichtung der Anteile parallel zur Einreichung zu klären).

Die Anteile des Promovenden/der Promovendin sowie der weiteren Doktoranden/Doktorandinnen als Koautoren an den Publikationen und zweitpublikationsrechten bei einer kumulativen Dissertation sind in der Anlage aufgeführt(Musterbeispiel),

Name des Promovenden/der Promovendin	Yanjun Shen		
<u>01. 03. 2018</u>	<u>Jena</u>		
Datum	Ort		Unterschrift

Ich bin mit der Abfassung der Dissertation als publikationsbasiert, d.h. kumulativ, einverstanden und bestätige die vorstehenden Angaben. Eine entsprechend begründete Befürwortung mit Angabe des wissenschaftlichen Anteils des Doktoranden/der Doktorandin an den verwendeten Publikationen werde ich parallel an den Rat der Fakultät der Chemisch-Geowissenschaftlichen Fakultät richten.

<u>Prof. Dr. Alexander Brenning</u>	<u>01. 03. 2018</u>	<u>Jena</u>	
Name Erstbetreuer(in)	Datum	Ort	Unterschrift

Musterbeispiel

Erklärung zu den Eigenanteilen des Promovenden/der Promovendenin sowie der weiteren Doktoranden/Doktorandinnen als Koautoren an den Publikationen und Zweitpublikationsrechten bei einer kumulativen Dissertation (bitte für jede in der kumulativen Dissertation verwendete Publikation ausfüllen, Erläuterungen ggf. auf Rückseite)

(in die kumulative Dissertation einbinden)

Falls eine Publikation schon in einer kumulativen Promotion Verwendung gefunden hat, bitter Art und Umfang der Verwendung aufführen.

Publikation(Vollständiges Zitat): Shen, Y.-J. , Y. Shen, M. Fink, S. Kralisch, Y. Chen, & A. Brenning. (2018), Trends and variability in streamflow and snowmelt runoff timing in the southern Tianshan Mountains, <i>Journal of Hydrology</i> , 557, 173-181, doi: https://doi.org/10.1016/j.jhydrol.2017.12.035 .						
Beteiligt an (Zutreffendes ankreuzen)	Yan-Jun Shen	Yanjun Shen	Manfred Fink	Sven Kralisch	Yaning Chen	Alexander Brenning
	Autor 1:	Autor 2:	Autor 3:	Autor 4:	Autor 5:	Autor 6:
Konzeption des Forschungsansatzes	×					
Planung der Untersuchungen	×	×				
Datenerhebung	×	×			×	
Datenanalyse und- interpretation	×		×			×
Schreiben des Manuskripts	×		×	×		×
Vorschlag Anrechnung Publikationsäquivalente	1.0					

Publikation(Vollständiges Zitat): Shen, Y.-J. , Y. Shen, J. Goetz, & A. Brenning. (2016), Spatial-temporal variation of near-surface temperature lapse rates over the Tianshan Mountains, central Asia, Journal of Geophysical Research: Atmospheres, 121, 14,006–14,017, doi: 10.1002/2016JD025711.					
Beteiligt an (Zutreffendes ankreuzen)	Yan-Jun Shen	Yanjun Shen	Jason Goetz	Alexander Brenning	
	Autor 1:	Autor 2:	Autor 3:	Autor 4:	
Konzeption des Forschungsansatzes	×			×	
Planung der Untersuchungen	×	×			
Datenerhebung	×	×			
Datenanalyse und-interpretation	×		×	×	
Schreiben des Manuskripts	×		×	×	
Vorschlag Anrechnung Publikationsäquivalente	1.0				

Publikation(Vollständiges Zitat): Shen, Y.-J. , Y. Shen, M. Fink, S. Kralisch, & A. Brenning. (2018), Unraveling the Hydrology of the Glacierized Kaidu Basin by Integrating Multisource Data in the Tianshan Mountains, Northwestern China, Water Resources Research, 54(1), 557-580, doi:10.1002/2017WR021806.					
Beteiligt an (Zutreffendes ankreuzen)	Yan-Jun Shen	Yanjun Shen	Manfred Fink	Sven Kralisch	Alexander Brenning
	Autor 1:	Autor 2:	Autor 3:	Autor 4:	Autor 5:
Konzeption des Forschungsansatzes	×			×	
Planung der Untersuchungen	×	×			
Datenerhebung	×	×			
Datenanalyse und-interpretation	×		×		×
Schreiben des Manuskripts	×		×	×	×
Vorschlag Anrechnung Publikationsäquivalente	1.0				

Acknowledgements

I still remember the excitement when I was awarded a scholarship (201304910343) from the China Scholarship Council (CSC). However, the period of searching for knowledge and finishing the dissertation are always filled with challenges. I was frustrated when the findings are undesirable and I was also content when the papers were accepted. After four years' study, I am proud of the final achievements. What I have learned from the period of doctoral study is the most cherished treasure in my life. It is my great honor to express deep gratitude to people who gave me help, support and encouragement during my study.

I thank Prof. Dr. Wolfgang-Albert Flügel, first, for offering me the opportunity to come to Department of Geography, Friedrich-Schiller-University Jena where allowed me to complete and appreciate my education. Your sincere help make my application goes smoother and my life easier at the very beginning in Jena. Your excellent advice and encouragement were much appreciated. I am grateful to Prof. Yuping Lei, Prof Hongjun Li and Prof. Yanjun Shen, for their kind support during my scholarship application and constructive suggestions throughout my PhD.

I am extremely grateful to Prof. Dr. Alexander Brenning for supervision and providing excellent research environment in the Geographic Information Science group. I benefited a lot from your motivation, suggestions and commenting. Your point of review and suggestions always help me to keep moving forward efficiently and get the papers to a higher level. You guided me how to improve the manuscripts in a scientific way.

I sincerely appreciate Prof. Dr. Yanjun Shen for providing data and supporting my research work. Part of my dissertation was also supported by your project. Hydro-meteorological data and model parameters collection would not be possible without your support. I warmly thank colleagues from the Center for Agricultural Resources Research, Chinese Academy of Sciences (CAS), for their kind support during field survey and data collection.

I would like to thank Dr. Manfred Fink, Dr. Sven Kralisch for their patience and continuous support during my research processes. Each time when I come to you, you are always available and willing to help me. Thank you for all the conversations, suggestions and feedbacks.

Many thanks to my office mate Miga for his generous help. You are the one who always give me valuable suggestions when I started my research, and help me a lot when I am in difficulties. We

Acknowledgements

had a good time in the past. I wish you a happy ending for your Ph.D. I wish to acknowledge Jason for valuable advices and all the contributions in the process of paper writing and revision. The experience in fitness with you was unforgettable. Thanks come to Helene, the books and music you and Jason recommended, the food you served and the conversions and discussions offered me inspiration and encouraged me a lot.

I can never give sufficient thanks to all my colleagues in the Geographic Information Science group for their friendship and kind help in research and my life in Jena. I thank all my colleagues who build tools, who guided me to use it efficient, who shared ideas and introduced me different cultures. They are: Anita, Annika, Benjamin, Bettina, Björn, Christian, Daniel, Franziska, Hannes, Hendrik, Hoffi, Jannes, José, Juliana, Laura, Melanie, Markus, Patrick, Peter, Sophie, Thomas. Although some of you have already left our department, I will never forget your help.

Special thanks to Xinli Pan, Xiaoyuan Zhang, Zhichao Wang and Zhenglong Zhang. I still remember your care and concern when I sprained my ankle. I appreciate all the wonderful moments we have been through in the past four years. There are still many friends who I haven't mentioned but certainly should be appreciated.

It is the best time to express heartfelt thanks to my family. For a long time, it seems I ignored my duties as a son. Thank you for your understanding and encouragement during my study in abroad. Your unwavering love is always my biggest motivation. Special gratitude to my girlfriend Dr. Yongjing Tian, you are the most beautiful and understanding woman who always encourages and supports me. It is your concern and love that accompany me to go through the good and hard times. Thank you for your love.

Jena, December 2017, Yanjun Shen

Abstract

The Tianshan Mountains, known as the “Water tower of Central Asia”, are an essential freshwater source for downstream rivers, residents, irrigation agriculture and ecosystems in Central Asia. Climate in this semiarid region has changed from warm-dry to warm-wet in the last decades. Water resources are highly sensitive to climate change, and their availability is expected to become more unstable in the future. However, hydrological processes in glacierized basins are poorly known due to data scarcity and complex snow and glacier melt dynamics. It is therefore particularly important to improve our understanding of climate change and its impacts on hydrological regimes in dry, glacierized mountain regions such as the Tianshan Mountains. Emphasizing the research gaps related to the scarcity of observational data and lack of understanding of climate variability and hydrological regimes, the aim of this thesis is to model hydrological responses to climate change in a data-scarce glacierized basin in the Tianshan Mountains to better understand mountain hydrology.

Spatio-temporal changes of climate change, climate extremes, hydrological and cryosphere were summarized based on data analysis and literature review. Trends and variability in streamflow and snowmelt runoff timing in four mountain basins in the southern Tianshan Mountains were analyzed by means of statistical tests applied to the winter/spring snowmelt runoff center time (WSCT). Correlations were analyzed to understand the relationships between climate variables, streamflow and WSCT. Spatio-temporal distribution of temperature lapse rates in the subregions (northern slopes, Kaidu basin and southern slopes) of the Tianshan Mountains were identified using simple linear regressions based on long term (1961-2011) weather stations and one year (09.2014-08.2015) temperature logger data. Given the lack of understanding of glacier controlled mountain hydrology in the Tianshan Mountains, the water balance and the distribution of runoff components in the glacierized Kaidu basin were unraveled by the distributed hydrological model J2000 driven by field data and bias-corrected gridded datasets. Monte-Carlo simulations, the Generalized Likelihood Uncertainty Estimation (GLUE) and the regional sensitivity analysis were further utilized to analyze parameter sensitivity and uncertainty with respect to simulated streamflow and different runoff components.

Streamflow and snowmelt runoff timing of mountain rivers are susceptible to climate change. Streamflow increased significantly in recent decades in the southern Tianshan basins, especially

in winter and spring seasons, with a sharp increase since the mid-1990s at annual and seasonal scales. The assessment of snowmelt runoff timing has demonstrated earlier snowmelt dates since the mid-1980s in the analyzed four basins. The variability of streamflow and snowmelt runoff timing differ in different basins due to different streamflow generation processes. They are closely related to the variability of temperature and precipitation, which have experienced an increasing trend over the last decades (1961-2011) in the southern Tianshan Mountains, especially during the second half of this period. Streamflow in the highly glacierized basin (Kunmalik) is mainly dominated by the change of temperature while in other basins depend on both changes of temperature and precipitation. Temperature lapse rates were found to be higher on the southern slopes than the northern slopes of the Tianshan Mountains and were found to be higher in summer than in winter months. The constant environmental temperature lapse rate of $6.5^{\circ}\text{C}/\text{km}$ is not representative of near-surface conditions and would give misleading results in temperature extrapolation in the Tianshan Mountains.

Data scarcity complicates the application of hydrological models in the glacierized basin in the Tianshan Mountains. Gridded precipitation products are affected by inconsistent biases based on a spatio-temporal comparison with the nearest weather stations, and should therefore be carefully evaluated before modelling. Driven by field data and bias-corrected gridded datasets (ERA-Interim and APHRODITE), J2000 showed a relatively good performance against observed daily streamflow in both calibration (Nash–Sutcliffe efficiency: 0.69) and validation periods (0.61). Logarithmic Nash–Sutcliffe efficiencies are 0.79 and 0.84 in the calibration and validation periods, respectively. Based on the model results, base flow (46%) and surface flow (31%) are two major runoff components of the total streamflow. However, 33% and 5% of the annual streamflow are contributed by snowmelt and glacier melt, respectively. Parameter sensitivity and uncertainty with respect to simulated streamflow and different runoff components were further examined.

This study highlighted key features of climatic and hydrological changes in data-scarce basins in the Tianshan Mountains. Changes of streamflow and snowmelt runoff timing can be important indicators for climate change and are useful for applications in flood risk regulation, future hydropower projects and integrated water resources management. Variations of temperature lapse rates are vital to applications such as temperature regionalization and hydrological modelling in the Tianshan Mountains. The application of hydrological models demonstrated the possibility of integrating gridded products into modelling in trying to unravel complex hydrological processes

in mountain regions. Although substantial uncertainties remain, the model-based simulation may deepen our understanding of the water balance and the distributions of runoff components in the glacierized Kaidu basin in the Tianshan Mountains in central Asia. Taken together, the underlying methodology of this study can be important for model applications and design in data-scarce mountainous regions elsewhere. The existence of parametric sensitivity and uncertainty assessment could contribute to improving model calibration and design in central Asia in the future, and it also sends a strong message regarding the need for adequate and sustainable observing systems that are required for modeling present and future water resources.

Zusammenfassung

Das Tianshan Gebirge, bekannt als der „Wasserturm“ von Zentralasien, liegt im Nordwesten von China und ist eine sehr wichtige Trinkwasserquelle für Flüsse, Einwohner, Ökosysteme und für Bewässerung in der Landwirtschaft in Zentralasien. Das Klima dieses semiariden Gebietes hat in den letzten Jahrzehnten einen Wandel von einem warm-trockenen zu einem warm-feuchten vollzogen. Besonders im Hinblick auf die Wasserversorgung ist diese Entwicklung bedeutend und eine größere Instabilität der Wasserversorgung aufgrund der hohen Sensibilität gegenüber dem Klimawandel wird erwartet. Jedoch können diese Erwartungen mit nur wenigen Daten bestätigt werden, da besonders in den vergletscherten Gebieten Zentralasiens sehr wenige Daten zu den hydrologischen Bedingungen vorliegen und die lokalen Schnee- und Gletscherschmelzdynamiken sehr komplex und bisher wenig verstanden sind. Um frühzeitig auf mögliche Probleme der Wasserversorgung in diesem semiariden Gebiet reagieren zu können, sind Forschungen zum besseren Verständnis des Klimawandels und dessen Auswirkungen auf den Wasserkreislauf und die Hydrologie der Gebirgsflüsse sehr wichtig und notwendig. Das Ziel dieser Dissertation ist die Modellierung der hydrologischen Auswirkungen des Klimawandels auf ein unbeobachtetes semiarides Einzugsgebiet im TianShan Gebirge mittels eines physikalisch basierten hydrologischen Modells. Dadurch wird die bestehende Forschungslücke bezüglich der lokalen Klimavariabilität und dem hydrologischen Regime des Gebirges aufgrund von Datenmangel adressiert.

In dieser Dissertation wurden raumzeitliche Veränderungen des Klimas, der Klimaextreme, der Hydrologie und Kryosphäre mittels statistischer Datenanalyse und Literaturrecherche analysiert. Trends und die Variabilität des Abflusses und im Zeitpunkt des Eintretens der Schneeschmelze wurden in vier Einzugsgebieten des südlichen Tianshan Gebirges mittels statistischer Tests zur Analyse der Winter/Frühlings Schneeschmelzabflusszeit („winter/spring snowmelt runoff center time“ – WSCT) untersucht. Zum besseren Verständnis der Beziehungen zwischen den Klimavariablen, dem Abfluss und der WSCT wurden Korrelationsfaktoren analysiert. Des Weiteren wurden räumliche Unterschiede im Temperaturgradienten in Subregionen des Tianshan Gebirges (nördliche Hänge, Kaidu Einzugsgebiet und südliche Hänge) mittels einfacher linearer Regression von Langzeit-Datenreihen zur Temperatur (1961-2011) und eigenen Temperaturdatenlogger Daten über ein Jahr (09.2014-08.2015) untersucht. Auf diesen

Erkenntnissen aufbauend wurde das J2000 Modell, ein Modell zur distributiven Beschreibung der hydrologischen bzw. ökohydrologischen Dynamik, verwendet um die Wasserbilanz und die Verteilung der Abflusskomponenten innerhalb des vergletscherten Einzugsgebiets Kaidu abzuschätzen. Das Modell wurde mit eigens im Gelände erhobenen Daten und mittels Bias-korrigierten gerasterten Klimadaten trainiert. Monte-Carlo Simulationen, die generalisierte Wahrscheinlichkeit-Unsicherheitsabschätzung (Generalized Likelihood Uncertainty Estimation - GLUE) und eine regionale Sensitivitätsanalyse wurden verwendet um die Sensitivität des Modells gegenüber der Eingangparameter und die Unsicherheit im simulierten Abfluss und den Abflussparametern abzuschätzen.

Die zentralen Ergebnisse dieser Dissertation können wie folgt zusammengefasst werden:

1. Wie generell angenommen ändern sich Abflussmengen in Gebirgsflüssen im Tianshan Gebirge und der Zeitpunkt des Einsetzens des Oberflächenabflusses mit der Schneeschmelze mit dem Klimawandel. Die Daten des Tianshan Gebirges zeigten einen Anstieg des Abflusses in den letzten Jahrzehnten in den südlichen Einzugsgebieten, besonders während dem Winter und dem Frühjahr. Besonders stark ist der Abfluss seit Mitte der 1990er Jahre auf jährlicher und saisonaler Skale angestiegen. In den vier analysierten Einzugsgebieten war der Zeitpunkt des Einsatzes von Oberflächenabfluss mit der Schneeschmelze deutlich früher seit Mitte der 1980er Jahre. Jedoch wurden auch Unterschiede dieser Kenngrößen innerhalb der vier Einzugsgebiete aufgrund unterschiedlicher Prozesse der Abflussgenerierung festgestellt. Dabei wurde ein enger Zusammenhang zwischen der Variabilität der Temperatur und des Niederschlages mit einem steigenden Trend zwischen 1961 und 2011 im südlichen Tianshan Gebirge, besonders in der zweiten Hälfte der untersuchten Periode, festgestellt. Der Abfluss des stark vergletscherten Einzugsgebiets Kunmalik ist hauptsächlich von Änderungen in der Temperatur dominiert. In den anderen Einzugsgebieten waren sowohl die Temperatur- als auch die Niederschlagsänderungen ausschlaggebend.

2. Die Analyse der raumzeitlichen Veränderungen des Oberflächentemperaturgradienten ergab eine höhere Magnitude des Oberflächentemperaturgradienten für die südlich orientierten Hänge und während der Sommermonate. Generell wurde durch diese Analysen festgestellt, dass ein konstanter Temperaturgradient von $6,5^{\circ}\text{C}/\text{km}$ nicht repräsentativ für die oberflächennahen

Bedingungen im Tianshan Gebirge ist und daher eine Extrapolation der Temperatur mit diesem Wert aus der Literatur zu falschen Ergebnissen führen würde.

3. Der vorliegende Datenmangel erschwert die hydrologische Modellierung der vergletscherten Einzugsgebiete im Tianshan Gebirge deutlich. Ein Modell zur distributiven Beschreibung der hydrologischen bzw. ökohydrologischen Dynamik und Abflusskomponenten angetrieben von Daten erhoben im Gelände und Bias-korrigierten Rasterdaten (ERA-Interim und APHRODITE Klimadaten) wurde angewendet, um Grundlagen für das Wasserressourcenmanagement und die Vorbereitung auf mögliche Klimawandelfolgen bereitzustellen.

Das hydrologische Modell zeigte eine relativ gute Performance verglichen zum beobachteten Abfluss in der Kalibrierungs (Nash-Sutcliffe Effizienz von 0,69)- und der Validierungsperiode (NS Effizienz von 0,61). Die logarithmische Nash-Sutcliffe Effizienz lag bei 0,79 und 0,84. Basierend auf den Modellergebnissen zeigte sich, dass der Basisabfluss (46%) und der Oberflächenabfluss (31%) die größten Bestandteile des Gesamtabflusses ausmachen. Zusätzlich tragen Schnee- und Gletscherschmelze mit jeweils 33% und 5% zum jährlichen Abfluss bei. Die Sensitivität des Modells gegenüber der Eingangsparameter und damit einhergehende Unsicherheiten der simulierten Abflusskomponenten wurden untersucht.

Mithilfe dieser Studie konnten zentrale Eigenschaften der klimatischen hydrologischen Veränderungen in Einzugsgebieten des Tianshan Gebirges mit großem Datenmangel aufgezeigt werden. Änderungen im Abfluss und im Zeitpunkt des Oberflächenabflusses mit der Schneeschmelze sind wichtige Indikatoren für den Klimawandel und deren Detektion ist wichtig für Anwendungen in der Hochwasserrisikoabschätzung, für den Bau oder Betrieb von Wasserkraftwerken und für integriertes Wasserressourcenmanagement. Das Wissen über räumliche Unterschiede im Temperaturgradienten ist für Anwendungen wie z.B. der Regionalisierung von Temperaturdaten oder das hydrologische Modellieren im Tianshan Gebirge von zentraler Bedeutung. Mit der Anwendung von distributiven hydrologischen Modellen konnte die Möglichkeit der Integration von gerasterten Klimadaten zur Erklärung der komplexen hydrologischen Prozesse in Gebirgsregionen aufgezeigt werden. Obwohl deutliche Unsicherheiten in den Modellergebnissen unumgänglich sind, ist die modellbasierte Simulation der Abflussparameter und der hydrologischen Auswirkungen des Klimawandels sehr gut geeignet um

Verständnis für die Wasserbilanz und die Abflusskomponenten des vergletscherten Einzugsgebiets Kaidu zu erlangen.

Die in dieser Dissertation angewendeten Methoden der Repräsentation von meteorologischen Daten, der hydrologischen Modellierung, der Abschätzung der parametrischen Sensitivität und Unsicherheiten sind besonders wichtig für Modellanwendungen und -Design in datenarmen Gebirgsregionen weltweit. Jedoch konnten mit der Modellierung nicht alle Fragen zur komplexen Gebirgshydrologie beantwortet werden, weshalb in diesem Gebiet noch weiterer Forschungsbedarf besteht. Des Weiteren wurde durch diese Analyse deutlich, dass eine Ausweitung des Monitoringnetzwerks zur Beobachtung der Klimavariablen und des Abflusses in Zentralasien dringend notwendig ist, um eine Aktualisierung der hydrologischen Modellierung mit den daraus gewonnenen Daten für zukünftige Forschungen zu aktuellen und zukünftigen Wasserressourcen zu ermöglichen.

Contents

Acknowledgements	I
Abstract	III
Zusammenfassung	VI
Contents	X
List of Figures	XIII
List of Tables	XVI
List of Symbols and Abbreviations	XVIII
Chapter 1 Introduction	1
1.1 Motivation.....	1
1.2 Mountains and hydrological cycle	2
1.2.1 Mountain in the hydrological cycle	2
1.2.2 Mountains as “Water Towers” in northwestern China.....	4
1.3 Climatic and hydrological changes	6
1.3.1 Observed climate change	6
1.3.2 Projected climate change	7
1.3.3 Changes in climate extremes.....	8
1.4 Cryospheric changes	9
1.4.1 Changes in snow and glacier cover fluctuations	9
1.4.2 Changes in streamflow	9
1.4.3 Changes in permafrost	10
1.5 Hydrological modelling and limitations	11
1.5.1 Classification of hydrological models.....	11
1.5.2 Hydrological models for snow and glacier melt	12
1.5.3 Hydrological modelling and challenges in the Tianshan Mountains	13
1.6 Objectives and research questions	14
1.7 Thesis outline	15
Chapter 2 Trends and variability in streamflow and snowmelt runoff timing in the southern Tianshan Mountains	17
2.1 Abstract.....	17
2.2 Introduction.....	18

2.3 Study area, data and methods.....	20
2.3.1 Study area.....	20
2.3.2 Data.....	23
2.3.3 Methods.....	23
2.4 Results.....	24
2.4.1 Trends and variability of streamflow	24
2.4.2 Streamflow links with temperature and precipitation	27
2.4.3 Changes of snowmelt runoff timing.....	29
2.4.4 Relations of WSCT to temperature and precipitation	30
2.5 Discussion.....	31
2.6 Conclusions.....	34
Chapter 3 Spatial-temporal variation of near-surface temperature lapse rates over the Tianshan Mountains, Central Asia	35
3.1 Abstract.....	35
3.2 Introduction.....	36
3.3 Study area, data sets and methods.....	38
3.3.1 Study area.....	38
3.3.2 Data sets	40
3.3.3 Exploratory analysis.....	42
3.4 Results.....	42
3.4.1 Annual variations: the southern slopes versus the northern slopes.....	42
3.4.2 Seasonal variations: the southern slopes versus the northern slopes	43
3.4.3 Geographic variability: the Kaidu Basin.....	44
3.5 Discussion.....	47
3.5.1 Mechanisms of seasonal variation	47
3.5.2 Mechanisms of spatial variation	49
3.5.3 Mechanisms of surface based temperature inversion.....	50
3.5.4 Implication for modelling Earth surface processes	50
3.6 Conclusions.....	51
Chapter 4 Unraveling the hydrology of the glacierized Kaidu Basin by integrating multi-source data in the Tianshan Mountains, northwestern China.....	53
4.1 Abstract.....	53
4.2 Introduction.....	54
4.3 Study area and datasets	57

4.3.1 Study area.....	57
4.3.2 Datasets	58
4.4 Methods.....	60
4.4.1 Gridded datasets comparison and correction	60
4.4.2 Hydrological model.....	62
4.4.3 Model calibration, validation and uncertainty analysis.....	64
4.5 Results.....	68
4.5.1 Evaluation of the precipitation products	68
4.5.2 Temperature and precipitation correction	74
4.5.3 Model performance	76
4.5.4 Uncertainty and sensitivity analysis.....	77
4.5.5 Temporal variation of the simulated water balance and runoff components	79
4.5.6 Spatial characters of simulated water balance and runoff components.....	81
4.6 Discussion	82
4.6.1 Comparison and correction of gridded meteorological data products	82
4.6.2 Remarks on calibration, uncertainty and sensitivity analysis	85
4.6.3 Simulated water balance and runoff components	86
4.6.4 Implications and future work	87
4.7 Conclusions.....	88
Chapter 5 Discussion	89
5.1 Hydro-meteorological research in this semiarid region	89
5.2 The applicability of gridded data	89
5.3 Hydrological modelling in mountain basins	90
5.4 Possible implications	91
Chapter 6 Conclusions and future research	93
6.1 Conclusions.....	93
6.2 Future research.....	95
References.....	97
Appendices.....	122
Selbständigkeitserklärung.....	135
Curriculum Vitae	136

List of Figures

Figure 1.1. Figure of global hydrologic cycle. Source: US Geological Survey.

Figure 1.2. Map showing mountains ranges and major rivers which have sources in Xinjiang province, northwestern China, central Asia. Elevation data comes from the HydroSheds SRTM (Lehner *et al.*, 2008) and map of permanent snow and glaciers was obtained from Randolph Glacier Inventory (RGI 6.0) (<http://www.glims.org/RGI/randolph60.html>) (RGI Consortium, 2017).

Figure 2.1. Location of river basins and gauge stations analyzed in this study.

Figure 2.2. Boxplots with seasonal normal (1961–2007) of temperature and precipitation for the Toxkon, Kunmalik, Kaidu and Huangshuigou basins in the southern Tianshan. Boxplots represent extreme values, lower and upper quartiles and median value of a variable. Seasons are defined as: SP= Spring (March, April, May), SU=Summer (June, July, August), AU=Autumn (September, October, November), WI=Winter (December, January and February) in this study.

Figure 2.3. Annual and cumulative anomalies of streamflow, temperature and precipitation in the Toxkon (1961-2007), Kunmalik (1961-2007), Kaidu (1972-2007) and Huangshuigou (1962-2007) basins. The panel scales for streamflow are different among basins.

Figure 2.4. Seasonal and cumulative anomalies of streamflow in the Toxkon (1961-2007), Kunmalik (1961-2007), Kaidu (1972-2008) and Huangshuigou (1962-2008) basins. The panel scales are different for each basin in different seasons.

Figure 2.5. Time series of historical WSCT in the Toxkon (1961-2007), Kunmalik (1961-2007), Kaidu (1972-2008) and Huangshuigou (1962-2008) basins.

Figure 3.1. Study area and spatial distribution of weather stations: (a) location within central Asia, (b) overview of subregions and climate stations over the Tianshan Mountains, (c) location of HOBO logger stations in the Kaidu Basin.

Figure 3.2. Altitudinal variation in mean annual temperature (T_{max} , T_{mean} and T_{min} , a-c) with their respective linear fit and γ_{local} for both the Southern slopes (circles) and Northern slopes (triangles) of the Tianshan Mountains. For comparison, the cross indicates the BYBLK station, located in the Kaidu Basin. Correlations in (a), Southern: $r = -0.91$, $p\text{-value} < 0.01$; Northern: $r = -0.81$, $p\text{-value} < 0.01$; in (b), Southern: $r = -0.74$, $p\text{-value} < 0.05$; Northern: $r = -0.82$, $p\text{-value} < 0.01$;

in (c): Southern: $r = -0.38$, $p\text{-value} = 0.35$; Northern: $r = -0.66$, $p\text{-value} = 0.05$. P-values correspond to the null hypothesis of zero correlation.

Figure 3.3. Seasonal variations of lapse rates [γ_{local} for Tmax (a), Tmean (b) and Tmin(c)] calculated by linear regression of temperature and elevation. Bold line indicates average value (averaged γ_{local} over the periods of 1961–2011). Seasonal conditions are divided into: Spr (spring: March, April and May), Sum (summer: June, July and August), Aut (autumn: September, October and November) and Win (winter: December, January and February).

Figure 3.4. Variations of γ_{local} for Tmax, Tmean and Tmin in monthly scales (April to October) in the Kaidu Basin (a) (09.2014-08.2015; winter months not included due to nonlinearity). The correlation between elevation and temperature in winter months (average temperature from November to March) and Loess smoothers (b).

Figure 3.5. Seasonal cycle of the relation between lapse rate (γ_{local} for Tmean) and climate factors [temperature (a), precipitation (b), relative humidity (c) and wind speed (d)] on the Southern and Northern slopes of Tianshan Mountains (1961-2011).

Figure 3.6. Annual cycle of the relationship between γ_{local} for Tmean with temperature (a) and relative humidity (b) in the Kaidu Basin (09.2014-08.2015).

Figure 4.1. (a) Location of the Kaidu Basin in Central Asia, elevation and location of observed and HOBO logger stations. Overview of the available geospatial data: (b) land cover classification, (c) soil types and (d) lithology.

Figure 4.2. General schematic representation of the J2000 model based on Krause (2001).

Figure 4.3. Spatial patterns of mean annual precipitation (mm) from the APHRODITE (1961–2007), CFSR (1979–2011), CRU (1961–2010), ERA-Interim (1979–2011), MERRA-2 (1980–2011) and TRMM (1998–2011) products over the Tianshan Mountains.

Figure 4.4. Same as Figure 4.3 but for seasonal mean precipitation.

Figure 4.5. Time series of precipitation at six weather stations (1961-2011) compared with gridded precipitation products from APHRODITE (1961–2011), CFSR (1979-2011), CRU (1961-2010), ERA-Interim (1979–2011), MERRA-2 (1980–2011) and TRMM (1998-2011).

Figure 4.6. Same as Figure 4.5 but for monthly mean precipitation.

Figure 4.7. Taylor diagrams for displaying correlation coefficient, SD and RMS of mean annual precipitation from observational stations and different gridded products based on the overlapping

period 1979–2007. The azimuthal position gives correlation coefficient. The blue radial coordinates and the green concentric semi-circles indicate SD and RMS values, respectively.

Figure 4.8. Relationships between mean daily temperatures observed at HOBO sites and bias-corrected ERA-Interim temperature (09.2014-08.2015).

Figure 4.9. Simulated and observed daily streamflow during the (a) calibration period of 1982–1986, (b) validation period of 1987–1991 and (c) post-reservoir period of 1992-2007 in the Kaidu Basin. Performance measures were calculated from daily data.

Figure 4.10. (a) Uncertainty band and observed streamflow during the period of 1982-1991 based on the GLUE method. (b) Boxplot of monthly uncertainty band of simulated streamflow (1982-1991). Boxplots represent extreme values, lower and upper quartiles and median value of a variable (similarly hereinafter).

Figure 4.11. Boxplots of the effect of parameter uncertainties on different simulated runoff components (1982-1991). Note: the panel of snowmelt is different with other figures.

Figure 4.12. Parameter sensitivity based on the LNS evaluation criterion.

Figure 4.13. (a) Simulated water balance, (b) streamflow, snowmelt and glacier melt, and (c) distributions runoff components in the Kaidu Basin (1982-2007).

Figure 4.14. Spatial distribution of simulated mean annual (a) precipitation, (b) ActET, (c) streamflow, (d) snowmelt, (e) RD1, (f) RD2, (g) RG1 and (h) RG2 in the Kaidu Basin (1982-2007).

List of Tables

Table 1.1. Mountain glaciers in northwestern China. The Kunlun Mountains includes glaciers both in Xinjiang and Qinhai-Tibet Plateau (Shi, 2005).

Table 1.2. Summary of reviewed studies on climatic and hydrological changes in Xinjiang. Tmax, Tmean and Tmin indicate the maximum, mean and minimum temperature. Numbers in parentheses in the table refer to the selected references.

Table 2.1. Summary of basins and gauge stations used in this study.

Table 2.2. Trends of streamflow in the Toxkon, Kunmalik, Kaidu and Huangshuigou basins.

Table 2.3. Trends of precipitation and temperature in the Toxkon, Kunmalik, Kaidu and Huangshuigou basins.

Table 2.4. Correlation coefficients between streamflow and average precipitation/temperature in the Toxkon, Kunmalik, Kaidu and Huangshuigou basins.

Table 2.5. Correlation coefficients between WSCT dates and average precipitation/temperature in the Toxkon, Kunmalik, Kaidu and Huangshuigou basins.

Table 3.1. Weather stations used in this study. H1-H9 indicates the HOBO logger data from field survey. S, N and Kaidu indicate Southern Slopes, Northern Slopes and Kaidu Basin, respectively. (Bayinbuluke station was excluded from the analysis in Kaidu Basin due to different data availability than logger data.)

Table 4.1. Information on long-term weather stations, gauging stations and HOBO logger temperature stations.

Table 4.2. Summary of global and regional gridded precipitation products. Time span shows the evaluation period used in this study.

Table 4.3. Monthly near surface temperature lapse rates in the Kaidu Basin. Temperature lapse rate from November to March were kept the same as October due to winter temperature inversion.

Table 4.4. Summary of model parameters, parameter ranges (for both calibration and uncertainty analysis purposes) and calibrated values in the J2000 model. Parameters included in the sensitivity analysis are shown in boldface.

Table 4.5. Mean values of the water balance for the Kaidu Basin (1982-2007). Storage change represents changes in channel, soil layer, snow cover, groundwater and surface storages. Values are in mm.

List of Symbols and Abbreviations

a.s.l.	Above Sea Level
ActET	Actual Evapotranspiration
ahum	Absolute Humidity
APHRODITE	Asian Precipitation-Highly-Resolved Observational Data Integration Towards Evaluation of Water Resources
CMA	China's Meteorological Administration
CAS	Chinese Academy of Sciences
CT	Center of Mass of Flow
DEM	Digital Elevation Model
ELR	Environmental Temperature Lapse Rate
ENSO	El Niño-Southern Oscillation
GCMs	General Circulation Models
GIS	Geographic Information System
GLUE	Generalized Likelihood Uncertainty Estimation
HBV	Hydrologiska Byråns Vattenbalansavdelning
HRUs	Hydrological Response Units
IDW	Inverse Distance Weighting
IPCC	Intergovernmental Panel on Climate Change
JAMS	Jena Adaptable Modeling System
LAI	Leaf Area Index
LNS	Logarithmic Nash-Sutcliffe Efficiency
LOESS	Locally weighted regression
LPS	Large Pore Storage
LULC	Land use/land cover

List of Symbols and Abbreviations

MPS	Middle Pore Storage
NSE	Nash–Sutcliffe Efficiency
PBIAS	Percent Bias
PMT	Penalized Maximal t Tests
PotET	Potential Evapotranspiration
r^2	Coefficient of Determination
RCP	Representative Concentration Pathways
RD1	Surface Runoff
RD2	Interflow 1
RG1	Interflow 2
RG2	Base flow
RSA	Regional Sensitivity Analysis
satLPS	Saturated Large Pore Storages
satMPS	Saturated Middle Pore Storages
rh _{um}	Relative Humidity
SPHY	Spatial Processes in Hydrology
SRM	Snowmelt Runoff Model
SRTM	Shuttle Radar Topography Mission
SWAT	Soil and Water Assessment Tool
T _{max}	Maximum Temperature
T _{mean}	Mean Temperature
T _{min}	Minimum Temperature
VHM	Veralgemeend Hydrologisch Model
WSCT	Winter/Spring Snowmelt Runoff Center Time
γ_{local}	Near-surface Temperature Lapse Rate

Chapter 1 Introduction

1.1 Motivation

Mountain regions supply a large amount of fresh water for lowland society and ecosystems (Viviroli & Weingartner, 2004), yet hydrological systems in mountain regions are susceptible to climate change (Barnett et al., 2005; Viviroli et al., 2011; Grafton et al., 2013; Piontek et al., 2014). Water resources from the Tianshan Mountains (known as the “Water Tower of Central Asia”) not only play a key role in sustaining downstream rivers, socio-economic development and ecosystems in semiarid Xinjiang, northwestern China but also important indicators of climate change which dramatic affects the variability of meltwater-depended streamflow (Shen & Chen, 2010; Sorg et al., 2012; Chen, 2014; Chen et al., 2016a). Water availability pressure will be aggravated by the ongoing climate change together with the increasing water demands (Shen et al., 2013b; Guo & Shen, 2016). There is a broad consensus about the variability and availability of water resources under the changing climate. However, the impacts of climate change and their hydrological significance are still not well understood, especially in glacierized basins (Chen et al., 2016b).

Currently, climate change is evidenced from rising temperature and precipitation trends in the Tianshan Mountains (Chen et al., 2006; Shi et al., 2007); which may result in an accelerated and unstable regional hydrological cycle (Shen & Chen, 2010). Examples can be seen from increased streamflow (Tao et al., 2011; Chen et al., 2016b), earlier snowmelt runoff timing (Liu et al., 2011) and remarkable glacier shrinkage (Yao et al., 2004; Ye et al., 2005; Yong et al., 2007). It was demonstrated that the changes of runoff are more significant in highly glacierized areas (Chen et al., 2016a). A comprehensive understanding of hydrological processes, especially in scarce monitored mountain basins, is one of the most important challenging works which needs to be solved in scientific community.

Overall, it is not well known how changes in climate will impact hydrological regimes in the meltwater-dependent basins due to the scarcity of observational data, complex snow and glacier melt processes. Additionally, the knowledge of the hydro-meteorological variations and hydrological modelling works must be improved. This thesis therefore aims to deepen our knowledge about mountain hydrology in this semiarid mountain region and improve the ability of hydrological modelling in mountain basin to coping with climate change impacts.

1.2 Mountains and hydrological cycle

1.2.1 Mountain in the hydrological cycle

Mountains occupy 25% of the earth's surface area and contribute nearly 32% of the total surface runoff (Meybeck et al., 2001). Approximately 40% of the global population rely on water sourced from mountain regions (Beniston, 2003). Mountain regions are therefore one of the most important components of the earth's ecosystems and undertake the responsibility for supplying water at global and regional scales (Beniston, 2003; de Jong et al., 2009). The importance of mountain regions on ecosystems is therefore far beyond themselves (Beniston, 2006), especially in arid and semiarid regions where water demand is high (Viviroli et al., 2007).

Mountain barriers obstruct moving moist air which is easily saturated due to temperature adiabatic cooling with lifted elevation, thus, lead to more precipitation (either rain or snow) than the surrounding lowlands (Barry, 2008; Whiteman, 2000). Additionally, mountains also have the capability to store solid water (snow and glaciers). Precipitation together with snow and glacier meltwater make mountains an important water sources for most rivers and provide a large portion of global runoff, thus, mountains are often regarded as "Water Tower" (Viviroli & Weingartner, 2004; Marston & Marston, 2017).

Mountain hydrology is a vital component of global water cycle (Figure 1.1) (<https://water.usgs.gov/edu/watercycle.html>). Water movement, the pathways (on, above and below the earth) and phase transition in mountain hydrology have been provided in detail by Marston (Marston & Marston, 2017). Since mountains can be regarded as the natural reservoirs that store water in the form of snow and glaciers and release water in warmer seasons (de Jong et al., 2009; Mote et al., 2005), meltwater from snow and glaciers contribute disproportionately large discharges and are an important connection between upstream and downstream (Viviroli & Weingartner, 2004; Nolin, 2012), especially in dry mountain regions where snow and glacier meltwater occupy approximately 50%-90% of the total discharge (Viviroli & Weingartner, 2004; Weingartner et al., 2007). Variation of streamflow, snowmelt volume and timing together with glacier melt are therefore of hydrological importance. However, the contribution of snowmelt water to total discharge, the amount and the timing of snowmelt vary in different regions due to different climate and terrain but have far-reaching consequences for lowland water resources (Bookhagen & Burbank, 2010).

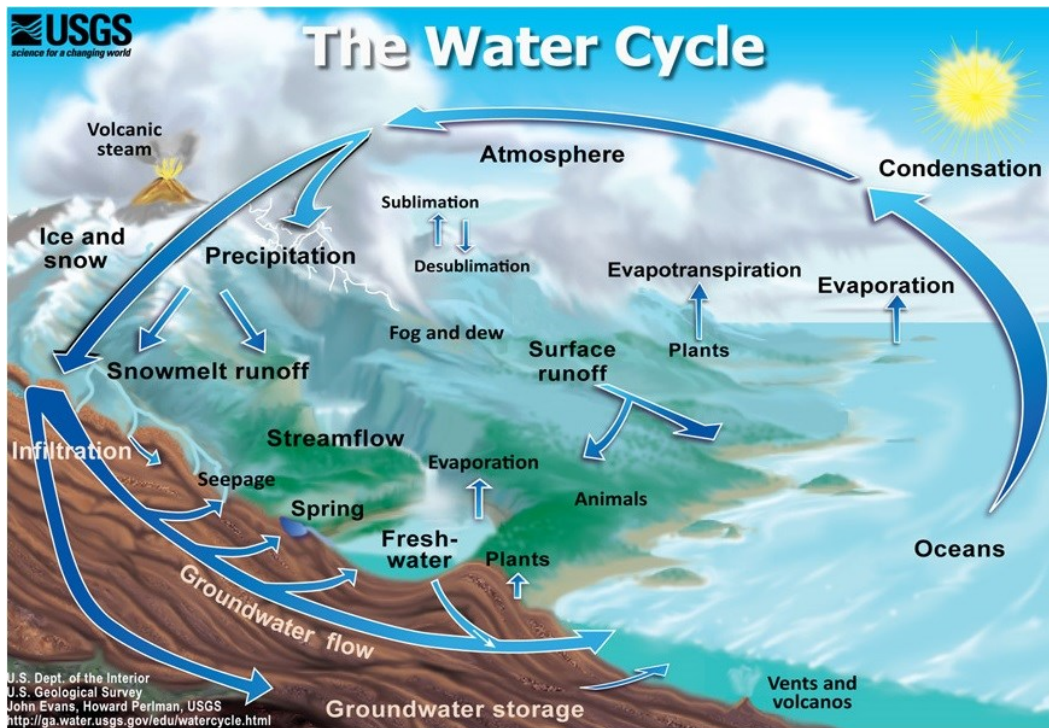


Figure 1.1 Figure of global hydrologic cycle. Source: US Geological Survey.

The significance of mountain hydrology is not only due to the freshwater they supplied but also an important indicator of climate change (Beniston, 2003; Viviroli et al., 2011). Climate change has been affecting cryosphere in past decades at global scale, including retreated Arctic sea ice cover, decreased spring snow cover in Northern Hemisphere, reduced glacier coverage and high-latitude near-surface permafrost extent (IPCC, 2013). Although there may have regional exceptions, elevation-dependent (or at a critical elevation) warming was found in most mountain regions (Mountain Research Initiative, 2015). Decreased snowmelt, shifted snowmelt timing and retreat of glaciers are expected to have the most important influence on water resources in mountain regions due to climate change (Justin et al., 2015; Barnett et al., 2005; Huss et al., 2010; Milner et al., 2017). Examples can be seen in central Asia (the Tianshan and Pamir mountains) (Deng et al., 2015; Chen et al., 2016a; Pohl et al., 2017), the European Alps (Beniston, 2006; Bogataj, 2007; de Jong, 2015; Huss et al., 2010), Himalayan mountains (Bookhagen & Burbank, 2010; Immerzeel & Bierkens, 2012; Immerzeel et al., 2010, 2013; Ragettli et al., 2016), Indus basins (Immerzeel et al., 2015), Central-Rocky mountains (Leppi et al., 2012) and west north America (Mote et al., 2005). Thus, mountain hydroclimate research should gain much attention.

The knowledge of climate changes and their hydrological consequences on mountain hydrology remain incomplete due to complex terrain, lack of measurement data, spatial and altitudinal variation in hydro-meteorological variables (Viviroli et al., 2011; Weingartner et al., 2007; Mountain Research Initiative, 2015). The combined factors of altitude, topography, wind circulation and meteorological variables are major elements for spatio-temporal variability in mountain climate (Barry, 2008; Barry & Chorley, 2009; Whiteman, 2000; Baigorria & Romero, 2012) but important triggers for hydrological processes; runoff stability is therefore highly impacted and results in different flow regimes (Viviroli et al., 2003; Viviroli & Weingartner, 2004). Thus, improve understanding of mountain hydrology is of cardinal significance.

1.2.2 Mountains as “Water Towers” in northwestern China

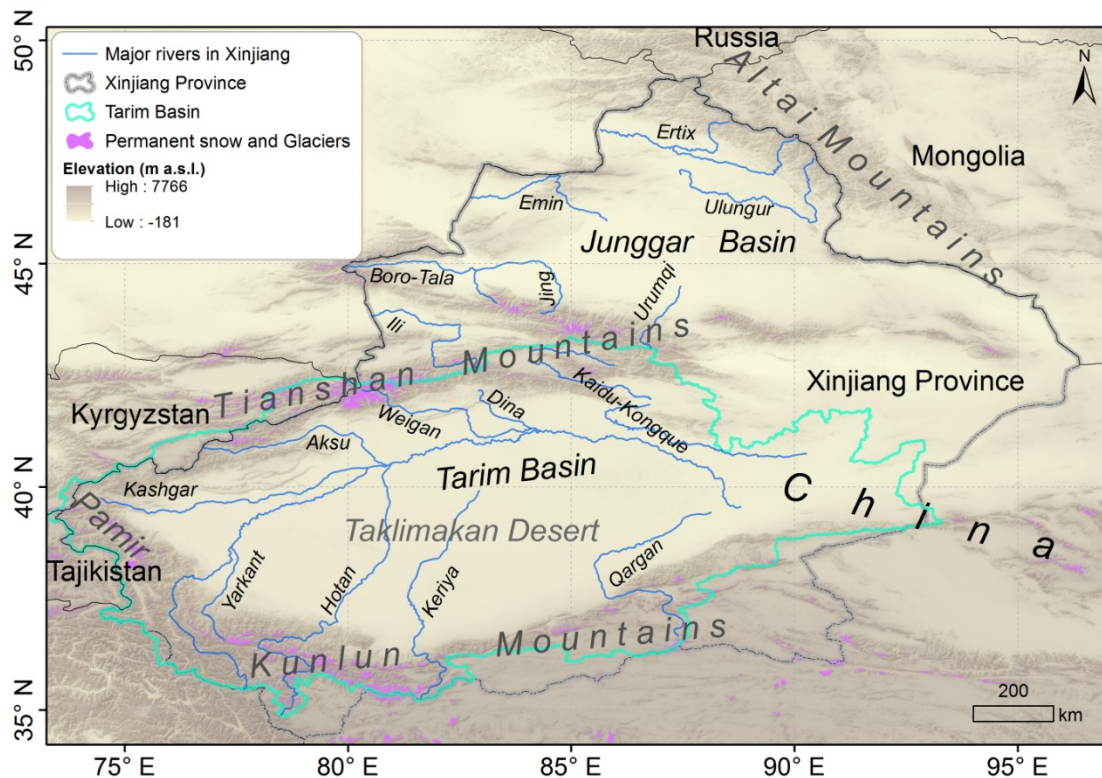


Figure 1.2 Map showing mountains ranges and major rivers which have sources in Xinjiang province, northwestern China, central Asia. Elevation data comes from the HydroSheds SRTM (Lehner et al., 2008) and map of permanent snow and glaciers was obtained from Randolph Glacier Inventory (RGI 6.0) (<http://www.glims.org/RGI/randolph60.html>) (RGI Consortium, 2017).

Mountain ranges are one of the major landform types in Xinjiang, northwestern China, with the Altay Mountains located in the northern, the Pamir Plateau located in the western, and the Tianshan

and Kunlun Mountains located in central and southern Xinjiang, respectively (Figure 1.2). Among these mountains, the Tianshan Mountains stretch from regions of Uzbekistan, Kazakhstan and Kyrgyzstan to Xinjiang and geographical separate the region into southern and northern Xinjiang; with the Tarim basin on the south and Junggar basin on the north (Figure 1.2) (Chen, 2014; Chen et al., 2016a). Xinjiang generally has a continental semiarid climate. Mountains block atmospheric circulation leads to uneven distributed temperature and precipitation, with southern Xinjiang is warmer and dryer than northern Xinjiang (Shi et al., 2007; Xu et al., 2010; Wu et al., 2010), while more precipitation occurs in high mountains due to orographic effect (Kundzewicz et al., 2015).

Glacier meltwater accounts for 30.6% of the total water recharge for downstream rivers in Xinjiang (Pang et al., 2011). Glaciers storage in Xinjiang are uneven distributed in different mountain ranges according to the first Glacier Inventory of China (Shi, 2005) (Table 1.1) and glacier ablation differs in different mountains, with glaciers in the Kunlun Mountains are relative stable while in the Tianshan Mountains are more sensitive, especially in the eastern Tianshan (Wang et al., 2008b).

Water resources from mountain regions account for more than 80% of the total surface water resources in Xinjiang, yet more than 45% are snow and glacier meltwater (Shen et al., 2013c). The Tianshan Mountains are the most important water source in Xinjiang based on the large stretches and the higher sensitivity to climate change. Take the largest inland Tarim river for example (covers an area of 1.03×10^6 km² and surrounds by 9 river systems) (Figure 1.2), near 50% of the total runoff are contributed by snow and glacier meltwater (Chen et al., 2015; Xu et al., 2009) and more than 75% of water in the Tarim basin were generated from the Tianshan Mountains (Pang, 2014). Thus, studies with the purpose of maintaining the water tower are an imperative.

Table 1.1 Mountains and glaciers in Xinjiang, northwestern China. The Karakorum and Kunlun Mountains includes glaciers both in Xinjiang and Qinhai-Tibet Plateau (Shi, 2005).

Mountain System	Mountain area (km ²)	Highest elevation (m)	Glacier		
			Number	Area (km ²)	Volume (km ³)
Altay	28800	4374	403	280	16
Tianshan	211900	7435	9035	9225	1011
Pamirs	23800	7649	1289	2696	249
Karakorum	26600	8611	3563	6262	692
Kunlun	478100	7167	7697	12267	1283

1.3 Climatic and hydrological changes

Global warming and its impacts are becoming one of the major issues in the 21st century (Piontek et al., 2014). Global surface temperature has increased 0.74 °C in the last 100 years (1906-2005), with a phenomenon that continental temperature increased faster than the oceans and higher northern latitudes temperature increased faster than the global average (Hallett et al., 2002; IPCC, 2007; Bates et al., 2008). Observed warming over several decades not only has serious impacts on the variability and intensity of precipitation, but also leads to a significant decrease in snow and glacier cover (IPCC, 2007). Ecosystems and environmental processes in mountain regions are even more sensitive to climate change (Beniston, 2003; Barry & Chorley, 2009).

1.3.1 Observed climate change

Annual mean temperature (T_{mean}) has increased at a rate of 0.36 °C /decade in the past decades (1960-2006) in northwestern China (Piao et al., 2010), which is higher than the average temperature increase rate of China (0.25°C/decade) (Li et al., 2012) and global (0.12 °C per decade) (1951–2012) (IPCC, 2013). Elevation-dependent warming through the whole Xinjiang was not found, yet higher latitudes were experienced a high magnitude of warming (Li et al., 2011b). In the Tianshan Mountains, T_{mean} increased at a rate of 0.3-0.45 °C per decade (Jiang et al., 2013; Chen et al., 2016a), which is higher than the global-average warming (IPCC, 2013). Precipitation generally experienced an increase trend (16% per decade) (1960-2006) (Piao et al., 2010), yet with more uncertainty. Aizen et al (Aizen et al., 1997) found that the precipitation increase rate is large under the elevation of 2000 m in the northern and western Tianshan. Yao et al (Yao et al., 2016) found that elevation-dependent precipitation trends are more obvious above the elevation of 500 to 1500 m). However, elevation-dependent increase in precipitation is still not clear.

Generally, the increase rate of temperature and precipitation and their spatio-temporal differences cannot be generalized in such a big area. The spatial and seasonal changes of temperature and precipitation and related references were summarized in Table 1.1. However, the abrupt increase in temperature and precipitation were found in the mid-1980s but more marked in the 1990s, respectively (Shi et al., 2007; Zhang et al., 2016a).

Table 1.1 Summary of reviewed studies on climatic and hydrological changes in Xinjiang. Tmax, Tmean and Tmin indicate the maximum, mean and minimum temperature. Numbers in parentheses in the table refer to the selected references.

	Key findings	Selected references
Temperature	Tmean increased (1) at a rate of 0.36°C /decade (1960-2006) in Xinjiang (2);	(1) (Shi et al., 2007); (2) (Piao et al., 2010);
	The magnitude of warming: Tmin> Tmax(3-5,42); northern Xinjiang > southern Xinjiang (6-8); high latitude >lower latitude(7);	(3) (Zhang et al., 2012b); (4) (Jiang et al., 2013); (5) (Xu et al., 2015a);
	Winter contributes the most to the annual temperature change (41,16); Abrupt change occurs in the mid-1980s in Xinjiang (1,5,8-10) and in the Tarim basin (11-15);	(6) (Wu et al., 2010); (7) (Li et al., 2011b); (8) (Xu et al., 2010); (9) (Bai et al., 2015b); (10) (Chen et al., 2014); (11) (Xu et al., 2004);
Precipitation	Increased precipitation but with more uncertain (1,3); precipitation increase at a rate of 16%/decade (1960-2006) (2) or 7.40 mm/decade (1961-2008) in Xinjiang (3);	(12) (Chen et al., 2006) ; (13) (Xu et al., 2006);
	The magnitude of increase: northern Xinjiang > southern Xinjiang (3,5,43) but mainly in winter (3,5,8,16);	(14) (Chen et al., 2007); (15) (Chen et al., 2009); (16) (Hu et al., 2016);
	Precipitation increase in winter in northern Xinjiang and in summer in southern Xinjiang(7); Abrupt change occurs in mid-1980s in Xinjiang (1) and in the Tarim basin(10-15);	(17) (Chen et al., 2016a); (18) (Shi, 2005); (19) (Xu et al., 2015b); (20) (Li et al., 2007); (21) (Li et al., 2011c); (22) (Li et al., 2011a);
Snow /glacier melt	Less snowfall and reduced snow cover (17);	(23) (Huai et al., 2015);
	Earlier snowmelt runoff peaks and snowmelt runoff timing (28);	(24) (Wang et al., 2017a); (25) (Huai et al., 2017);
	Glacier retreat in Xinjiang (1, 18) but mainly in the Tianshan Mountains (17,25,27); Glacier retreat rate: western and eastern Tianshan > cenreal Tianshan (25);	(26) (Shangguan et al., 2009); (27) (Farinotti et al., 2015); (28) (Sun et al., 2015); (29) (Chen et al., 2008);
Streamflow	Glaciers were found to decrease in the Ili basin (19), the Urumqi basin (No. 1 Glacier) (20-22,28), the western Tianshan (Tomur Peak) (23); Ebinur lake basin (24) and the Tarim basin (26);	(30) (Yao et al., 2007); (31) (Yang et al., 2010); (32) (Jianhua Xu et al., 2009); (33) (Bai et al., 2015a); (34) (Wang et al., 2013c);
	Streamflow in most rivers increased in Xinjiang and more obvious in the 1990s (1,2 8,12,31, 34);	(35) (Tao et al., 2011); (36) (Krysanova et al., 2015);
	Earlier spring floods and increasing summer flood peaks (8,13); Streamflow increased in the Aksu (12, 32,34,36,37), Yarkand (12, 32), Kaidu basin (33,34,38) , Urumqi (40) and the whole Tarim basins (29-31,35,39); High glacierized basins are more correlated with temperature change, while low latitude basins (less or no glacier) are more correlated with precipitation change (16, 37);	(37) (Kundzewicz et al., 2015); (38) (Xu et al., 2016a); (39) (Xu et al., 2011); (40) (Li et al., 2010); (41) (Li et al., 2012); (42) (Ling et al., 2012); (43) (Zhang et al., 2010);

1.3.2 Projected climate change

Global average temperature is likely to continue to increase at ranges between 0.3-1.7 °C (RCP2.6) and 2.6-4.8°C (RCP8.5) in 2081–2100 relative to the baseline period (1986–2005). Precipitation was expected to increase at high latitudes but with more variability (IPCC, 2013). Although uncertainties remain in the extent and pace of climate change (Piao et al., 2010; Guo et al., 2017), temperature and precipitation in northwestern China are expected to increase in future (Shi et al.,

2007; Wang et al., 2014; Guo & Shen, 2016; Wang & Qin, 2017) and even warm faster than other regions in China (Wang & Chen, 2014).

Temperature is projected to increase by 3 °C in northern Xinjiang and 1-2 °C in southern Xinjiang in the period of 2046-2075 relative to the baseline period (1971-2100) based on different climate scenarios (RCP2.6, RCP4.5 and RCP8.5) (Guo & Shen, 2016). The projected increase in precipitation ranges from 5 to 10% in northwestern China (Wang et al., 2014) and more significant in summer and winter, in northern and eastern Xinjiang and in mountainous regions (Guo & Shen, 2016). The generally warmer and wetter tendency was found in other basins (e.g. the Kaidu and Tarim basins) (Shi et al., 2007; Chen et al., 2013a; Xu et al., 2016a; Doris et al., 2016). In view of the uncertainties, future climate change in this area needs to be addressed.

1.3.3 Changes in climate extremes

Climate change not only expresses in the trends of climate elements but also leads to unexpected extreme events (Easterling et al., 2000; Coumou & Rahmstorf, 2012). Changes in temperature and precipitation extremes were investigated over northwestern China based on the ETCCDMI climate indices (Zhang et al., 2011). The changes of climate extremes are less conclusive and with uncertainties but generally consistent with the climate change tendency in this arid region.

The magnitude and frequency of temperature and precipitation extremes were found to increase in northwestern China (Hu et al., 2016). It is very likely that the warm days (daily $T_{max} >$ the 90th percentile) and warm nights (daily $T_{min} >$ the 90th percentile) have an increase trend while the frost days (annual count when daily minimum < 0 °C) and ice days (annual count when daily minimum < 0 °C) decreased significantly in past decades in northwestern China (Zhai & Pan, 2003; You et al., 2011; Wang et al., 2013a; Wang et al., 2013d). The diurnal temperature range exhibited a decreasing trend (Wang et al., 2013a) while the growing season was lengthen (Zhang et al., 2006; Hu et al., 2016), which is coincident with the increased warm days and nights.

The frequency and intensity of precipitation showed up trends in the past decades (Zhai et al., 2005; Wang et al., 2013a, 2013b). Extreme rainfall events had experienced an uptrend (Fu et al., 2013a; Wang et al., 2013d) and occurs more in northern Xinjiang (Wang et al., 2013a). Impacted by climate change, rainstorm-induced and temperature-induced floods increased after the 1980s in the Tarim basin and the frequency of extreme floods (return periods > 10 years) become more

frequently after the 1990s (Zhang et al., 2016a). The intensity of warm extremes and precipitation extremes are projected to increase with warming climate in the long run (Zhang et al., 2006; 2017).

1.4 Cryospheric changes

1.4.1 Changes in snow and glacier cover fluctuations

Warmer temperature can reduce winter snow accumulation and possibly alter the rate and time of the subsequent snowmelt runoff (Barnett et al., 2005; Molini et al., 2011). The Tianshan Mountains are vulnerable by the impacts of warming climate, precipitation variability and changes of snow and glacier dynamics (Chen et al., 2016a; Shen & Chen, 2010).

The maximum snow depth, duration and the ratio of snowfall to precipitation experienced a decrease trend in the Tianshan Mountains due to climate warming (Aizen et al., 1997; Chen et al., 2016a). Snow accumulation is therefore less in winter and the onset of snowmelt becomes earlier. Additionally, glacier coverage has continued to decline in past decades in the Tianshan Mountains (Chen et al., 2016a), yet the decline trends showed an accelerated tendency since 1985 (Li et al., 2007) and become more obvious in the 1990s (Yao et al., 2004). Glacier hydrology therefore becomes more unstable (Shen & Chen, 2010; Chen, 2014).

Glacier area in Chinese Tianshan Mountains has decreased by near 22% (approximately 287 km²) (Huai et al., 2017). However, glacier retreat varies in different regions across the Tianshan Mountains based on topographic maps and remote sensing images (Landsat ETM+) (Shangguan et al., 2009; Huai et al., 2017). For instance, glacier coverage in the western Tianshan (the Tomur Peak, Huai et al., 2015), Ebinur lake basin (Wang et al., 2017a); the Glacier No. 1 (Ye et al., 2005; Li et al., 2007) and the Bogda and Harlik mountains (Li et al., 2011a) were found to decrease but with different magnitude in past decades (Table 1.1). Geographically, glaciers area in western and eastern Chinese Tianshan are generally decreased faster than in the central Tianshan (Huai et al., 2017; Chen et al., 2016a), and the magnitude of glacier volume change was found more obvious in the Tarim River Basin than other basins (Yao et al., 2004; Liu et al., 2006).

1.4.2 Changes in streamflow

Water cycle can be intensified by a warmer climate (Labat et al., 2004) and possibly experiences a dominant rise in the spring streamflow peak in the coldest basins (Nijssen et al., 2001). Warmer temperature may lead to significant decrease of snow and glacier coverage which contribute a large

amount of water for increasing water levels of mountain lakes (Shi et al., 2007; Ye et al., 2017) and, streamflow in most downstream rivers (Yao et al., 2004; Ye et al., 2005; Li et al., 2010; Liu et al., 2006; Tao et al., 2011; Chen et al., 2013b, 2016a; Krysanova et al., 2015) (Table 1.1). Nevertheless, the changes of streamflow generally consist with the increase tendency of temperature, with more obvious increase in the 1990s (Yao et al., 2004; Li et al., 2010)

Streamflow showed spatial and temporal variability due to different climate and basin characteristics in northwestern China (Table 1.1). Spatially, streamflow in northern Xinjiang is more impacted by the precipitation variability, while in the middle and south Xinjiang is more affected by temperature changes (Wang et al., 2013c), and streamflow in highly glacierized basins are likely dominated by the changes of temperature (Kundzewicz et al., 2015; Chen et al., 2016a). Seasonal, regional study showed that streamflow increase in spring and autumn is highly depend on temperature, while precipitation mainly dominated the changes of streamflow in summer (Deng et al., 2015).

Streamflow was expected to increase in future based on regional climate model-RegCM2 (Shi et al., 2007). However, streamflow was projected increase to some extent first and then may decrease in the long run (Xu et al., 2016a; Chen et al., 2016b). Northwestern China is therefore forecasted one of the most critical regions where vanishing glaciers will negatively affect water supply in the future (Barnett et al., 2005).

1.4.3 Changes in permafrost

Permafrost and seasonally frozen ground are widely distributed in high latitude (Voigt et al., 2017) and altitudinal mountain regions (e.g. the European Alps, the Chilean Andes, the Qinghai-Tibet plateau and Tianshan Mountains), yet are sensitive to climate change (Jin et al., 2000; Boeckli et al., 2012; Guido et al., 2016; Lu et al., 2017; Azócar et al., 2017).

High-elevation permafrost and seasonally frozen ground are widely distributed in northwestern China (Jin et al., 2000; Marchenko et al., 2007; Imbery et al., 2013; Peng et al., 2017). The altitude height of continuous permafrost, discontinuous zone and sporadic zone in the central northern Tianshan Mountains distribute above 3600, 3200-3600 and 2700-3200 m a.s.l (above sea level), respectively (Zhao et al., 2010). However, the maximum depth of frozen soil is deeper in the northern than southern Xinjiang (Fu et al., 2013).

Generally, the permafrost temperatures increased in past decades (Jin et al., 2000; Xiao et al., 2007; Qin & Xiao, 2009), approximately 0.3-0.68 °C (1974–2004) in the northern Tian Shan based on geothermal observations (Marchenko et al., 2007; Zhao et al., 2010). Additionally, the duration of soil frozen has become shorter in Xinjiang (Wang et al., 2005; Qin & Xiao, 2009) and the total area of permafrost and frozen soil have decreased in different parts of the Tianshan Mountains (Xiao et al., 2007; Marchenko et al., 2007; Qin et al., 2014). The distribution of permafrost has moved northward 8-10.5 m/year (1972-1991) in the central Tianshan (Ding, 1998) and the altitudinal lower limits of permafrost have risen in the Altai and Tianshan Mountains (Jin et al., 2000; Marchenko et al., 2007). Moreover, the active-layer thickness has increased while varies due to the calculation year, altitude, aspect, slope and lithology (Ding, 1998; Wang et al., 2005; Marchenko et al., 2007; Imbery et al., 2013; Tian et al., 2016). Zhao et al (Zhao et al., 2010) found the active-layer thickness in central Asia has increased from 3.2-4 m to 5.2 m from the mid-1970s to 2009.

Changes of permafrost are impacted by climate change. However, the feedback from variations of permafrost also can be an important factor for accelerating climate warming due to the amounts of organic carbon it release (Koven et al., 2011). Changes of alpine permafrost and frozen soil have implications for the surface energy, hydrothermal conditions, water balance and ecosystems (Tian et al., 2016; Peng et al., 2017) and therefore need further research.

1.5 Hydrological modelling and limitations

1.5.1 Classification of hydrological models

Hydrological models have been widely applied in understanding and evaluating hydrological processes in the past and present (Hagg et al., 2007; Praskievicz & Chang, 2009). Hydrological models represent the natural systems in a simplified form and vary classified based on the purpose and the methodologies used in the model (Xu, 2002). Generally, hydrological models can be classified into empirical models, lumped conceptual models and physical-based models (Refsgaard & Knudsen, 1996). Empirical models (also called black-box models) are largely depend on the relationships between input and output rather than physical processes. Normally, the whole basin is treated as a homogeneous area and statistical methods are used to describe hydrological processes (Xu, 2002; Devia et al., 2015). Lumped conceptual models (grey-box models) are regarded as the transition zone between empirical models and physical-based models,

which take physical processes into consideration but in a simplified way (e.g. HBV model (Bergström, 1992; Xu, 2002). Physical-based models (theoretical models) are the most complex models which have logical structure and try to describe detail physical processes during the simulation (Beven, 2001). Moreover, physical-based models can be classified into distributed and semi-distributed models in terms of spatial discretization of the watershed (Xu, 2002). Distributed hydrological models divide a basin into homogeneous elementary units like grid or Hydrological Response Units (HRUs) [e.g. MIKE SHE model (Jayatilaka et al., 1998), J2000 model (Krause, 2002)], Spatial Processes in Hydrology (SPHY) (Terink et al., 2015), while semi-distributed hydrological models calculate water components based on separate areas or sub-basins (SWAT, Arnold et al., 1998). Normally, physically based models are applied to better understand hydrological processes in a catchment.

1.5.2 Hydrological models for snow and glacier melt

As important input components for hydrological systems, snow and glacier melt are of great importance for hydrological cycle, especially in mountain catchments. However, snow and glacier melt processes representation remains a complex task in hydrological community. Currently, snow and glacier melt are generally simulated based on a simple temperature index approach (Hock, 2003; 2005), sophisticated energy-balance models (Anderson, 1976; Marks et al., 1999; Liston & Elder, 2006) and combination of index and energy budget methods (Senese et al., 2014).

Constrained by observational data, temperature-index models (or degree days) generally assume empirical relationships between ablation and positive air-temperature sums. However, with the increased computational power and research progress, the temperature-index model received significant attention in including more climatic variables and accounting for spatial variability of melt rates (Hock, 1999). The air temperature threshold for melt is an important factor in the temperature-index model which controls the melt start (Kuhn, 1987; Senese et al., 2014). Energy-balance models account energy exchanges at the snow-air interface, which are represented by important physical relationships, such as radiation transfer, latent and sensible heat transfer, heat storage and heat transfer by rain water (Anderson, 1976). However, as the meteorological conditions are always variable and the model is rather complicated, whether an energy-balance model is valid or not largely depends on forcing data (Anderson, 1976; Marks et al., 1999). Thus, this complex model sometimes cannot be used due to the scarcity of data. Therefore, a combination

of energy budget and temperature-index methods was adapted in snowmelt simulations which try to take more variables and meanwhile with some lumped parameters (Hock, 2003; Tahir et al., 2011; Senese et al., 2014).

1.5.3 Hydrological modelling and challenges in the Tianshan Mountains

Hydrological modelling is a useful approach to unraveling hydrological processes in mountain regions (Hagg et al., 2007; Chen et al., 2016b). Snowmelt runoff model (SRM), which based on the temperature-index approach, has been widely used in the Tianshan Mountains. Current studies indicated that temperature representation plays an important role on mode prediction and accuracy based on the SRM (Zhang et al., 2007; Dou et al., 2011). Yong et al (Yong et al., 2007) had applied a modified degree-day model which based on the method developed by Hock (Hock, 1999) in the glacierized Keqicar Baqi basin in the southern Tianshan. The improved method has taken potential clear-sky solar radiation into consideration. Their results indicated that in the data scarcity area, the simple degree-day model is suitable for snowmelt modelling. However, degree-day factors are always constant in space and time in the simulation. Zhang et al (Zhang et al., 2012a) had modified a monthly degree-day model by integrated glacier area variation in seven sub-basins of the Tarim basin. Similarly, poorly known temperature lapse rates and precipitation gradients were found to be the major sources of uncertainty for the model simulation.

Physical conditions and dynamics of glacier extent are not well represented in most conceptual and physically-based hydrological models. The conceptual precipitation-runoff model HBV, which regards sub-basins as geographically and climatologically heterogeneous units, was found not appropriate for representing local physical conditions in the Urumqi basin in the Tianshan Mountains (Sun et al., 2015). A lumped conceptual model (VHM) and a physically-based model (MIKE SHE) was applied in the glacierized Kaidu basin for understanding hydrological response to climate change, showing that the lumped model inadequate simulated streamflow due to constant temperature threshold for snowmelt, yet the distributed hydrological model performs better due to spatial variation in temperature. However, glacier was assumed constant in the model (Liu et al., 2011). Furthermore, an algorithm of modelling glacier melt processes was included in the physical-based SWAT model for simulating glacier retreat and its response to climate change in the Manas basin (Luo et al., 2013). However, solar radiation and topographic factors were

excluded. Multi-method integrated model approaches (hybrid model) were found to better simulate runoff than a single model (Xu et al., 2016b), which may be the alternative option in future research.

1.6 Objectives and research questions

Climate change is substantial and plays an important role in affecting water resources and ecosystems in the Tianshan Mountains in northwestern China. Snow and glacier meltwater are critical in water cycle in mountainous basin, yet the processes are complex and have not been discussed in detail. Emphasizes the need for better understanding mountain hydrology, physical-based hydrological models are highly required. The objectives of this thesis are therefore modelling hydrological responses to climate change in a data-scarce glacierized basin in the Tianshan Mountains with the purposes of better understanding water balance and quantifying the contribution of different runoff components, which can be of great value in supporting water resources management in the Tianshan mountain basins under the changing climate.

This thesis tends to integrating studies of climate change, changes of hydrology regimes, changes of near-surface temperature lapse rates and the application of glacierized hydrological model together in the Tianshan Mountain regions. Accordingly, several research questions are raised in the following:

1. What is the status of climatic and hydrological changes in northwestern China?

Ecosystems and environmental processes are highly sensitive to climate change in northwestern China. Understanding the climate variability is the fundamental question for investigating the impacts of climate change and adopts further solutions in water resources management.

2. How are the hydrological regimes expected to change under the changing climate?

The timing and volume of streamflow and snowmelt runoff can be particularly sensitive to climate change. However, it is not well known how changes in climate will impact streamflow and snowmelt runoff timing in different basins of the Tianshan Mountains. This research question seeks to estimate how changes in temperature and precipitation could affect streamflow and snowmelt runoff timing and their relationships in four mountain basins in the southern Tianshan.

3. What are the variations of temperature lapse rate in the Tianshan Mountains?

Near-surface temperature lapse rates are needed to regionalize air temperature in mountain regions where with scarce instrumental records. However, actual lapse rates vary at a given place and time.

As climates differ substantially between the northern and southern slopes of the Tianshan Mountains and between its mountain valleys, it is necessary to evaluate the variations of near-surface temperature lapse rates in the Tianshan Mountains.

4. How can we unravel the hydrology in the glacierized mountain basin, especially to understand the contribution of snow/glacier meltwater and different runoff components?

Snow and glacier meltwater play an important role in regional water balance and supplies a large amount of water for downstream rivers, yet the hydrological processes of glacierized basins are poorly known due to data scarcity and complex snow/glacier melt dynamics. In addition, different runoff components have not been identified in detail. This research question welcomes studies that: (1) to fill the gaps in data-scarcity basin by considering gridded metrological data as well as high-elevation field survey data; (2) to understand hydrological processes and quantify the contribution of different runoff components in the glacierized Kaidu basin using the high resolution (spatial and temporal) distributed hydrological model; and (3) to obtain the key parameters for hydrological modelling and assess uncertainties related to the model parameters and design.

1.7 Thesis outline

This thesis addresses different research questions under the frame of understanding hydrological processes in the glacierized data-scarce basin in the Tianshan Mountains. Every chapter tends to answer a specific question in the form of a peer reviewed paper. The thesis is therefore structured as follows:

- Chapter 1 provides a general overview of research background. Climatic and hydrological changes in northwestern China were summarized. The limitations of current research and hydrological models were discussed, which highlight the urgent to conduct research in this semiarid region (the chapter 1 and chapter 5 are part of a manuscript in preparation for a review paper in Journal X);
- Chapter 2 shows the impacts of climate change on river streamflow and snowmelt runoff timing in the southern Tianshan basins;
- Chapter 3 examines the variations of near-surface temperature lapse rate which can be used to regionalizing temperature in mountain basins and further valuable used in hydrological model;
- Chapter 4 is served as a case study for applying the distributed hydrological model and understanding hydrological processes in the glacierized Kaidu basin;

- Chapter 5 and 6 provide discussions, conclusions and recommendations of the whole topic.

(Author's note: the captions of figures, tables and literature format underwent modifications for composition in this dissertation. Please check the journal version.).

Chapter 2 Trends and variability in streamflow and snowmelt runoff timing in the southern Tianshan Mountains

Acknowledgments:

This research was supported by the National Natural Science Foundation of China [41630859] and the Key Project of Chinese Academy of Sciences [KZZD-EW-12-1]. China Scholarship Council (CSC) is acknowledged for the PhD scholarship awarded to the first author. The authors wish to thank Jason Goetz for his constructive comments on the manuscript. We appreciate the editor and anonymous reviewers for their constructive comments

Published as:

Shen, Y.-J., Y. Shen, M. Fink, S. Kralisch, Y. Chen, & A. Brenning. (2018), Trends and variability in streamflow and snowmelt runoff timing in the southern Tianshan Mountains, *Journal of Hydrology*, 557, 173-181, doi: 10.1016/j.jhydrol.2017.12.035.

Key points:

1. Streamflow increased significantly, especially in winter and spring in the southern Tianshan.
2. Streamflow has shown a sharp increase since the mid-1990s at annual and seasonal scales.
3. Snowmelt runoff timing shifted earlier dates since the mid-1980s in the southern Tianshan.
4. Variabilities of streamflow and snowmelt timing differ in different basins due to different streamflow generation processes.

2.1 Abstract

Streamflow and snowmelt runoff timing of mountain rivers are susceptible to climate change. Trends and variability in streamflow and snowmelt runoff timing in four mountain basins in the southern Tianshan were analyzed in this study. Streamflow trends were detected by Mann-Kendall tests and changes in snowmelt runoff timing were analyzed based on the winter/spring snowmelt runoff center time (WSCT). Pearson's correlation coefficient was further calculated to analyze the relationships between climate variables, streamflow and WSCT. Annual streamflow increased significantly in past decades in the southern Tianshan, especially in spring and winter months. However, the relations between streamflow and temperature/precipitation depend on the different

streamflow generation processes. Annual precipitation plays a vital role in controlling recharge in the Toxkon basin, while the Kaidu and Huangshuigou basins are governed by both precipitation and temperature. Seasonally, temperature has a strong effect on streamflow in autumn and winter, while summer streamflow appears more sensitive to changes in precipitation. However, temperature is the dominant factor for streamflow in the glacierized Kunmalik basin at annual and seasonal scales. An uptrend in streamflow begins in the 1990s at both annual and seasonal scales, which is generally consistent with temperature and precipitation fluctuations. Average WSCT dates in the Kaidu and Huangshuigou basins are earlier than in the Toxkon and Kunmalik basins, and shifted towards earlier dates since the mid-1980s in all the basins. It is plausible that WSCT dates are more sensitive to warmer temperature in spring period compared to precipitation, except for the Huangshuigou basin. Taken together, these findings are useful for applications in flood risk regulation, future hydropower projects and integrated water resources management.

Keyword:

Climate change; Winter/spring snowmelt runoff time; WSCT; Tarim basin; Central Asia.

2.2 Introduction

Snowmelt contributes substantially to the springtime runoff and streamflow in mountain regions with colder climates. The timing and volume of snowmelt runoff and streamflow can be particularly sensitive to climate change (Barnett et al., 2005; Stewart et al., 2004; Clow, 2010; Viviroli et al., 2011; Leppi et al., 2012). The rivers flowing from the Tianshan Mountains (known as the “Water tower of Central Asia”) are an important freshwater source for Central Asia (Sorg et al., 2012; Chen et al., 2016a, 2016b). Additionally, the snowmelt in the Tianshan Mountains, as in other cold mountain regions, contributes substantially to the springtime runoff and streamflow portions of the regional water balance (Chen et al., 2016b). Average temperature and precipitation have been increasing over recent decades in northwestern China where the Tianshan Mountains are located (Xu et al., 2004; Chen et al., 2006; Kong & Pang, 2012). As precipitation influences streamflow directly, while temperature mainly affects evapotranspiration, snow/glacier melt and the form (rain or snow) of precipitation (Singh & Singh, 2001; Molini et al., 2011); warmer and wetter conditions may result in an accelerated and unstable regional hydrological cycle in this semiarid region (Shen & Chen, 2010; Chen, 2014). Streamflow variability is therefore remarkably important for studying the impacts of climate change.

Streamflow and snowmelt runoff timing in the Tianshan Mountains are expected to change under a changing climate. Streamflow experienced a remarkable increase with climate warming (Chen et al., 2009, 2013; Liu et al., 2011) which-combined with glacier shrinkage-leads to a significant increase in streamflow volume and earlier snowmelt runoff in the Urumqi basin (Sun et al., 2015). According to model simulations, the timing of snowmelt runoff is projected to shift earlier due to temperature increase in spring (Wang et al., 2010; Liu et al., 2011). However, the impacts of climate change on streamflow differ in different basins. The Xinjiang province portion of the Tianshan mountains in China runs from west to east (around 1700 km long), and therefore intercepts moist air coming from the westerlies and results in unevenly distributed precipitation and water resources (Chen, 2014). The northern and western slopes of the Tianshan receive more precipitation than the southern and eastern parts (Xu et al., 2010), while temperature on the southern slopes is higher than on the northern slopes (Shen et al., 2016). The climate-related impacts on streamflow are even more complex in glacierized catchments. For instance, streamflow change in the Kaidu basin in summer is mainly attributed to changes in mountain precipitation (Deng et al., 2015), while temperature dominates streamflow changes in the highly glacierized Kunmalik basin (Kundzewicz et al., 2015). Generally, the distribution of streamflow and snowmelt runoff timing are undergoing significant changes due to climate variability, which motivates the need to identify the streamflow variability and snowmelt runoff timing in meltwater-dependent basins.

Changes in streamflow and snowmelt runoff timing have become evident in other regions in recent decades. Global streamflow has tended to increase in the warming climate (Labat et al., 2004). In addition, streamflow increases have been projected due to increased temperature and precipitation in a glacierized river basin in Nepal (Immerzeel et al., 2012). Quantified by means of center of volume date (CT) and spring pulse onset, streamflow and snowmelt runoff timing were shifted earlier due to temperature increase in New England (Hodgkins et al., 2003) and Colorado (Clow, 2010). These changes are also observed in western North America and Eurasian Arctic rivers (Stewart et al., 2004, 2005; Cayan et al., 2001; Tan et al., 2011). Based on GCM models, the projected streamflow in Quebec, Canada, is expected to increase in winter and decrease in spring (Boyer et al., 2010). Taken together, changes in streamflow and snowmelt runoff timing are important indicators of climate-related changes (Hodgkins et al., 2003). However, climate change and its impacts on streamflow are still poorly described, especially with respect to snowmelt runoff

changes in glacierized catchments in the Tianshan Mountains (Chen et al., 2016b). Currently, not much research in the Tianshan Mountains focuses on the streamflow variability at the basin scale, while much of the recent work has focused on large regional areas (Shi et al., 2007; Chen et al., 2009; Tao et al., 2011; Xu et al., 2010; Wang et al., 2013c). Therefore, it is not well known how changes in climate might impact streamflow and snowmelt runoff timing in different basins of the Tianshan Mountains. To improve our general understanding of the impacts of climate change, the knowledge of seasonal relationships between hydro-meteorological variables at the basin scale must be improved.

This study therefore seeks to estimate the trends and variability of streamflow and snowmelt runoff timing in four mountain basins in the southern Tianshan (from west to east) and their possible sensitivity to climate change. The objectives are: (1) to estimate annual, seasonal and monthly historical streamflow characteristics in four glacierized basins in the Tianshan Mountains; (2) to characterize possible changes in snowmelt runoff timing; (3) to obtain insights into hydrological processes and to identify the relationships between hydrological changes associated with climate variables.

2.3 Study area, data and methods

2.3.1 Study area

Four glacierized basins (Toxkon, Kunmalik, Kaidu and Huangshuigou, respectively) in the southern Tianshan were chosen based on the location and data availability (Figure 2.1 and Table 2.1). Mean elevations of the Toxkon, Kunmalik, Kaidu and Huangshuigou basins are 3634, 3707, 3008 and 2840 m above sea level (a.s.l), respectively. The Toxkon and Kunmalik basins drain approximately 19,166 and 12,816 km² upstream from the Shaliguilanke and Xiehela stations (Table 2.1). They are the main headwater subcatchments of the Aksu River, which is the main tributary of the Tarim basin, accounting for about 80% of its annual streamflow. In addition, approximately 4% and 20% of the Toxkon and Kunmalik basins, respectively, are glacierized (Doris et al., 2016). The Kaidu and Huangshuigou basins are located in the central southern part of the Tianshan Mountains and cover 18,649 and 4,298 km² upstream from the Dashankou and Huangshuigou gauge stations. Streamflow from the Kaidu and Huangshuigou basins finally arrive at Bosten Lake which is another important water source for the Tarim basin.

The basins are characterized by a continental semiarid climate. Mean annual streamflow in the Toxkon, Kunmalik, Kaidu and Huangshuigou basins are 148, 381, 189 and 69 mm/year, respectively (Table 2.1). Temperature and precipitation (from APHRODITE, see the Data section) are highly heterogeneous due to large elevational gradients and complex topography. The Kaidu basin has the coldest winters (mean winter temperature $-20.4\text{ }^{\circ}\text{C}$), followed by the Kunmalik ($-17.2\text{ }^{\circ}\text{C}$), Huangshuigou ($-15.8\text{ }^{\circ}\text{C}$) and Toxkon ($-15.2\text{ }^{\circ}\text{C}$) basins (Figure 2). The highest mean summer temperature is found in the Huangshuigou basin ($10.4\text{ }^{\circ}\text{C}$). Average summer temperatures in the Toxkon, Kunmalik and Kaidu basins are 9.3 , 6.9 and $9.2\text{ }^{\circ}\text{C}$, respectively. Generally, temperature in winter is more variable than in summer, while the opposite holds true for precipitation (Figure 2). Winter is the driest season for all the basins (15, 23, 11 and 6 mm for the Toxkon, Kunmalik, Kaidu and Huangshuigou basins, respectively). Precipitation mainly occurs in summer (115, 152, 138 and 127 mm for the Toxkon, Kunmalik, Kaidu and Huangshuigou basins). Moreover, average precipitation in spring is higher in the Toxkon and Kunmalik (65 and 79 mm) than the Kaidu and Huangshuigou (37 and 30 mm, respectively) basins.

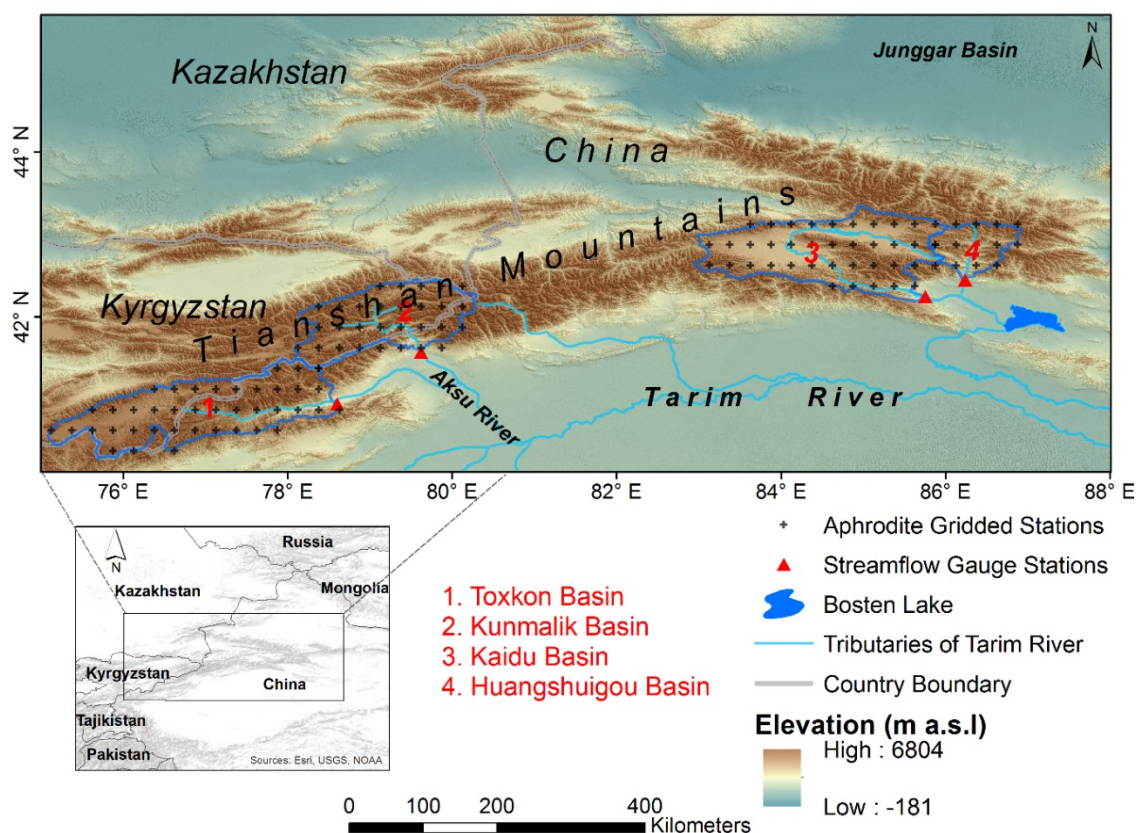


Figure 2.1. Location of river basins and gauge stations analyzed in this study.

Table 2.1. Summary of basins and gauge stations used in this study.

River Basin	Area (km ²)	Gauge Station	Latitude (N)	Longitude (E)	Elevation (m a.s.l)	Data Availability	Annual Streamflow (m ³ s ⁻¹)	Annual Streamflow (mm)
Toxkon	19166	Shaliguilanke	40.95	78.6	2000	1961-2007	89.5	148
Kunmalik	12816	Xiehela	41.57	79.62	1478	1961-2007	153.7	378
Kaidu	18649	Dashankou	42.22	85.73	1340	1972-2008	111.2	189
Huangshuigou	4298	Huangshuigou	42.45	86.23	1320	1962-2008	9.3	69

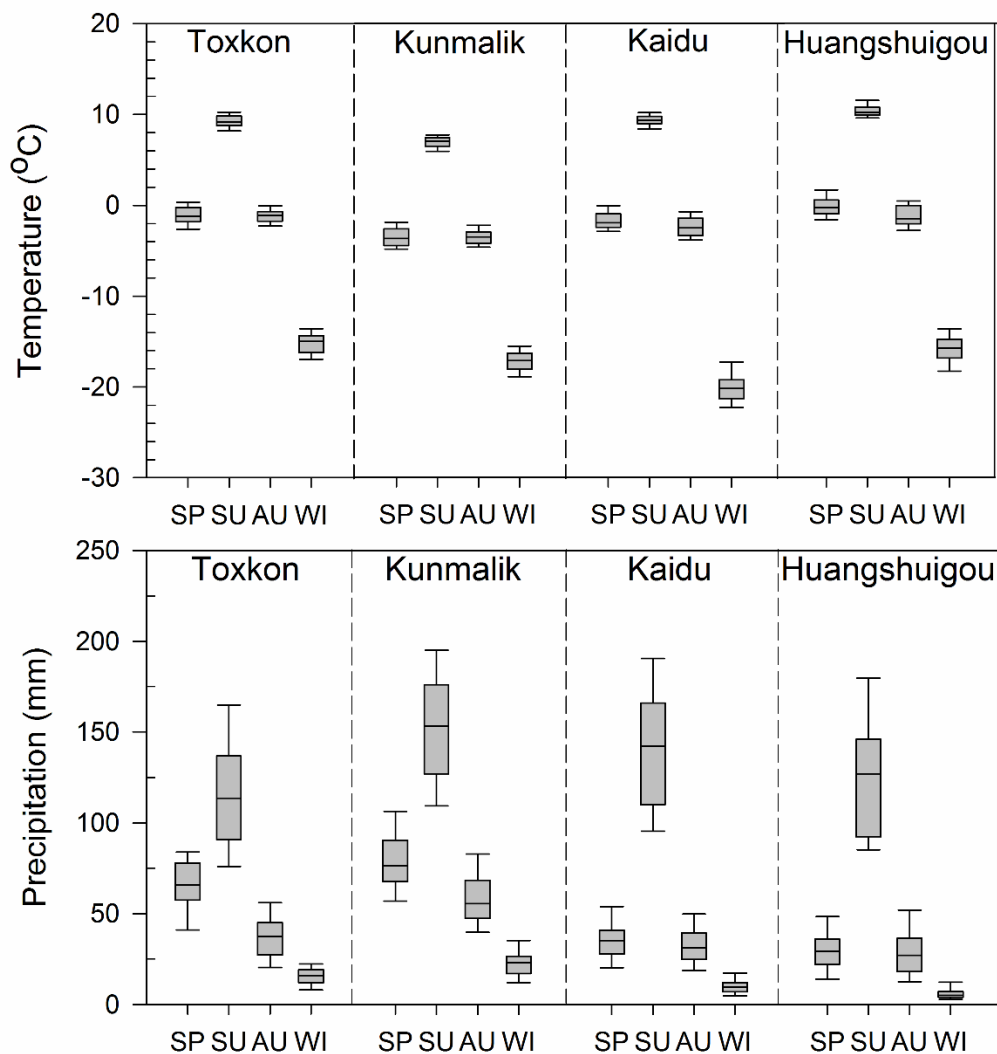


Figure 2.2. Boxplots with seasonal normal (1961–2007) of temperature and precipitation for the Toxkon, Kunmalik, Kaidu and Huangshuigou basins in the southern Tianshan. Boxplots represent extreme values, lower and upper quartiles and median value of a variable. Seasons are defined as: SP= Spring (March, April, May), SU=Summer (June, July, August), AU=Autumn (September, October, November), WI=Winter (December, January and February) in this study.

2.3.2 Data

Streamflow gauge data were obtained from the Hydrology and Water Resources Bureau of Xinjiang. Four stations with daily streamflow data are available in the Tianshan Mountains. The gauge locations are shown in Figure 2.1 and the corresponding summary information is listed in Table 2.1. The streamflow data cover a period of more than 30 years and all the data were strictly checked for homogeneity. There are a few days of missing data (<1% of the daily values) for the daily streamflow in the Shaliguilanke, Xiehela and Huangshuigou stations. However, monthly data are available. We interpolated the missing data using linear regression with neighboring data. Although uncertainties remain, we assume that they won't have much influence on the trend detection.

There is only one observation station in each basin, which cannot represent the spatial climate for the whole basin. Therefore, time series of mean temperature and precipitation data within these basins were extracted from APHRODITE (Asian Precipitation-Highly-Resolved Observational Data Integration Towards Evaluation of Water Resources) gridded data (Yatagai et al., 2012). APHRODITE covers time span more than 45 years (1951-2007 for precipitation and 1961-2007 for temperature) and it features a spatial resolution of $0.25^\circ \times 0.25^\circ$. APHRODITE is an interpolated dataset that can provide a basic description for the local climate and has been widely applied in central Asia (Immerzeel et al., 2015; Shea et al., 2015; Krysanova et al., 2015). Climate stations are sparse in the Tianshan Mountains and most of the stations are located in the valley; APHRODITE may therefore underestimate the mountain precipitation due to the high orographic influence of the Tianshan Mountains. However, in terms of analyzing the streamflow and climate change variability, the trend of climate and their relationship with discharge can also give valuable information. We acknowledge that uncertainties related to the representation of climate in mountain areas remain. The river basins were delineated by using HydroSHEDS elevation data (approx. $90 \text{ m} \times 90 \text{ m}$ resolution; Lehner et al., 2008).

2.3.3 Methods

Temporal trends of streamflow were evaluated using non-parametric Mann-Kendall tests (Mann, 1945; Kendall, 1975) at annual and monthly scales for each basin. Sen's slope (Sen, 1968) was applied to analyze the linear rate of change. To reduce the expected proportion of false discoveries that may occur by chance alone, an adjustment for multiple comparisons was conducted by using

the Benjamini–Hochberg procedure (Benjamini & Hochberg, 1995). The false discovery rate was controlled at a level of 0.05, i.e. it is expected that no more than 5% of all null hypotheses rejected in this study were incorrectly rejected. All statistical analyses were performed using R (R Core Team, 2016).

Snowmelt runoff timing was carried out using the theory of “the center of mass of flow” (CT), which is a flow-weighted timing that represents the center of mass of the streamflow curve (Stewart et al., 2004). CT is not necessarily related to the actual snowmelt timing but the change of CT can present as evidence for observed earlier actual melting (Stewart et al., 2005). As most precipitation in the Tianshan Mountains falls in summer, to avoid the impact of large amounts of seasonal rainfall to the flow-weight, we computed CT only for the winter/spring period (January 1st to May 31st) when streamflow is snowmelt dominated. Thus, the annual winter/spring snowmelt runoff center time (WSCT) was calculated from:

$$\text{WSCT} = \sum(t_i q_i) / \sum q_i$$

where t_i is time in months (or days) from the beginning of the year (January 1st), q_i is the corresponding streamflow for month i (or day, i). Therefore, WSCT is a date which is given in months or days and smoothed by locally weighted regression (LOESS; Cleveland & Devlin, 1988). The correlations between streamflow, WSCT, temperature and precipitation were furthermore measured using Pearson’s correlation coefficient (R).

2.4 Results

2.4.1 Trends and variability of streamflow

Annual streamflow showed an increasing trend in four basins in past decades based on the Mann-Kendall test and Sen’s slope estimator (9.29, 14.35, 18.02 and 4.34 mm per decade for the Toxkon, Kunmalik, Kaidu and Huangshuigou basins, respectively). However, the streamflow increase was more strongly significant in the winter and spring months (from November to March) in four basins (Table 2.2, Figure 2.4). Seasonally, streamflow amounts of the Toxkon and Kaidu basins appear to increase in every season, while there are no significant trends in streamflow in the Kunmalik and Huangshuigou basins in summer and autumn, respectively.

Annual streamflow is expected to show the largest increase from the mid-1990s for each basin (Figure 2.3). Seasonal patterns of streamflow are generally similar to the change patterns of

annual streamflow that also increased since the early 1990s in terms of the cumulative anomalies (Figure 2.4). However, seasonal changes are more variable in spring than changes for other seasons as well as at the annual scale.

Table 2.2. Trends of streamflow in the Toxkon, Kunmalik, Kaidu and Huangshuigou basins.

	Toxkon (1961-2007)		Kunmalik (1961-2007)		Kaidu (1972-2008)		Huangshuigou (1962-2008)	
	mm/decade	P-value	mm/decade	P-value	mm/decade	P-value	mm/decade	P-value
Jan	0.22	<0.01	0.24	<0.01	1.51	<0.001	0.14	0.04
Feb	0.20	<0.01	0.23	<0.01	0.98	<0.001	0.14	0.02
Mar	0.20	<0.01	0.18	<0.01	0.99	<0.001	0.20	<0.001
Apr	0.55	0.14	0.23	0.15	0.74	0.1	0.24	<0.01
May	1.22	0.01	0.55	0.05	0.34	0.62	0.21	0.22
Jun	1.49	0.09	0.55	0.48	-0.39	0.66	-0.03	0.93
Jul	1.88	<0.01	6.49	<0.01	2.77	0.01	1.21	0.1
Aug	0.47	0.47	5.30	<0.01	3.85	<0.01	0.80	0.15
Sep	0.84	0.02	1.94	0.06	2.08	<0.01	0.61	0.04
Oct	0.55	<0.01	0.84	0.06	1.32	<0.01	0.40	<0.01
Nov	0.35	<0.01	0.36	0.02	1.60	<0.001	0.27	<0.01
Dec	0.28	<0.01	0.25	0.02	1.49	<0.001	0.28	<0.01
Annual	9.29	<0.001	14.35	<0.001	18.02	<0.02	4.34	0.03
Spring	1.94	<0.01	0.91	<0.01	2.11	0.045	0.75	<0.01
Summer	4.23	<0.01	10.43	<0.01	6.04	0.03	1.97	0.19
Autumn	1.71	<0.01	2.86	0.09	5.43	<0.001	1.33	0.01
Winter	0.72	<0.001	0.60	<0.001	4.08	<0.001	0.57	<0.01

Chapter 2

Trends and variability in streamflow and snowmelt runoff timing in the southern Tianshan Mountains

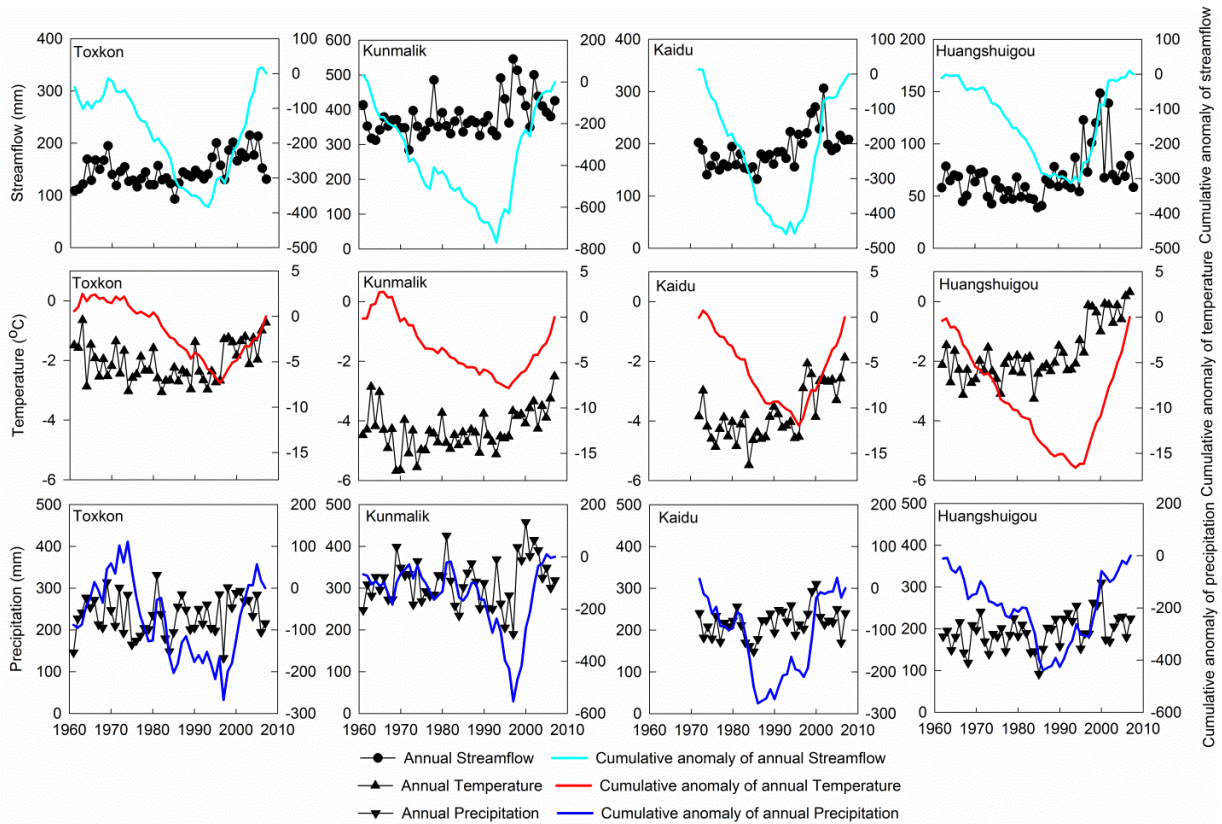


Figure 2.3. Annual and cumulative anomalies of streamflow, temperature and precipitation in the Toxkon (1961-2007), Kunmalik (1961-2007), Kaidu (1972-2007) and Huangshuigou (1962-2007) basins. The panel scales for streamflow are different among basins.

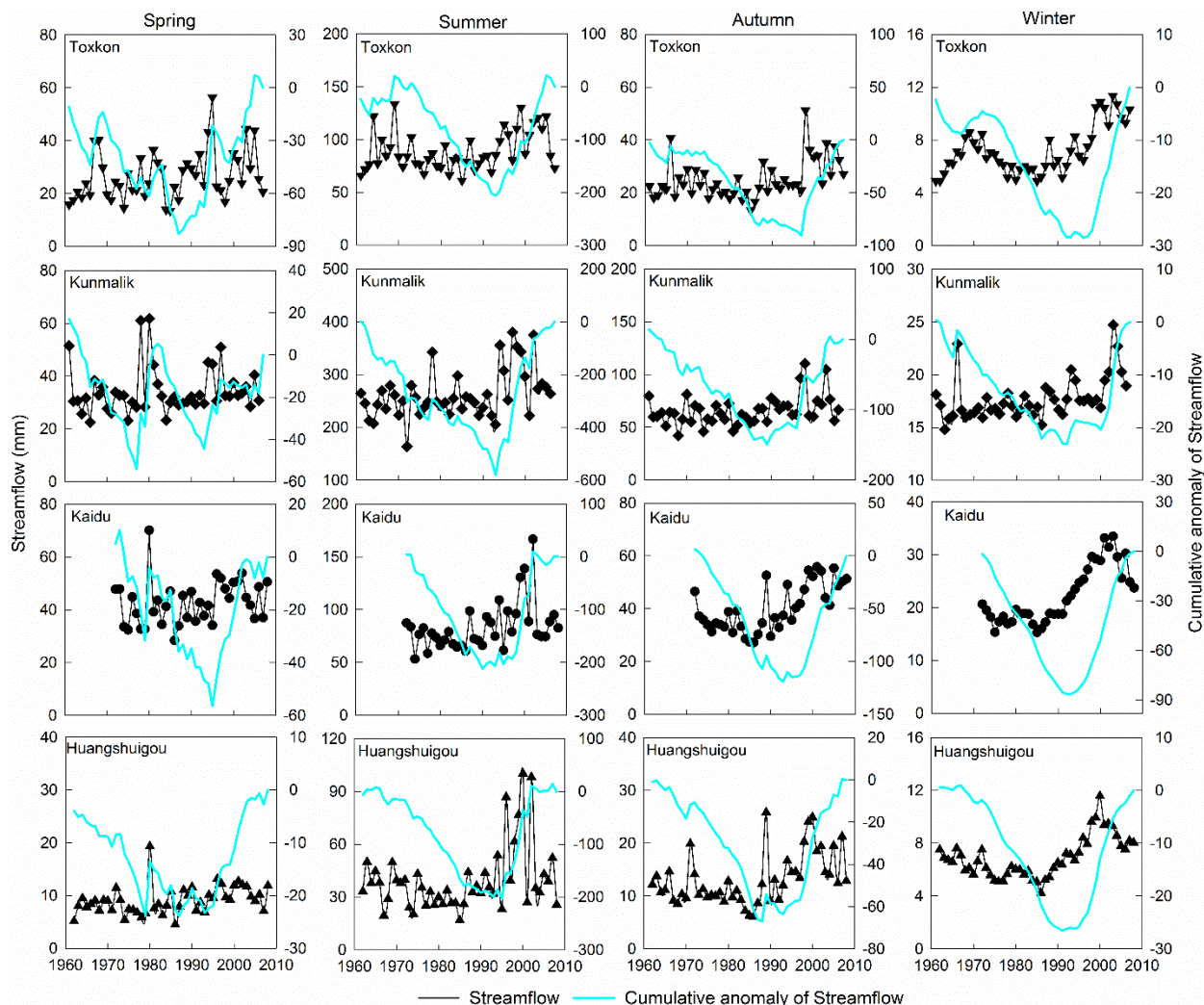


Figure 2.4. Seasonal and cumulative anomalies of streamflow in the Toxkon (1961-2007), Kunmalik (1961-2007), Kaidu (1972-2008) and Huangshuigou (1962-2008) basins. The panel scales are different for each basin in different seasons.

2.4.2 Streamflow links with temperature and precipitation

Changes in streamflow at annual and seasonal scales can be linked to the variations of temperature and precipitation. Annual temperature increased significantly in all basins (0.2, 0.5, 0.5 °C per decade for the Kunmalik, Kaidu and Huangshuigou basins) except for the Toxkon basin. Seasonally, temperature in autumn and winter has significantly increased in all the basins (Table 2.3). However, only temperature in the Kaidu basin rose significantly in all the seasons. Precipitation tended to increase in all basins, but with more uncertainty, as a significant trend was only detected in the Huangshuigou basin (Table 2.3). Winter precipitation increased significantly

in all the basins, except for the Toxkon basin. However, annual streamflow increased substantially since the mid-1990s, which very likely coincides with change patterns of annual precipitation and temperature. Annual temperature and precipitation also showed significant positive trends since the 1990s (Figure 2.3). Seasonal change patterns of temperature and precipitation were also estimated based on the seasonal cumulative anomaly of temperature and precipitation (Figure S2.1 and S2.2 in supporting information). We found consistent evidence that seasonal temperature had a steep change after the mid-1990s. However, seasonal precipitation is more variable than temperature.

Table 2.3. Trends of precipitation and temperature in the Toxkon, Kunmalik, Kaidu and Huangshuigou basins.

Time period	Toxkon (1961-2007)				Kunmalik (1961-2007)				Kaidu (1972-2007)				Huangshuigou (1962-2007)			
	Precipitation		Temperature		Precipitation		Temperature		Precipitation		Temperature		Precipitation		Temperature	
	mm/decade	P-value	°C/decade	P-value	mm/decade	P-value	°C/decade	P-value	mm/decade	P-value	°C/decade	P-value	mm/decade	P-value	°C/decade	P-value
Annual	5.0	0.37	0.1	0.28	8.2	0.26	0.2	0.01	10.3	0.07	0.5	<0.001	10.9	0.01	0.5	<0.001
Spring	0.3	0.87	-0.2	0.23	3.4	0.20	-0.1	0.46	-0.7	0.69	0.5	0.02	-0.6	0.58	0.3	0.06
Summer	0.9	0.84	-0.1	0.47	-1.8	0.66	0.1	0.26	10.3	0.08	0.4	<0.001	8.2	0.02	0.3	<0.001
Autumn	2.2	0.15	0.2	0.02	3.6	0.05	0.3	0.01	-0.6	0.82	0.6	<0.01	0.00	1.00	0.6	<0.001
Winter	0.4	0.57	0.3	0.02	2.1	0.04	0.4	<0.01	1.7	<0.01	0.7	<0.01	0.9	<0.01	0.8	<0.001

Average precipitation and temperature were compiled at annual and seasonal scales to identify the relationship between streamflow and climate variables (Table 2.4). Annual and summer streamflows have a positive relation with precipitation in all the basins, except for the glacierized Kunmalik basin. There has been no consistent relationship between streamflow and precipitation in the other seasons. Temperature has a significant positive relation with autumn and winter streamflow in the Toxkon, Kaidu and Huangshuigou basins. However, streamflow in the glacierized Kunmalik basin generally has a significant relationship with temperature at annual and seasonal scales.

Table 2.4. Correlation coefficients between streamflow and average precipitation/temperature in the Toxkon, Kunmalik, Kaidu and Huangshuigou basins.

Time period	Toxkon (1961-2007)				Kunmalik (1961-2007)				Kaidu (1972-2007)				Huangshuigou (1962-2007)			
	Precipitation		Temperature		Precipitation		Temperature		Precipitation		Temperature		Precipitation		Temperature	
	R	P-value	R	P-value	R	P-value	R	P-value	R	P-value	R	P-value	R	P-value	R	P-value
Annual	0.49	<0.001	0.07	0.66	-0.02	0.83	0.35	0.02	0.57	<0.001	0.60	<0.001	0.59	<0.001	0.52	<0.001
Spring	0.19	0.19	-0.23	0.13	-0.04	0.77	0.35	0.02	0.50	<0.01	-0.03	0.86	0.13	0.40	0.07	0.65
Summer	0.42	<0.01	-0.07	0.63	-0.24	0.09	0.47	<0.001	0.46	<0.01	0.26	0.12	0.56	<0.01	0.15	0.31
Autumn	0.45	<0.001	0.37	0.01	-0.01	0.94	0.38	<0.01	0.17	0.31	0.61	<0.001	0.23	0.12	0.51	<0.001
Winter	-0.04	0.80	0.32	0.02	0.18	0.21	0.14	0.345	0.38	0.02	0.54	<0.001	0.29	0.05	0.62	<0.001

2.4.3 Changes of snowmelt runoff timing

Long-term changes in WSCT showed no significant trend based on the Mann–Kendall tests, except for the Kaidu basin (-3.4 days/decade, $p < 0.01$), whose significant negative trend may have been enhanced by the short data period. From west to east, WSCT shifts towards earlier dates. Average WSCT during the study period for the Toxkon, Kunmalik, Kaidu and Huangshuigou basins are Julian day 111, 98, 94 and 87, respectively. A general nonlinear pattern was apparent according to which the WSCT dates rose first and then decreased after mid-1980s based on the loess smooth line (Figure 2.5). All the gauge stations show consistent fluctuations in WSCT, which indicates earlier snowmelt runoff timing and increased winter/spring runoff (Table 2.2). WSCT shifted toward earlier dates after the mid-1980s: 11 days (Julian day range: 103-114) in the Toxkon basin, 5 days (94-99) in the Kunmalik basin, 8 days (88-97) in the Kaidu basin, and 8 days (82-90) in the Huangshuigou basin, respectively.

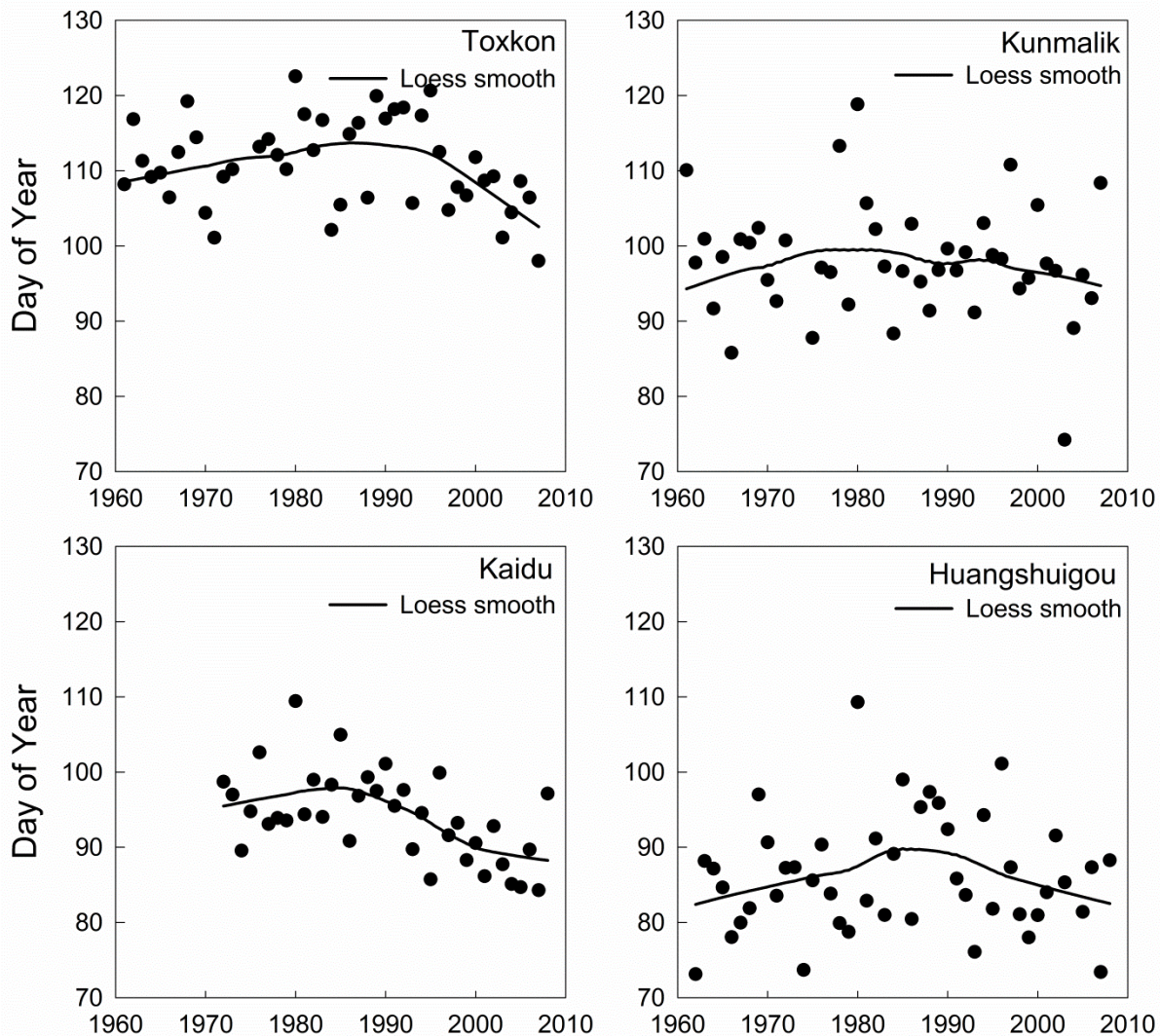


Figure 2.5. Time series of historical WSCT in the Toxkon (1961-2007), Kunmalik (1961-2007), Kaidu (1972-2008) and Huangshuigou (1962-2008) basins.

2.4.4 Relations of WSCT to temperature and precipitation

Changes in WSCT may be additional indicators of changing precipitation and temperature. Rivers that originate from the Tianshan Mountains are mainly supplied by precipitation and meltwater from snow and glaciers; correlations between monthly precipitation and temperature with WSCT dates were therefore explored (Table 2.5). There was no significant relationship between WSCT dates and precipitation in the Toxkon basin. However, average precipitation was found to have weak but significant positive correlation with WSCT dates in May ($r = 0.39$, $p=0.02$) in the Kaidu basin and in March ($r = 0.37$, $p=0.01$) in the Huangshuigou basin. Nevertheless, the strongest

correlation between WSCT dates and temperature in the Toxkon basin was found in the period of February to April ($r = -0.46$, $p < 0.01$). The strongest correlation between WSCT dates and temperature in the Kaidu basin was found in the period of March to April ($r = -0.66$, $p < 0.001$); while no significant relationships were found in the Huangshuigou basin. However, WSCT dates were found to have a negative relationship with precipitation in the period of January to April ($r = -0.34$, $p = 0.02$) and a positive relationship with temperature in May ($r = 0.59$, $p < 0.001$) in the Kunmalik basin.

Table 2.5. Correlation coefficients between WSCT dates and average precipitation/temperature in the Toxkon, Kunmalik, Kaidu and Huangshuigou basins.

Time period	Toxkon (1961-2007)				Kunmalik (1961-2007)				Kaidu (1972-2007)				Huangshuigou (1962-2007)			
	Precipitation		Temperature		Precipitation		Temperature		Precipitation		Temperature		Precipitation		Temperature	
	R	P-value	R	P-value	R	P-value	R	P-value	R	P-value	R	P-value	R	P-value	R	P-value
Jan	0.13	0.37	-0.21	0.16	-0.15	0.31	-0.05	0.73	-0.19	0.26	-0.23	0.18	0.07	0.62	-0.12	0.42
Feb	-0.03	0.82	-0.36	0.01	-0.40	0.01	-0.16	0.29	0.10	0.56	-0.27	0.11	-0.04	0.80	-0.13	0.38
Mar	0.04	0.80	-0.16	0.28	-0.15	0.31	0.03	0.83	0.27	0.11	-0.64	<0.001	0.37	0.01	-0.12	0.42
Apr	0.14	0.36	-0.42	<0.01	-0.20	0.19	0.31	0.03	0.11	0.51	-0.43	<0.01	0.03	0.86	0.06	0.70
May	0.08	0.59	0.01	0.96	0.07	0.63	0.59	<0.001	0.39	0.02	-0.23	0.19	0.09	0.54	0.19	0.20
Jan to Mar	0.05	0.72	-0.36	0.01	-0.30	0.04	-0.09	0.53	0.11	0.52	-0.45	<0.01	0.29	0.05	-0.16	0.30
Jan to Apr	0.14	0.36	-0.45	<0.01	-0.34	0.02	0.03	0.85	0.14	0.41	-0.52	<0.01	0.19	0.21	-0.11	0.45
Feb to Mar	0.02	0.91	-0.36	0.01	-0.29	0.05	-0.09	0.53	0.24	0.16	-0.49	<0.01	0.31	0.03	-0.15	0.31
Feb to Apr	0.12	0.44	-0.46	<0.01	-0.33	0.02	0.06	0.71	0.22	0.20	-0.58	<0.001	0.19	0.21	-0.10	0.53
Mar to Apr	0.14	0.37	-0.36	0.01	-0.25	0.09	0.21	0.16	0.22	0.20	-0.66	<0.001	0.20	0.18	-0.04	0.81
Mar to May	0.15	0.30	-0.27	0.07	-0.11	0.46	0.36	0.01	0.41	0.01	-0.64	<0.001	0.19	0.2	0.04	0.78

2.5 Discussion

The relationships between streamflow on the one side and temperature and precipitation on the other side vary among the basins at annual and seasonal scales, which may be due to different streamflow generation processes. Basins in mountain areas are mainly recharged by both precipitation and meltwater, as is the case in the Kaidu and Huangshuigou basins (Zhou et al., 2016). However, large amounts of precipitation are stored in the form of snow or glaciers. In the strongly glacierized Kunmalik basin, streamflow is therefore highly dependent on temperature controlled snow and glacier meltwater (Krysanova et al., 2015; Kundzewicz et al., 2015; Doris et al., 2016). The Toxkon basin has less glacier area and relatively lower elevation compare to the Kunmalik basin, which leads to a faster response of streamflow to precipitation (Krysanova et al.,

2015; Kundzewicz et al., 2015). Precipitation accumulated in winter as snow will be released as meltwater in the later warmer months. Thus, increased winter precipitation and temperature can possibly explain the positive trends in streamflow in winter and spring (Table 2.3 and 2.4). Nevertheless, owing to high glacier coverage in the Kunmalik basin, streamflow is generally more affected by temperature variability in any season.

Streamflow increased more obviously in these four basins after the 1990s, which further confirmed that streamflow is highly affected by the warmer temperature and higher precipitation in this period. This result is consistent with previous research (Chen et al., 2009; Xu et al., 2010; Tao et al., 2011; Wang et al., 2013c). The atmospheric water vapor content, which increased in the 1990s, together with the intensified water cycle caused by global warming could further have strengthened the streamflow variability (Shi et al., 2007; Chen et al., 2008). However, the mechanisms behind the abrupt changes need further research.

Changes in snowmelt runoff timing provide another indication that streamflow are susceptible to climate fluctuation in the Tianshan Mountains. Average snowmelt runoff timing in the western basins is later than in the eastern basins. This finding may demonstrate that the Toxkon and Kunmalik basins are more influenced by the westerlies (Chen, 2014), while the Kaidu and Huangshuifou basins are located in central Xinjiang where the climate is warmer and dryer (Figure 2). The changes of WSCT dates are coherent in all the basins; snowmelt runoff timing shifted towards earlier dates since the mid-1980s. Since these basins are not heavily influenced by human activities, the substantial changes of WSCT could be primarily driven by the changes of precipitation and temperature. A break point of temperature change was also identified in the mid-1980s (Chen et al., 2006, 2007; Xu et al., 2010).

The association of WSCT with temperature and precipitation in different periods in the Toxkon and Kaidu basins indicated that WSCT happens earlier when spring temperature is higher. Meanwhile, significant correlations of temperature are generally stronger than the precipitation correlations, which further confirms that WSCT is more sensitive to temperature variability. This finding is consistent with previous studies, according to which the changes of spring streamflow are related to the spring temperature change (Liu et al., 2011; Zhuang et al., 2015). However, precipitation is weakly but positively correlated with the WSCT. Precipitation accumulated in spring will lead to greater snow depth and longer snow cover duration, which will lead to a later

meltwater peak in the warm months; the snowmelt runoff center time therefore will be delayed. WSCT in the Huangshuigou basin did not have a significant relationship with temperature, which could be explained by its small area and relatively lower elevation reducing the importance of snowmelt. The Kunmalik basin has a highly snow cover and glaciers extent, which may be the reason for a stronger relationship between streamflow and temperature but poor relationship with precipitation. Previous study had already indicated that the spring streamflow is dominated by changes in temperature (Kundzewicz et al., 2015).

Streamflow runoff changes presumably reflect a complex response to climate change. However, uncertainties remain. The process of snow and glacier melt is a complex issue in terms of orographic effects and data availability in mountain regions. In addition, data length, quality and analysis methods are also contribute to uncertainties in the estimation. Furthermore, since discharge data for artificial reservoirs was not available; the investigation of snowmelt and hydrological changes may be biased in the Kaidu basin. Even though the two reservoirs (Dashankou and Chahanwusu) have small capacity (5.8% of the annual streamflow) since 1992, they can still influence streamflow during the dry season. However, the positive trend and presence of a break point are comparable to the adjacent Huangshuigou basin.

Mountain basins shoulder the task of suppling fresh water for downstream rivers. Since streamflow is substantially influenced by the variability of climate and climate change, the variability of streamflow and snowmelt runoff timing can be important indicators for climate change. Additionally, snowmelt runoff shifted earlier which may lead to less water released in summer when irrigation water demand is high; the changes of streamflow and snowmelt runoff timing could therefore threaten seasonal water availability (Shen et al., 2013b). Furthermore, streamflow in spring and summer is expected to increase in the near future in the Tianshan Mountains (Hagg et al., 2007); and fresh water supply is expected to be pushed towards its limits in the future in northwestern China (Guo & Shen, 2016). This study gives important insights into the spatial variability of streamflow and snowmelt runoff timing, which is of great significance for flood control, hydropower plants adaption and integrated water resources management under the changing climate. In the future, enhanced climate and streamflow observations are required and more comprehensive studies of the impacts of climate change on streamflow in the Tianshan regions based on hydrological modelling are an important next step.

2.6 Conclusions

Our study provides a comprehensive overview of streamflow variability and snowmelt runoff timing in four mountain basins in the southern Tianshan. Annual streamflow in this area exhibits a significant positive trend in all basins. Seasonally, streamflow mainly increased in winter and spring months. The relationships between streamflow and climate variables revealed that temperature plays a great role on streamflow in autumn and winter, while streamflow is dominated by precipitation in summer in the Toxkon, Kaidu and Huangshuigou basins. The glacierized Kunmalik basin shows a different behavior in which temperature plays a key role for streamflow variability at annual and seasonal scales. Streamflow had an abrupt change in the mid-1990s at annual and seasonal scales, a pattern that can also be identified in precipitation and temperature data from the southern Tianshan. The analysis of winter/spring snowmelt runoff center time has shown that average WSCT dates in the Kaidu and Huangshuigou basins are earlier than in the Toxkon and Kunmalik basins. A clear shift towards earlier WSCT was found since the mid-1980s, which reflects the combined influences of temperature and precipitation. It is particularly noteworthy that WSCT is negatively related to temperature but positively related to precipitation in spring. However, the opposite relationship between WSCT and temperature/precipitation was found in the glacierized Kunmalik basin. Although uncertainties remain, this study is essential to understanding the variability of streamflow and its relationship with climate variables. Besides, it is distinctly important for regional water resources management. Streamflow variability and snowmelt runoff change in semiarid mountain basins still require further attention.

Chapter 3 Spatial-temporal variation of near-surface temperature lapse rates over the Tianshan Mountains, Central Asia

Acknowledgments:

This study was supported by the Key Project of Chinese Academy of Sciences (KZZD-EW-12-1). Thanks to China Scholarship Council (CSC) for a PhD scholarship (201304910343). The data was provided by the China's meteorological administration (CMA) (<http://data.cma.cn/>). The fieldwork data in this study has been acquired in collaboration with Key Laboratory of Agricultural Water Resources, Center for Agricultural Resources Research, CAS. The authors express their sincere thanks to colleagues from Center for Agricultural Resources Research, CAS, for their kind support during field survey and data collection. Field data may be obtained from Yanjun Shen (email: yjshen@sjziam.ac.cn). We also wish to acknowledge Manfred Fink, Sven Kralisch and Miga Magrnika Julian for their valuable suggestions. We appreciate the Editor and three anonymous reviewers for their constructive and insightful comments.

Published as:

Shen, Y.-J., Y. Shen, J. Goetz, & A. Brenning. (2016), Spatial-temporal variation of near-surface temperature lapse rates over the Tianshan Mountains, central Asia, *J. Geophys. Res. Atmos.*, 121, 14,006–14,017, Doi: 10.1002/2016JD025711.

Key Points:

1. Magnitudes of near-surface temperature lapse rate are found higher on the Southern slopes than the Northern Slopes over Tianshan Mountains
2. Seasonal variations of near-surface temperature lapse rate are found higher in summer than in winter months
3. The constant environmental temperature lapse rate of 6.5 °C / km is not representative of near-surface conditions in the Tianshan Mountains

3.1 Abstract

Adequate estimates of near-surface temperature lapse rate (γ_{local}) are needed to represent air temperature in remote mountain regions with sparse instrumental records such as the mountains of Central Asia. To identify the spatial and temporal variation of γ_{local} in the Tianshan Mountains,

long term (1961-2011) daily maximum, mean and minimum temperature (T_{\max} , T_{mean} and T_{\min}) data from 17 weather stations and one year of temperature logger data were analyzed considering three subregions: Northern Slopes, Kaidu Basin and Southern Slopes. Simple linear regression was performed to identify relationships between elevation and temperature, revealing spatial and seasonal variation in γ_{local} . γ_{local} are higher on the Southern slopes than the Northern slopes due to topography and regional climate conditions. Seasonally, γ_{local} are more pronounced higher in the summer than in the winter months. γ_{local} are generally higher for T_{\max} than T_{mean} and T_{\min} . The Kaidu Basin shows similar seasonal variability, but with the highest γ_{local} for T_{mean} and T_{\min} occurring in the spring. Formation of γ_{local} patterns is associated with the interactions of climate factors in different subregions. Overall, annual mean γ_{local} for T_{\max} , T_{mean} and T_{\min} in the study's subregions are lower than the standard atmospheric lapse rates ($6.5 \text{ }^{\circ}\text{C km}^{-1}$), which would therefore be an inadequate choice for representing the near-surface temperature conditions in this area. Our findings highlight the importance of spatial and temporal variation of γ_{local} in hydro-meteorological research in the data-sparse Tianshan Mountains.

3.2 Introduction

Mountain regions, as an important supplier of snow or rain-fed freshwater to lowlands, are significant hydrological and climatological drivers (De Jong et al., 2005). Ecosystems and environmental processes in mountain regions are highly sensitive to climate change (Beniston, 2003; Barry, 2008). The Tianshan Mountains, known as the “water tower of Central Asia”, are a large system of mountain ranges located in Central Asia and are highly susceptible to climate variations (Sorg et al., 2012; Chen, 2014; Hu et al., 2014). Climate in this region has been changing from warm-dry to warm-wet based on historical recorded data (Shi et al., 2007), and water resources are expected to become more unstable in this semi-arid alpine region (Piao et al., 2010; Shen et al., 2010). Water resource assessments and the investigation of other climatically driven earth surface phenomena such as mountain permafrost require the accurate regional representation of near-surface air temperature, which is strongly dependent on elevation. However, insufficient measurements and the complex topography pose a challenge for temperature extrapolation and hydrological modelling over mountain regions (Minder et al., 2010; Ayala et al., 2015; Jobst et al., 2016). Spatial and temporal variability of climate drivers (i.e. temperature and precipitation) in Tianshan Mountains are poorly understood owing to the sparsity of recording data.

Constant or spatially uniform temperature lapse rate were typically adopted for extrapolating air temperature from meteorological stations to different elevations (Minder et al., 2010). Temperature lapse rate (γ) is the rate of temperature change with elevation, also known as the vertical temperature gradient (Whiteman, 2000). From atmospheric physics, unsaturated air parcel cools at the dry adiabatic lapse rate of $9.8\text{ }^{\circ}\text{C km}^{-1}$ when displaced upward, while the saturated adiabatic lapse rate varies with temperature and local conditions due to the condensation process (Whiteman, 2000; Barry, 2008; Barry & Chorley, 2009). The environmental temperature lapse rate (ELR) is the actual temperature decrease with height at a given place and time, which depends on the local vertical profile air temperature (Dodson & Marks, 1997; Barry & Chorley, 2009). In general, it is often replaced by the standard atmospheric lapse rate in the troposphere (6 or $6.5\text{ }^{\circ}\text{C km}^{-1}$) (Harlow et al., 2004; Barry, 2008; Minder et al., 2010). The standard atmosphere lapse rate is commonly used for temperature extrapolation due to lack of measurements (Wang et al., 2010; Luo et al., 2012). However, applying a standard lapse rate has its challenges since spatio-temporal patterns of temperature lapse rate can be influenced by diurnal cycles (Pepin et al., 1999; Pepin, 2001; Sheridan et al., 2010), direction of wind (i.e., windward or leeward side differences; Minder et al., 2010), and general contrasts between slope sites (Rolland, 2003; Tang & Fang, 2006; Kattel et al., 2015). Many studies suggest that γ_{local} values are typically higher for maximum temperatures than minimum, and generally lower in winter than in summer or spring (Rolland 2003; Tang & Fang, 2006; Blandford et al., 2008). It has been found that in air temperature extrapolation, regionally defined near-surface temperature lapse rates perform better than the constant lapse rate (Harlow et al., 2004; Lundquist et al., 2007; Blandford et al., 2008; Petersen et al., 2013). Near-surface temperature lapse rate is the rate of change in temperature with elevation observed typically at 2 m above the surface. It is typically decrease with increasing elevation, however, the opposite effect may occur under certain conditions (Blandford et al., 2008). It was therefore explored from observed temperature data (recorded at 2 m above the surface) using linear regression. From here forward, we use γ_{local} ($\gamma_{\text{local}} = -\partial T/\partial Z$) to refer to the locally computed near-surface temperature lapse rate. Throughout this paper, a positive temperature lapse rate refers to when temperature decreases with elevation and a higher/steeper γ_{local} refers to a rapid temperature decrease (lower/shallower γ_{local} refers slow decrease) with elevation as done in previous studies (Minder et al., 2010; Petersen & Pellicciotti, 2011).”

γ_{local} is a critical factor for mountain hydrology. Adequate estimate of γ_{local} is not only important for temperature downscaling (Gardner et al., 2009), it is also essential for distinguishing the precipitation form (rain or snow) (Minder et al., 2010). In addition, γ_{local} is of great significant for snowmelt runoff and glacier melt change (Chutko et al., 2009; Lundquist et al., 2007; Deng et al., 2015). Previous studies have emphasized the spatial and temporal pattern of γ_{local} in mainland China, whereas they subjectively divided the whole China into different climate zones or Southern and Northern parts (Li et al. 2013; Li et al., 2015), the patterns of γ_{local} may not reveal regional details in mountain areas due to irregular distribution and sparse weather stations at higher elevations. At a regional scale, Zhang et al. (2012) modified a monthly degree-day model for semi-arid Northwestern China by considering different monthly γ_{local} based on latitude zones; however, the range of latitude zones is too coarse to adequately capture γ_{local} variations which vary with time and topography in mountainous regions. Some researchers adopted $6\text{ }^{\circ}\text{C km}^{-1}$ as a regional temperature lapse rate (Luo et al., 2012) while others applied $5\text{ }^{\circ}\text{C km}^{-1}$ (Yang et al., 2014) in the Tianshan Mountains. Furthermore, climate differs substantially between the Northern/Southern slopes and Kaidu Basin in the Tianshan Mountains (Chen, 2014). As described previously, there is still a lack of knowledge on possible spatial and seasonal variations of γ_{local} in the Tianshan Mountains, and in particular possible surface based temperature inversions in winter are rarely discussed.

This study aims to evaluate the spatial and temporal variations of γ_{local} by separating the Tianshan Mountain into three subregions based on topography and different climate regimes: the North-facing slopes (Northern slopes), the inner mountain region (Kaidu Basin) and the South-facing slopes (Southern slopes). 51 years of climate records and a one-year record of temperature logger data were used to illustrate the spatial and temporal patterns of γ_{local} in this area. This Study is not only important for hydro-meteorological research in Tianshan region; it would also be most useful for water resource research in Central Asia.

3.3 Study area, data sets and methods

3.3.1 Study area

The Xinjiang Tianshan Mountains (located 41° - 45°N and 80° - 88.5°E) are surrounded by the Taklamakan Desert to the South and the Junggar Basin to the North (Figure 3.1). The study area is characterized by an arid continental climate and elevations ranging from -65 to 6804 m above

sea level (a.s.l). The Tianshan Mountains can be divided into three general subregions according to topography and climatic conditions: Northern Slopes, the Kaidu Basin and Southern slopes. Yining and Zhaosu stations are influenced by westerly winds and their climatic features are more similar to the Northern slopes; they will be used to characterize the climate of the Northern slopes. The distribution and summary of stations are shown in Figure 3.1 and Table 3.1. Annual mean temperature on the Southern slopes (9.7 °C) is higher than on the Northern slopes (6.7 °C).

The distribution of precipitation also shows important spatial variation (Figure S3.1 in the supporting information). Annual average precipitation is 90 mm on Southern slopes and 220 mm on the Northern slopes according to recorded data. The Kaidu basin drains approximately 18649 km² and has a mean elevation of 3100 m a.s.l. It is a typical snowmelt and precipitation fed basin that stretches over parts of central Tianshan Mountains and Mountainous valley, and it can be recognized as an independent mountain climate system. The Tianshan Mountains are the most important water source for downstream rivers, which lead to the Tarim Basin on the Southern slope, the Yili valley and Junggar Basin on the Northern slope.

Overall, temperature in the Tianshan Mountains is highly elevation dependent, and is characterized by warm summers (Southern slopes: 23.2 °C; Northern slopes: 21.8 °C) and cool winters (Southern slopes: -6.7 °C; Northern slopes: -11.3 °C) based on average temperature. Precipitation in mountain areas is more than the lower part depending on elevation (Chen, 2014). Snowfall can also occur in summer at higher elevations (i.e., the snowline at 4000-4100 m a.s.l. in Urumqi River Basin on the Northern slopes of Tianshan Mountains; Zhao et al., 2006); the precipitation and hydrothermal processes in this region are very complex due to the vertical differentiation of temperature.

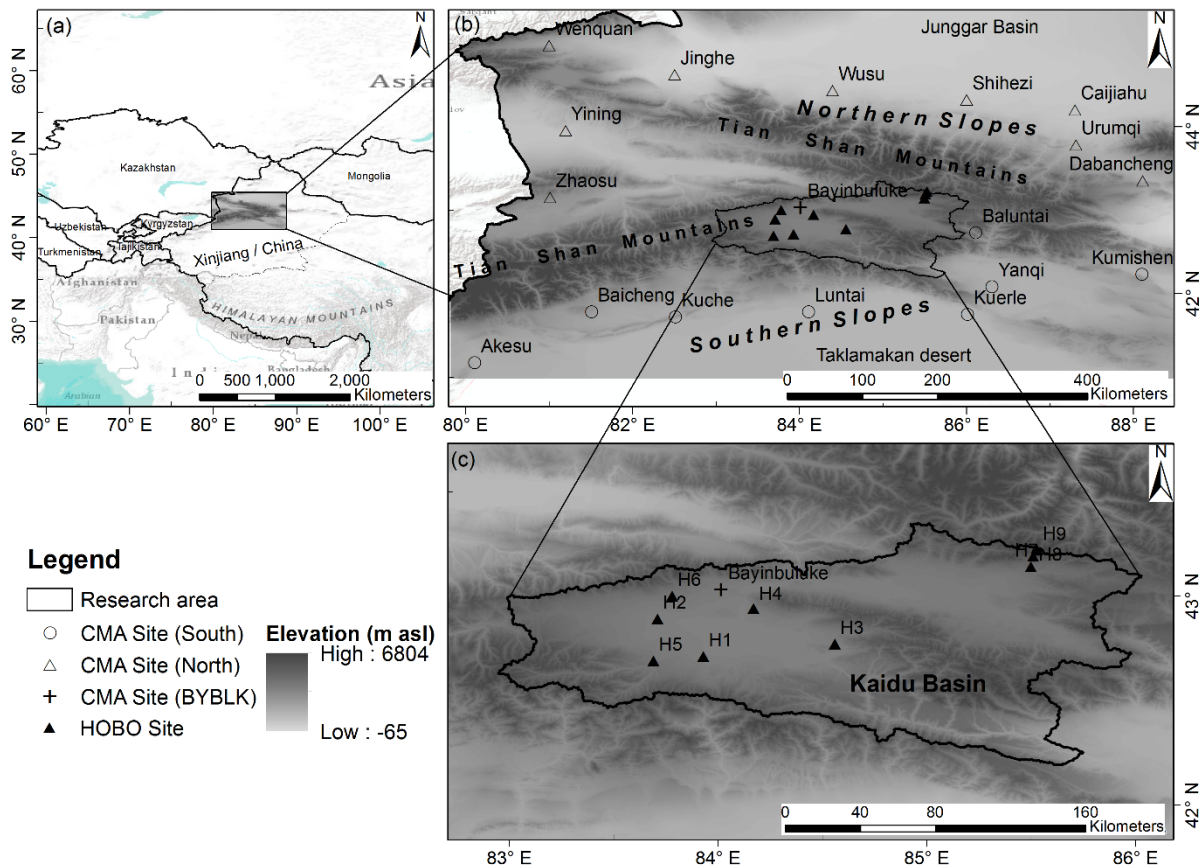


Figure 3.1. Study area and spatial distribution of weather stations: (a) location within central Asia, (b) overview of subregions and climate stations over the Tianshan Mountains, (c) location of HOBO logger stations in the Kaidu Basin.

3.3.2 Data sets

Long-term time series of daily maximum, mean and minimum temperature (T_{max} , T_{mean} and T_{min} , respectively), precipitation, relative humidity and wind speed data were obtained from China's Meteorological Administration (CMA). Stations record observation data four times a day (Beijing time 02, 08, 14, 20h). The T_{max} and T_{min} were determined from these four measurements, while T_{mean} is the average. This dataset is comprised of 18 climate stations covering the period of 1961–2011 in and around the mountain area (Figure 3.1b, Table 3.1). The homogeneity of the meteorological data was assessed by using penalized maximal t (PMT) tests to detect multiple change points in data series (Wang et al., 2007; Wang, 2008; Wang & Feng, 2013; RHtestsV4 package, available from the ETCCDI website:

<http://etccdi.pacificclimate.org/software.shtml>). A 1.5 °C temperature shift was detected from the Baluntai station in 1995, which could be explained by a change in the station's location. The closest station (Yanqi station) was chosen as a reference, which is assumed has the same climate signal (trend and periodic components). Data from Baluntai was adjusted by quantile matching (Wang et al., 2010; Vincent et al., 2012).

Table 3.1. Weather stations used in this study. H1-H9 indicates the HOBO logger data from field survey. S, N and Kaidu indicate Southern Slopes, Northern Slopes and Kaidu Basin, respectively. (Bayinbuluke station was excluded from the analysis in Kaidu Basin due to different data availability than logger data.)

ID	Name	Subregions	Lat (N)	Lon(E)	Elevation (m a.s.l.)	Tmean (°C)	Precipitation (mm)	Start year–end year
1	Yanqi	S	42.08	86.31	1055	8.58	76	1961-2011
2	Kuerle	S	41.75	86.01	932	11.78	55	1961-2011
3	Kuche	S	41.72	82.51	1082	11.30	70	1961-2011
4	Luntai	S	41.78	84.11	976	11.20	65	1961-2011
5	Baicheng	S	41.78	81.51	1229	7.94	119	1961-2011
6	Akesu	S	41.17	80.11	1104	10.45	74	1961-2011
7	Baluntai	S	42.73	86.11	1739	7.12	208	1961-2011
8	Kumishen	S	42.23	88.11	922	9.51	53	1961-2011
9	Urumqi	N	43.78	87.32	935	7.22	264	1961-2011
10	Shihezi	N	44.32	86.01	443	7.48	212	1961-2011
11	Wusu	N	44.43	84.4	479	8.14	170	1961-2011
12	Caijiahu	N	44.2	87.30	441	6.19	143	1961-2011
13	Dabancheng	N	43.35	88.12	1104	6.66	70	1961-2011
14	Yining	N	43.95	81.2	663	9.16	278	1961-2011
15	Jinghe	N	44.62	82.51	320	7.92	104	1961-2011
16	Wenquan	N	44.97	81.00	1358	3.98	232	1961-2011
17	Zhaosu	N	43.15	81.01	1851	3.40	509	1961-2011
18	Bayinbuluke	Kaidu	43.03	84.02	2458	-4.25	272	1961-2011
19	H1	Kaidu	42.71	83.93	2428	-2.37	--	09.2014-08.2015
20	H2	Kaidu	42.89	83.71	2470	-4.52	--	09.2014-08.2015
21	H3	Kaidu	42.77	84.56	2483	-2.06	--	09.2014-08.2015
22	H4	Kaidu	42.94	84.17	2525	0.36	--	09.2014-08.2015
23	H5	Kaidu	42.69	83.69	2663	-2.65	--	09.2014-08.2015
24	H6	Kaidu	42.92	83.33	2791	-0.90	--	09.2014-08.2015
25	H7	Kaidu	43.14	85.50	2986	-0.96	--	09.2014-08.2015
26	H8	Kaidu	43.19	85.51	3427	-2.67	--	09.2014-08.2015
27	H9	Kaidu	43.22	85.53	3771	-4.35	--	09.2014-08.2015

Since CMA climate stations have poor coverage of the inner-mountain Kaidu basin, field data collection was necessary to improve our estimation of γ_{local} . Thus, HOBO Pro V2 (U23-001) temperature/relative humidity data-loggers (HOBO) were set up in the Kaidu basin to monitor near-surface temperature (2 m above surface) and relative humidity between 2428 to 3771 m a.s.l (Figure 3.1c and Table 3.1) from September 2014 to August 2015. Monthly and annual data were computed based on daily data. The HOBO data-loggers can better represent the monthly temperature pattern in the Tianshan Mountains (Figure S3.2 in the supporting information). The HydroSHEDS void-filled Digital Elevation Model (DEM) at 3 arc-second resolution was furthermore used (approx. 90 m; Lehner et al., 2008; <http://www.worldwildlife.org/hydrosheds>).

3.3.3 Exploratory analysis

Annual temperatures were averaged for T_{max} , T_{mean} and T_{min} from 51 years of data records. The spatial and temporal variations in γ_{local} were explored using simple linear regressions of temperature and elevation for each of the three regions (Northern slopes, Kaidu Basin and Southern slopes; Figure 3.1 b and c). Loess models (Cleveland & Devlin, 1988) were furthermore used to examine nonlinear altitudinal temperature gradients. We analyzed these datasets separately due to different data availability: 51 years of climate records for the Northern slopes and Southern slopes and only one year of field survey data for the Kaidu Basin, respectively. Furthermore, we explored the relationship between γ_{local} for T_{mean} with climate factors. The Pearson's correlation coefficient (r) was used to measure the strength of linear associations between elevation and temperature.

3.4 Results

3.4.1 Annual variations: the southern slopes versus the northern slopes

The mean annual γ_{local} shows very strong variation and in particular substantial differences between different slopes (Figure 2 a-c). The γ_{local} for T_{max} , T_{mean} and T_{min} on the Southern slopes are 5.2, 4.8 and 3 °C km⁻¹ and on the Northern slopes are 3.1, 3 and 2.5 °C km⁻¹ respectively. The γ_{local} on the Southern slopes are substantially higher than the Northern slopes. Additionally, mean annual γ_{local} for T_{max} is the highest, followed by mean annual γ_{local} for T_{mean} and T_{min} . Comparatively, mean annual γ_{local} for T_{max} , T_{mean} and T_{min} on both sides of Tianshan Mountains are lower than the standard atmospheric lapse rate of 6.5 °C km⁻¹. Thus, an extrapolation of air temperature using this standard lapse rate would be expected to produce a substantial bias in regional scale estimates.

The correlation of mean annual Tmax with elevation on the Southern slopes is stronger than on the Northern slopes ($r = -0.91$ and $r = -0.81$ respectively). The reverse holds true for mean annual Tmean, whose correlation with elevation on the Southern slopes ($r = -0.74$) is weaker than on and the Northern slopes ($r = -0.82$). However, the relationship between mean annual Tmin and elevation is not robust (Southern slopes: -0.38 , Northern slopes: -0.66) (Figures S3-S4 in the supporting information).

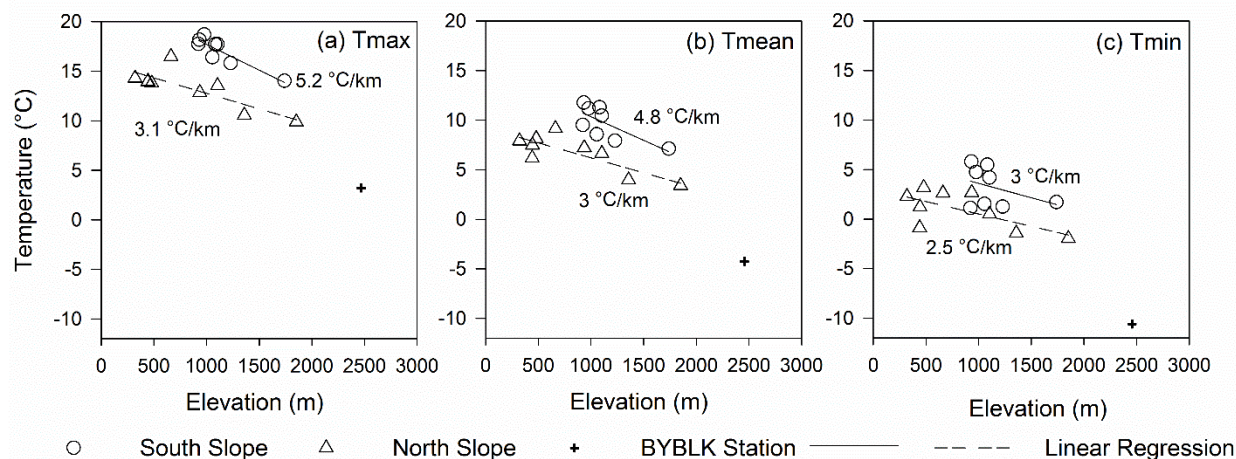


Figure 3.2. Altitudinal variation in mean annual temperature (Tmax, Tmean and Tmin, a-c) with their respective linear fit and γ_{local} for both the Southern slopes (circles) and Northern slopes (triangles) of the Tianshan Mountains. For comparison, the cross indicates the BYBLK station, located in the Kaidu Basin. Correlations in (a), Southern: $r = -0.91$, $p\text{-value} < 0.01$; Northern: $r = -0.81$, $p\text{-value} < 0.01$; in (b), Southern: $r = -0.74$, $p\text{-value} < 0.05$; Northern: $r = -0.82$, $p\text{-value} < 0.01$. in (c): Southern: $r = -0.38$, $p\text{-value} = 0.35$; Northern: $r = -0.66$, $p\text{-value} = 0.05$. P-values correspond to the null hypothesis of zero correlation.

3.4.2 Seasonal variations: the southern slopes versus the northern slopes

The seasonal γ_{local} over the Tianshan Mountains shows remarkable differences on the different slopes (Figure 3.3 a-c). Overall, the seasonal cycle of γ_{local} for Tmean is higher on Southern slopes than Northern slopes in all seasons. The γ_{local} for Tmax and Tmin follow the same distribution except for Tmin in autumn where the average γ_{local} for Tmin on the Northern slopes exceeded the value for the Southern slopes (2.6 and 2.4 $^{\circ}\text{C km}^{-1}$ respectively). However, γ_{local} for Tmax is higher in summer than γ_{local} for Tmean and Tmin on both sides of Tianshan Mountains. In addition, the lapse rates (γ_{local} for Tmax, Tmean and Tmin) in summer were 8.6 , 8.2 and 6.7 $^{\circ}\text{C km}^{-1}$ for the

Southern slopes and were 7, 6.7 and 5.7 °C km⁻¹ for the Northern slopes respectively (Figure 3.3). Notably, the lapse rates (γ_{local} for Tmax, Tmean and Tmin) in autumn were lower than in spring.

The winter season lapse rates on both sides of Tianshan Mountain are more variable than in other seasons (Figure 3.3). The average ranges of year-to-year variation in seasonal average γ_{local} were 1.8 (std.dev. = 0.44), 2.9 (0.66), 1.9 (0.46) and 4.6 (1.16) °C km⁻¹ for spring, summer, autumn and winter on the Southern slopes, and 3.1 (0.55), 2.5 (0.32), 2.3 (0.50) and 3.5 °C km⁻¹(0.86) on the Northern slopes. However, the lapse rates in winter were observed to have either lower or negative values, i.e. surface based temperature inversions on both sides of Tianshan Mountains.

3.4.3 Geographic variability: the Kaidu Basin

The Kaidu Basin differs in elevation, topography and local climate from the Northern and Southern slopes. Seasonal variation of γ_{local} shows slight differences compared to the other sites. Monthly γ_{local} for Tmax between April and October is higher than γ_{local} for Tmean and Tmin in the Kaidu Basin (Figure 3.4a). The highest γ_{local} for Tmax occurs in September (8.4 °C km⁻¹) while γ_{local} for Tmean and Tmin occur in April (6.9 and 5.8 °C km⁻¹, respectively). γ_{local} for Tmean and Tmin have a decreasing trend after April.

A non-linear trend for lapse rates in the Kaidu Basin was observed in the winter months related to surface based temperature inversion (Figure 3.4b, Figure S3.5 in the supporting information); the temperature (Tmax, Tmean and Tmin) generally increases in the valleys and lowlands with increasing elevation, and then tends to decrease at higher elevations. For Tmax and Tmean, the inflection elevation is around 3000 m a.s.l. However, Tmin becomes flat above 2800 m a.s.l. We cannot identify the top of the inversion layer inside Kaidu Basin due to the data sparsity and complexity of inversion process.

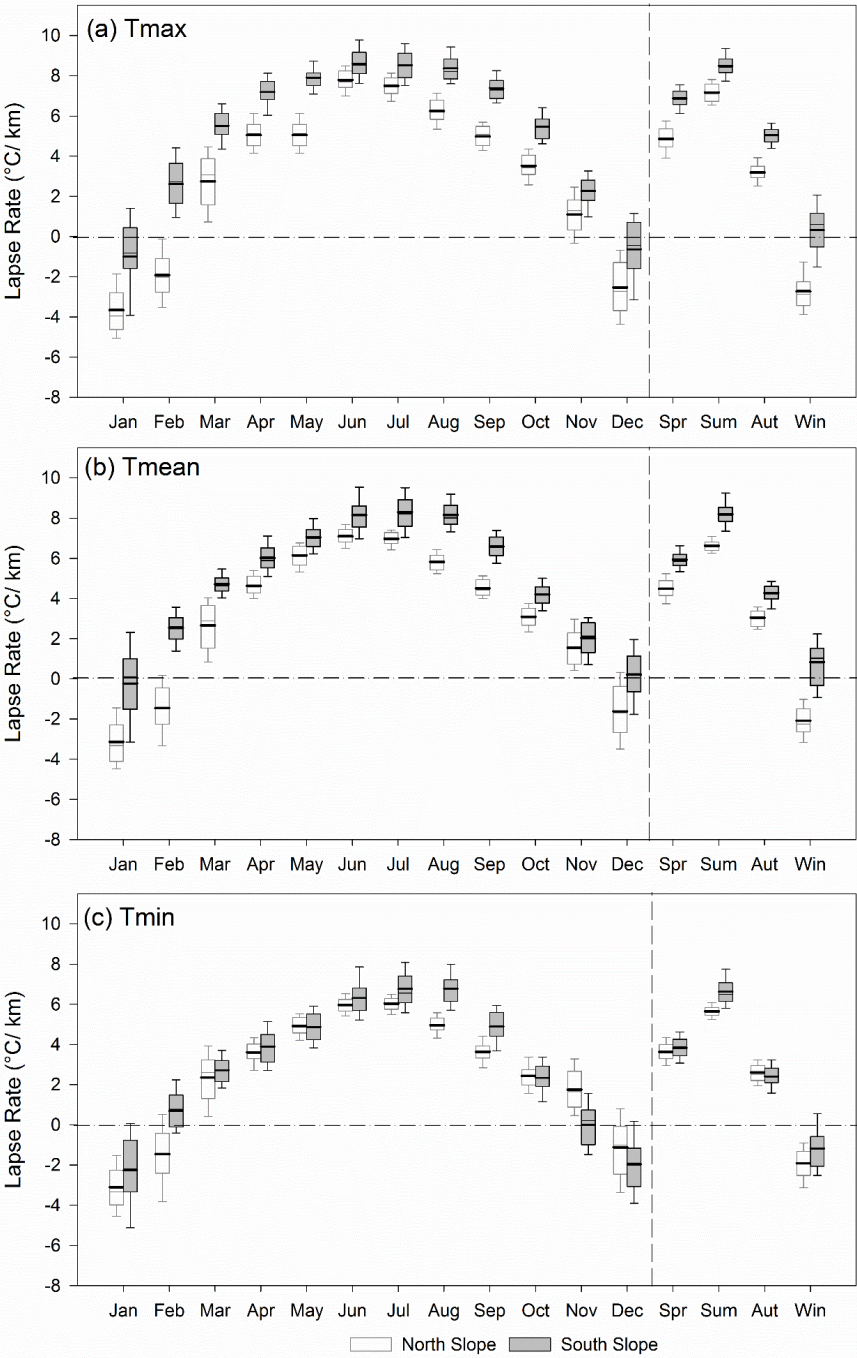


Figure 3.3. Seasonal variations of lapse rates [γ_{local} for Tmax (a), Tmean (b) and Tmin(c)] calculated by linear regression of temperature and elevation. Bold line indicates average value (averaged γ_{local} over the periods of 1961–2011). Seasonal conditions are divided into: Spr (spring: March, April and May), Sum (summer: June, July and August), Aut (autumn: September, October and November) and Win (winter: December, January and February).

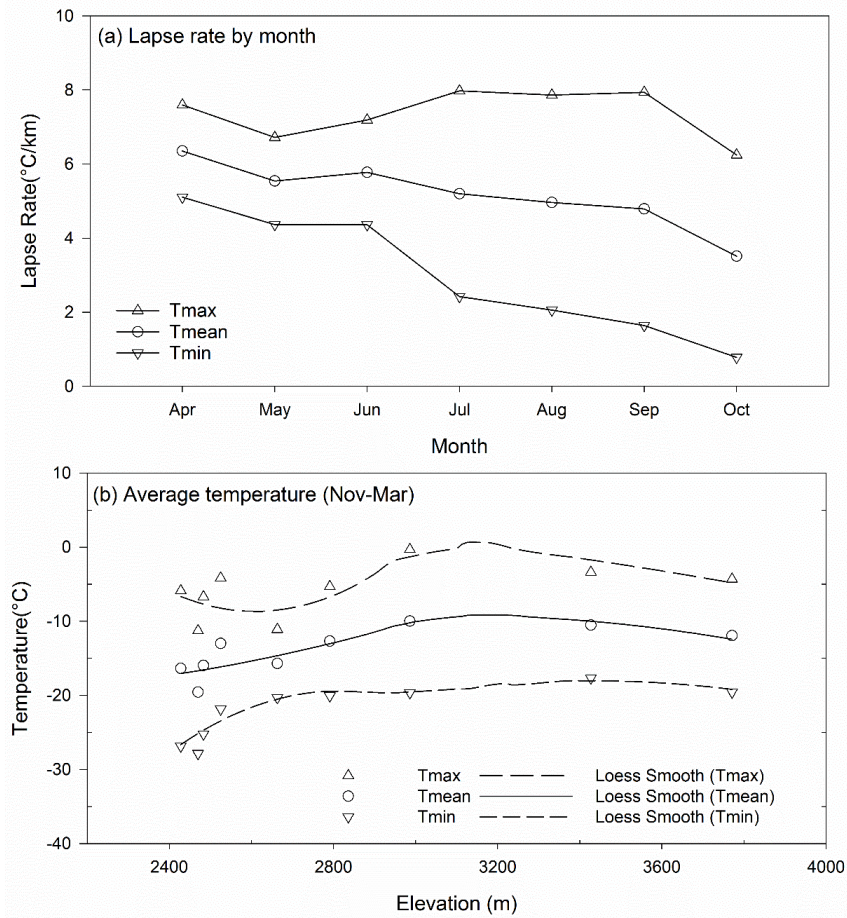


Figure 3.4. Variations of γ_{local} for Tmax, Tmean and Tmin in monthly scales (April to October) in the Kaidu Basin (a) (09.2014-08.2015; winter months not included due to nonlinearity). The correlation between elevation and temperature in winter months (average temperature from November to March) and Loess smoothers (b).

3.5 Discussion

3.5.1 Mechanisms of seasonal variation

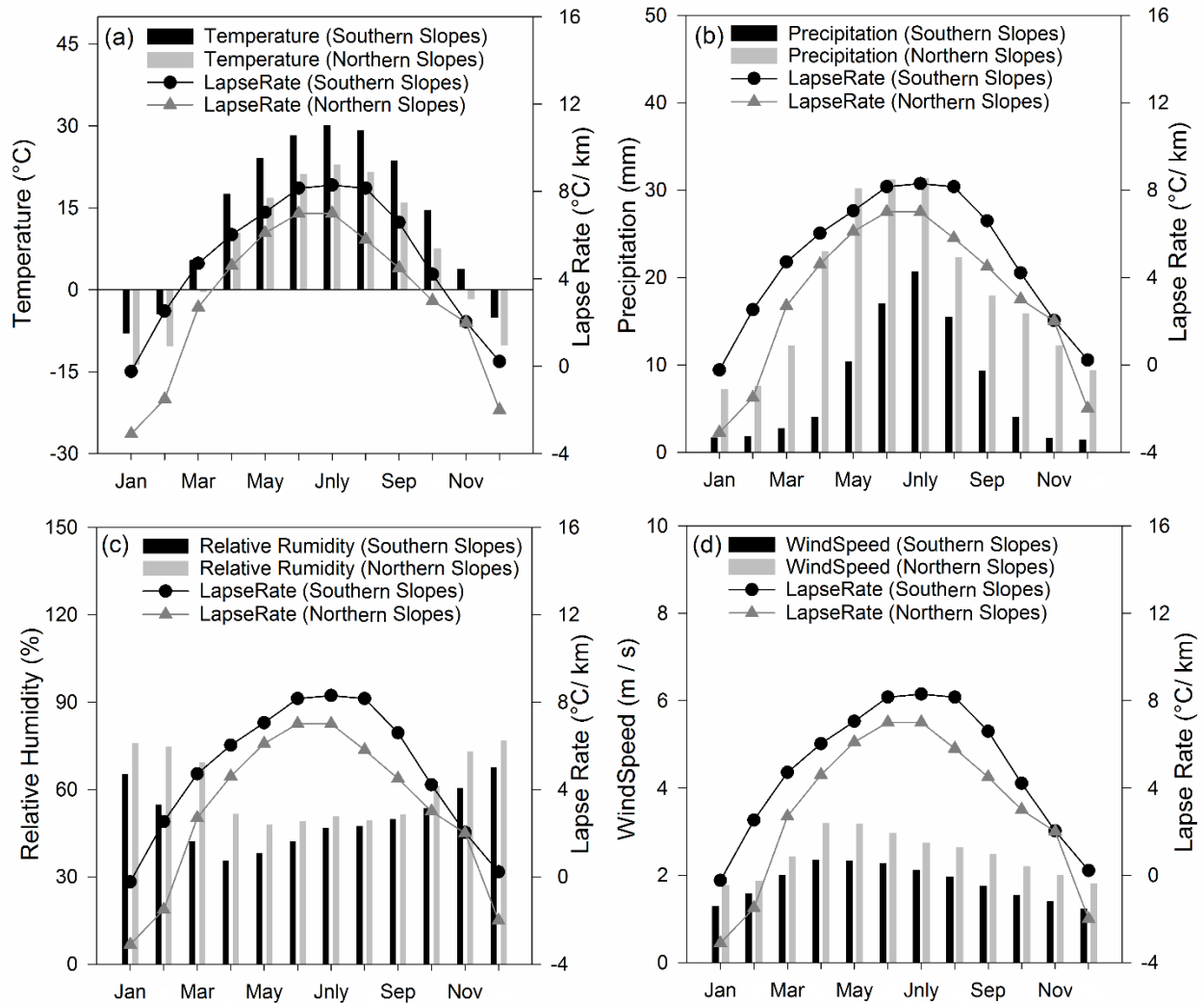


Figure 3.5. Seasonal cycle of the relation between lapse rate (γ_{local} for T_{mean}) and climate factors [temperature (a), precipitation (b), relative humidity (c) and wind speed (d)] on the Southern and Northern slopes of Tianshan Mountains (1961-2011).

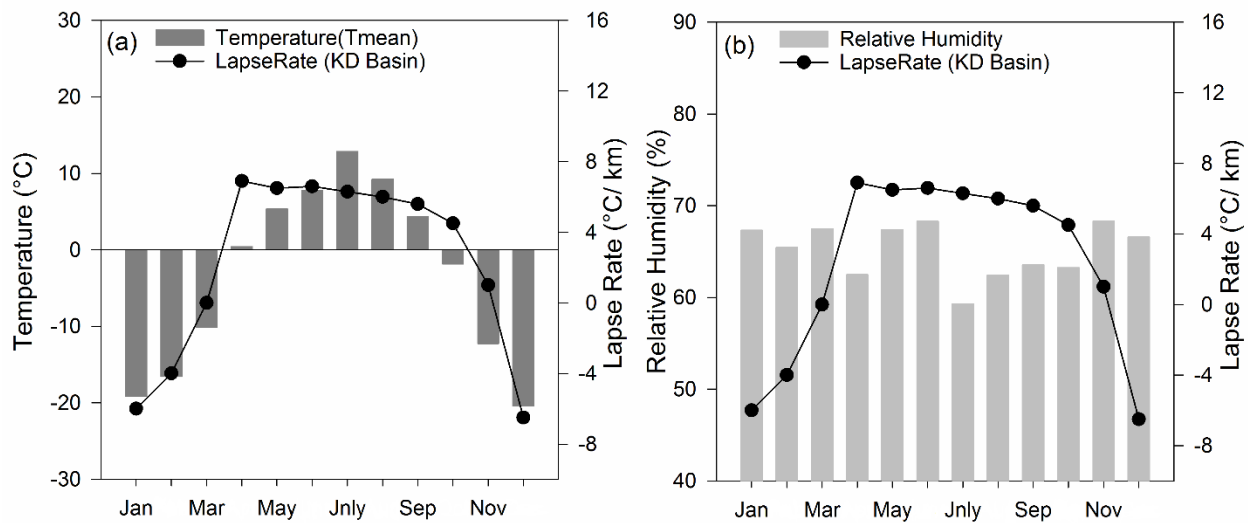


Figure 3.6. Annual cycle of the relationship between γ_{local} for Tmean with temperature (a) and relative humidity (b) in the Kaidu Basin (09.2014-08.2015).

The variations of γ_{local} (γ_{local} only refer to γ_{local} for Tmean here and after since γ_{local} for Tmax, Tmean and Tmin have very similar distribution patterns at the monthly scale) show seasonality throughout the year with higher γ_{local} in the summer months and shallower γ_{local} in the winter months in all subregions (Figure 3.3-3.4), which is consistent with previous research (Rolland, 2003; Blandford et al., 2008; Kirchner et al., 2013; Li et al., 2013). As seasonally modified radiative and turbulent heat exchanges can significantly affect the temperature structure and the adiabatic process (Barry & Chorley, 2009), we suggest that the seasonal variation of γ_{local} can be explained by the seasonal variation of solar radiation. Regions in the middle latitudes in the northern hemisphere receive more radiation in summer than in winter, which leads to a similar seasonal temperature variation (higher in summer and lower in winter) (Figure 3.5a, 3.6a). However, there is regional exception in the Kaidu Basin, where the maximum lapse rate occurs in April (Figure 3.6a). The instability of atmosphere between snow-free ground in lowland and snow-covered mountain slopes could modify lapse rates (Barry & Chorley, 2009). Melting snow is evident in Kaidu Basin in the spring, which is likely the cause for the higher lapse rates in April.

Surface based winter temperature inversions are another possible cause for the seasonal variation of γ_{local} . Surface based temperature inversion is known to weaken the relationship between air temperature and elevation (Marshall et al., 2007, 2011; Cullen et al., 2011; Kattel et al., 2013).

Winter temperature inversions are common phenomenon in Tianshan mountain area. The temperature lapse rates can be reversed from positive to negative due to winter temperature inversion, thus the γ_{local} in the winter months are lower than in the summer months.

3.5.2 Mechanisms of spatial variation

Near-surface temperature lapse rates for all months are higher on the Southern slopes than on the Northern slopes over Tianshan Mountains, which may result from the difference of slope sites and local climatic conditions. The role of water vapor in the air is essential for the spatial pattern of γ_{local} . Previous research indicated that shallower γ_{local} is typically associated with relatively warmer and moister atmospheric conditions (Pepin et al., 1999; Barry & Chorley, 2009; Li et al., 2013; Jobst et al., 2016). Air parcels cool more slowly in a humid environment than dry climates as it rises because of greater amounts of latent heat that can be released from vapor condensation (Whiteman, 2000; Barry & Chorley, 2009). Thus, the magnitude of temperature changes with elevation are reduced. This mechanism can be revealed by the spatial variability of precipitation and humidity which are higher on the Northern slopes than the Southern slopes (Figure 3.5 b-c). Although, an opposite sign was found in temperature that Southern slopes are warmer than the Northern slopes (Figure 3.5a), the Southern slopes are generally dryer and more limited by precipitation compare to the Northern slopes (annual precipitation are 90 and 220 mm for Southern and Northern slopes, respectively). Therefore, the modification of the lapse rate is still largely due to less latent heat that can be released by the condensation process. Furthermore, the spatial variability of γ_{local} is also consistent with the pattern of wind speed. Higher wind speed can enhance the air turbulences and the mixing of air masses, which will decrease the temperature gradient (Barry & Chorley, 2009). Wind speed on the Northern slopes is higher than Southern slopes (Figure 3.5d), this mechanism might be another explanation for the lower γ_{local} on the Northern slopes while higher γ_{local} on the Southern slopes.

Data source and length between Northern and Southern slopes with Kaidu Basin are different, thus, γ_{local} values from different subregions may not be spatially comparable. Specifically, it is unclear why higher relative humidity occurred in May and June in the Kaidu Basin (Figure 3.6b). Field measurement show that there is a vast wetland located in the central Kaidu Basin which may influence the surrounding climate and introduces additional uncertainty to the relative humidity

calculation. We acknowledge that some uncertainty remains. More measurement data are required for detailed analysis.

3.5.3 Mechanisms of surface based temperature inversion

Surface based temperature inversion during the winter was observed for all sites in Tianshan Mountains (Southern slopes, Kaidu Basin and Northern slopes; Figures 3-6). There are some possible reasons for this phenomenon in the Tianshan Mountains. Solar radiation will heat ground surface temperature during the day, in turn, the ground will release the sensible heat flux in the night, which will cool down surface temperature. Thus, nocturnal radiative cooling at the surface leads to diurnal change in surface temperature might be the reason for surface based temperature inversion (Whiteman et al., 1999, 2000; Barry & Chorley, 2009). Local topography (i.e. mountain valley) can also modify the atmospheric structure. Cold air drainage above the ground will limit temperature exchange between high elevation and low lands, which leads to atmosphere subsidence; furthermore, reduces cloud formation and enhances longwave cooling of the surface temperature, and further yields strong inversion (Vihma, 2011). Specifically, the relationship between temperature and elevation in winter is nonlinear in Kaidu Basin (Figure 3.4b). Cullen et al. (2011) recommended to use piecewise linear models for the regionalization of air temperature where inversion and non-inversion periods exist. However, challenges still remain in understanding the surface based temperature inversion since inversion depth and intensity always change with season and local climate.

3.5.4 Implication for modelling Earth surface processes

The findings in this study illustrate that γ_{local} has a spatio-temporal distribution pattern in Tianshan Mountains and the constant environmental temperature lapse rate ($6.5 \text{ }^{\circ}\text{C km}^{-1}$) throughout the year cannot represent the variability of the temperature-elevation relationship in complex terrain areas. The behaviors of γ_{local} can be quite important for ecosystems and mountain hydrological processes research. For instance, higher (lower) γ_{local} will result in lower (higher) temperature from lower to higher elevations in temperature interpolation, errors therefore not only increase in temperature extrapolation and downscaling (Komatsu et al., 2010; Sheridan et al., 2010), but also result in a reduction on modeled melt when higher lapse rate are used (Gardner et al., 2009; Petersen & Pellicciotti, 2011). In addition, locally computed temperature lapse rate plays a great role in identifying the form of rain or snow (Singh & Singh, 2001). Furthermore, the choice of

temperature lapse rate has a significant influence on the seasonal discharge variation (Minder et al., 2010; Deng et al., 2015). It has been observed that the timing of summer melt can shift a full month earlier when the lapse rate is changed from 6.5 to 4° C km⁻¹ (Minder et al., 2010). In particular, the application of reasonable lapse rate can effectively improve the accuracy of hydrological modeling in data-sparse alpine catchments (Immerzeel et al., 2014; Jobst et al., 2016). Additionally, spatial and seasonal changes of γ_{local} are vital for vegetation–climate relationships in mountainous areas (Tang & Fang, 2006; Bendix et al., 2010) and modelling the distribution of mountain permafrost based on the significant impact on ground temperatures (Lewkowicz & Bonnaventure, 2011; Gruber, 2012). Besides, the topography information (valley or slopes) appears influence the temperature interpolation reliability as well; the interpolation error may be reduced when taking the topographic differences into account in an Alpine region (Rolland, 2003). Spatial and seasonal γ_{local} are vital to applications such as temperature extrapolation and hydrological modelling in the Tianshan Mountains. Previous study indicated that the runoff change in spring and autumn is highly sensitive to the γ_{local} in the Kaidu River Basin (Deng et al., 2015). Since snow and glaciers are widespread in the Tianshan Mountains and temperature needs to be extrapolated from the lower elevation due to data sparsity and incomplete coverage, we have suggested to use the seasonal γ_{local} to reduce uncertainties in related climatic and hydrological research. The constant lapse rate should only be considered as a last resort. This knowledge is also transferable to research in mountainous areas in central Asia where with similar topographic complexity and climatic contrasts.

3.6 Conclusions

Spatial and temporal variations of γ_{local} in different slopes sites and Kaidu Basin were investigated in the Tianshan Mountains by simple linear regression base on the recorded and field survey data. Seasonally, lapse rates are higher in summer than in winter months in all subregions. Lapse rates for T_{max} are higher than that for T_{mean} and T_{min} . Spatially, lapse rates are higher on the Southern slopes than the Northern slopes, except for the Kaidu Basin which has the special mountain climate. The standard atmospheric lapse rate (6.5 °C km⁻¹) throughout the whole year would therefore mislead results in temperature extrapolation. The spatial and temporal variations of γ_{local} in Tianshan Mountain are linked to the geographic differences and climate factors and should be taken into account in meteorological and hydrological applications. In addition, it is reasonable to consider surface based winter temperature inversions (i.e., nonlinear relationship) in models

Chapter 3

Spatial-temporal variation of near-surface temperature lapse rates over the Tianshan Mountains, Central Asia

extrapolating temperature in winter time. The knowledge of this study is useful for hydrometeorology research in the Tianshan Mountain region and regions in central Asia.

Chapter 4 Unraveling the hydrology of the glacierized Kaidu Basin by integrating multi-source data in the Tianshan Mountains, northwestern China

Acknowledgements:

The research is supported by the Key Research Program of National Natural Science Foundation of China (D91425302) and the National Natural Science Foundation of China (41630859). Thanks to China Scholarship Council (CSC) for a PhD scholarship (201304910343). The meteorological datasets and field data can be obtained from the Kaidu River Basin Information System (KaiduRBIS): <http://leutra.geogr.uni-jena.de/kaiduRBIS/metadata/start.php>. Colleagues from the Key Laboratory of Agricultural Water Resources, Center for Agricultural Resources Research, CAS, are gratefully acknowledged for their support during field survey. We thank Jason Goetz and Miga Magenika Julian for their valuable suggestions

Published as:

Shen, Y.-J., Shen, Y., Fink, M., Kralisch, S., & Brenning, A. (2018). Unraveling the hydrology of the glacierized Kaidu Basin by integrating multisource data in the Tianshan Mountains, Northwestern China. *Water Resources Research*, 54, 557–580. Doi:10.1002/2017WR021806.

Key Points:

1. Gridded products have inconsistent biases and need to be evaluated before using them in modeling studies.
2. The water balance and the distribution of runoff components were estimated in the glacierized Kaidu Basin based on a hydrological model.
3. Meteorological data representation, parametric sensitivity and uncertainty need further research in data-scarce mountainous basins.

4.1 Abstract

Understanding the water balance, especially as it relates to the distribution of runoff components, is crucial for water resource management and coping with the impacts of climate change. However, hydrological processes are poorly known in mountainous regions due to data scarcity and the

complex dynamics of snow and glaciers. This study aims to provide a quantitative comparison of gridded precipitation products in the Tianshan Mountains, located in Central Asia and in order to further understand the mountain hydrology and distribution of runoff components in the glacierized Kaidu Basin. We found that gridded precipitation products are affected by inconsistent biases based on a spatio-temporal comparison with the nearest weather stations and should be evaluated with caution before using them as boundary conditions in hydrological modelling. Although uncertainties remain in this data-scarce basin, driven by field survey data and bias-corrected gridded datasets (ERA-Interim and APHRODITE), the water balance and distribution of runoff components can be plausibly quantified based on the distributed hydrological model (J2000). We further examined parameter sensitivity and uncertainty with respect to both simulated streamflow and different runoff components based on an ensemble of simulations. This study demonstrated the possibility of integrating gridded products in hydrological modelling. The methodology used can be important for model applications and design in other data-scarce mountainous regions. The model-based simulation quantified the water balance and how the water resources are partitioned throughout the year in Tianshan Mountain basins, although the uncertainties present in this study result in important limitations.

Key words

Hydrological modelling; Glacier melt; Runoff components; Tianshan Mountains; Central Asia.

4.2 Introduction

The assessment of hydrological response to climate change is a vital research field in the Tianshan Mountains and many other mountain regions (Viviroli et al., 2007; Doris et al., 2016; Biskop et al., 2016; Chen et al., 2016b; Ragettli et al., 2016). Water resources supplied from the Tianshan Mountains (known as the “Water Tower of Central Asia”) are of great importance for downstream rivers, residents, irrigation agriculture and ecosystems (Hagg et al., 2007; Shen & Chen, 2010; Sorg et al., 2012; Chen, 2014). Climate-driven changes have a significant influence on hydrological regimes in snow- and glacier-fed basins (Barnett et al., 2005); the Tianshan Mountains were found to be critical in forcing large-scale circulation changes (Baldwin & Vecchi, 2016). It is therefore an important research task to improve our understanding of mountain hydrological processes in high-elevation catchments in the Tianshan Mountains.

High-altitude basins are vulnerable to the combined impacts of warming temperature, precipitation variability and changes in snow and glacier dynamics in the Tianshan Mountains (Duethmann et al., 2015; Sun et al., 2015). Temperature shows a positive trend (Chen et al., 2006; Shi et al., 2007) and snow cover extent and glacier sizes have been decreasing (Yao et al., 2004; Ye et al., 2005; Yong et al., 2007). However, streamflow has been increasing (Tao et al., 2011; Chen et al., 2016b). The water cycle is likely to become more unstable (Shen & Chen, 2010). Additionally, rising temperatures have changed glacier mass balances and snowfall fraction, which leads to less snow accumulation and alters the role of meltwater in the regional water balance (Chen et al., 2016a). In the Kaidu Basin on the southern slope of the Tianshan Mountains, climate-driven changes not only increase the volume of streamflow (Chen et al., 2009; Tao et al., 2011; Wang et al., 2013; Deng et al., 2015; Chen et al., 2016b; Shen et al., 2018), but also the seasonal variability of streamflow (Liu et al., 2011) and glacier melt (Liu et al., 2006). Snowmelt runoff timing is expected to shift towards earlier dates due to spring temperature increases (Liu et al., 2011; Shen et al., 2018). Snow and glacier meltwater play an important role in seasonal patterns of streamflow in this glacierized catchment. Although statistical analyses of observational data have revealed changes of hydrological regimes due to climate change (Chen et al., 2013), it is still necessary to quantify the contributions of different runoff components to streamflow in glacierized basins in order to gain a better understanding of the ongoing changes.

Hydrological modelling is widely used to understand hydrological processes at the basin scale. However, the application of hydrological models in glacierized basins is complicated either by inadequate observational data (Zhang et al., 2007; Dou et al., 2011; Fang et al., 2015; Ragetti et al., 2013; Biskop et al., 2016) or the limited knowledge of snow and glacier melt dynamics (Sun et al., 2015; Chen et al., 2016b), which are the main obstacles for the application of hydrological models in the Tianshan Mountains and downstream basins. For instance, insufficient and coarse datasets posed a major challenge in the optimization of the grid-based Variable Infiltration Capacity (VIC) model in the Tarim Basin (Liu et al., 2010). In other earlier studies near our study region, glacier ablation was not fully represented by the Hydrologiska Byråns Vattenbalansavdelning (HBV) model in the glacierized Urumqi Basin (Sun et al., 2015), or neglected by the MIKE SHE model in the Tarim Basin (Liu et al., 2013). Furthermore, the SWAT model was enhanced to include glacier melt processes for simulating glacier retreat and its response to climate change in the Manas Basin in the Tianshan Mountains (Luo et al., 2013), yet

solar radiation and topographic factors were excluded in the degree-day factors. In the glacierized Kaidu Basin, the lack of observational data and the omission of glacier melt processes have been two major sources of uncertainty in earlier studies (Zhang et al., 2007; Dou et al., 2011; Liu et al., 2012; Xu et al., 2016a; Zhang et al., 2016; Chen et al., 2016b). Efforts have been made to correct model parameters and apply hybrid models (Fang et al., 2015; Xu et al., 2016b); in a comparative study, a physically-based model (MIKE SHE) performed better than a lumped conceptual model for spatially representing climate variability (Liu et al., 2011). In existing studies, glacier melt was excluded (Zhang et al., 2007; Dou et al., 2011; Xu et al., 2016a; Zhang et al., 2016; Chen et al., 2016b), and the distribution of runoff components was not addressed (Xu et al., 2016a; Liu et al., 2011; Sun et al., 2015). To our knowledge, high (spatial and temporal) resolution physically-based modelling has not been conducted in the glacierized Kaidu Basin, where it would be important to characterize the water balance and determine the relative contributions of different runoff components.

Gridded datasets offer the potential to fill data gaps, and have been widely used over the years for representing climatic patterns in mountainous regions (Immerzeel et al., 2015; Shea et al., 2015; Biskop et al., 2016). Remote sensing data can partly overcome data scarcity in hydrological modelling, yet their limitations in accuracy and temporal resolution need to be addressed in detail (Liu et al., 2012). Besides, gridded data quality is affected by complex topography and elevation effects in the semiarid Tianshan Mountains (Wang et al., 2015). The Global Precipitation Climatology Centre (GPCC V7) was previously utilized to investigate variations of annual precipitation in Central Asia (Hu et al., 2017), yet different precipitation products show large discrepancies in mountainous areas. The gridded datasets show different uncertainties and biases and therefore cannot be used directly without quality assessment and comparison, especially in mountainous regions (Gao et al., 2012; Wang et al., 2015). Taken together, the reliability of gridded datasets has not sufficiently been addressed and compared in the Tianshan Mountains, and their suitability for driving hydrological models remains unexplored.

Field data have the potential to further improve bias corrections and hydrological model performance (Immerzeel et al., 2014; Ragetti et al., 2015). Nevertheless, field data in the Tianshan Mountains are very limited due to inaccessible terrain. For instance, the temperature lapse rate is crucial for representing mountain temperature and simulating snowmelt runoff in high-elevation

basins (Lundquist & Cayan, 2007; Li & Williams, 2008; Deng et al., 2015; Immerzeel et al., 2014). According to our field research, temperature lapse rates vary spatially and seasonally in the Tianshan Mountains (Shen et al., 2016), which has not been addressed in previous hydrological modelling studies (Zhang et al., 2007; Dou et al., 2011; Xu et al., 2016a; Zhang et al., 2016). Moreover, vegetation structure, soil type, geology and morphological features were not considered in sufficient detail in previous studies (Liu et al., 2011; Sun et al., 2015; Xu et al., 2016b).

In the light of the mentioned limitations, the main objectives of this study are to unravel the glacierized mountain hydrology and characterize the distribution of runoff components in order to better cope with the variability of water resources. To achieve these goals, the applicability of gridded climate datasets was evaluated, and suitable datasets were subsequently corrected based on field data. Driven by multiple input datasets, a fully distributed hydrological model was applied. Moreover, uncertainty and sensitivity related to model parameters and equifinality were assessed. This study sheds light on hydrological processes in a data-scarce glacierized basin. The results – although somewhat preliminary due to data scarcity– are of great importance for better understanding of the vulnerability of water resources in Central Asia and other mountainous regions with limited data availability.

4.3 Study area and datasets

4.3.1 Study area

This study focuses on the Kaidu Basin, which is located on the central southern slopes of the Tianshan Mountains ($42^{\circ} 14' N - 43^{\circ} 21' N$, $82^{\circ} 58' E - 86^{\circ} 05' E$) in northwestern China (Figure 4.1). The basin drains an area of 18,649 km² with a mean elevation of 3100 m above sea level (a.s.l.) above the Dashankou gauge station (Figure 4.1 a, Table 4.1). The Kaidu river originates from the Tianshan Mountains, flows through the Bayinbuluk grassland and finally arrives at Lake Bosten (Figure 4.1a), for which it is the largest tributary, accounting for about 87% of its mean annual inflow (Chen, 2014). Water released from Lake Bosten is used for irrigation and is of critical importance for ecosystems located further downstream.

Situated in northwestern China, the Kaidu Basin has a continental semiarid climate. Mean annual precipitation and temperature at the Bayinbuluke weather station are 272 mm and $-4.25^{\circ}C$ respectively (1961-2011) (Table 4.1). Precipitation generally increases with altitude in the

mountainous regions, and temperature experiences distinct spatial-temporal variation (Chen, 2014; Shen et al., 2016). Precipitation and temperature are highly variable. More than 60% of the average annual precipitation at the Bayinbuluke occurs in the summer months. Year-to-year precipitation variation is highest in summer and lowest in winter; the opposite holds true for temperature. Seasonal mean temperatures at the Bayinbuluke are -1.5, 10.1, 2.1 and -20.3°C in spring, summer, autumn and winter, respectively.

The Kaidu Basin is a rainfall- and snow/glacier meltwater-fed basin with very little human land use. The main land cover types are grassland and barren land (62% and 30%, respectively) (Figure 4.1b). Annual streamflow at the Dashankou gauging station is approximately 189 mm/year (1972-2008). The observed increase of streamflow in the Kaidu Basin could be either due to the uptrend of precipitation or an increase of snow and glacier meltwater (Shi et al., 2007). Snow accumulates from November to March and is released in the spring and summer. Thus, spring streamflow is dominated by snowmelt, and glacier meltwater contributes to summer streamflow, yet precipitation is the main source of discharge in summer (Deng et al., 2015; Fu et al., 2013). Base flow also contributes a vast proportion (41%) of water throughout the year (Chen et al., 2009). However, the distribution of runoff components is insufficiently studied..

4.3.2 Datasets

Daily stream discharge data from the Dashankou gauging station were collected from the Hydrology and Water Resources Bureau of Xinjiang. Daily precipitation and temperature data were obtained from the China Meteorological Data Service Center (CMDC) (<https://data.cma.cn/en>). HOBO Pro V2 (U23-001) temperature loggers (HOBO) were furthermore installed in the field about 2 m above the ground surface between 2428 to 3771 m a.s.l. in the Kaidu Basin. Location and summary information of hydro-meteorological stations are provided in Figure 4.1 and Table 4.1.

Several global and regional gridded precipitation products were evaluated in this study (Table 4.2). They include interpolated data: Asian Precipitation-Highly-Resolved Observational Data Integration Towards Evaluation (APHRODITE) (Yatagai et al., 2012) and Climatic Research Unit (CRU) (Harris et al., 2014); reanalysis data: ERA-Interim (conducted by European Centre for Medium-Range Weather Forecasts, ECMWF) (Dee et al., 2011), Modern-Era Retrospective Analysis for Research and Applications, version 2 (MERRA-2) (Reichle et al., 2017) and Climate

Forecast System Reanalysis (CFSR) (Dile & Srinivasan, 2014); and satellite data (Tropical Rainfall Measuring Mission, TRMM) (Huffman et al., 2007). These datasets have relatively good spatial (Figure S4.1 in the supplementary information) and temporal coverage (Table 4.2). The original spatial resolution of ERA-Interim is $0.75^{\circ} \times 0.75^{\circ}$; we use the resampled data with a $0.125^{\circ} \times 0.125^{\circ}$ resolution.

The HydroSHEDS void-filled digital elevation model (approx. $90 \text{ m} \times 90 \text{ m}$ resolution) was used in this study (Lehner et al., 2008) (Figure 4.1a). A land use/land cover (LULC) dataset was created using Landsat TM/ETM+ satellite imagery by unsupervised classification followed by classification based on the interpretation of Google Earth imagery (Figure 4.1b; overall accuracy 89%). A soil map (1:1,000,000) was obtained from the Institute of Soil Science, Chinese Academy of Science (CAS) (Shi et al., 2004) (Figure 4.1c). Soil texture parameters were derived from the Soil Map of China (National Soil Survey Office, 1995) and field sampling in September 2014 (Figure 4.1a). Laboratory analysis was carried out by employing a Laser Particle Size Analyzer (Malvern Mastersizer 3000). A lithology dataset was derived from the 1:2,500,000 scale geological map of China (Figure 4.1d).

Table 4.1. Information on long-term weather stations, gauging stations and HOBO logger temperature stations.

Category	Name	Lon ($^{\circ}$ E)	Lat ($^{\circ}$ N)	Elevation (m a.s.l.)	Tmean ($^{\circ}$ C)	Precipitation (mm)	Time period
Long-term weather stations	Bayinbuluke	84.02	43.03	2458	-4.25	272	1961-2011
	Baluntai	86.11	42.73	1739	7.12	208	1961-2011
	Kuche	82.51	41.72	1082	11.30	70	1961-2011
	Yanqi	86.31	42.08	1055	8.58	76	1961-2011
	Luntai	84.11	41.78	976	11.20	65	1961-2011
	Kuerle	86.01	41.75	932	11.78	55	1961-2011
Gauging stations	Dashankou	85.74	42.25	1340	--	--	1972-2008
	H1	83.93	42.71	2428	-2.37	--	09.2014-08.2015
	H2	83.71	42.89	2470	-4.52	--	09.2014-08.2015
	H3	84.56	42.77	2483	-2.06	--	09.2014-08.2015
HOBO temperature stations	H4	84.17	42.94	2525	0.36	--	09.2014-08.2015
	H5	83.69	42.69	2663	-2.65	--	09.2014-08.2015
	H6	83.33	42.92	2791	-0.90	--	09.2014-08.2015
	H7	85.50	43.14	2986	-0.96	--	09.2014-08.2015
	H8	85.51	43.19	3427	-2.67	--	09.2014-08.2015
	H9	85.53	43.22	3771	-4.35	--	09.2014-08.2015

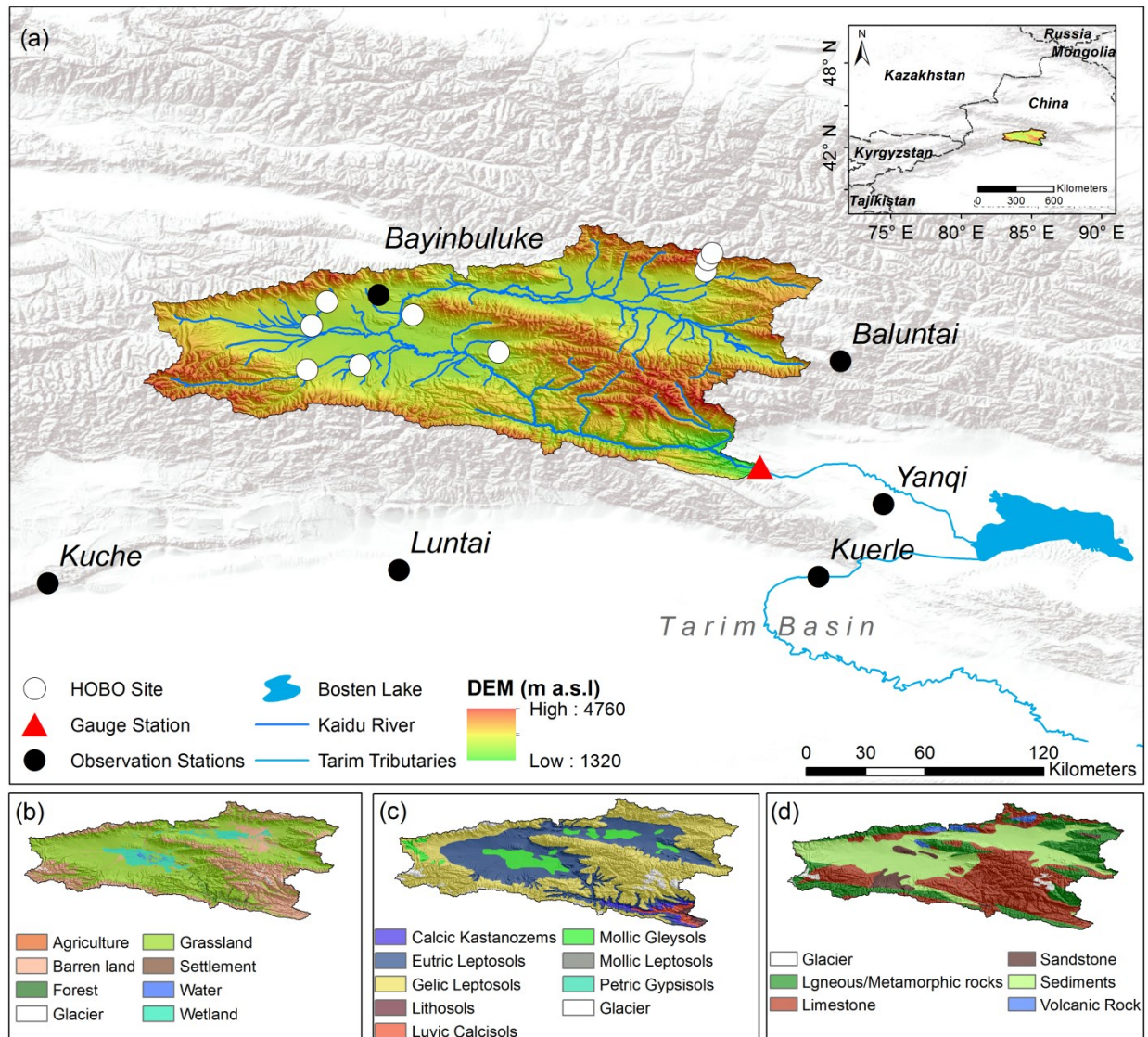


Figure 4.1. (a) Location of the Kaidu Basin in Central Asia, elevation and location of observed and HOBO logger stations. Overview of the available geospatial data: (b) land cover classification, (c) soil types and (d) lithology.

4.4 Methods

4.4.1 Gridded datasets comparison and correction

Gridded products need to be evaluated before modelling. As precipitation is the most important uncertainty source in mountainous regions (Hu et al., 2017), here, we evaluate the accuracy of six kinds of gridded precipitation products in and around the southern Tianshan where the Kaidu Basin

is located. Precipitation extracted from gridded precipitation products were compiled at annual and monthly scales and compared directly with the nearest neighbor weather stations (Table 4.1). Correlation coefficient (R), standard deviation (SD) and root-mean-square (RMS) difference were presented in the Taylor diagrams (Taylor, 2001) in order to assess the feasibility of multiple gridded precipitation data in the Tianshan Mountains.

APHRODITE precipitation data were chosen eventually in terms of the best performance of seasonal distributions and time series dynamics at annual and seasonal scales (see section 4.5.1). However, APHRODITE has been reported to underestimate precipitation in mountain regions (Shea et al., 2015; Krysanova et al., 2015). In the Kaidu Basin, the mean annual precipitation from APHRODITE is 277 mm (1972-2007) while the recorded annual discharge at the Dashankou gauging station is 188 mm (1972-2007) and the ActET is approximately 198 mm/year (2001-2013) based on remote sensing estimation (Liu et al., 2017), which implies that APHRODITE underestimates precipitation in the Kaidu Basin based on the water balance. Precipitation shows spatial variation and a substantial altitudinal gradient caused by orographic effects (Chen, 2014). As the elevation of gridded APHRODITE differs from the measurement stations, we took the altitudinal gradient into account and statistically adjusted the precipitation in the Kaidu Basin.

$$P_{adjusted} = P_{APHRODITE} + (H_{APHRODITE} - H_{Obs}) \times PG$$

$H_{APHRODITE}$ is the elevation of gridded APHRODITE data; H_{Obs} is the elevation of observation data (here it refers to the Bayinbuluke station). PG is the precipitation gradient (0.15 mm/m/year, Figure S4.2 in the supporting information) which was calculated by relating annual precipitation amounts to elevation at the southern slope stations (Figure 4.1a and Table 4.1); $P_{APHRODITE}$ is the annual precipitation of gridded APHRODITE. This simple adjustment based on a correction factor was used due to limited data availability, yet precipitation gradient was wide adoption in mountain hydrological studies (Liu et al., 2011; Immerzeel et al., 2015; Ragettli et al., 2015).

ERA-Interim temperature data offer the potential to fill data gaps in the mountain regions after elevation correction (Gao et al., 2012). Here, ERA-Interim temperature (maximum and minimum temperature) data were bias-corrected using one-year HOBO logger temperature dataset (September 2014 to August 2015) (Figure 4.1a, Table 4.1) as suggested in previous studies (Gao et al., 2012; Shea et al., 2015). Daily corrected gridded temperature data can be calculated as:

$$T = \gamma_{local}\Delta Z + T_{ERA} + Bias$$

where T is the corrected gridded temperature, γ_{local} is the monthly near surface temperature lapse rate which was calculated from HOBO temperature stations (Table 4.3); ΔZ is the elevation difference between ERA-Interim height and local elevation (in km, extracted from the HydroSHEDS elevation model). Biases are the monthly mean difference between the corrected ERA-Interim gridded data and nine independent HOBO temperature stations.

Relative humidity, solar radiation and wind speed datasets were furthermore extracted from ERA-Interim. They showed no strong relationship with station data, which can be attributed to the difference between grid box and point measurement. However, to share the same model physical mechanics with temperature, these datasets were kept unchanged.

Table 4.2. Summary of global and regional gridded precipitation products. Time span shows the evaluation period used in this study.

Data set	Coverage	Category	Spatial (temporal) resolution	Time Span	References
APHRODITE(V1101)	Asia	Interpolation	0.25°(daily)	1961-2007	Yatagai et al, 2012
CRU	Global	Interpolation	0.5° (monthly)	1961-2010	Harris et al, 2014
CFSR	Global	Reanalysis	0.3125° (daily)	1979-2011	Dile & Srinivasan, 2014
ERA-Interim	Global	Reanalysis	0.125° (daily)	1979-2011	Dee et al, 2011
MERRA-2	Global	Reanalysis	0.625° × 0.5° (hourly)	1980-2011	Reichle et al., 2017
TRMM(3B43)	Global	Satellite	0.25° (daily)	1998-2011	Huffman et al, 2007

Table 4.3. Monthly near surface temperature lapse rates in the Kaidu Basin. Temperature lapse rate from November to March were kept the same as October due to winter temperature inversion.

	Jan	Feb	Mar	Apr	May	June	July	Aug	Sep	Oct	Nov	Dec
Lapse rate (°C /km)	3.7	3.7	3.7	6.5	6.1	6.3	5.8	5.4	5.0	3.7	3.7	3.7

4.4.2 Hydrological model

The distributed and process-based J2000 model (Krause, 2002), which is built upon the Jena Adaptable Modeling System (JAMS) (Kralisch & Krause, 2006; Kralisch et al., 2007), includes flexible components and modules for representing hydrological processes at the basin scale. It was successfully applied to simulate hydrological processes in mountainous regions (Nepal et al., 2014;

Biskop et al., 2016), and therefore fits this study's purpose. The spatial heterogeneity of data and processes in the basin are represented by means of Hydrological Response Units (HRUs) (Flügel, 1995). HRUs were delineated by overlaying DEM derived information (elevation, slope angle and slope aspect), lithology, land cover information and soil datasets. All datasets were resampled to the spatial resolution of the DEM (90 m × 90 m), resulting in a total of 19,206 HRUs (Figure S4.3 in the supplementary information). A short description of different modules is given below. Detailed information about J2000 can be found in references on model design (Krause, 2002; Nepal, 2012).

Climate inputs are mapped to HRUs by means of a spatial regionalization approach based on inverse distance weighting and elevation regression. Precipitation is distributed into rain, snow and rain-snow mixtures by means of daily mean temperature and calibration parameters (*Trs* and *Trans*; Table 4.4). Maximum interception storage by vegetation coverage is modeled based on the Leaf Area Index (LAI) and its seasonal variability (Dickinson, 1984). From climate inputs, potential evapotranspiration is calculated according to the Penman–Monteith method (Allen et al., 1998).

Snowmelt is simulated based on the approach suggested by Knauf (1980). As water from rain or snow can be stored in the snowpack, runoff from snowmelt occurs only when the storage capacity of the snowpack is exceeded. Thus, snow accumulation, compaction and melt phases are included in the J2000 model. Snowmelt calculation considers two water fractions and snow densities: dry snow with an initial snow density and dry snow plus the stored liquid water with a modified snow density. This represents the ability of the snowpack to store liquid water without producing snowmelt runoff (Bertle, 1966; Krause, 2002). Even though snow sublimation affects evapotranspiration (Li et al., 2017), it was neglected in the model due to limited input data and should be regarded as a limitation.

A glacier simulation component was integrated into the model by using a degree-day-factor method (Hock, 1999), yet including more state variables (slope aspect, slope angle and debris cover; Nepal, 2012). Snow processes on glaciers were modelled by the snowmelt model described above, while glacier melt only occurs once the surface snow has disappeared and the air temperature is higher than the glacier melt threshold. The glacierized HRUs are treated separately in the model, allowing glacier meltwater to create surface runoff directly. Glacierized HRUs with

a slope angle below 30° are regarded as debris-covered glaciers, allowing to account for their modified energy balance in the model. The glacier extent is represented as being constant over time in the J2000 model (Nepal, 2012; Nepal et al., 2014).

Streamflow is calculated from four different runoff components which are simulated in the J2000, i.e. surface runoff (RD1), interflow from soil zone (RD2), interflow from the upper part of the aquifer (RG1), and base flow (RG2; Figure 4.2; Krause, 2002). Using this approach, both lateral and vertical fluxes are represented in the model. RD1 represents runoff from depression storage (DPS) which in turn is filled by infiltration and saturation excess water. Additionally, RD1 is fed by glacier runoff. Infiltrated water is distributed into two soil storages: the middle pore storage (MPS; pore diameter of 0.2–50 μm) and large pore storage (LPS; pore diameter $>50 \mu\text{m}$). Water stored in MPS is depleted by evapotranspiration while LPS is emptied by gravity. RD2 represents lateral flow from LPS in the soil layer, which reacts slower than RD1. Water from LPS can further percolate into the groundwater zone, representing the vertical water flux from the soil. The groundwater zone feeds two additional runoff components, namely the faster (RG1) and the slower (RG2) groundwater fluxes. Processes related to permafrost are not explicitly represented in the model.

The J2000 model takes reach routing into account based on the kinematic wave approach (Miller, 1984). The rate and velocity of flow in each stream segment was estimated by the Manning-Strickler equation (Krause, 2001). A routing coefficient (TA) which is subject of model calibration influences the velocity of the runoff waves in the channel until it reaches the catchment outlet.

4.4.3 Model calibration, validation and uncertainty analysis

A multi-objective genetic algorithm (Non-dominated Sorting Genetic Algorithm-II, NSGA-II) was used to optimize model parameters (Deb et al., 2002). Three thousand simulations were performed with user-defined parameter ranges (Table 4.4). The considered performance criteria were the Nash–Sutcliffe efficiency (NSE; Nash & Sutcliffe, 1970), percent bias (PBIAS; Gupta et al., 1999), logarithmic Nash–Sutcliffe efficiency (LNS; Krause et al., 2005), and coefficient of determination (r^2). The time series of simulated and observed streamflow were split into subperiods based on reservoir operation: 1979-1981 for model initialization, 1982-1986 for calibration, and 1987-1991 (before reservoir construction) for validation. Considering the impacts of reservoirs since 1992 (Figure S4.4 in the supplementary information), we do not expect the simulation to capture the

hydrograph well after reservoir construction; simulation results for the 1992-2007 period are therefore shown only for information.

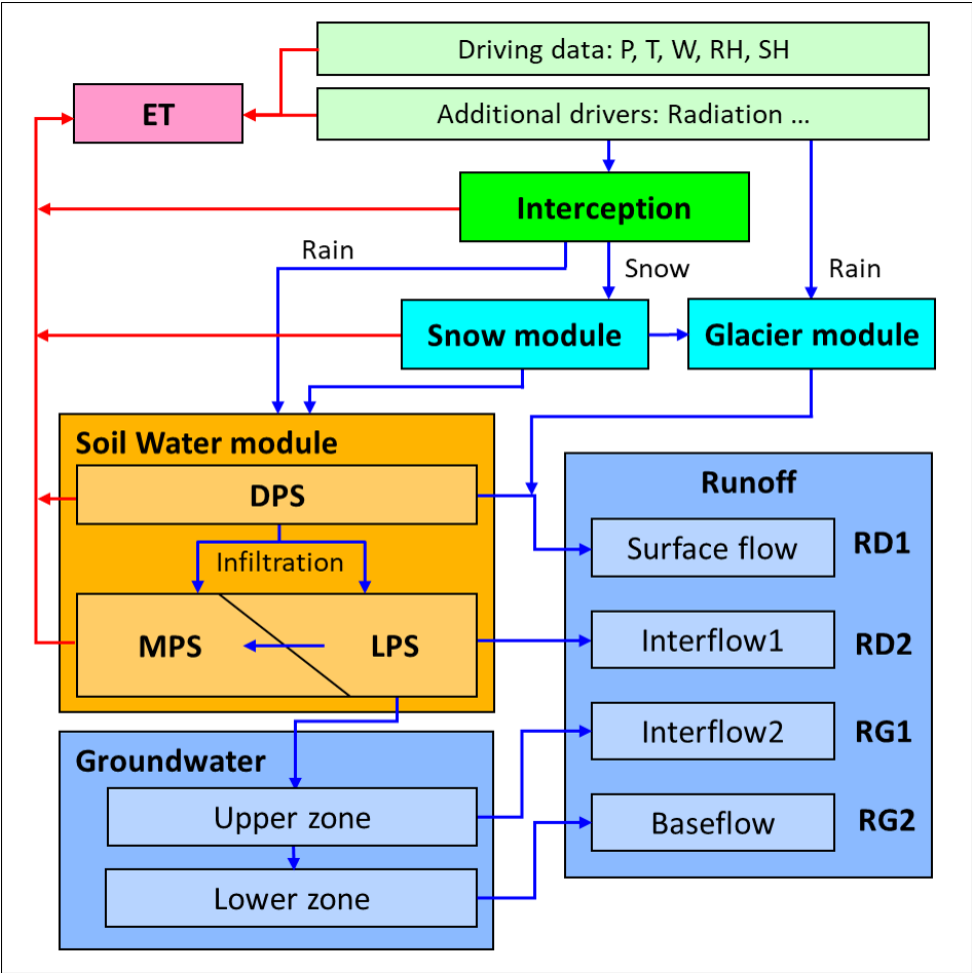


Figure 4.2. General schematic representation of the J2000 based on Krause (2001).

As different parameter sets may lead to equally accurate predictions, the prediction uncertainty was evaluated using the Generalized Likelihood Uncertainty Estimation (GLUE) procedure (Beven & Binley, 1992). The general idea behind GLUE is to run the model with random parameter sets, selecting behavioral Monte-Carlo simulations while ruling out non-behavioral ones in further analyses (Beven & Binley, 1992; Beven & Freer, 2001). It should be noted that simulations that are acceptable based on a goodness-of-fit criterion are referred to as behavioral models, although the acceptance threshold is subjectively determined. Each set of parameters from the behavioral simulations are assigned likelihood values, while unrealistic simulations are assigned zero. Finally, a measure of uncertainty of predictions is obtained based on the behavioral

simulations. OPTAS (Fischer, 2013) with 7,734 Monte-Carlo simulations was applied based on the parameter ranges (Table 4.4). To avoid the influence of reservoirs, the GLUE method was applied in the period of 1982-1991. In this study, simulations with $LNS > 0.7$ were considered as behavioral simulations. Based on this criterion, 80 parameter combinations were chosen as the behavioral ensemble. The 5th and 95th percentile was used to characterize the parameter uncertainties of the total streamflow and runoff components (RD1, RD2, RG1 and RG2). As meltwater is an important water source in the Kaidu Basin, uncertainties of snowmelt and glacier melt were also assessed separately using the GLUE method.

A Regional Sensitivity Analysis (RSA) was furthermore performed (Hornberger & Spear, 1981) to assess the parameter sensitivity of simulated streamflow. Monte-Carlo simulations were implemented in the RSA analysis based on parameter ranges (Table 4.4). The RSA method separates various model simulations into behavioral (good) and non-behavioral (bad) groups based on user defined evaluation criteria. The cumulative distributions of a single parameter associated with many model simulations are therefore indicators of parameter sensitivity. Large discrepancies in cumulative frequency distributions indicate a higher sensitivity (Fischer et al., 2012; Nepal et al., 2014). Sensitive parameters (Table 4.4) for the model output were singled out and discussed below (section 4.5.3).

Table 4.4. Summary of model parameters, parameter ranges (for both calibration and uncertainty analysis purposes) and calibrated values in the J2000 model. Parameters included in the sensitivity analysis are shown in boldface.

Modules	parameter acronym	Description [Units]	Range	Calibrated Value
Initialising	ACAdaptation	Multiplier for air capacity [-]	0.5 to 2	1.26
	FCAdaptation	Multiplier for field capacity [-]	0.5 to 2	1.79
Precipitation distribution	Trs	Temperature threshold for snow and rain [°C]	-1 to +1	-0.92
	Trans	Temperature range for mixed rain and snow [°C]	0-2	0.48
Interception module	a_rain	Interception storage factor for rain [mm]	0-5	0.60
	a_snow	Interception storage factor for snow [mm]	0-5	1.09
Snow module	snowCritDens	Critical snow density [g/cm ³]	0.1 - 1	0.29
	baseTemp	Threshold temperature for snowmelt [°C]	-1 - 1	-0.7
	t_factor	Melt factor by sensible heat [mm/K]	1 - 5	4.77
	r_factor	Melt factor by liquid precipitation [-]	1 - 5	2.09
	g_factor	Melt factor by soil heat flow [mm]	1 - 10	9.48
	ccf	cold content factor [-]	0.001 - 0.01	0.0014
Glacier module	meltfactor	Melt factor for ice melt [mm/K]	0.2 - 5	0.32
	alphaIce	Radiation melt factor for ice [mm/(K*M)]	0.1 - 1	0.1
	ddfIce	Day degree factor for ice melt [mm/K]	0.1 - 2	1.85
	kIce	Routing coefficient for ice melt [-]	1 - 8	2.1
	kSnow	Routing coefficient for snowmelt [-]	1 - 8	3.58
	kRain	Routing coefficient for rain runoff [-]	1 - 8	3.63
	debrisFactor	Debris factor for ice melt [-]	1 - 5	2.52
Soil module	Tbase	Threshold temperature for melt [°C]	-2 to 2	-0.25
	soilMaxDPS	Maximum depression storage [mm]	0.3 - 2	1.73
	soilPolRed	polynomial reduction coefficient for actual evapotranspiration [-]	1 - 5	2.96
	soilMaxInfSummer	Maximum infiltration in summer [mm]	60 - 150	82.10
	soilMaxInfWinter	Maximum infiltration in winter [mm]	60 - 150	65.15
	soilMaxInfSnow	Maximum infiltration in snow cover areas [mm]	40 - 120	43.19
	soilImpGT80	Infiltration for areas greater than 80% sealing [-]	0.1 - 1	0.34
	soilImpLT80	Infiltration for areas lesser than 80% sealing [-]	0.1 - 1	0.30
	SoilDistMPSLPS	MPS-LPS distribution coefficient [-]	0.2 - 2	0.64
	SoilDiffMPSLPS	MPS-LPS diffusion coefficient [-]	0.1 - 1	0.13
	soilOutLPS	Outflow coefficient for LPS [-]	0.1 - 1	0.23
	soilLatVertLPS	Calibration coefficient for the distribution of interflow and percolation water [-]	0.2 - 2	0.87
	soilMaxPerc	Maximum percolation rate [mm]	3 - 20	8.34
	soilConcRD1	Recession coefficient for overland flow [-]	1 - 3	1.25
	soilConcRD2	Recession coefficient for interflow [-]	1 - 4	2.8
Groundwater module	gwRG1RG2dist	RG1-RG2 distribution coefficient [-]	0.5 - 3	1.39
	gwRG1Fact	Adaptation for RG1 flow [-]	0.5 - 3	1.80
	gwRG2Fact	Adaptation for RG2 flow [-]	0.5 - 5	2.19
Reach routing	flowRouteTA	Run time of the outflow route [-]	2 - 18	14.43

4.5 Results

4.5.1 Evaluation of the precipitation products

4.5.1.1 Spatial distribution of precipitation products

The spatial distribution of precipitation in the different gridded products is shown in Figures 4.3 and 4.4. Although the averaging periods from different gridded products are different (but overlapping), we believe that this should not impact the spatial distribution of precipitation fundamentally. Most of the gridded products can generally capture the spatial distribution of precipitation with higher values in the Tianshan Mountains in the northern and western part of the Kaidu Basin (Figure 4.3). CFSR, ERA-Interim, MERRA-2 and TRMM products generally overestimate precipitation in the western and northern parts of the Kaidu Basin where precipitation is approximately 400 to 800 mm per year (Chen, 2014). Particularly, annual CFSR, MERRA-2 and TRMM have some extreme values (from 1000 mm to more than 3000 mm) which are unrealistic in this semiarid region (Figure 4.3). APHRODITE and CRU data have lower precipitation compared with the other precipitation datasets, yet CRU data mismatch the spatial pattern of precipitation at high elevations in general.

Overall, precipitation products can capture known seasonal precipitation patterns with a higher precipitation in summer and lower precipitation in winter (Chen, 2014) (Figure 4.4). Consistent with annual distribution, seasonal CFSR, ERA-Interim, MERRA-2 and TRMM overestimate summer precipitation which is even higher than the indicated sum of the entire year as mentioned above. To our knowledge, CFSR, ERA-Interim, MERRA-2 and TRMM data mostly overestimate spring precipitation, especially for CFSR (Figure 4.4). APHRODITE and CRU data have relatively reliable performance at seasonal scales for this semiarid mountain region. However, CRU showed less summer precipitation in the mountain chain.

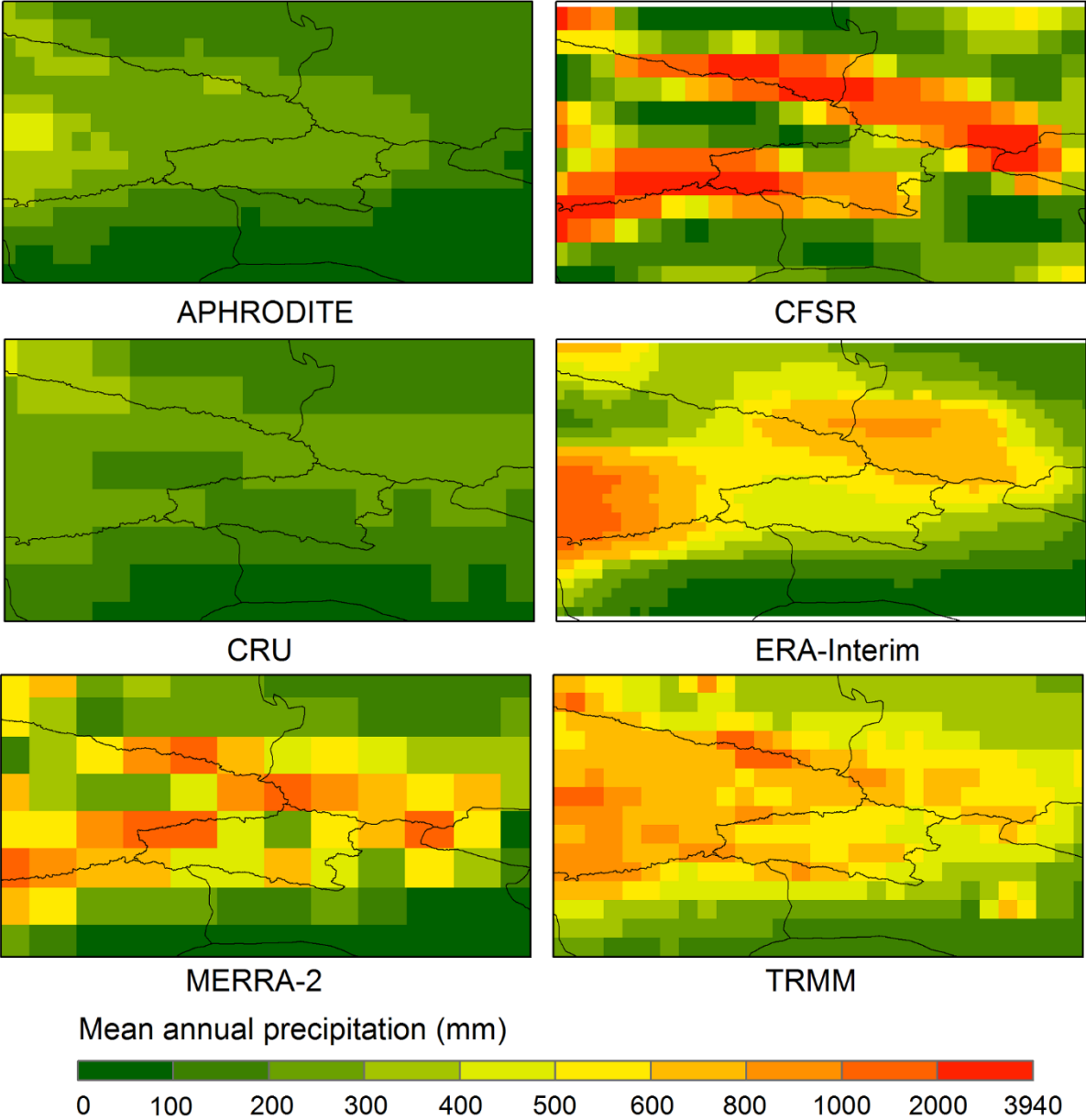


Figure 4.3. Spatial patterns of mean annual precipitation (mm) from the APHRODITE (1961–2007), CFSR (1979–2011), CRU (1961–2010), ERA-Interim (1979–2011), MERRA-2 (1980–2011) and TRMM (1998–2011) products over the Tianshan Mountains.

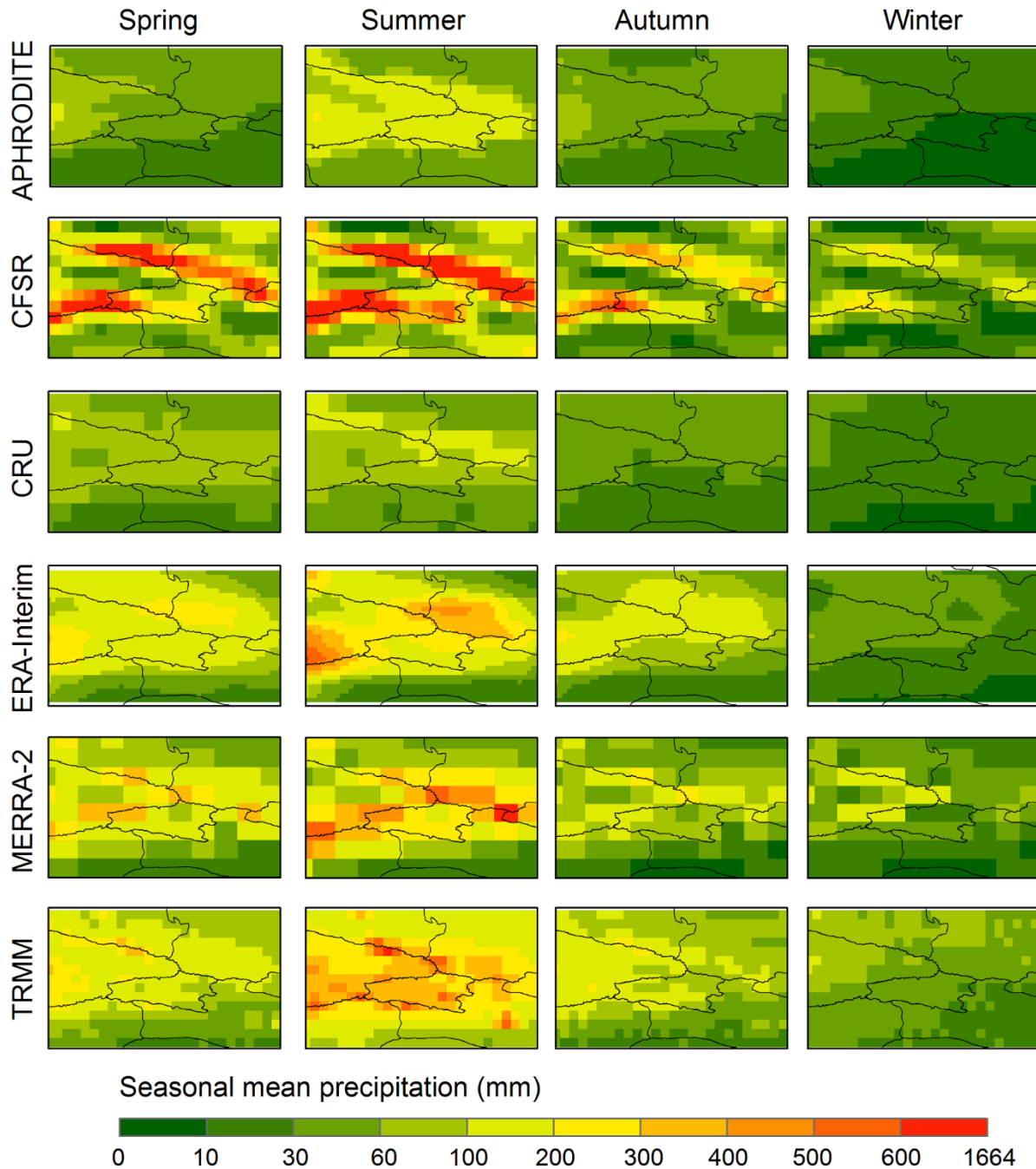


Figure 4.4. Same as Figure 4.3 but for seasonal mean precipitation.

4.5.1.2 Grid-based comparison of gridded precipitation products

Time series of precipitation at six weather stations were compared directly to the corresponding gridded data from each gridded product at annual and seasonal scales (Figures 4.5 and 4.6). Annual TRMM data overestimated precipitation at all stations and had an abruptly decreasing slope after the end of 1990s. The non-systematic over- or underestimation errors and extremes at different

stations indicate an insufficient quality of ERA-Interim and CFSR data in this study region. MERRA-2 data showed better annual consistency at the lower elevation stations than the mountain region (e.g. Bayinbuluke station). APHRODITE and CRU generally showed similar consistency with observation at most stations (Figure 4.5). Seasonally, most datasets captured the precipitation variability better than ERA-Interim and CFSR, which had the precipitation maximum in June while the largest precipitation occurs in July normally (Figure 4.6). MERRA-2 does not perform well as it overestimates seasonal precipitation at the Bayinbuluke and Luntai stations and exhibits implausible seasonality at the Yanqi and Kuerle stations. TRMM revealed the highest positive bias in summer and with an unrealistic behavior in spring. CRU underestimates the summer precipitation at all the stations. APHRODITE is generally close to the observation data although it underestimates summer precipitation at the mountainous Bayinbuluke station.

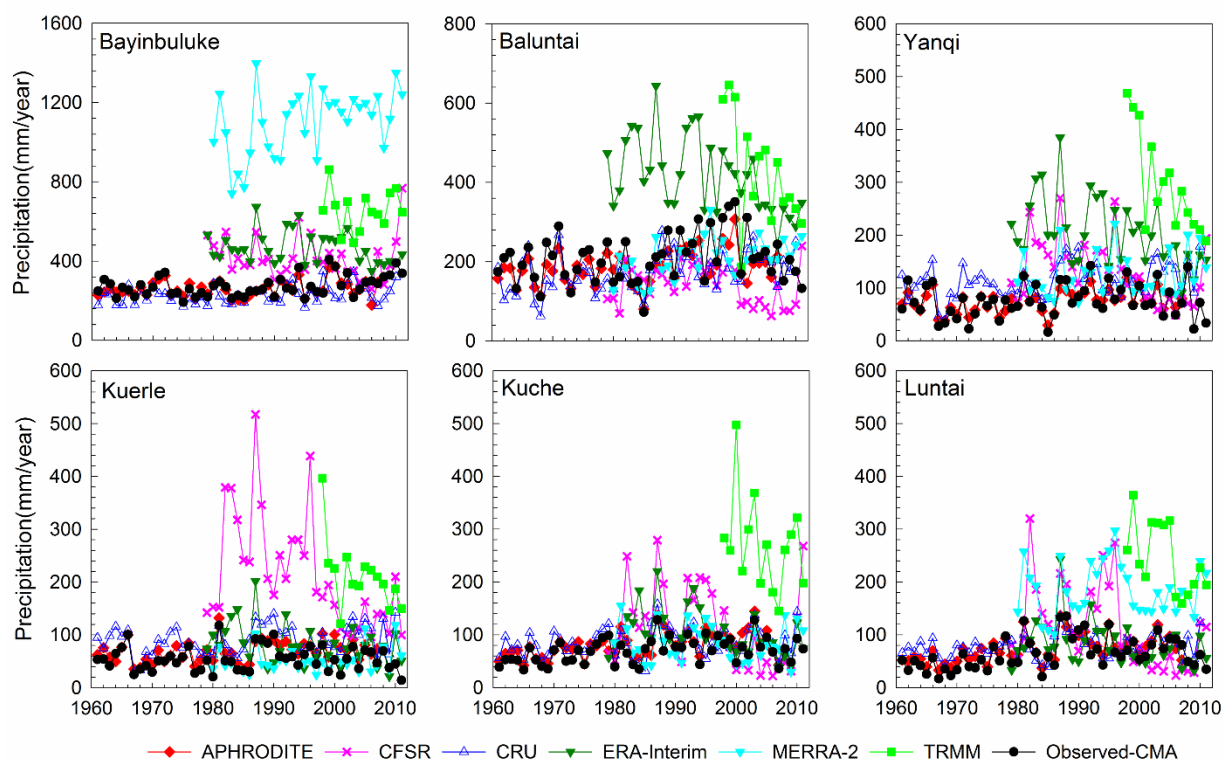


Figure 4.5. Time series of precipitation at six weather stations (1961-2011) compared with gridded precipitation products from APHRODITE (1961–2011), CFSR (1979-2011), CRU (1961-2010), ERA-Interim (1979–2011), MERRA-2 (1980–2011) and TRMM (1998-2011).

Taylor diagrams were applied to evaluate all the comparable datasets except for TRMM, which was excluded from the comparison due to the short overlapping time period (Figure 4.7). ERA-

Interim and CFSR are unreliable at all the stations, having a higher SD and RMS and relatively weak correlations with precipitation at weather stations. MERRA-2 generally had higher SD and RMS than CRU at all the stations, and had the highest SD and RMS overall at the Bayinbuluke mountainous station. APHRODITE performed best in terms of the higher correlation, lower SD and RMS at all the stations at annual scale.

Seasonally, most gridded products had a dissatisfactory performance (Figures S4.5-S4.8 in supplementary information). CFSR and ERA-Interim had higher SD and RMS than the other datasets, and the correlations with the station data were below 0.5 in nearly all the seasons, except for the Bayinbuluke station. CRU and MERRA-2 were inconsistent in most seasons and at various stations. At the mountainous Bayinbuluke station, MERRA-2 had the highest SD and RMS in all the seasons. The highest correlation coefficient and smallest RMS were found in APHRODITE in all the seasons. Overall, APHRODITE achieved a good performance at annual and monthly scales and performed substantially better than the other available gridded precipitation products.

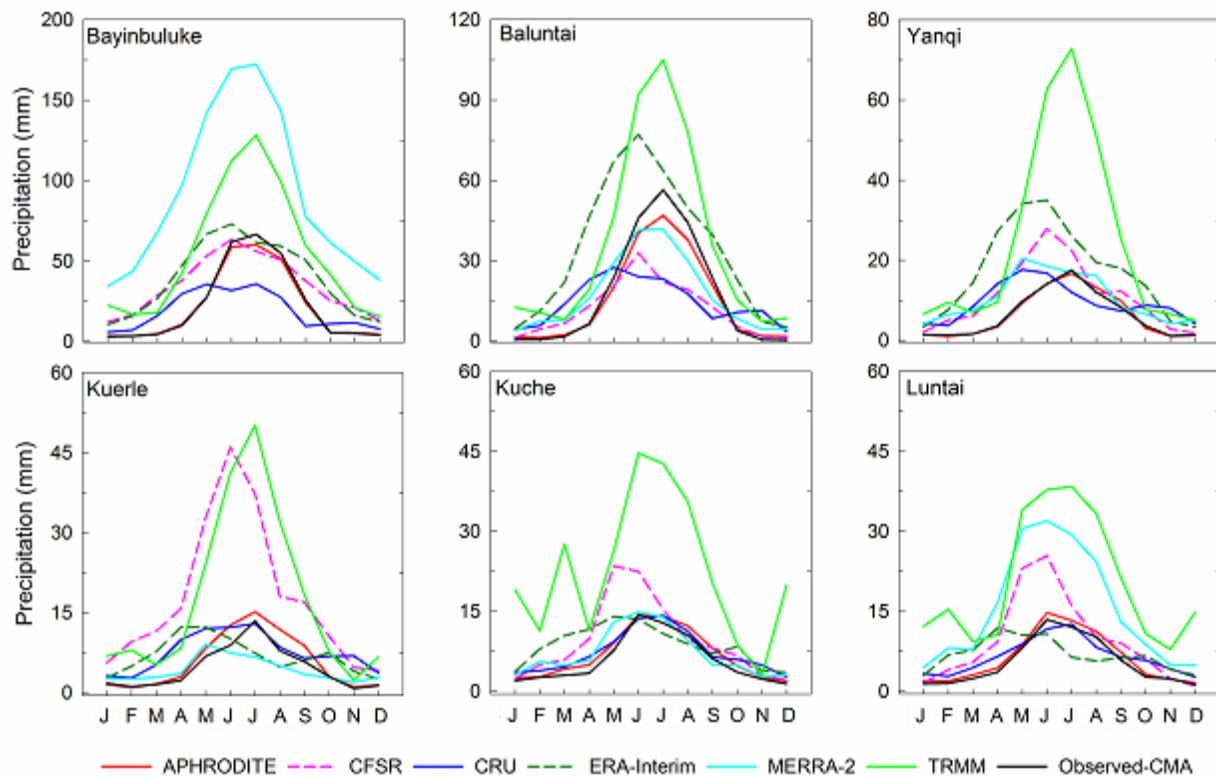


Figure 4.6. Same as Figure 4.5 but for monthly mean precipitation.

Seasonally, most gridded products had a dissatisfactory performance (Figures S5-S8 in supplementary information). CFSR and ERA-Interim had higher SD and RMS than the other datasets, and the correlations with the station data were below 0.5 in nearly all the seasons, except for the Bayinbuluke station. CRU and MERRA-2 were inconsistent in most seasons and at various stations. At the mountainous Bayinbuluke station, MERRA-2 had the highest SD and RMS in all the seasons. The highest correlation coefficient and smallest RMS were found in APHRODITE in all the seasons. Overall, APHRODITE achieved a good performance at annual and monthly scales and performed substantially better than the other available gridded precipitation products.

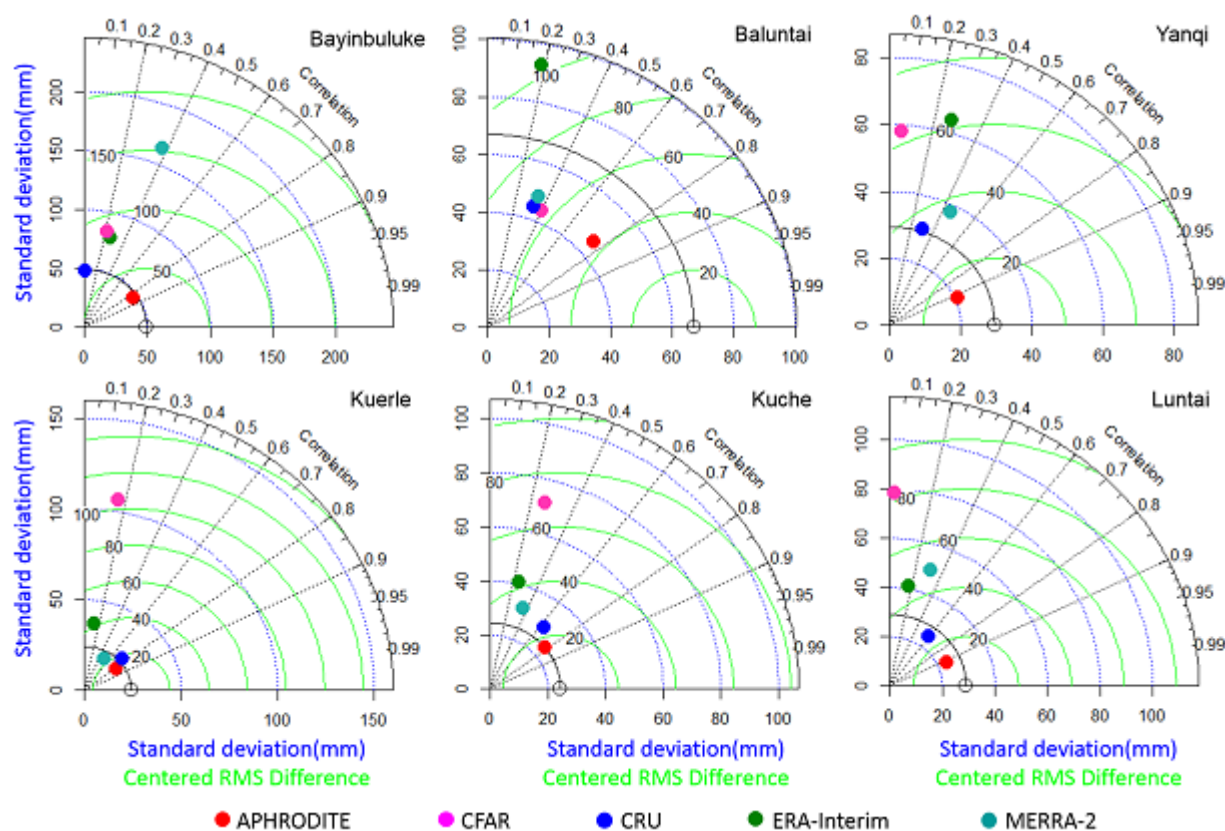


Figure 4.7. Taylor diagrams for displaying correlation coefficient, SD and RMS of mean annual precipitation from observational stations and different gridded products based on the overlapping period 1979–2007. The azimuthal position gives correlation coefficient. The blue radial coordinates and the green concentric semi-circles indicate SD and RMS values, respectively.

4.5.2 Temperature and precipitation correction

At all HOBO stations, the monthly mean temperature from ERA-Interim were greater than the observed data. The gradients of bias were higher in winter time (November to March) (Figure S4.9 in the supplementary information). We corrected ERA-Interim temperature based on monthly mean bias from these nine HOBO stations. The bias-corrected daily temperatures had strong correlations with the HOBO station (Figure 4.8), with root mean squared errors (RMSE) of 2.2 °C to 5.1°C mean absolute errors (MAE) of 1.8°C to 3.7°C.

The adjusted precipitation exhibited a strong increase (nearly 50% compared to Bayinbuluke station) based on the elevation difference. The adjusted mean annual precipitation in the Kaidu Basin was 425 mm (discussed in section 4.5.6, Figure 4.14a), which is generally consistent with precipitation ranges of 200-500 mm mentioned by previous studies (Fu et al., 2013). Spatially, regionalized precipitation is consistent with the general precipitation distribution in the Tianshan Mountains where the western and northern Tianshan receive more precipitation (400 to 800 mm) (Chen, 2014). Although substantial uncertainties still remain, our experience so far shows that it is necessary to take the precipitation gradient into consideration, and the adjusted precipitation can fulfill the model requirement and represent the orographic effect.

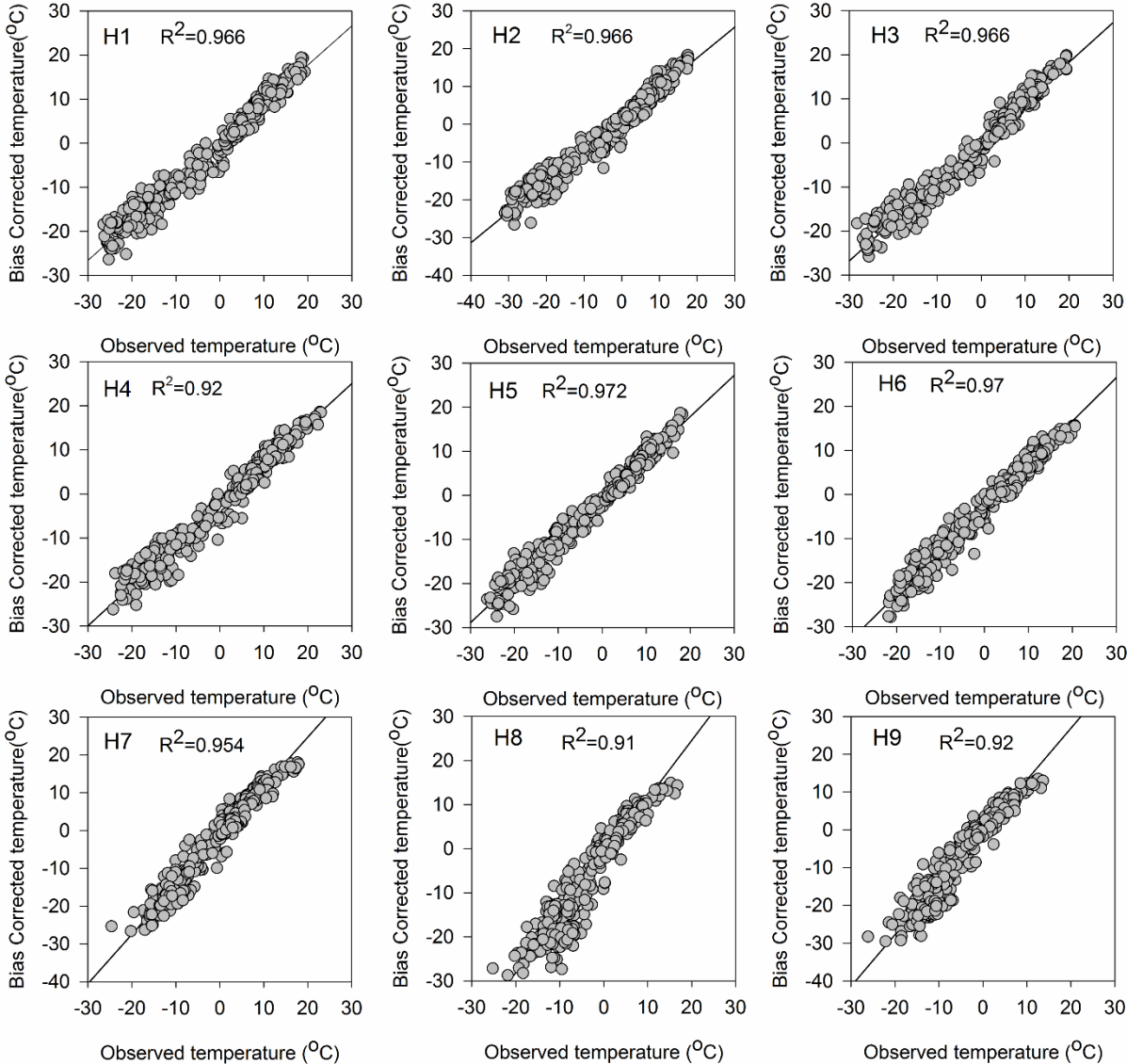


Figure 4.8. Relationships between mean daily temperatures observed at HOBO sites and bias-corrected ERA-Interim temperature (09.2014-08.2015).

4.5.3 Model performance

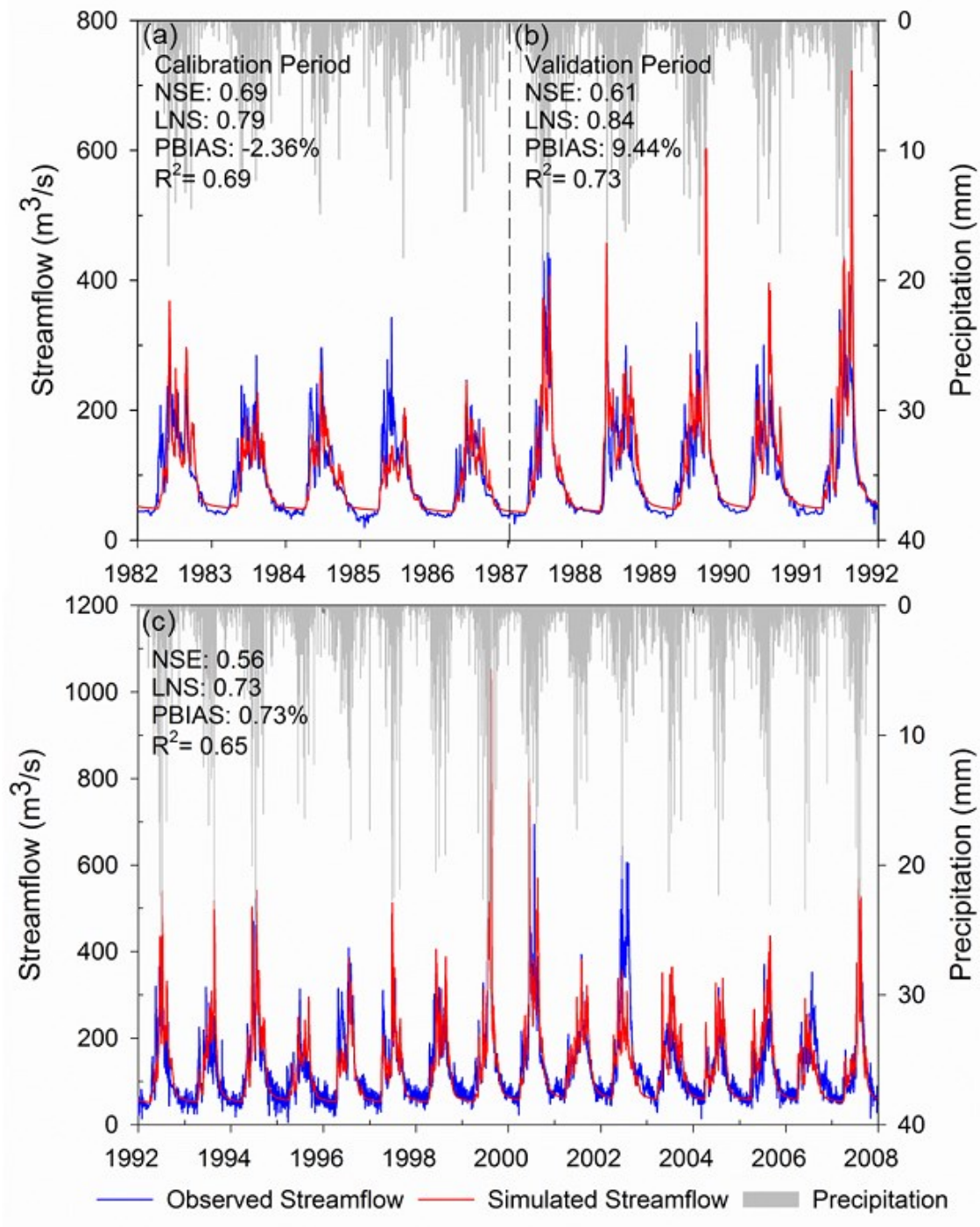


Figure 4.9. Simulated and observed daily streamflow during the (a) calibration period of 1982–1986, (b) validation period of 1987–1991 and (c) post-reservoir period of 1992–2007 in the Kaidu Basin. Performance measures were calculated from daily data.

Driven by the gridded precipitation and temperature datasets, the J2000 model could generally represent the regional hydrological dynamics, with NSE values of 0.69 and 0.61 and r^2 values of 0.69 and 0.73 for the calibration and validation periods, respectively (Figures 4.9a and 4.9b). Simulated and observed monthly streamflow during calibration and validation period indicate a reasonably good fit as well (Figure S4.10 in the supplementary information). For the post-reservoir period, the NSE and r^2 are 0.56 and 0.65, respectively (Figure 4.9c). It is worth noting that the model is not capturing reservoir effects, thus, we do not expect the model simulation to capture the hydrograph as well. The post-reservoir period is therefore only shown for information.

Although the rising and recession limbs are generally captured by the model, the spring snowmelt in the calibration period was underestimated (Figure 4.9a). However, the simulated base flow is relatively reliable in the basin based on the LNS, which is more closely related to the low flow. The LNS values are 0.79 and 0.84 for the calibration and validation periods (Figures 4.9a and 4.9b). Additionally, some overprediction peaks still can be seen in the post-reservoir periods when the model is not intended to simulate regulated flow due to reservoirs.

4.5.4 Uncertainty and sensitivity analysis

Based on the GLUE uncertainty analysis, the observed streamflow is generally within the 5th to 95th percentile of uncertainty ranges (1982-1991; Figure 4.10a). However, the uncertainty ranges are not constant in the simulated years; they are larger in the summer (high flow) periods when both precipitation and snow/glacier melt play an important role while they are relatively small in the winter (low flow) periods (Figure 4.10b). Furthermore, the streamflow in April and October are not well represented by the simulations as it falls outside of the uncertainty ranges (Figure 4.10b).

Figure 4.11 shows the average dynamics in the centerline of the box of the behavioral models for snowmelt, glacier melt and the runoff components RD1, RD2, RG1 and RG2. The range of the boxes and whiskers can be interpreted by GLUE-based uncertainty. The snowmelt shows two peak dynamics with maximum values in May and September. The uncertainty in May ($\pm 16\%$) is lower than in April and June ($\pm 38\%$ and $\pm 35\%$ respectively) while the uncertainties from August to October are $\pm 56\%$, $\pm 31\%$ and $\pm 30\%$, respectively. The uncertainty in simulated glacier melt is more obvious in July and August ($\pm 61\%$ and $\pm 50\%$, respectively). The patterns of RD1, RD2 and RG1 are generally similar, with the absolute uncertainty range higher in summer months. The

annual average relative uncertainties are $\pm 34\%$, $\pm 53\%$ and $\pm 43\%$, respectively. RG2 has a more stable uncertainty ($\pm 21\%$) throughout the year.

Model performance was particularly sensitive to four parameters (flowRouteTA, alphaIce, gwRG1RG2dist, ccf; Figure 4.12) based on RSA analysis. The model performance is moderately sensitive to additional parameters of the groundwater module (gwRG2Fact), the glacier module (meltFactorIce, debrisFactor and tbase) and the snowmelt module (g_factor, t_factor). The remaining parameters are less sensitive based on the LNS evaluation criterion (Figure 4.12).

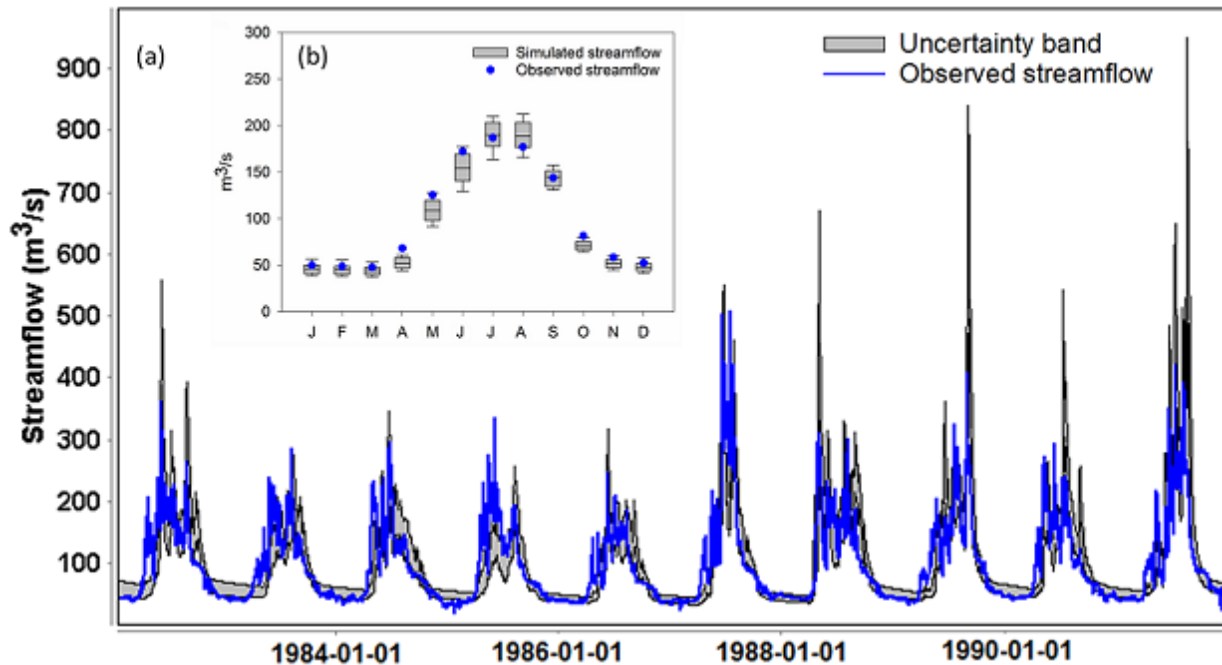


Figure 4.10. (a) Uncertainty band and observed streamflow during the period of 1982-1991 based on the GLUE method. (b) Boxplot of monthly uncertainty band of simulated streamflow (1982-1991). Boxplots represent extreme values, lower and upper quartiles and median value of a variable (similarly hereinafter).

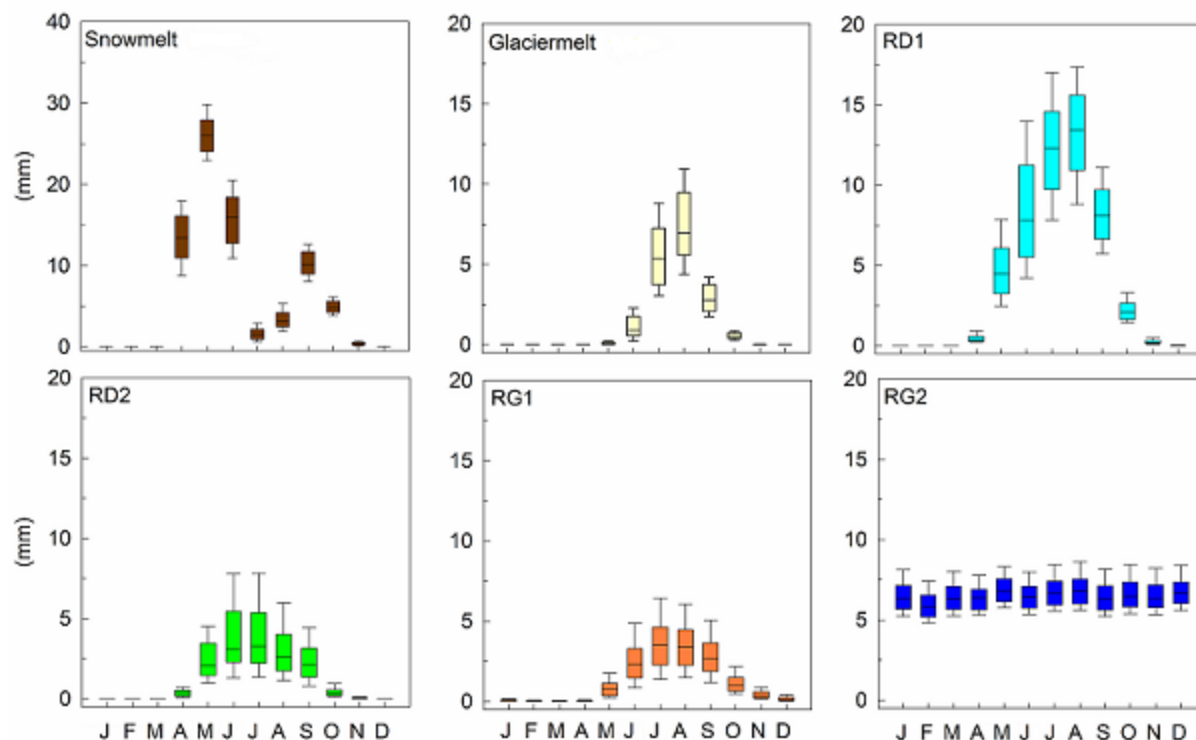


Figure 4.11. Boxplots of the effect of parameter uncertainties on different simulated runoff components (1982-1991). Note: the panel of snowmelt is different with other figures.

4.5.5 Temporal variation of the simulated water balance and runoff components

Annual and monthly distributions of the simulated water balance are shown in Table 4.5 and Figure 4.13a. As major inputs for the water balance, precipitation and glacier melt account for 425 mm and 9 mm, respectively. As for the output from the hydrological system, ActET and simulated streamflow account for 233 mm and 199 mm, respectively. Annual storage changes according to the model sum up to 2 mm. The summer season dominates the major hydrological processes in the Kaidu Basin, with peak values of precipitation, temperature, ActET and runoff in summer (Table 4.5).

As important water resources in the glacierized basin, snowmelt and glacier melt were extracted and analyzed individually (Figure 4.13b). Snowmelt mainly takes place in April (26 mm) and May (17 mm), while glacier melt is most evident in July and August (3 mm each). Snowmelt in September (8 mm) and October (6 mm) are also remarkable. Overall, snowmelt and glacier melt

contribute 33% (66 mm) and 5% (9 mm) to the simulated annual streamflow, respectively.

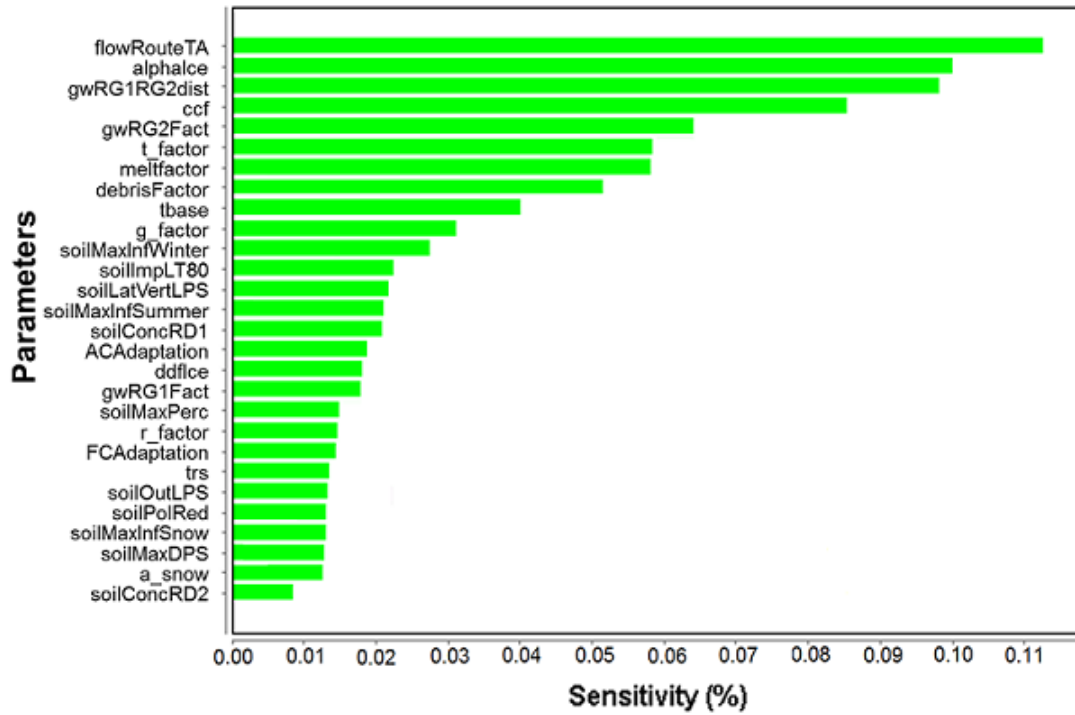


Figure 4.12. Parameter sensitivity based on the LNS evaluation criterion.

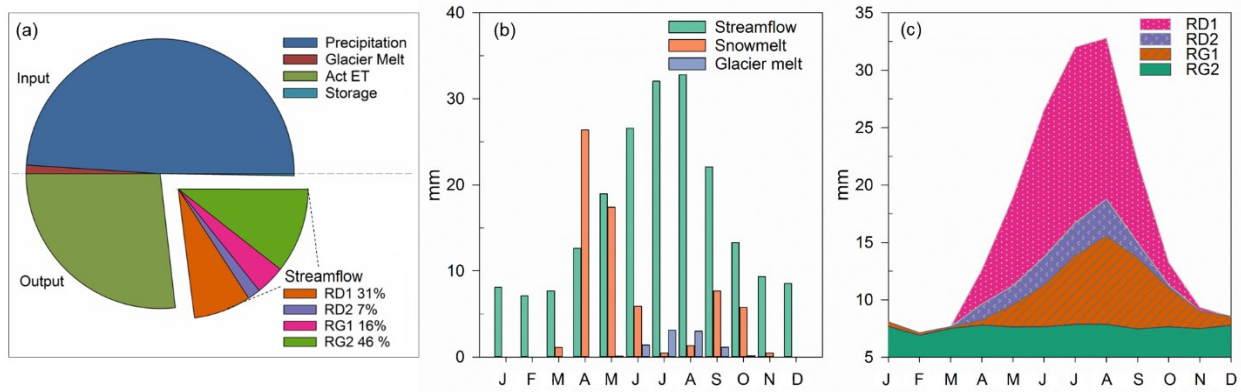


Figure 4.13 (a) Simulated water balance, (b) streamflow, snowmelt and glacier melt, and (c) distributions runoff components in the Kaidu Basin (1982-2007).

Table 4.5 Mean values of the water balance for the Kaidu Basin (1982-2007). Storage change represents changes in channel, soil layer, snow cover, groundwater and surface storages. Values are in mm.

	Precipitation	Glacier melt	ActET	Simulated Runoff	Storage Change
Jan	8.1	0.0	3.7	8.1	-3.6
Feb	8.9	0.0	4.3	7.1	-2.6
Mar	11.7	0.0	11.4	7.7	-7.3
Apr	20.2	0.0	24.1	12.6	-16.5
May	43.9	0.1	30.21	19.0	-5.2
Jun	88.4	1.4	35.8	26.6	27.4
Jul	92.3	3.1	41.8	32.0	21.6
Aug	74.3	3.0	35.6	32.8	8.8
Sep	37.3	1.1	22.5	22.1	-6.2
Oct	14.9	0.2	12.4	13.3	-10.6
Nov	13.9	0.0	7.0	9.4	-2.5
Dec	11.3	0.0	4.0	8.6	-1.2
Annual	424.9	8.9	232.6	199.2	2.0

Concerning the monthly distribution of different runoff components, RG2 (91 mm) and RD1 (62 mm) are the most important contributors, which account for 46% and 31% of the simulated annual total streamflow, respectively (Figure 4.13a). RD2 (13 mm) and RG1 (32 mm) account for 7% and 16% of the simulated annual total streamflow, respectively. Additionally, RD1, RD2 and RG1 showed similar seasonal patterns with peaks in summer and lows in winter, while RG2 was relatively stable throughout the whole year (Figure 4.13c).

4.5.6 Spatial characters of simulated water balance and runoff components

To explore the spatial distribution of water balance and runoff components, we aggregated these components to mean annual values (Figure 4.14). Mean annual precipitation varies regionally from 223 mm to 560 mm in the basin, with more humid areas located in the western and northern parts while the drier areas are in the southeastern basin (Figure 4.14a). The simulated ActET is partly impacted by elevation, with a lower ActET in the mountain regions. The highest ActET was concentrated in the lower reaches of the river and in the middle of the Kaidu Basin where wetlands are located (Figure 4.14b). The ActET rates are lower in the southeastern basin than in the higher elevated central part due to the limited water supply. The spots of lower ActET rates in the northeastern plane are caused by the barren land which leads to relative lower ActET values. The annual streamflow is mainly generated in the mountain regions in the middle, western and northern

part of the Kaidu Basin (Figure 4.14c). The snowmelt distribution shows higher values in the western mountain regions (Figure 4.14d). Apart from the greater water availability due to higher precipitation rates, RD1 and RD2 are mainly generated in the mountain regions, which is associated with higher slopes and less developed soils (Figure 4.14e and 4.14f). Barren land increases RD1 because of lower infiltration rates while gentle slopes and well-developed soils are associated with less RD2 in the lowlands. As the distribution of RG1 and RG2 depends on the HRUs' slope gradients, less RG1 is generated in the plain areas (Figure 4.14g). The distribution of modeled RG2 mainly depends on the total water balance. The changes of RG2 can be regarded as compensation with other runoff components, which can be observed in barren land where RD1 is greatly generated while RG2 is less distributed (Figure 4.14e and 4.14h).

4.6 Discussion

4.6.1 Comparison and correction of gridded meteorological data products

No consistent error pattern could be identified in the comparison of several gridded precipitation products and weather stations in our study (Figures 4.3-4.7). As different gridded datasets utilized different assimilation methodologies, we believe that the non-systematic errors can be due to limitations of the data assimilation processes and lack of representative weather stations in this mountainous region. However, gridded datasets need to be evaluated and used carefully, and the reasons for the spatial and temporal errors in different gridded data products need further study.

APHRODITE performed better in terms of an acceptable SD, RSM and R, which is related to the fact that APHRODITE was produced by interpolating rain gauge stations (Yatagai et al., 2012). However, APHRODITE underestimates precipitation in mountainous regions. Precise estimates of the amount of precipitation in the Kaidu Basin are not yet available due to scarcity of observational data and complex terrain. We have considered a spatial downscaling methodology, yet it will lead to unrealistic results in this data-scarce mountain region. The precipitation factor method has been proposed as an acceptable option in data-scarce mountain regions (Immerzeel et al., 2015; Biskop et al., 2016). APHRODITE was therefore simply corrected by a basin-wide factor (1.5) based on the annual precipitation gradient and elevation difference between the grid box and weather station. We adopted this approach because it may be more accurate in complex terrain where precipitation generally increases with elevation and it also provided a clear improvement in simulating regional streamflow in the Kaidu Basin. The adjustment of precipitation provides a

plausible estimation of annual precipitation, resulting in the simulated ActET being in much closer agreement with a previous study by Liu et al. (2016). These results support the chosen precipitation correction and modelling approach. However, uncertainty remains in the precipitation input.

A constant lapse rate is often a poor description of the spatial or temporal temperature structure (Lundquist & Cayan, 2007; Immerzeel et al., 2014). Thus, monthly temperature lapse rates were used for temperature correction and hydrological modeling in this study. Similar bias correction methods have frequently been used in the literatures (Gao et al., 2012; Liu et al., 2011; Shea et al., 2015). The largest bias in winter temperature during the correction processes might be interpreted as a temperature inversion (Shen et al., 2016) which can be captured by local monitoring stations but not the ERA-Interim temperature data.

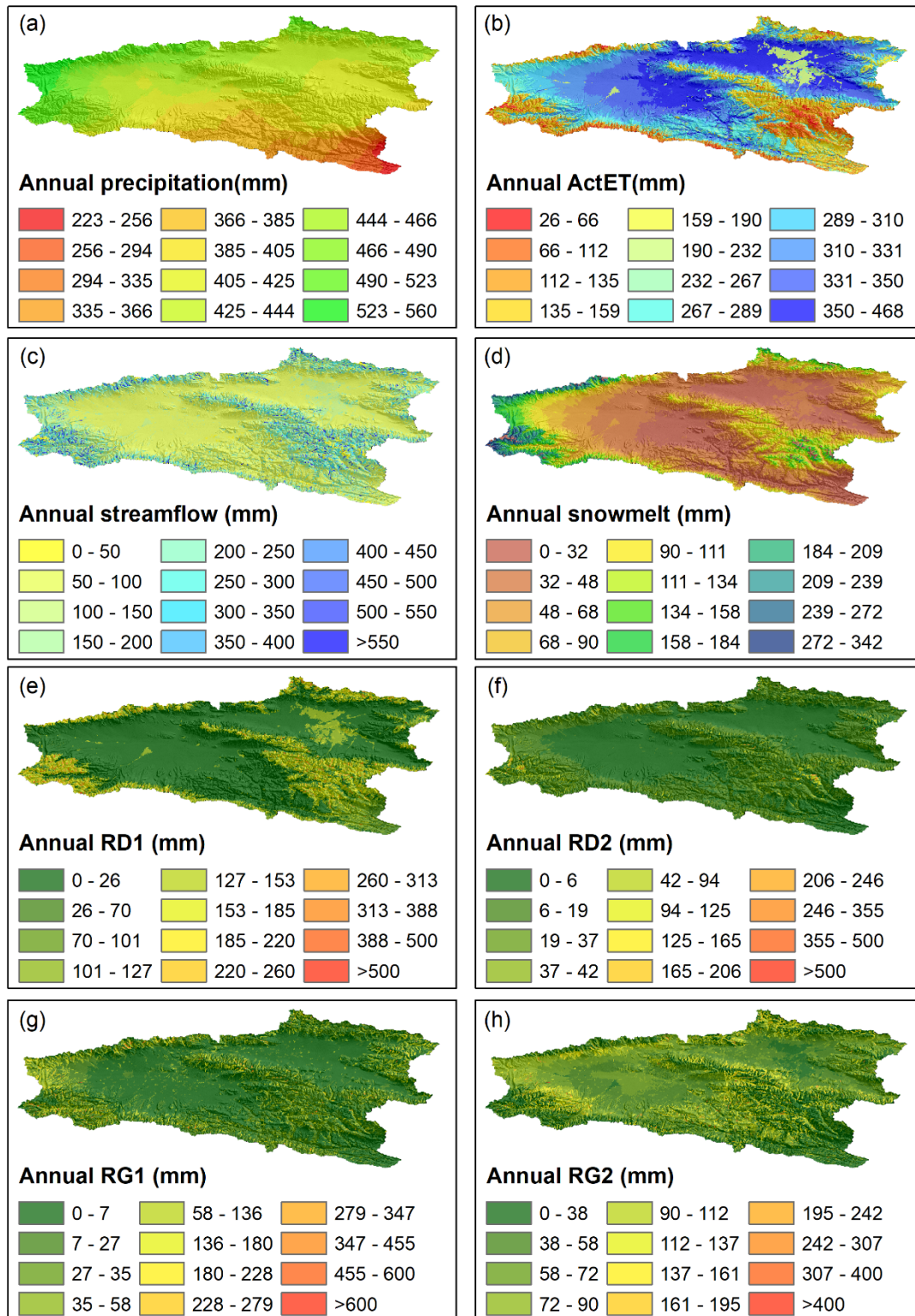


Figure 4.14. Spatial distribution of simulated mean annual (a) precipitation, (b) ActET, (c) streamflow, (d) snowmelt, (e) RD1, (f) RD2, (g) RG1 and (h) RG2 in the Kaidu Basin (1982-2007).

4.6.2 Remarks on calibration, uncertainty and sensitivity analysis

The performance of hydrological models in glacierized catchments is strongly constrained by various uncertainties: quality of the input data, model structure, model parameters, and the limited knowledge of hydrological regimes (Montanari et al., 2009; Ragettli et al., 2013; Nepal et al., 2014; Shea et al., 2015; Chen et al., 2016b). Existing studies utilized different model approaches for modelling snowmelt in different basins, which makes the parameters not transferable (Zhang et al., 2007; Dou et al., 2011; Zhang et al., 2015). Some of the model parameters were derived from modelling studies in other mountain regions (Nepal et al., 2014; Ragettli et al., 2015; Biskop et al., 2016) and adapted to our regional setting. However, calibration parameters in the model are often related to each other (Figure 4.2, Table 4.4). Their values therefore need to be chosen with care. Although we defined plausible parameter ranges based on literatures and our knowledge about the study region, different parameter sets might lead to the same prediction as suggested by Beven and Freer (2001). Indeed, there is not a single ‘best’ parameter set, and we therefore conclude that hydrological regimes can best be represented by the behavioral parameter ensemble based on calibration and uncertainty analysis.

Although previous research indicated that model nonlinearity, parameter uncertainty and model structure errors can be implicitly reflected in the GLUE method (Beven & Binley, 1992; Beven & Freer, 2001), the GLUE method has still been criticized for its subjective selection of behavioral models (Mantovan & Todini, 2006) and inconsistency with statistical theory (Stedinger et al., 2008; Montanari et al., 2009). However, subjectivity is unavoidable and expert knowledge is highly needed where data are scarce (Montanari et al., 2009; Beven & Binley, 2014). Given that epistemic errors make it hard to fit the assumptions of probabilistic models in real-world applications, GLUE remains a widely used technique applicable in data-scarce regions, we believe that the GLUE uncertainty assessment is acceptable in this study while its limitations should be acknowledged.

Snowmelt is too complex to be fully represented due to data scarcity and some unpredictable processes (e.g., snow drift), which may be the reason for the large range of snowmelt uncertainties (Figure 4.11) and underprediction of spring snowmelt in the calibration period (Figure 4.9a). In absolute terms, the great summer uncertainties of glacier melt can be explained by the dynamics of temperature and precipitation, which impact glacier melt the most (Figure 4.11). Runoff

components RD1, RD2 and RG1 show a larger uncertainty range in summer than in winter time, which is due to the fact that surface and subsurface runoff react relatively quickly in summer to the changes of hydro-meteorological conditions. In addition, the variability of precipitation and glacier melt in the summer season could strengthen these runoff uncertainties. Uncertainty of the base flow component RG2 was less pronounced, which is not surprising since base flow varies more slowly in the water cycle (Nepal et al., 2014).

The most sensitive parameters were identified based on RSA and provide starting points for further reducing model uncertainty in future studies (Table 4.4). The Kaidu Basin is a large basin in which large portions of the stream network have weak gradients. Streamflow is therefore greatly affected by the calibration parameter flowRouteTA, which refers to the velocity of the streamflow waves (Figure 4.12). Base flow plays an important role in sustaining streamflow, especially in the winter time. The gwRG2Fact and gwRG1RG2dist influence the runoff retention time and the distribution of water between RG1 and RG2, which is the reason for the sensitivity of model performance to these parameters. The water budgets of mountain areas also partly depend on meltwater from glaciers (Chen et al., 2016a). Streamflow variability is therefore also highly sensitive to alphaIce, meltfactor, debrisFactor and tbase, which affect glacier melt calculation directly in J2000 (Nepal et al., 2014). The sensitivity to ccf, t_factor and g_factor can be explained by the importance of snow cold content in snow accumulation and snowmelt (Krause, 2002). The soil module dominates the water transfer between surface and subsurface, which plays an important role in the simulated streamflow. The simulated streamflow is therefore also sensitive to parameters of the soil module (Figure 4.2 and Table 4.4).

4.6.3 Simulated water balance and runoff components

Although uncertainties remain and it is impossible to validate the volume of annual precipitation in the Kaidu Basin without additional measurement data, the amount of precipitation in this study (approximately 425 mm per year) is in reasonable agreement with other studies according to which precipitation amounts range from about 200 to 500 mm in the Kaidu Basin (Fu et al., 2013). Spatially, the distribution of precipitation broadly agrees with the previously known precipitation patterns in the Tianshan Mountains according to which precipitation is higher in the adjacent northern Tianshan and the Yili river valley (400 to 800 mm per year; Chen, 2014), and the western Tianshan (Chinese part) receives more precipitation than the eastern part (Xu et al., 2010; Chen,

2014). The simulated mean annual ActET (233 mm) is slightly higher than the satellite-based estimation (2001-2013) of mean annual ActET (above 190 mm) in the Kaidu Basin (Liu et al., 2017). Although little data is available to validate ActET in both our study and the satellite-based estimation (MODIS), we believe the estimation of regional ActET can be trusted owing to the good performance of the hydrological model and the closed water balance.

The large amount of simulated base flow (46% of the total streamflow) suggests that groundwater related processes play an important role in the Kaidu Basin. The simulated base flow volumes are in good agreement with results from other study (approximate 41%; Chen et al., 2009). The seasonal distribution of base flow is stable, which is reasonable since groundwater has a longer recession time (Figure 4.13c). According to our model results most of the high-intensity rainfall drained as surface flow due to the mountainous topography; this may explain the large contribution (31%) of RD1. The smaller contribution of RD2 (7%) is possibly due to poorly developed soils on the steep slopes where most of the surface runoff is generated. The proportion of infiltrated water is less due to the small pore storage, which saturates quickly and leads to a major contribution to surface runoff.

4.6.4 Implications and future work

Climate change substantially influences hydrological regimes in basins with high runoff contributions from snow and glacier meltwater, which could lead to more pressure on the water availability in future (Sorg et al., 2012). The water cycle has already started to intensify and could become more unstable under a warming climate in the Tianshan Mountains (Shi et al., 2007; Shen & Chen, 2010). Additionally, irrigation agriculture consumes large amounts of water further downstream and relies heavily on stream discharge, which is generated primarily by mountain meltwater or summer rainfall (Shen et al., 2013). However, snowmelt runoff occurs earlier in a warming climate (Liu et al., 2011; Sun et al., 2015), which may reduce water availability in summer when irrigation demand is at its peak. The water balance and the distributions of runoff components in the glacierized Kaidu Basin were quantified. Therefore, we believe the results of this study explained a significant part of mountain hydrology and could be helpful for adopting better water resource management.

This study is of interest as hydrological modelling in this data-scarce basin has not previously been described in detail. Integrating meteorological data from multiple sources shed light on modelling

mountain hydrology, which could be important for model applications and design in data-scarce mountainous regions elsewhere. The existence of parametric sensitivity and uncertainty could contribute to improving model calibration and design in central Asia in the future, and it also sends a strong message regarding the need for adequate and sustainable observing systems that are required for modeling present and future water resources.

4.7 Conclusions

In this study, we evaluated the performance of different gridded meteorological datasets in the Tianshan Mountains in order to identify the most appropriate inputs for driving hydrological models. Additionally, we statistically bias-corrected gridded climate data based on in situ data and analyzed the spatio-temporal patterns of water balance and the distribution of runoff components in the glacierized Kaidu Basin using the J2000 model. Moreover, we have identified parameter uncertainties and sensitivities that affect model performance, which need to be considered and further constrained in future research.

Overall, none of the available gridded precipitation products is perfect, but the interpolated APHRODITE data represented the annual and seasonal precipitation dynamics best, although it underestimates precipitation in the Tianshan Mountains. Driven by the corrected gridded climate datasets, the simulated daily streamflow is in good agreement with observed streamflow in the calibration and validation periods. Parameter uncertainty and sensitivity analyses were conducted, which are essential for modelling studies in data-scarce mountain basins. Regional water balance and the distribution of runoff components were further quantified, and uncertainties in streamflow and runoff components were estimated, which can be used to reduce hydrological uncertainties in future work. We acknowledge that uncertainty remains due to limited data availability. However, this study provides insights into mountain hydrology, which could contribute to hydrological research and water resource management in the Tianshan mountain area and other mountain regions with limited measurement data. Further studies are required to address the limitations and uncertainties.

Chapter 5 Discussion

5.1 Hydro-meteorological research in this semiarid region

Although temperature and precipitation were found to abruptly change in the mid-1980s in Xinjiang and internal river basins (Xu et al., 2004; 2006; Chen et al., 2006, 2007, 2009; Shangguan et al., 2009) and the magnitude of changes is more obvious in the 1990s (Shi et al., 2007; Chen et al., 2015; Zhang et al., 2016), the reason for abrupt changes of temperature and precipitation are still not clear. As climate in Xinjiang is dominated by moisture from the westerlies (Shen et al., 2013a; Tian et al., 2007; Yin et al., 2014), it is logical to correlate the changes with global atmosphere cycle, such as El Niño–Southern Oscillation (ENSO). However, there have no solid evidences for the relationships between temperature/precipitation with ENSO (Chen et al., 2013a; Hu et al., 2017; Xu et al., 2004). Shi et al (2007) indicated that the enhanced water cycle and increased atmospheric vapor content which were caused by global warming are possible reasons for the abrupt changes. Li et al (2012) indicated that the increase of temperature might be because of the weakening of the Siberian High in the 1980s to 1990s. Chen et al (2014) found that the Tibetan Plateau index can be another possible factor for the abrupt changes of climate variables. However, the mechanisms behind these abrupt changes need further research.

The assessment of climate change and its impacts on water resources cannot be generalized since spatial heterogeneity is apparent in mountain regions. Climate change and its effects differ evidently among different regions in northwestern China (Shi et al., 2007; Chen, 2014). For instance, the changes of streamflow and snowmelt timing differ in different regions due to different distribution of temperature and different streamflow generation processes (rain or snow-dominated) (Kundzewicz et al., 2015). Additionally, the results from climate change are not transferable to different regions, which needs to be evaluated in detail (Immerzeel et al., 2010).

5.2 The applicability of gridded data

Constrained by the scarcity of data, gridded hydro-meteorological products have been widely used to estimate climate change and drive hydrological models in mountain regions (Hughes, 2006; Shen et al., 2010b; Yatagai et al., 2012; Immerzeel et al., 2013; Shea et al., 2015). However, gridded data were demonstrated have different performance in different regions (Worqlul et al., 2014; You et al., 2015; Blacutt et al., 2015), which needs to be evaluated with caution.

The assessment of gridded data might be biased in mountain regions. The baseline of observational data are incomplete due to data scarcity and inaccessible topography. The observation-based datasets are always based on point measurement (point stations) and normally located in the valley (You et al., 2013). Additionally, gridded products have used different sources of data and methodologies in the process of data assimilation (Frauenfeld et al., 2005). In most cases, they have different resolution in the horizon and temporal scales (Mooney et al., 2011; Cornes & Jones, 2013; Worqlul et al., 2014).

Regardless of the uncertainties mentioned above, spatio-temporally evaluation of gridded is still needed. It would be better to take orographic effects (temperature lapse rate or precipitation gradient) into consideration when bias correcting or evaluating gridded products (Gao et al., 2012; Ehret et al., 2012; Wang et al., 2015). Gridded datasets may not reflect the mesoscale reality but can be representative on regional scales. Regional adjustment would be another considerable option (Immerzeel et al., 2015; Shea et al., 2015; Biskop et al., 2016). Combination of multiple datasets provides a new option for hydroclimate researches in mountainous regions (Knoche et al., 2014; Pohl et al., 2017).

5.3 Hydrological modelling in mountain basins

Hydrological models are heavily restrained by the driving and calibration data (Chen et al., 2016b). Concerning the driving data, as one of the key factors influencing model performance, precipitation has more variability than temperature which is elevation dependent (Barnett et al., 2005). The lack of reliable measurement data in mountain basins not only impedes a successful implementation of hydrological modelling work but also leads to more uncertainties in model simulations (Kobold, 2005; Knoche et al., 2014; Engelhardt et al., 2014; Biskop et al., 2016). Although it is possible to employ precipitation gradients and precipitation-factor into hydrological simulation, precipitation gradient differs spatio-temporally in mountain regions (Immerzeel et al., 2015; Shea et al., 2015) and precipitation-factors are not comparable (Biskop et al., 2016).

Currently, hydrological models have been widely applied in the Tianshan Mountains in different basins. However, as the energy and mass balance in snow and glacier melt processes are relatively complex and observational data are scarce, physical details in hydrological modelling still need to be addressed (Chen et al., 2016b). For instance, snow drift and sublimation (Biskop et al., 2016), snow redistribution (Ragettli et al., 2015), unknown debris cover (Pohl et al., 2017) and glacier

dynamics (Ragetti et al., 2013) should be included and analyzed in detail. Moreover, freezing soil was neglected in most of hydrological models, which play an important role and need to be considered in future.

Uncertainties in the application of hydrological model should be considered as a priority in hydrological simulations (Montanari, 2007). Uncertainties in hydrological simulations were found to associate with the quantity and quality of input data, model structure, parameters and the limited knowledge of hydrological regimes (Beven & Binley, 1992; Biskop et al., 2016; Beven & Binley, 2014; Ragetti et al., 2013; Shea et al., 2015; Chen et al., 2016b), which can be found in Chapter 4 in the application of J2000 model into the glacierized Kaidu Basin. However, parametric uncertainty was found to be the major uncertainty among climate uncertainty and natural climate variability in glacierized basin (Ragetti et al., 2013). Tarasova et al (2016) found that increase model complexity in including distributed/semi-distributed parameters does not increase model performance in a glacierized basin. The applicability of simple modelling approaches is still required in mountain basins where observation datasets are unavailable (Shea et al., 2015).

5.4 Possible implications

Climate-driven changes in snow and glacier meltwater-fed basins have direct implications on water availability, irrigation and hydropower (Sorg et al., 2012). The impacts of climate change are expressed in many ways in the Tianshan Mountains, including enhanced evapotranspiration (Shen & Chen, 2010), variation of precipitation patterns (Shen et al., 2013a), onset of vegetation growing seasons (Wang et al., 2008a; Wang et al., 2014), shrinking glaciers (Yao et al., 2004; Liu et al., 2006) and alternation of streamflow and snow runoff timing (Tao et al., 2011; Ling et al., 2014, Shen et al, 2017). Meltwater from the Tianshan Mountains is the important water supply for downstream rivers but their role in sustaining freshwater will be significantly altered by these changes.

Warmer temperatures and the corresponding alteration of hydrological regimes may threaten seasonal water availability, which have direct implications on water resources management. The fact is that agriculture sector consumes the majority (more than 90%) of water withdrawal in arid Xinjiang, and oasis agriculture highly depends on river streamflow which depends on meltwater from mountainous regions (Shen et al., 2013a; 2013b). Summer warming can greatly increase evapotranspiration which might lead to water shortage for agriculture (Piao et al., 2010; Shen et

al., 2013a). Additionally, high temperatures reduce winter snow accumulation and alter the snowmelt runoff timing in spring in the snow/glacier-fed basins (Middelkoop et al., 2001; Barnett et al., 2005; Molini et al., 2011; Sun et al., 2015, Shen et al., 2017), which may lead to less water released in summer when irrigation water demand is high (Shen et al., 2013b). Moreover, the irrigation water demand increased in past decades due to the expansion of irrigation area (Shen et al., 2013b). Therefore, the changes of seasonal distribution of streamflow could threaten agriculture water resources management. More attention should be paid to irrigation projects; for instance, water use efficiency should be improved and new irrigation management needs to be adapted.

A warmer climate possible has implications on vegetation response. For instance, the warm-wet conditions become more suitable for vegetation growth, with vegetation vigor and coverage improved in past decades (1982-2006) in the Tarim basin (Wang et al., 2013e). The favorable climate condition also possible lengthen vegetation growing season (Hu et al., 2016), especially in the Tianshan Mountains and the southern Xinjiang based on in situ observations and satellite-based normalized difference vegetation index (NDVI) (Wang et al., 2014). The changes of climate condition could also impact crop type and crop yield. Such a warm-wet condition tendency could become more suitable for improving cotton production rather than winter wheat (Wang et al., 2008a), yet the irrigation water requirement of cotton is higher than other crops (wheat, corn, oilseed and sugar beet) (Shen et al., 2013b).

Melting snow and glaciers lead to increased streamflow in a short term in glacier-fed basins, which could alter regional hydrological cycle by changing seasonal runoff (Barnett et al., 2005). However, glacier meltwater will become more stressed with the disappearance of glaciers in the long run, which could threaten long-term water availability (Barnett et al., 2005; Chen et al., 2016a; Guo & Shen, 2016). Additionally, the consequences of climate warming accompanied with intensify precipitation could also inevitably lead to high risk of flood (Zhang et al., 2016; 2016a), which impact downstream environments and livelihoods. Ecosystems are vulnerable to climate change in this arid region (Shen & Chen, 2010; Hu et al., 2016), such as environmental degradation in the Tarim basin (Wu, 2012). Water resources management, which relates to both the water shortage and extremes, is urgently needed to be adapted in coping with the ongoing climate change. Considering seasonal streamflow is substantially altered due to climate change; changes in regulations of reservoirs and hydropower plans might be unavoidable.

Chapter 6 Conclusions and future research

6.1 Conclusions

Climate impacts are apparent from rising temperatures, variable precipitation and retreating snow and glacier coverage in northwestern China. In this thesis, integrated analysis and hydrological modelling have been conducted to estimate climate change and unravel the glacierized mountain hydrology in the Tianshan Mountains. The framework of this thesis consists of several issues that need to be addressed by studying climate change and applying a distributed hydrological model in data-poor mountain regions where with snow and glacier dynamics. The status of climatic and hydrological changes were highlighted and analyzed by using statistical and GIS methodologies. Additionally, to overcome the shortcomings during hydrological model application, driving data, parameter preparation and snow/glacier dynamics were addressed. The main conclusions can be summarized as follows:

1. Climate change is substantial in northwestern China in past decades as evidenced by the uptrends of average temperature and precipitation. However, the increase tendencies of temperature and precipitation are more obvious after the mid-1980s and 1990s, respectively. Concurrently, the increase of average temperature has a high confidence based on historical observation data, with the T_{min} increased more obvious than T_{max} and the increase tendency is more obvious on the northern than the southern slopes of the Tianshan Mountains. The changes of precipitation vary significantly, with a more remarkable increase in the northern Tianshan. Seasonally, temperature increased more significantly in winter and spring, while precipitation mainly increased in winter and summer months. Climate extremes were found to change along with climate change, including increased warm days, warm nights and frequency of intense precipitation.
2. Hydrological regimes were affected by climate change based on the comprehensive analysis of streamflow variability and snowmelt runoff timing in four mountain basins in the southern Tianshan. Annual streamflow exhibited a significant positive trend in all basins and increased more sharply since the mid-1990s at annual and seasonal scales. The changes of annual streamflow generally consist with the changes of temperature and precipitation. Snowmelt runoff timing has shifted towards earlier dates since the mid-1980s. The relationships between climate variables with streamflow vary due to different season and streamflow generation processes. Precipitation plays

a vital role for streamflow changes in summer. Streamflow in autumn and winter are dominated by temperature changes in the snow-dominated basins (the Toxkon, Kaidu and Huangshuigou basins), while temperature plays a great role in affecting streamflow dynamics on annual and seasonal scales in the glacierized Kunmalik basin. Snowmelt runoff timing negatively correlated with temperature but positively correlated with precipitation accumulation in spring. However, an opposite relationship was found in the glacierized Kunmalik basin.

3. Near-surface temperature lapse rates were presented based on historical records and field survey data. The near-surface temperature lapse rates vary spatially and temporally on the southern and northern slopes of the Tianshan Mountains and in the Kaidu basin. Geographically, the variations of temperature lapse rates are found higher on the northern slopes than the southern slopes. Seasonally, temperature lapse rates are higher in summer than in winter months. Additionally, lapse rates for T_{max} are higher than that for T_{mean} and T_{min} . The results demonstrated that the standard atmospheric lapse rate of $6.5^{\circ}\text{C km}^{-1}$ could be an inadequate choice for temperature regionalization.

4. The performance of different gridded meteorological datasets were compared and evaluated in the Tianshan Mountains, and mountain hydrology in the specific glacierized Kaidu basin was revealed driving by the regionally bias-corrected and adjusted gridded meteorological data. The combination of physical-based model with the integration of multiple gridded dataset has proven a promising methodology for hydrological modelling application in scarcely monitored mountain basin. Water balance and the distribution of runoff components were revealed in the Kaidu basin. In terms of the runoff components, base flow is the most important contributor (46% of the annual streamflow), followed by surface flow (31%), interflow from the vadose zone (16%) and lateral flow (7%). Additionally, snow and glacier meltwater contribute of 33% and 5% to the annual total streamflow based on the model simulation, respectively. Seasonally, snowmelt mainly contributes to the streamflow in April and May; while glacier melt mainly occur in July and August. A parameter sensitivity analysis was conducted and annual and seasonal uncertainties of simulated runoff components were examined within acceptable simulation ensembles. However, the sources of uncertainty (input data, model structure and parameters) still need further research.

6.2 Future research

This thesis provided insights into mountain hydrology in northwestern China. Although uncertainties remain, research in data scarce mountain basins can be benefited from the processes of data preparation, model simulation and calibration. Considering climate warming is projected to continue and the role of mountains as “Water Tower” will in the face of critical situation, recommendations are therefore provided below, from climate research, data preparation and evaluation to hydrological modelling perspectives, for improving our understanding of climate variability and the corresponding hydrological consequences in the future.

Measurement data are not only critical in investigating spatio-temporal characteristics of historical climate state but also serve as the baseline for evaluating future projections (Shi et al., 2007; Immerzeel, 2008). In addition, hydro-meteorological assessments in mountain regions are highly hindered by the scarcity of observation-based data (Deng et al., 2015; Shen et al., 2016; Chen et al., 2016b; Biskop et al., 2016). Monitoring and observations, both in quantity and quality, are therefore should be enhanced in mountain regions. Projection changes in climate and hydrological regimes should be addressed in future research.

Climatic and hydrological changes cannot be generalized in mountain basins in Xinjiang due to the complex terrain. The impact of climate change on hydrological regimes differs in different basins based on different climate and physical characteristics of the basins. In addition, many factors (meteorological variables, groundwater, permafrost etc.) interact simultaneously, which makes assessment of climate change and their hydrological consequences a big challenge. The contributions of ground water (Sun et al., 2016), the changes of land use/land cover (Wu et al., 2010) and the variation of evaporation and meteorological variables (Shen et al., 2010a) need to be addressed in future.

An in-depth assessment of mountain hydrology is still lacking in mountain basins in northwestern China due to complex terrain, spatial and altitudinal variation in hydro-meteorological variables and complex snow and glacier melt dynamics (Luo et al., 2013; Chen et al., 2016b). Hydrological models can be strengthened by using different sources of hydro-meteorological data and with a flexible structure for regional utilization (Konz et al., 2007; Zhang et al., 2016b). As simulated snow and glacier melt greatly depend on the degree-day factor, changes of glacier extent and the combination of mass and energy balance therefore should be considered and represented by

hydrological models. The distribution and processes of rock glaciers need to be investigated as well (Wang et al., 2017b). Additionally, comprehensive uncertainty and sensitivity analysis should be enhanced to reduce uncertainties in model simulation in future research (Chen et al., 2016b). Isotopic composition can be a useful method for cross-validating model results (Kong et al., 2013; Pang et al., 2011; Sun et al., 2016; Tian et al., 2007).

Climatic and hydrological changes have implications on mountainous ecosystems and water resources management. Since land degradation are serious in the Tarim basin (Zhao et al., 2014; Chen, 2014), the ecological water conveyance project and reservoirs should be taken into consideration in future due to their substantial influence on the streamflow variability. With the increasing population and extending irrigation area, water demand will increase in the long run (Wu et al., 2010; Shen et al., 2013b). As the alterations of hydrological regimes could bring new challenges for agriculture irrigation and hydropower generation, thus, effective water resources management requires a comprehensive understanding of the linkage between upstream and downstream. The impacts of land use change on water quantity and quality and corresponding adaptive plans should also gain much attention in mountain regions and lowlands in order to coping with the ongoing climate change. Furthermore, effective water resources management requires the integration of relevant disciplines and enhancement of knowledge exchanges.

References

- Aizen, V. B., E. M. Aizen., J. M. Melack., & J. Dozier. (1997). Climatic and Hydrologic Changes in the Tien Shan, Central Asia. *Journal of climate*, 10(6), 1393-1404. doi:10.1175/1520-0442(1997)010<1393:CAHCIT>2.0.CO;2.
- Allen, R. G., L. S. Pereira., D. Raes., & M. Smith. (1998). Crop evapotranspiration-Guidelines for computing crop water requirements-FAO Irrigation and drainage paper 56. *FAO, Rome*, 300(9), D05109.
- Anderson, E. A. (1976). A point energy and mass balance model of a snow cover. Silver Spring, MD US. National Oceanic and Atmospheric Administration (NOAA), *Technical Report NWS*, 19.
- Arnold, J. G., R. Srinivasan, R. S. Muttiah, and J. R. Williams. (1998). LARGE AREA HYDROLOGIC MODELING AND ASSESSMENT PART I: MODEL DEVELOPMENT1. *Journal of the American Water Resources Association*, 34(1), 73-89. doi:10.1111/j.1752-1688.1998.tb05961.x.
- Ayala, A., F Pellicciotti., & JM Shea. (2015). Modeling 2 m air temperatures over mountain glaciers: Exploring the influence of katabatic cooling and external warming. *Journal of Geophysical Research: Atmospheres*, 120, 3139–3157. doi:10.1002/2015JD023137.
- Azócar, G. F., A. Brenning., & X. Bodin. (2017). Permafrost distribution modelling in the semi-arid Chilean Andes. *The Cryosphere*, 11(2), 877-890. doi:10.5194/tc-11-877-2017.
- Bai, L., J. Xu., Z. Chen., W. Li., Z. Liu., B. Zhao., & Z. Wang. (2015b). The regional features of temperature variation trends over Xinjiang in China by the ensemble empirical mode decomposition method. *International Journal of Climatology*, 35(11), 3229-3237. doi:10.1002/joc.4202.
- Bai, L., Z. Chen., J. Xu., & W. Li. (2015a). Multi-scale response of runoff to climate fluctuation in the headwater region of Kaidu River in Xinjiang of China. *Theoretical and Applied Climatology*, 1-10. doi:10.1007/s00704-015-1539-2.
- Baigorria, G. A., & C. C. Romero (2012). *Applications of Climatic Resources in Mountainous Regions*, edited, Guide to Agricultural Meteorological Practices (GAMP). World Meteorological Organization, WMO.
- Baldwin, J., & Vecchi, G. (2016). Influence of the Tian Shan on Arid Extratropical Asia. *Journal of Climate*, 29(16), 5741-5762. DOI:10.1175/JCLI-D-15-0490.1.
- Barnett, T. P., J. C. Adam., & D. P. Lettenmaier. (2005). Potential impacts of a warming climate on water availability in snow-dominated regions. *Nature*, 438(7066), 303-309. doi:10.1038/nature04141.
- Barry R G & R J Chorley. (2009). *Atmosphere, weather and climate*. 9th ed., Routledge, Oxon, U.K.
- Barry, R. G. (2008). *Mountain Weather and Climate*. 3rd ed., Cambridge Univ. Press, Cambridge, U.K.

- Bates, B.C., Z.W. Kundzewicz., S. Wu., & J.P. Palutikof. (Eds.). (2008). *Climate Change and Water. Technical Paper of the Intergovernmental Panel on Climate Change*. IPCC Secretariat, Geneva, 210 pp.
- Bendix, J., H. Behling., T. Peters., M. Richter., & E. Beck. (2009). *Functional biodiversity and climate change along an altitudinal gradient in a tropical mountain rainforest*. In: Tschardtke, T., Leuschner, C., Veldkamp, E., Faust, H. (Eds.). *Tropical Rainforests and Agroforests under Global Change*. Springer, Berlin. 239-268, doi:10.1007/978-3-642-00493-3_11.
- Beniston M. (2003). Climatic change in mountain regions: a review of possible impacts, *Climate Change*, 59:5–31. doi:10.1023/A:1024458411589.
- Beniston, M. (2006). Mountain weather and climate: a general overview and a focus on climatic change in the Alps. *Hydrobiologia*, 562(1), 3-16. doi:10.1007/s10750-005-1802-0.
- Benjamini, Y., & Hochberg, Y. (1995). Controlling the false discovery rate: a practical and powerful approach to multiple testing. *Journal of the Royal Statistical Society: Series B (Methodological)*, 57(1): 289-300. DOI: 10.2307/2346101.
- Bergström, S. (1992). The HBV model: Its structure and applications. *Swedish Meteorological and Hydrological Institute*. doi:10.5194/nhess-10-2713-2010.
- Bertle FA. (1966). Effects of snow compaction on runoff from rain and snow. *Bureau of Reclamation, Engineering Monograph No. 35*, Washington.
- Beven, K. (2001). How far can we go in distributed hydrological modelling?. *Hydrology and Earth System Sciences*, 5(1), 1-12, doi:10.5194/hess-5-1-2001.
- Beven, K., & A. Binley (1992). The future of distributed models: Model calibration and uncertainty prediction. *Hydrological Processes*, 6(3), 279-298. doi:10.1002/hyp.3360060305.
- Beven, K., & A. Binley. (2014). GLUE: 20 years on. *Hydrological Processes*, 28(24), 5897-5918. doi:10.1002/hyp.10082.
- Beven, K., & J. Freer. (2001). Equifinality, data assimilation, and uncertainty estimation in mechanistic modelling of complex environmental systems using the GLUE methodology. *Journal of Hydrology*, 249(1–4), 11-29. doi: 10.1016/S0022-1694(01)00421-8.
- Biskop, S., F. Maussion., P. Krause., & M. Fink. (2016). Differences in the water-balance components of four lakes in the southern-central Tibetan Plateau. *Hydrology and Earth System Sciences*, 20(1), 209-225. doi:10.5194/hessd-20-209-2016.
- Blacutt, L. A., D. L. Herdies., L. G. G. de Gonçalves., D. A. Vila., & M. Andrade. (2015). Precipitation comparison for the CFSR, MERRA, TRMM3B42 and Combined Scheme datasets in Bolivia. *Atmospheric Research*, 163, 117-131. doi: 10.1016/j.atmosres.2015.02.002.
- Blandford T R., K S Humes., B J Harshburger., B C Moore., V P Walden., & H Ye. (2008). Seasonal and Synoptic Variations in Near-Surface Air Temperature Lapse Rates in a Mountainous Basin, *Journal of Applied Meteorology and Climatology*, 47, 249–261. doi: 10.1175/2007JAMC1565.1.

- Boeckli, L., A. Brenning., S. Gruber., & J. Noetzli. (2012). Permafrost distribution in the European Alps: calculation and evaluation of an index map and summary statistics. *The Cryosphere*, 6(4), 807-820. doi:10.5194/tc-6-807-2012.
- Bogataj, L. (2007). How will the Alps Respond to Climate Change. *Alpine space–man & environment*, 3, 43-51. doi: 10.1007/s00024-005-2684-9.
- Bookhagen, B., & D. W. Burbank. (2010). Toward a complete Himalayan hydrological budget: Spatiotemporal distribution of snowmelt and rainfall and their impact on river discharge. *Journal of Geophysical Research: Earth Surface*, 115(F3), F03019. doi:10.1029/2009JF001426.
- Boyer, C., Chaumont, D., Chartier, I., & Roy, A.G. (2010). Impact of climate change on the hydrology of St. Lawrence tributaries. *Journal of Hydrology*, 384(1–2): 65-83. DOI: 10.1016/j.jhydrol.2010.01.011.
- Cayan, D.R., Dettinger, M.D., Kammerdiener, S.A., Caprio, J.M., & Peterson, D.H. (2001). Changes in the Onset of Spring in the Western United States. *Bulletin of the American Meteorological Society*, 82(3): 399-415. DOI:10.1175/1520-0477(2001)082<0399:CITOOS>2.3.CO;2.
- Chen, Y., C. Xu., Y. Chen., Y. Liu., & W. Li. (2013a). Progress, Challenges and Prospects of Eco-Hydrological Studies in the Tarim River Basin of Xinjiang, China. *Environmental Management*, 51(1), 138-153. doi:10.1007/s00267-012-9823-8.
- Chen, Y., H. Deng., B. Li., Z. Li., & C. Xu. (2014). Abrupt change of temperature and precipitation extremes in the arid region of Northwest China. *Quaternary International*, 336, 35-43. doi: 10.1016/j.quaint.2013.12.057.
- Chen, Y., K. Takeuchi., C. Xu., Y. Chen., & Z. Xu. (2006). Regional climate change and its effects on river runoff in the Tarim Basin, China. *Hydrological Processes*, 20(10), 2207-2216. doi:10.1002/hyp.6200.
- Chen, Y., Pang, Z., Hao., X., Xu., C., & Chen, Y. (2008). Periodic changes of stream flow in the last 40 years in Tarim River Basin, Xinjiang, China. *Hydrological Processes*, 22(21): 4214-4221. DOI:10.1002/hyp.7024.
- Chen, Y., W. Li, G. Fang., & Z. Li. (2016b). Hydrological modeling in glacierized catchments of Central Asia: status and challenges, *Hydrology and Earth System Sciences*, 1-23. doi:10.5194/hess-2016-325.
- Chen, Y., W. Li., H. Deng., G. Fang., & Z. Li. (2016a). Changes in Central Asia's Water Tower: Past, Present and Future. *Scientific Reports*, 6, 35458. doi:10.1038/srep35458.
- Chen, Y., Xu, C., Hao, X., Li, W., Chen, Y., Zhu, C., & Ye, Z. (2009). Fifty-year climate change and its effect on annual runoff in the Tarim River Basin, China. *Quaternary International*, 208(1): 53-61. doi:10.1016/j.quaint.2008.11.011.
- Chen, Y., Z. Li., Y. Fan., H. Wang., & H. Deng. (2015). Progress and prospects of climate change impacts on hydrology in the arid region of northwest China. *Environmental Research*, 139, 11-19. doi: 10.1016/j.envres.2014.12.029.

- Chen, Y.-n., Li, W.-h., Xu., C.-c., Hao., & X.-m. (2007). Effects of climate change on water resources in Tarim River Basin, Northwest China. *Journal of Environmental Sciences*, 19(4): 488-493. DOI: 10.1016/S1001-0742(07)60082-5.
- Chen, YN. (2014). *Water resources research in Northwest China*. Springer, New York. Doi:10.1007/978-94-017-8017-9.
- Chen, Z., Y. Chen., & B. Li (2013). Quantifying the effects of climate variability and human activities on runoff for Kaidu River Basin in arid region of northwest China. *Theoretical and applied climatology*, 111(3-4), 537-545. Doi:10.1007/s00704-012-0680-4.
- Chutko, K. J., & S. F. Lamoureux. (2009). The influence of low-level thermal inversions on estimated melt-season characteristics in the central Canadian Arctic. *International Journal of Climatology*, 29(2), 259-268. doi:10.1002/joc.1722.
- Cleveland, W.S., & Devlin, S.J. (1988). Locally weighted regression: an approach to regression analysis by local fitting. *Journal of the American Statistical Association*, 83(403): 596-610. DOI:10.2307/2289282.
- Clow, D.W. (2010). Changes in the timing of snowmelt and streamflow in Colorado: a response to recent warming. *Journal of Climate*, 23(9): 2293-2306. DOI: 10.1175/2009JCLI2951.1.
- Cornes, R. C., & P. D. Jones. (2013) How well does the ERA-Interim reanalysis replicate trends in extremes of surface temperature across Europe?. *Journal of Geophysical Research: Atmospheres*, 118(18), 10,262-210,276. doi:10.1002/jgrd.50799.
- Coumou, D., & S. Rahmstorf. (2012). A decade of weather extremes, *Nature Climate Change*, 2(7), 491-496. doi:10.1038/nclimate1452.
- Cullen R M., & S J Marshall. (2011). Mesoscale temperature patterns in the rocky mountains and foothills region of Southern Alberta. *Atmosphere-Ocean*, 49: 189-205. DOI: 10.1080/07055900.2011.592130.
- De Jong C., Collins D., & Ranzi R. (2005). *Climate and Hydrology in Mountain Areas*. Wiley: West Sussex, England. DOI: 10.1002/0470858249.
- de Jong, C. (2015). Challenges for mountain hydrology in the third millennium. *Frontiers in Environmental Science*, 3, 38. doi: 10.3389/fenvs.2015.00038.
- de Jong, C., D. Lawler., & R. Essery. (2009). Mountain Hydroclimatology and Snow Seasonality—Perspectives on climate impacts, snow seasonality and hydrological change in mountain environments. *Hydrological Processes*, 23(7), 955-961. doi:10.1002/hyp.7193.
- Deb, K., A. Pratap, S. Agarwal., & T. Meyarivan. (2002). A fast and elitist multiobjective genetic algorithm: NSGA-II. *IEEE Transactions on Evolutionary Computation*, 6(2), 182-197. doi:10.1109/4235.996017.
- Dee, D. P., Uppala, S. M., Simmons, A. J., Berrisford, P., Poli, P., et al. (2011). The ERA-Interim reanalysis: configuration and performance of the data assimilation system. *Quarterly Journal of the Royal Meteorological Society*, 137(656), 553-597. doi:10.1002/qj.828.

- Deng, H., Y. Chen., H. Wang., & S. Zhang. (2015). Climate change with elevation and its potential impact on water resources in the Tianshan Mountains, Central Asia. *Global and Planetary Change*, 135, 28-37. doi:10.1016/j.gloplacha.2015.09.015.
- Devia, G. K., B. P. Ganasri., & G. S. Dwarakish. (2015). A Review on Hydrological Models. *Aquatic Procedia*, 4, 1001-1007. doi: doi.org/10.1016/j.aapro.2015.02.126.
- Dickinson, R. E. (1984). *Modeling Evapotranspiration for Three-Dimensional Global Climate Models*, in *Climate Processes and Climate Sensitivity* (eds J. E. Hansen and T. Takahashi). Washington, DC: American Geophysical Union. doi: 10.1029/GM029p0058.
- Dile, Y. T., & R. Srinivasan (2014). Evaluation of CFSR climate data for hydrologic prediction in data-scarce watersheds: an application in the Blue Nile River Basin. *Journal of the American Water Resources Association*, 50(5), 1226-1241. doi:10.1111/jawr.12182.
- Dodson, R., & D. Marks. (1997). Daily air temperature interpolated at high spatial resolution over a large mountainous region. *Climate Research*, 8,1–20. doi:10.3354/cr008001.
- Doris, D., M. Christoph., J. Tong., & V. Sergiy. (2016). Projections for headwater catchments of the Tarim River reveal glacier retreat and decreasing surface water availability but uncertainties are large. *Environmental Research Letters*, 11(5), 054024. doi:10.1088/1748-9326/11/5/054024.
- Dou, Y., X. Chen., A. Bao., & L. Li (2011). The simulation of snowmelt runoff in the ungauged Kaidu River Basin of TianShan Mountains, China. *Environmental Earth Sciences*, 62(5), 1039-1045. DOI: 10.1007/s12665-010-0592-5.
- Duethmann, D., T. Bolch., D. Farinotti., D. Kriegel., S. Vorogushyn., B. Merz., T. Pieczonka., T. Jiang., B. Su., & A. Güntner. (2015). Attribution of streamflow trends in snow and glacier melt-dominated catchments of the Tarim River, Central Asia. *Water Resources Research*, 51(6), 4727-4750. doi:10.1002/2014WR016716.
- Easterling, D. R., G. A. Meehl., C. Parmesan., S. A. Changnon., T. R. Karl., & L. O. Mearns. (2000), Climate Extremes: Observations, Modeling, and Impacts, *Science*, 289(5487), 2068-2074. DOI: 10.1126/science.289.5487.2068.
- Ehret, U., E. Zehe., V. Wulfmeyer., K. Warrach-Sagi., & J. Liebert. (2012). HESS Opinions "Should we apply bias correction to global and regional climate model data?". *Hydrology and Earth System Sciences*, 16(9), 3391-3404. doi:10.5194/hess-16-3391-2012.
- Engelhardt, M., T. V. Schuler., & L. M. Andreassen. (2014). Contribution of snow and glacier melt to discharge for highly glacierised catchments in Norway. *Hydrology and Earth System Sciences*, 18(2), 511-523. doi:10.5194/hess-18-511-2014.
- Fang, G., J. Yang., Y. Chen., C. Xu., & P. De Maeyer. (2015). Contribution of meteorological input in calibrating a distributed hydrologic model in a watershed in the Tianshan Mountains, China. *Environmental Earth Sciences*, 74(3), 2413-2424. doi:10.1007/s12665-015-4244-7.
- Farinotti, D., L. Longuevergne., G. Moholdt., D. Duethmann., T. Molg., T. Bolch., S. Vorogushyn., & A. Guntner. (2015). Substantial glacier mass loss in the Tien Shan over the past 50 years. *Nature Geoscience*, 8(9), 716-722. doi:10.1038/ngeo2513.

- Fischer C., Kralisch S., & Flügel W-A. (2012). *An integrated, fast and easily useable software toolbox which allows comparative and complementary application of various parameter sensitivity analysis methods* (Seppelt R, Voinov AA, Lange S, Bankamp D (eds). International Congress on Environmental Modelling and Software.). In *Managing Resources of a Limited Planet, Sixth Biennial Meeting*, Leipzig, Germany.
- Fischer, C. (2013). *Automatische Kalibrierung hydrologischer Modelle: Entwicklung und Anwendung des Kalibrierungssystems OPTAS* (Doctoral dissertation). Faculty of Chemistry and Earth Sciences, Friedrich Schiller University Jena, Germany.
- Flügel, W.-A. (1995). Delineating hydrological response units by geographical information system analyses for regional hydrological modelling using PRMS/MMS in the drainage basin of the River Bröl, Germany. *Hydrological Processes*, 9(3-4), 423-436. doi:10.1002/hyp.3360090313.
- Frauenfeld, O. W., T. Zhang., & M. C. Serreze. (2005). Climate change and variability using European Centre for Medium-Range Weather Forecasts reanalysis (ERA-40) temperatures on the Tibetan Plateau. *Journal of Geophysical Research: Atmospheres*, 110, D02101, doi:10.1029/2004JD005230.
- Fu C.B., D. Li., W. Jian., & Wie. R.Q. (2013). Variation and abrupt change of maximum depth of frozen soil over Xinjiang under the background of global warming, 1961-2005. *Journal of Glaciology and Geocryology*, 35(6): 1410-1418. doi:10.7522/j.issn.1000-0240.2013.0156.(In Chinese with English abstract).
- Fu, A. H., Y. N. Chen., W. H. Li., B. F. Li., Y. H. Yang., & S. H. Zhang. (2013). Spatial and temporal patterns of climate variations in the Kaidu River Basin of Xinjiang, Northwest China. *Quaternary International*, 311(0), 117-122. doi: 10.1016/j.quaint.2013.08.041.
- Fu, G., J. Yu., X. Yu., R. Ouyang., Y. Zhang., P. Wang., W. Liu., & L. Min. (2013a). Temporal variation of extreme rainfall events in China, 1961–2009. *Journal of Hydrology*, 487, 48-59. doi: 10.1016/j.jhydrol.2013.02.021.
- Gao, L., M. Bernhardt., & K. Schulz. (2012). Elevation correction of ERA-Interim temperature data in complex terrain. *Hydrology and Earth System Sciences*, 16(12), 4661-4673. doi:10.5194/hess-16-4661-2012.
- Gardner, A. S., M. J. Sharp., R. M. Koerner., C. Labine., S. Boon., S. J. Marshall., D. O. Burgess., & D. Lewis. (2009). Near-surface temperature lapse rates over Arctic glaciers and their implications for temperature downscaling. *Journal of Climate*, 22(16), 4281–4298. doi:10.1175/2009JCLI2845.1.
- Grafton, R. Q., Grafton, R. Q., Pittock, J., Davis, R., Williams, J., Fu, G., Warburton, M., Udall, B., McKenzie, R., Yu, X., Che, N., Connell, D., Jiang, Q., Kompas, T., Lynch, A., Norris, R., Possingham, H., & Quiggin, J. (2013). Global insights into water resources, climate change and governance. *Nature Climate Change*, 3(4), 315-321. doi:10.1038/nclimate1746.
- Gruber, S. (2012). Derivation and analysis of a high-resolution estimate of global permafrost zonation. *The Cryosphere*, 6(1), 221-233. doi:10.5194/tc-6-221-2012.

- Guido, G., G. Scott., A. D. McGuire., E. R. Vladimir., & A. G. S. Edward. (2016). Changing permafrost in a warming world and feedbacks to the Earth system. *Environmental Research Letters*, 11(4), 040201. doi:10.1088/1748-9326/11/4/040201.
- Guo, Y., & Y. Shen. (2016). Agricultural water supply/demand changes under projected future climate change in the arid region of northwestern China. *Journal of Hydrology*, 540, 257-273. doi:10.1016/j.jhydrol.2016.06.033.
- Gupta, H. V., S. Sorooshian., & P. O. Yapo. (1999). Status of automatic calibration for hydrologic models: Comparison with multilevel expert calibration. *Journal of Hydrologic Engineering*, 4(2), 135-143. DOI:10.1061/(ASCE)1084-0699(1999)4:2(135).
- Hagg, W., L. Braun., M. Kuhn., & T. Nesgaard. (2007). Modelling of hydrological response to climate change in glacierized Central Asian catchments. *Journal of Hydrology*, 332(1), 40-53. doi:10.1016/j.jhydrol.2006.06.021.
- Hallett, J. (2002). Climate change 2001: The scientific basis. Edited by J. T. Houghton, Y. Ding, D. J. Griggs, N. Noguer, P. J. van der Linden, D. Xiaosu, K. Maskell & C. A. Johnson. Contribution of Working Group I to the Third Assessment Report of the Intergovernmental Panel on Climate Change, Cambridge University Press, Cambridge. 2001. 881 pp. ISBN 0521 01495 6. *Quarterly Journal of the Royal Meteorological Society*, 128: 1038–1039. doi:10.1002/qj.200212858119.
- Hao, X., W. Li, & H. Deng. (2016). The oasis effect and summer temperature rise in arid regions - case study in Tarim Basin. *Scientific Reports*, 6, 35418, doi:10.1038/srep35418.
- Harlow R C., E J Burke., R L Scott., W J Shuttleworth., C M Brown., & J R Petti. (2004). Derivation of temperature lapse rates in semi-arid south-eastern Arizona. *Hydrology and Earth System Sciences*, 8:1179-1185.
- Harris, I., P. D. Jones., T. J. Osborn., & D. H. Lister. (2014). Updated high-resolution grids of monthly climatic observations – the CRU TS3.10 Dataset. *International Journal of Climatology*., 34(3), 623-642. doi:10.1002/joc.3711.
- Hock, R. (1999). A distributed temperature-index ice- and snowmelt model including potential direct solar radiation. *Journal of Glaciology*, 45(149), 101-111. doi: 10.1017/S0022143000003087.
- Hock, R. (2003). Temperature index melt modelling in mountain areas. *Journal of Hydrology*, 282(1–4), 104-115. doi: 10.1016/S0022-1694(03)00257-9.
- Hock, R. (2005). Glacier melt: a review of processes and their modelling. *Progress in Physical Geography*, 29(3), 362-391. doi:10.1191/0309133305pp453ra.
- Hodgkins, G.A., Dudley, R.W., & Huntington, T.G. (2003). Changes in the timing of high river flows in New England over the 20th Century. *Journal of Hydrology*, 278(1-4): 244-252. DOI:10.1016/S0022-1694(03)00155-0.
- Hornberger, G. M., & R. C. Spear. (1981). Approach to the preliminary analysis of environmental systems. *Journal of Environmental Management*, 12(1), 7-18. DOI:10.1007/978-3-642-82054-0_3.
- Hu, Z., C. Zhang, Q. Hu, & H. Qin. (2014). Temperature changes in central Asia from 1979 to 2011 based on multiple datasets. *Journal of Climate*, 27(3), 1143–1167. doi:10.1175/JCLI-D-13-00064.1.

- Hu, Z., Q. Li., X. Chen., Z. Teng., C. Chen., G. Yin, & Y. Zhang. (2016). Climate changes in temperature and precipitation extremes in an alpine grassland of Central Asia. *Theoretical and Applied Climatology*, 126(3), 519-531. doi:10.1007/s00704-015-1568-x.
- Hu, Z., Q. Zhou., X. Chen., C. Qian., S. Wang., & J. Li. (2017). Variations and changes of annual precipitation in Central Asia over the last century. *International Journal of Climatology*, 37: 157–170. doi:10.1002/joc.4988.
- Huai, B., L. Zhongqin., S. Meiping., W. Wenbin., J. Shang., & L. Kaiming. (2015). Change in glacier area and thickness in the Tomur Peak, western Chinese Tien Shan over the past four decades. *Journal of Earth System Science*, 124(2), 353-363. doi:10.1007/s12040-015-0541-5.
- Huai, B., S. Weijun., W. Yetang., & L. Zhongqin. (2017). Glacier Shrinkage in the Chinese Tien Shan Mountains from 1959/1972 to 2010/2012. *Arctic, Antarctic, and Alpine Research*, 49(2), 213-225. doi:10.1657/AAAR0015-032.
- Huffman, G. J., D. T. Bolvin., E. J. Nelkin., D. B. Wolff., R. F. Adler., G. Gu., Y. Hong., K. P. Bowman., & E. F. Stocker. (2007). The TRMM Multisatellite Precipitation Analysis (TMPA): Quasi-Global, Multiyear, Combined-Sensor Precipitation Estimates at Fine Scales. *Journal of Hydrometeorology*, 8(1), 38-55. doi:10.1175/JHM560.1.
- Hughes, D. A. (2006). Comparison of satellite rainfall data with observations from gauging station networks. *Journal of Hydrology*, 327(3), 399-410. DOI: 10.1016/j.jhydrol.2005.11.041.
- Huss, M., G. Jouvett., D. Farinotti., & A. Bauder. (2010). Future high-mountain hydrology: a new parameterization of glacier retreat. *Hydrology and Earth System Sciences*, 14(5), 815-829. doi:10.5194/hess-14-815-2010.
- Imbery, S., M. Duishonakunov., Z. Sun., & L. King. (2013). Spatial and temporal variability of mean annual ground surface temperatures (MAGST) in the Gukur catchment, Central Tian Shan. *Neogeographie*, 2(1), 1-17.
- Immerzeel, W. (2008). Historical trends and future predictions of climate variability in the Brahmaputra basin. *International Journal of Climatology*, 28(2), 243-254. doi:10.1002/joc.1528.
- Immerzeel, W. W., & M. F. P. Bierkens. (2012). Asia's water balance. *Nature Geoscience*, 5(12), 841-842. DOI: 10.1038/ngeo1643.
- Immerzeel, W. W., F. Pellicciotti., & M. F. P. Bierkens. (2013). Rising river flows throughout the twenty-first century in two Himalayan glacierized watersheds. *Nature Geoscience*, 6(9), 742-745. doi:10.1038/ngeo1896.
- Immerzeel, W. W., L. P. H. van Beek., & M. F. P. Bierkens. (2010). Climate Change Will Affect the Asian Water Towers. *Science*, 328(5984), 1382-1385. DOI: 10.1126/science.1183188.
- Immerzeel, W. W., L. Petersen., S. Ragetti., & F. Pellicciotti. (2014). The importance of observed gradients of air temperature and precipitation for modeling runoff from a glacierized watershed in the Nepalese Himalayas. *Water Resources Research*, 50(3), 2212-2226. doi:10.1002/2013WR014506.

- Immerzeel, W. W., N. Wanders., A. F. Lutz., J. M. Shea., & M. F. P. Bierkens. (2015). Reconciling high-altitude precipitation in the upper Indus basin with glacier mass balances and runoff. *Hydrology and Earth System Sciences*, 19(11), 4673-4687. doi:10.5194/hess-19-4673-2015.
- Immerzeel, W.W., van Beek, L.P.H., Konz, M., Shrestha, A.B., Bierkens, & M.F.P. (2012). Hydrological response to climate change in a glacierized catchment in the Himalayas. *Climate Change*, 110(3): 721-736. DOI:10.1007/s10584-011-0143-4.
- IPCC, 2013: Summary for Policymakers. In: Climate Change. (2013), *The Physical Science Basis. Contribution of Working Group I to the Fifth Assessment Report of the Intergovernmental Panel on Climate Change* [Stocker, T.F., D. Qin, G.-K. Plattner, M. Tignor, S.K. Allen, J. Boschung, A. Nauels, Y. Xia, V. Bex and P.M. Midgley (eds.)]. Cambridge University Press, Cambridge, United Kingdom and New York, NY, USA.
- IPCC. (2007), Climate Change.2007: Synthesis Report. *Contribution of Working Groups I, II and III to the Fourth Assessment Report of the Intergovernmental Panel on Climate Change* [Core Writing Team, Pachauri, R.K and Reisinger, A.(eds.)]. IPCC, Geneva, Switzerland, 104 pp. Pang Z. (2014), Mechanism of water cycle changes and implications on water resources regulation in Xinjiang Uygur Autonomous Region. *Quaternary Sciences*, 2014, 34(5): 907-917 (In Chinese with English abstract).
- Jayatilaka, C. J., B. Storm., & L. B. Mudgway. (1998). Simulation of water flow on irrigation bay scale with MIKE-SHE. *Journal of Hydrology*, 208(1), 108-130. doi: 10.1016/S0022-1694(98)00151-6.
- Jiang Y-A, J., C. Ying, Z. Yi-Zhou, C. Peng-Xiang, Y. Xing-Jie, F. Jing, & B. Su-Qin. (2013). Analysis on Changes of Basic Climatic Elements and Extreme Events in Xinjiang, China during 1961–2010, *Advances in Climate Change Research*, 4(1), 20-29, doi: 10.3724/SP.J.1248.2013.020.
- Jin, H., S. Li., G. Cheng., W. Shaoling., & X. Li. (2000). Permafrost and climatic change in China. *Global and Planetary Change*, 26(4), 387-404. doi: 10.1016/S0921-8181(00)00051-5.
- Jobst A M., D G Kingston., N J Cullen., & P Sirguey. (2016). Combining thin-plate spline interpolation with a lapse rate model to produce daily air temperature estimates in a data-sparse alpine catchment. *International Journal of Climatology*, 37: 214–229. doi:10.1002/joc.4699.
- Justin, S. M., V. Daniel., S. Deepti., Y. H. Arjen., & S. D. Noah. (2015). The potential for snow to supply human water demand in the present and future. *Environmental Research Letters*, 10(11), 114016. DOI: 10.1088/1748-9326/10/11/114016.
- Kattel D B., T Yao., W Yang., Y Gao., & L Tian. (2015). Comparison of temperature lapse rates from the northern to the southern slopes of the Himalayas. *International Journal of Climatology*, 35: 4431–4443. doi:10.1002/joc.4297.
- Kattel, D. B., T. Yao., K. Yang., L. Tian., G. Yang., & D. Joswiak. (2013). Temperature lapse rate in complex mountain terrain on the southern slope of the central Himalayas. *Theoretical and Applied Climatology*, 113, 671–682. doi:10.1007/s00704-012-0816-6.
- Kendall, M., 1975. Multivariate analysis. Charles Griffin.

- Kirchner M., T Faus-Kessler., G Jakobi., M Leuchner., L Ries., H-E Scheel., & P Suppan. (2013). Altitudinal temperature lapse rates in an Alpine valley: trends and the influence of season and weather patterns. *International Journal of Climatology*, 33: 539–555. doi:10.1002/joc.3444.
- Knauf, D. (1980). *Die Berechnung des Abflusses aus einer Schneedecke*. Analyse und Berechnung oberirdischer Abflüsse DVWK-Schriften, Heft 46, Bonn.
- Knoche, M., C. Fischer., E. Pohl., P. Krause., & R. Merz. (2014). Combined uncertainty of hydrological model complexity and satellite-based forcing data evaluated in two data-scarce semi-arid catchments in Ethiopia. *Journal of Hydrology*, 519, 2049-2066, doi: 10.1016/j.jhydrol.2014.10.003.
- Kobold, M. (2005). Precipitation forecasts and their uncertainty as input into hydrological models. *Hydrology and Earth System Sciences*, 9(4), 322-332. doi:10.5194/hess-9-322-2005.
- Komatsu H., Hashimoto H., Kume T., Tanaka N., Yoshifuji N., Otsuki K., Suzuki M., & Kumagai T. (2010). Modeling seasonal changes in the temperature lapse rate in a northern Thailand mountainous area. *Journal of Applied Meteorology and Climatology*, 49(6): 1233–1246. DOI: 10.1175/2010JAMC2297.1.
- Kong, Y., & Pang, Z. (2012). Evaluating the sensitivity of glacier rivers to climate change based on hydrograph separation of discharge. *Journal of Hydrology*, 434–435: 121-129. DOI: 10.1016/j.jhydrol.2012.02.029.
- Kong, Y., Z. Pang., & K. Froehlich. (2013). Quantifying recycled moisture fraction in precipitation of an arid region using deuterium excess. *Tellus. Series B, Chemical and Physical Meteorology*, 65(1), 19251. doi:10.3402/tellusb.v65i0.19251.
- Konz, M., S. Uhlenbrook., L. Braun., A. Shrestha., & S. Demuth. (2007). Implementation of a process-based catchment model in a poorly gauged, highly glacierized Himalayan headwater. *Hydrology and Earth System Sciences*, 11(4), 1323-1339. doi:10.5194/hess-11-1323-2007.
- Koven, C. D., B. Ringeval., P. Friedlingstein., P. Ciais., P. Cadule., D. Khvorostyanov., G. Krinner., & C. Tarnocai. (2011). Permafrost carbon-climate feedbacks accelerate global warming. *Proceedings of the National Academy of Sciences*, 108(36), 14769-14774. doi: 10.1073/pnas.1103910108.
- Kralisch, S., and P. Krause (2006), *JAMS-A framework for natural resource model development and application*. In Proceedings of the International Environmental Software Society (IEMSS), Vermont, USA.
- Kralisch, S., P. Krause., M. Fink., C. Fischer., & W. A. Flügel. (2007). *Component based environmental modelling using the JAMS framework*. In MODSIM 2007 International Congress on Modelling and Simulation. Christchurch, New Zealand.
- Krause, P. (2001). *Das hydrologische Modellsystem J2000: Beschreibung und Anwendung in großen Flußeinzugsgebieten*. Schriften des Forschungszentrums Jülich. Reihe Umwelt/Environment; Band 29.
- Krause, P. (2002). Quantifying the impact of land use changes on the water balance of large catchments using the J2000 model. *Physics and Chemistry of the Earth, Parts A/B/C*, 27(9), 663-673. DOI:10.1016/S1474-7065(02)00051-7.

- Krause, P., D. P. Boyle., & F. Bäse. (2005). Comparison of different efficiency criteria for hydrological model assessment. *Advances in Geosciences*, 5, 89-97. doi:10.5194/adgeo-5-89-2005.
- Krysanova, V., M. Wortmann., T. Bolch., B. Merz., D. Duethmann., J. Walter., S. Huang., J. Tong., S. Buda., & Z. W. Kundzewicz. (2015). Analysis of current trends in climate parameters, river discharge and glaciers in the Aksu River basin (Central Asia). *Hydrological Sciences Journal*, 60(4), 566-590. doi:10.1080/02626667.2014.925559.
- Kuhn, M. (1987), Micro-meteorological conditions for snow melt. *Journal of Glaciology*, 33(113), 24-26. DOI: 10.1017/S002214300000530X.
- Kundzewicz, Z. W., B. Merz., S. Vorogushyn., H. Hartmann., D. Duethmann., M. Wortmann., S. Huang., B. Su., T. Jiang., & V. Krysanova. (2015). Analysis of changes in climate and river discharge with focus on seasonal runoff predictability in the Aksu River Basin. *Environmental Earth Sciences*, 73(2), 501-516. doi:10.1007/s12665-014-3137-5.
- Labat, D., Godd eris, Y., Probst, J.L., & Guyot, J.L. (2004). Evidence for global runoff increase related to climate warming. *Advances in Water Resources*, 27(6): 631-642. DOI: 10.1016/j.advwatres.2004.02.020.
- Lehner, B., K. Verdin., & A. Jarvis. (2008). New Global Hydrography Derived From Spaceborne Elevation Data. *Eos, Transactions American Geophysical Union*, 89(10), 93-94. doi:10.1029/2008EO100001.
- Leppi, J.C., DeLuca, T.H., Harrar, S.W., & Running, S.W. (2012). Impacts of climate change on August stream discharge in the Central-Rocky Mountains. *Climate Change*, 112(3): 997-1014. DOI:10.1007/s10584-011-0235-1.
- Lewkowicz A G, & P P Bonnaventure. (2011). Equivalent Elevation: A New Method to Incorporate Variable Surface Lapse Rates into Mountain Permafrost Modelling. *Permafrost and Periglacial Processes*, 22: 153-162. DOI:10.1002/ppp.720.
- Li Z., L. I., S. Yong-ping., & W. Teng-fei. (2007). Response of the melting Urumqi Glacier No. 1 in eastern Tianshan to climate change. *Advances in Climate Change Research*, 3(3), 132-137.
- Li, B., Y. Chen., & X. Shi. (2012). Why does the temperature rise faster in the arid region of northwest China?. *Journal of Geophysical Research: Atmospheres*, 117, D16115. doi:10.1029/2012JD017953.
- Li, D., M.L. Wrzisien., M. Durand., J.C. Adam., & D.P. Lettenmaier. (2017). How much western United States streamflow originates as snow? *Geophysical Research Letters*, 44(12), 6163-6172. doi: 10.1002/2017GL073551.
- Li, K., Z. Li., W. Gao., & L. Wang. (2011a). Recent glacial retreat and its effect on water resources in eastern Xinjiang. *Chinese Science Bulletin*, 56(33), 3596-3604. doi:10.1007/s11434-011-4720-8.
- Li, Q., Y. Chen., Y. Shen., X. Li., & J. Xu. (2011b). Spatial and temporal trends of climate change in Xinjiang, China. *Journal of Geographical Sciences*, 21(6), 1007-1018. DOI: 10.1007/s11442-011-0896-8.

- Li, X., & M. W. Williams. (2008). Snowmelt runoff modelling in an arid mountain watershed, Tarim Basin, China. *Hydrological Processes*, 22(19), 3931-3940. doi:10.1002/hyp.7098.
- Li, X., L. Wang., D. Chen., K. Yang., B. Xue., & L. Sun. (2013). Near-surface air temperature lapse rates in the mainland China during 1962–2011. *Journal of Geophysical Research: Atmospheres*, 118, 7505–7515. doi:10.1002/jgrd.50553.
- Li, X., Y. Ding., B. Ye., & T. Han. (2011c). Changes in physical features of Glacier No. 1 of the Tianshan Mountains in response to climate change. *Chinese Science Bulletin*, 56(26), 2820. doi:10.1007/s11434-011-4621-x.
- Li, Y., Z. Zeng., L. Zhao., & S. Piao. (2015). Spatial patterns of climatological temperature lapse rate in mainland China: A multi-time scale investigation. *Journal of Geophysical Research: Atmospheres*, 120, 2661–2675. doi:10.1002/2014JD022978.
- Li, Z., W. Wang., M. Zhang., F. Wang., & H. Li. (2010). Observed changes in streamflow at the headwaters of the Urumqi River, eastern Tianshan, central Asia. *Hydrological Processes*, 24(2), 217-224. doi:10.1002/hyp.7431.
- Ling, H., H. Xu., & J. Fu. (2014). Changes in intra-annual runoff and its response to climate change and human activities in the headstream areas of the Tarim River Basin, China. *Quaternary International*, 336, 158-170. doi: 10.1016/j.quaint.2013.08.003.
- Ling, H., H. Xu., J. Fu., Q. Zhang., & X. Xu. (2012). Analysis of temporal-spatial variation characteristics of extreme air temperature in Xinjiang, China. *Quaternary International*, 282, 14-26. DOI: 10.1016/j.quaint.2012.01.033.
- Liston, G. E., & K. Elder. (2006). A Distributed Snow-Evolution Modeling System (SnowModel). *Journal of Hydrometeorology*, 7(6), 1259-1276. doi:10.1175/JHM548.1.
- Liu, S., Y. Ding., D. Shangguan., Y. Zhang., J. Li., H. Han., J. Wang., & C. Xie. (2006). Glacier retreat as a result of climate warming and increased precipitation in the Tarim river basin, northwest China. *Annals of Glaciology*, 43(1), 91-96. DOI:10.3189/172756406781812168.
- Liu, T., H. Fang., P. Willems., A. M. Bao., X. Chen., F. Veroustraete., & Q. H. Dong. (2013). On the relationship between historical land-use change and water availability: the case of the lower Tarim River region in northwestern China. *Hydrological Processes*, 27(2), 251-261. doi:10.1002/hyp.9223.
- Liu, T., P. Willems., X. Pan., A. M. Bao., X. Chen., F. Veroustraete., & Q. Dong. (2011). Climate change impact on water resource extremes in a headwater region of the Tarim basin in China. *Hydrology and Earth System Sciences*, 15 (11)(4), p6593. DOI:10.5194/hessd-8-6593-2011.
- Liu, T., P. Willems., X. W. Feng., Q. Li., Y. Huang., A. M. Bao., X. Chen., F. Veroustraete & Q. H. Dong. (2012). On the usefulness of remote sensing input data for spatially distributed hydrological modelling: case of the Tarim River basin in China. *Hydrological Processes*, 26, 335-344. DOI:10.1002/hyp.8129.
- Liu, X., Y. Shen., H. Li., Y. Guo., H. Pei., & W. Dong. (2017). Estimation of land surface evapotranspiration over complex terrain based on multi-spectral remote sensing data. *Hydrological Processes*, 31:446–461. doi:10.1002/hyp.11042.

- Liu, Z., Z. Xu., J. Huang., S. P. Charles., & G. Fu. (2010). Impacts of climate change on hydrological processes in the headwater catchment of the Tarim River basin, China. *Hydrological Processes*, 24(2), 196-208. doi:10.1002/hyp.7493.
- Lu, Q., D. Zhao, & S. Wu. (2017). Simulated responses of permafrost distribution to climate change on the Qinghai–Tibet Plateau. *Scientific Reports*, 7(1), 3845. doi:10.1038/s41598-017-04140-7.
- Lundquist, J. D., & D. R. Cayan. (2007). Surface temperature patterns in complex terrain: Daily variations and long-term change in the central Sierra Nevada, California. *Journal of Geophysical Research: Atmospheres*, 112(D11). DOI:10.1029/2006JD007561
- Luo Y., J Arnold., P Allen., & X Chen. (2012). Baseflow simulation using SWAT model in an inland river basin in Tianshan Mountains, Northwest China. *Hydrology and Earth System Sciences*, 16: 1259-1267. doi:10.5194/hess-16-1259-2012.
- Luo, Y., J. Arnold., S. Liu., X. Wang., & X. Chen. (2013). Inclusion of glacier processes for distributed hydrological modeling at basin scale with application to a watershed in Tianshan Mountains, northwest China. *Journal of Hydrology*, 477, 72-85. doi:10.1016/j.jhydrol.2012.11.005.
- Mann, H.B., (1945). Nonparametric tests against trend. *Econometrica*, 33: 245-259. DOI: 0012-9682(194507)13:3<245:NTAT>2.0.CO;2-U.
- Mantovan, P., & E. Todini. (2006). Hydrological forecasting uncertainty assessment: Incoherence of the GLUE methodology. *Journal of Hydrology*, 330(1), 368-381. doi:10.1016/j.jhydrol.2006.04.046.
- Marchenko, S. S., A. P. Gorbunov., & V. E. Romanovsky. (2007). Permafrost warming in the Tien Shan mountains, central Asia. *Global and Planetary Change*, 56(3), 311-327. DOI: 10.1016/j.gloplacha.2006.07.023.
- Marks, D., J. Domingo., D. Susong., T. Link., & D. Garen. (1999). A spatially distributed energy balance snowmelt model for application in mountain basins. *Hydrological Processes*, 13(12-13), 1935-1959. DOI: 10.1002/(SICI)1099-1085(199909)13:12/13<1935::AID-HYP868>3.0.CO;2-C.
- Marshall, S. J., Sharp, M. J., Burgess, D. O. & Anslow, F. S. (2007). Near-surface-temperature lapse rates on the Prince of Wales Icefield, Ellesmere Island, Canada: implications for regional downscaling of temperature. *International Journal of Climatology*, 27: 385–398. doi:10.1002/joc.1396.
- Marshall, S., & M. Losic. (2011). *Temperature Lapse Rates in Glacierized Basins*, in Encyclopedia of Earth Sciences Series. Encyclopedia of Snow, Ice and Glaciers.
- Marston, R., & B. K. Marston. (2017). In book: International Encyclopedia of Geography, Edition: 1st, Publisher: Wiley, Editors: D. Richardson, N.Castree, M.F. Goodchild, A Kobayashi, W.Liu, R.A. Marston, pp.4532-4540.Meybeck, M., P. Green, xf, xf, and C. smarty. (2001), A New Typology for Mountains and Other Relief Classes: An Application to Global Continental Water Resources and Population Distribution, *Mountain Research and Development*, 21(1), 34-45. doi:10.1659/0276-4741(2001)021[0034:ANTFMA]2.0.CO;2.

- Middelkoop, H., K. Daamen., D. Gellens., W. Grabs., J. C. J. Kwadijk., H. Lang., B. W. A. H. Parmet., B. Schädler., J. Schulla., & K. Wilke. (2001). Impact of Climate Change on Hydrological Regimes and Water Resources Management in the Rhine Basin. *Climate Change*, 49(1), 105-128. doi:10.1023/A:1010784727448.
- Miller, J.E. (1984). Basic concepts of Kinematic-wave models. U.S. Geological Survey Professional Paper, 1302:32p. Washington.
- Milner, A. M., Khamis, K., Battin, T. J., Brittain, J. E., Barrand, N. E., Füreder, L., & Hodson, A. J. (2017). Glacier shrinkage driving global changes in downstream systems. *Proceedings of the National Academy of Sciences*, 114(37), 9770-9778. doi: 10.1073/pnas.1619807114.
- Minder, J. R., P. W. Mote., & J. D. Lundquist. (2010). Surface temperature lapse rates over complex terrain: Lessons from the Cascade Mountains. *Journal of Geophysical Research*, 115, D14122. doi:10.1029/2009JD013493.
- Molini, A., Katul, G.G., Porporato, A. (2011). Maximum discharge from snowmelt in a changing climate. *Geophysical Research Letters*, 38(5): L05402. DOI:10.1029/2010GL046477.
- Montanari, A. (2007). What do we mean by ‘uncertainty’? The need for a consistent wording about uncertainty assessment in hydrology. *Hydrological Processes*, 21(6), 841-845. doi:10.1002/hyp.6623.
- Montanari, A., C. A. Shoemaker., & N. van de Giesen. (2009). Introduction to special section on Uncertainty Assessment in Surface and Subsurface Hydrology: An overview of issues and challenges. *Water Resources Research*, 45, W00B00. doi:10.1029/2009WR008471.
- Mooney, P. A., F. J. Mulligan., & R. Fealy. (2011). Comparison of ERA-40, ERA-Interim and NCEP/NCAR reanalysis data with observed surface air temperatures over Ireland. *International Journal of Climatology*, 31(4), 545-557. doi:10.1002/joc.2098.
- Mote, P. W., A. F. Hamlet., M. P. Clark., & D. P. Lettenmaier. (2005). Declining mountain snowpack in western North America. *Bulletin of the American Meteorological Society*, 86(1). doi:10.1175/BAMS-86-1-39.
- Mountain Research Initiative, E. D. W. W. G. (2015). Elevation-dependent warming in mountain regions of the world. *Nature Climate Change*, 5(5), 424-430. doi:10.1038/nclimate2563.
- Nash, J. E., & J. V. Sutcliffe. (1970). River flow forecasting through conceptual models part I — A discussion of principles. *Journal of Hydrology*, 10(3), 282-290. doi: 10.1016/0022-1694(70)90255-6.
- National Soil Survey Office. (1995). *Soil Map of China (in Chinese)*. Beijing: China Map Press.
- Nepal S. (2012). *Evaluating upstream–downstream linkages of hydrological dynamics in the Himalayan region*(Doctoral dissertation). Faculty of Chemistry and Earth Sciences, Friedrich Schiller University Jena, Germany.
- Nepal, S., P. Krause., W. A. Flügel., M. Fink., & C. Fischer. (2014). Understanding the hydrological system dynamics of a glaciated alpine catchment in the Himalayan region using the J2000 hydrological model. *Hydrological Processes*, 28(3), 1329-1344. doi:10.1002/hyp.9627.

- Nijssen, B., G. M. O'Donnell., A. F. Hamlet., & D. P. Lettenmaier. (2001). Hydrologic sensitivity of global rivers to climate change. *Climate Change*, 50(1-2), 143-175.
- Nolin, A. W. (2012). Perspectives on Climate Change, Mountain Hydrology, and Water Resources in the Oregon Cascades, USA. *Mountain Research and Development*, 32(S1), S35-S46. doi:10.1659/MRD-JOURNAL-D-11-00038.S1.
- Pang, Z., Y. Kong., K. Froehlich., T. Huang., L. Yuan., Z. Li., & F. Wang. (2011). Processes affecting isotopes in precipitation of an arid region. *Tellus B*, 63(3), 352-359. doi:10.1111/j.1600-0889.2011.00532.x.
- Peng, X., T. Zhang., O. W. Frauenfeld., K. Wang., B. Cao., X. Zhong., s. Hang., & C. Mu. (2017). Response of seasonal soil freeze depth to climate change across China. *The Cryosphere*, 11, 1059-1073. doi:10.5194/tc-11-1059-2017.
- Pepin, N. C. (2001). Lapse rate changes in northern England. *Theoretical and Applied Climatolog*, 68(1-2), 1-16. doi:10.1007/s007040170049.
- Pepin, N. C., D. Benham., & K. Taylor. (1999). Modeling lapse rates in the maritime uplands of northern England: Implications for climate change. *Arctic, Antarctic and Alpine Research*, 31(2), 151-164.
- Petersen, L., & F. Pellicciotti. (2011). Spatial and temporal variability of air temperature on a melting glacier: Atmospheric controls, extrapolation methods and their effect on melt modeling, Juncal Norte Glacier, Chile. *Journal of Geophysical Research*, 116, D23109. doi:10.1029/2011JD015842.
- Petersen, L., F. Pellicciotti., I. Juszak., M. Carezzo., & B. W. Brock. (2013). Suitability of a constant air temperature lapse rate over an Alpine glacier: Testing the Greuell and Böhm model as an alternative. *Annals of Glaciology*, 54(63), 1-1. doi:10.3189/2013AoG63A477.
- Piao, S., P. Ciais., Y. Huang., Z. Shen., S. Peng., J. Li., L. Zhou., H. Liu., Y. Ma., & Y. Ding. (2010). The impacts of climate change on water resources and agriculture in China. *Nature*, 467(7311), 43-51. doi:10.1038/nature09364.
- Piontek, F., Müller, C., Pugh, T. A., Clark, D. B., Deryng, D., Elliott, J., & Frieler, K. (2014). Multisectoral climate impact hotspots in a warming world, PNAS, 111(9), 3233-3238. DOI: 10.1073/pnas.1222471110.
- Pohl, E., R. Gloaguen., C. Andermann., & M. Knoche. (2017). Glacier melt buffers river runoff in the Pamir Mountains. *Water Resources Research*, 53(3), 2467-2489. doi:10.1002/2016WR019431.
- Praskievicz, S., & H. Chang. (2009). A review of hydrological modelling of basin-scale climate change and urban development impacts. *Progress in Physical Geography*, 33(5), 650-671. doi:10.1177/0309133309348098.
- QIN D., B. Zhou., & C. Xiao. (2014). Progress in studies of cryospheric changes and their impacts on climate of China. *Acta Meteorologica Sinica*, 72(5): 869-879. (In Chinese with English abstract).
- Qin, D., & C. Xiao. (2009). Global climate change and cryospheric evolution in China. *EDP Sciences*. DOI:10.1140/epjconf/e2009-00907-x.

- R Core Team. (2016). *R: A language and environment for statistical computing*. R Foundation for Statistical Computing, Vienna, Austria. URL <https://www.R-project.org/>.
- Ragetti, S., F. Pellicciotti., R. Bordoy., & W. W. Immerzeel. (2013). Sources of uncertainty in modeling the glaciohydrological response of a Karakoram watershed to climate change. *Water Resources Research*, 49(9), 6048-6066. doi:10.1002/wrcr.20450.
- Ragetti, S., F. Pellicciotti., W. W. Immerzeel., E. S. Miles., L. Petersen., M. Heynen., J. M. Shea., D. Stumm., S. Joshi., & A. Shrestha. (2015). Unraveling the hydrology of a Himalayan catchment through integration of high resolution in situ data and remote sensing with an advanced simulation model. *Advances in Water Resources*, 78, 94-111. doi:10.1016/j.advwatres.2015.01.013.
- Ragetti, S., W. W. Immerzeel., & F. Pellicciotti. (2016). Contrasting climate change impact on river flows from high-altitude catchments in the Himalayan and Andes Mountains. *Proceedings of the National Academy of Sciences*, 113(33), 9222-9227. doi:10.1073/pnas.1606526113.
- Refsgaard, J. C., & J. Knudsen. (1996). Operational Validation and Intercomparison of Different Types of Hydrological Models. *Water Resources Research*, 32(7), 2189-2202. doi:10.1029/96WR00896.
- Reichle, R. H., C. S. Draper., Q. Liu., M. Girotto., S. P. P. Mahanama., R. D. Koster., & G. J. M. De Lannoy. (2017). Assessment of MERRA-2 land surface hydrology estimates. *Journal of Climate*, 30, 2937–2960. doi:10.1175/JCLI-D-16-0720.1.
- RGI Consortium. (2017). *Randolph Glacier Inventory – A Dataset of Global Glacier Outlines: Version 6.0*: Technical Report, Global Land Ice Measurements from Space, Colorado, USA. Digital Media. DOI: 10.7265/N5-RGI-60.
- Rolland, C. (2003). Spatial and seasonal variations of air temperature lapse rates in Alpine regions. *Journal of Climate*, 16, 1032–1046. doi:10.1175/1520-0442(2003)016<1032:SASVOA>2.0.CO;2.
- Salinger, M. J. (2005). *Climate Variability and Change: Past, Present and Future — an Overview*. in *Increasing Climate Variability and Change: Reducing the Vulnerability of Agriculture and Forestry*, edited by J. Salinger, M. V. K. Sivakumar and R. P. Motha, pp. 9-29, Springer Netherlands, Dordrecht. doi:10.1007/1-4020-4166-7_3.
- Sen, P.K. (1968). Estimates of the regression coefficient based on Kendall's tau. *Journal of the American Statistical Association*, 63(324): 1379-1389. DOI:10.2307/2285891.
- Senese, A., M. Maugeri., E. Vuillermoz., C. Smiraglia., & G. Diolaiuti. (2014). Using daily air temperature thresholds to evaluate snow melting occurrence and amount on Alpine glaciers by T-index models: the case study of the Forni Glacier (Italy). *The Cryosphere*, 8(5), 1921-1933. doi:10.5194/tc-8-1921-2014, 2014.
- Shangguan, D., S. Liu., Y. Ding., L. Ding., J. Xu., & L. Jing. (2009). Glacier changes during the last forty years in the Tarim Interior River basin, northwest China. *Progress in Natural Science*, 19(6), 727-732. doi:10.1016/j.pnsc.2008.11.002.

- Shea, J. M., W. W. Immerzeel, P. Wagnon, C. Vincent, & S. Bajracharya. (2015). Modelling glacier change in the Everest region, Nepal Himalaya. *The Cryosphere*, 9(3), 1105-1128. doi:10.5194/tc-9-1105-2015.
- Shen, Y., & Y. Chen (2010). Global perspective on hydrology, water balance, and water resources management in arid basins. *Hydrological Processes*, 24(2), 129-135. doi:10.1002/hyp.7428.
- Shen, Y., A. Xiong, Y. Wang, & P. Xie. (2010b). Performance of high-resolution satellite precipitation products over China. *Journal of Geophysical Research: Atmospheres*, 115, D02114. doi:10.1029/2009JD012097.
- Shen, Y., C. Liu, M. Liu, Y. Zeng, & C. Tian. (2010a). Change in pan evaporation over the past 50 years in the arid region of China. *Hydrological Processes*, 24(2), 225-231. doi:10.1002/hyp.7435.
- Shen, Y., H. Su, G. Wang, W. Mao, S. Wang, P. Han, N. Wang, & Z. Li. (2013c). The responses of glaciers and snow cover to climate change in Xinjiang (1): hydrological effect. *Journal of Glaciology and Geocryology*, 35(3), 513-527 (In Chinese with English abstract).
- Shen, Y., S. Li, Y. Chen, Y. Qi, & S. Zhang. (2013). Estimation of regional irrigation water requirement and water supply risk in the arid region of Northwestern China 1989–2010. *Agricultural Water Management*, 128, 55-64. doi:10.1016/j.agwat.2013.06.014.
- Shen, Y., Y. Chen, C. Liu, & K. Smettem. (2013a). Ecohydrology of the inland river basins in the Northwestern Arid Region of China. *Ecohydrology*, 6(6), 905-908. doi:10.1002/eco.1441.
- Shen, Y.-J., Y. Shen, J. Goetz, & A. Brenning. (2016). Spatial-temporal variation of near-surface temperature lapse rates over the Tianshan Mountains, Central Asia. *Journal of Geophysical Research: Atmospheres*, 121, 14,006–14,017. doi:10.1002/2016JD025711.
- Shen, Y.-J., Y. Shen, M. Fink, S. Kralisch, Y. Chen, & A. Brenning. (2018). Trends and variability in streamflow and snowmelt runoff timing in the southern Tianshan Mountains, *Journal of Hydrology*, 557, 173-181, doi:10.1016/j.jhydrol.2017.12.035.
- Sheridan, P., S. Smith, A. Brown, & S. Vosper. (2010). A simple height- based correction for temperature downscaling in complex terrain. *Meteorological Applications*, 17, 329–339. doi:10.1002/met.177.
- Shi Y F. (2005). *Concise Chinese Glacier Inventory* (Shanghai: Shanghai Scientific Popularization Press), pp. 17–188.
- Shi, X., D. Yu, E. D. Warner, X. Pan, G. W. Petersen, Z. G. Gong, & D. C. Weindorf (2004). Soil database of 1:1,000,000 digital soil survey and reference system of the Chinese genetic soil classification system. *Soil Survey Horizons*, 45, 129–136. DOI: 10.2136/sh2004.4.0129.
- Shi, Y., Y. Shen, E. Kang, D. Li, Y. Ding, G. Zhang, & R. Hu. (2007). Recent and future climate change in northwest China. *Climatic Change*, 80(3–4), 379–393. DOI:10.1007/s10584-006-9121-7.
- Singh, P., & V. P. Singh. (2001). *Snow and Glaciers Hydrology*, (Doctoral dissertation). Kluwer Acad., Netherlands.

- Sorg, A., T. Bolch., M. Stoffel., O. Solomina., & M. Beniston. (2012). Climate change impacts on glaciers and runoff in Tien Shan (Central Asia). *Nature Climate Change*, 2(10), 725-731. doi:10.1038/nclimate1592. .
- Stedinger, J. R., R. M. Vogel., S. U. Lee., & R. Batchelder. (2008). Appraisal of the generalized likelihood uncertainty estimation (GLUE) method. *Water Resources Research*, 44, W00B06. doi:10.1029/2008WR006822.
- Stewart, I.T., Cayan, D.R., & Dettinger, M.D. (2004). Changes in Snowmelt Runoff Timing in Western North America under a 'Business as Usual' Climate Change Scenario. *Climate Change*, 62(1): 217-232. DOI:10.1023/B:CLIM.0000013702.22656.e8.
- Stewart, I.T., Cayan, D.R., & Dettinger, M.D. (2005). Changes toward Earlier Streamflow Timing across Western North America. *Journal of Climate*, 18(8): 1136-1155. DOI:10.1175/JCLI3321.1.
- Sun, C., J. Yang., Y. Chen., X. Li., Y. Yang., & Y. Zhang. (2016). Comparative study of streamflow components in two inland rivers in the Tianshan Mountains, Northwest China. *Environmental Earth Sciences*, 75(9), 727. doi:10.1007/s12665-016-5314-1.
- Sun, M., Z. Li., X. Yao., M. Zhang., & S. Jin. (2015). Modeling the hydrological response to climate change in a glacierized high mountain region, northwest China. *Journal of Glaciology*, 61(225), 127-136. doi:10.3189/2015JoG14J033.
- Tahir, A. A., P. Chevallier., Y. Arnaud., L. Neppel., & B. Ahmad. (2011). Modeling snowmelt-runoff under climate scenarios in the Hunza River basin, Karakoram Range, Northern Pakistan. *Journal of Hydrology*, 409(1–2), 104-117. doi: 10.1016/j.jhydrol.2011.08.035.
- Tan, A., Adam, J.C., & Lettenmaier, D.P. (2011). Change in spring snowmelt timing in Eurasian Arctic rivers. *Journal of Geophysical Research: Atmospheres*, 116: D03101. DOI:10.1029/2010JD014337.
- Tang, Z., & J. Fang. (2006). Temperature variation along the northern and southern slopes of Mt. Taibai, China. *Agricultural and Forest Meteorology*, 139, 200–207. doi:10.1016/j.agrformet.2006.07.001.
- Tao, H., M. Gemmer., Y. Bai., B. Su., & W. Mao. (2011). Trends of streamflow in the Tarim River Basin during the past 50 years: Human impact or climate change?. *Journal of Hydrology*, 400(1–2), 1-9. doi: 10.1016/j.jhydrol.2011.01.016.
- Tarasova, L., M. Knoche., J. Dietrich., & R. Merz. (2016). Effects of input discretization, model complexity, and calibration strategy on model performance in a data-scarce glacierized catchment in Central Asia. *Water Resources Research*, 52(6), 4674-4699. doi:10.1002/2015WR018551.
- Taylor, K. E. (2001). Summarizing multiple aspects of model performance in a single diagram. *Journal of Geophysical Research: Atmospheres*, 106(D7), 7183-7192. doi:10.1029/2000JD900719.
- Terink, W., A. F. Lutz., G. W. H. Simons., W. W. Immerzeel., & P. Droogers. (2015). SPHY v2.0: Spatial Processes in HYdrology. *Geoscientific Model Development*, 8(7), 2009-2034. doi:10.5194/gmd-8-2009-2015.

- Tian, D. H., Z. P. Hong., C. Peng., & Q. J. Ke. (2016). Hydrological effects of alpine permafrost in the headwaters of the Urumqi River, Tianshan Mountains. *Sciences in Cold and Arid Regions*, 8(3), 241-249. doi: 10.1002/hyp.7201.
- Tian, L., T. Yao., K. MacClune., J. W. C. White., A. Schilla., B. Vaughn., R. Vachon., & K. Ichiyangi. (2007). Stable isotopic variations in west China: A consideration of moisture sources, *Journal of Geophysical Research: Atmospheres*, 112, D10112. doi:10.1029/2006JD007718.
- Vihma, T. (2011). *Atmosphere-snow/ice interactions*, in *Encyclopedia of Snow, Ice and Glaciers*, 66-75. DOI:10.1007/978-90-481-2642-2_31.
- Vincent, L. A., X. L. Wang., E. J. Milewska., H. Wan., F. Yang., & V. Swail. (2012). A second generation of homogenized Canadian monthly surface air temperature for climate trend analysis. *Journal of Geophysical Research*, 117, D18110. doi:10.1029/2012JD017859.
- Viviroli, D., & R. Weingartner. (2004). The hydrological significance of mountains: from regional to global scale. *Hydrology and Earth System Sciences*, 8(6), 1017-1030. doi:10.5194/hess-8-1017-2004.
- Viviroli, D., et al. (2011), Climate change and mountain water resources: overview and recommendations for research, management and policy, *Hydrology and Earth System Sciences*, 15(2), 471-504. doi:10.5194/hess-15-471-2011.
- Viviroli, D., H. H. Dürr., B. Messerli., M. Meybeck., & R. Weingartner. (2007). Mountains of the world, water towers for humanity: Typology, mapping, and global significance. *Water Resources Research*, 43, W07447. doi:10.1029/2006WR005653.
- Viviroli, D., R. Weingartner., & B. Messerli. (2003). Assessing the Hydrological Significance of the World's Mountains. *Mountain Research and Development*, 23(1), 32-40. DOI: 10.1659/0276-4741(2003)023[0032:ATHSOT]2.0.CO;2.
- Voigt, C., et al. (2017). Increased nitrous oxide emissions from Arctic peatlands after permafrost thaw. *Proceedings of the National Academy of Sciences*, 114(24), 6238-6243. DOI: 10.1073/pnas.1702902114.
- Wang J, H Li., & X Hao. (2010). Responses of snowmelt runoff to climatic change in an inland river basin, Northwestern China, over the past 50 years. *Hydrology and Earth System Sciences*, 14: 1979-1987. doi:10.5194/hess-14-1979-2010.
- Wang X L., & Y Feng. (2013). RHtestsV4 user manual. http://etccdi.pacificclimate.org/RHtest/RHtestsV4_UserManual_10Dec2014.pdf.
- Wang, B., M. Zhang., J. wie., S. Wang., S. Li., Q. Ma., X. Li., & S. Pan. (2013a). Changes in extreme events of temperature and precipitation over Xinjiang, northwest China, during 1960–2009. *Quaternary International*, 298, 141-151.
- Wang, H. L., Y. T. Gan., R. Y. Wang., J. Y. Niu., H. Zhao., Q. G. Yang., & G. C. Li. (2008a). Phenological trends in winter wheat and spring cotton in response to climate changes in northwest China. *Agricultural and Forest Meteorology*, 148(8), 1242-1251. doi: 10.1016/j.agrformet.2008.03.003.

- Wang, H., Y. Chen., & Z. Chen. (2013b). Spatial distribution and temporal trends of mean precipitation and extremes in the arid region, northwest of China, during 1960–2010. *Hydrological Processes*, 27(12), 1807-1818. doi:10.1002/hyp.9339.
- Wang, H., Y. Chen., S. Xun., D. Lai., Y. Fan., & Z. Li. (2013d). Changes in daily climate extremes in the arid area of northwestern China. *Theoretical and Applied Climatology*, 112(1-2), 15-28. doi:10.1007/s00704-012-0698-7.
- Wang, H., Y. Chen., W. Li., & H. Deng. (2013). Runoff responses to climate change in arid region of northwestern China during 1960–2010. *Chinese Geographical Science*, 23(3), 286-300. doi:10.1007/s11769-013-0605-x.
- Wang, J., Li, H., & Hao, X. (2010). Responses of snowmelt runoff to climatic change in an inland river basin, Northwestern China, over the past 50 years. *Hydrology and Earth System Sciences*, 14(10): 1979-1987. DOI:10.5194/hess-14-1979-2010.
- Wang, L., & W. Chen. (2014). A CMIP5 multimodel projection of future temperature, precipitation, and climatological drought in China. *International Journal of Climatology*, 34(6), 2059-2078. doi:10.1002/joc.3822.
- Wang, L., Z. Li., F. Wang., & R. Edwards. (2017a). Glacier shrinkage in the Ebinur lake basin, Tien Shan, China, during the past 40 years. *Journal of Glaciology*, 60(220), 245-254. doi:10.3189/2014JoG13J023.
- Wang, Q., Li, H. J., Wei, R. Q., & Wang, X. M. (2005). Annual change and abrupt change of the seasonal frozen soil in Xinjiang, China during 1961–2002. *Journal of Glaciology and Geocryology*, 27(6), 820-826(In Chinese with English abstract).
- Wang, S., M. Zhang., M. Sun., B. Wang., X. Huang., Q. Wang., & F. Feng. (2015). Comparison of surface air temperature derived from NCEP/DOE R2, ERA-Interim, and observations in the arid northwestern China: a consideration of altitude errors. *Theoretical and Applied Climatology*, 119(1-2), 99-111. DOI:10.1007/s00704-014-1107-1.
- Wang, X. (2007). Penalized maximal t test for detecting undocumented mean shift without trend change. *Journal of Applied Meteorology and Climatology*, 46, 916–931. doi:10.1175/JAM2504.1.
- Wang, X. (2008a). Accounting for autocorrelation in detecting mean shifts in climate data series using the penalized maximal t or F test. *Journal of Applied Meteorology and Climatology*, 47, 2423–2444. doi:10.1175/2008JAMC1741.1.
- Wang, X. L., H. Chen., Y. Wu., Y. Feng., & Q. Pu. (2010). New techniques for detection and adjustment of shifts in daily precipitation data series. *Journal of Applied Meteorology and Climatology*, 49 (12), 2416-2436. DOI:10.1175/2010JAMC2376.1.
- Wang, X., L. Liu., L. Zhao., T. Wu., Z. Li., & G. Liu. (2017b). Mapping and inventorying active rock glaciers in the northern Tien Shan of China using satellite SAR interferometry. *The Cryosphere*, 11(2), 997-1014. doi:10.5194/tc-11-997-2017.
- Wang, X., Z. Xie., Q. Li., S. Wang., & L. Cheng. (2008b). Sensitivity analysis of glacier systems to climate warming in China. *Journal of Geographical Sciences*, 18(2), 190. doi:10.1007/s11442-008-0190-6.

- Wang, Y., Y. Shen., F. Sun., & Y. Chen. (2014). Evaluating the vegetation growing season changes in the arid region of northwestern China. *Theoretical and Applied Climatology*, 118(3), 569-579. doi:10.1007/s00704-013-1078-7.
- Wang, Y., Y. Shen., Y. Chen., & Y. Guo. (2013e). Vegetation dynamics and their response to hydroclimatic factors in the Tarim River Basin, China. *Ecohydrology*, 6(6), 927-936. doi:10.1002/eco.1255.
- Wang, Y.-J., & D.-H. Qin. (2017). Influence of climate change and human activity on water resources in arid region of Northwest China: An overview. *Advances in Climate Change Research*, DOI: 10.1016/j.accre.2017.08.004.
- Weingartner, R., D. Viviroli., & B. Schädler. (2007). Water resources in mountain regions: a methodological approach to assess the water balance in a highland-lowland-system. *Hydrological Processes*, 21(5), 578-585. doi:10.1002/hyp.6268.
- Whiteman C D. (2000). *Mountain meteorology: fundamentals and applications*. Oxford University Press. New York, p 355.
- Whiteman, C. D., X. Bian., & S. Zhong. (1999). Wintertime evolution of the temperature inversion in the Colorado Plateau Basin. *Journal of Applied Meteorology*, 38, 1103 – 1117.
- Worqlul, A. W., B. Maathuis., A. A. Adem., S. S. Demissie., S. Langan., & T. S. Steenhuis. (2014). Comparison of rainfall estimations by TRMM 3B42, MPEG and CFSR with ground-observed data for the Lake Tana basin in Ethiopia. *Hydrology and Earth System Sciences*, 18(12), 4871-4881. doi:10.5194/hess-18-4871-2014.
- Wu, J. (2012). Evaluation of the water resource reproducible ability on Tarim River Basin in south of Xinjiang, northwest China. *Environmental Earth Sciences*, 66(7), 1731-1737. DOI 10.1007/s12665-011-1396-y.
- Wu, Z., H. Zhang., C. M. Krause., & N. S. Cobb. (2010). Climate change and human activities: a case study in Xinjiang, China. *Climate Change*, 99(3), 457-472. doi:10.1007/s10584-009-9760-6.
- Xiao, C., et al. (2007). Observed changes of cryosphere in China over the second half of the 20th century: an overview. *Annals of Glaciology*, 46, 382-390. doi:10.3189/172756407782871396.
- Xu, C., Chen, Y., Yang, Y., Hao, X., & Shen, Y. (2010). Hydrology and water resources variation and its response to regional climate change in Xinjiang. *Journal of Geographical Sciences*, 20(4): 599-612. DOI: 10.1007/s11442-010-0599-6.
- Xu, C., J. Li., J. Zhao., S. Gao., & Y. Chen. (2015a). Climate variations in northern Xinjiang of China over the past 50 years under global warming. *Quaternary International*, 358, 83-92. doi: 10.1016/j.quaint.2014.10.025.
- Xu, C., J. Zhao, H. Deng., G. Fang., J. Tan., D. He., Y. Chen., Y. Chen., & A. Fu. (2016a). Scenario-based runoff prediction for the Kaidu River basin of the Tianshan Mountains, Northwest China. *Environmental Earth Sciences*, 75(15), 1126. doi:10.1007/s12665-016-5930-9.
- Xu, C., Y. Chen., W. Li., & Y. Chen. (2006). Climate change and hydrologic process response in the Tarim River Basin over the past 50 years. *Chinese Science Bulletin*, 51(1), 25-36. doi:10.1007/s11434-006-8204-1.

- Xu, C., Y. Chen., Y. Yang., X. Hao., & Y. Shen. (2010). Hydrology and water resources variation and its response to regional climate change in Xinjiang. *Journal of Geographical Sciences*, 20(4), 599-612. doi:10.1007/s11442-010-0599-6.
- Xu, C.-y. (2002). Hydrologic models, Uppsala University, Department of Earth Sciences and Hydrology.
- Xu, H., B. Zhou., & Y. Song. (2011). Impacts of climate change on headstream runoff in the Tarim River Basin. *Hydrology Research*, 42(1), 20. DOI: 10.2166/nh.2010.069.
- Xu, J., S. Liu., W. Guo., Z. Zhang., J. wie., & T. Feng. (2015b). Glacial Area Changes in the Ili River Catchment (Northeastern Tian Shan) in Xinjiang, China, from the 1960s to 2009. *Advances in Meteorology*, 12. doi:10.1155/2015/847257.
- Xu, J., Y. Chen., L. Bai., & Y. Xu. (2016b). A hybrid model to simulate the annual runoff of the Kaidu River in northwest China. *Hydrology and Earth System Sciences*, 20(4), 1447-1457. doi:10.5194/hess-20-1447-2016.
- Xu, J., Y. Chen., W. Li., M. Ji., & S. Dong. (2009). The complex nonlinear systems with fractal as well as chaotic dynamics of annual runoff processes in the three headwaters of the Tarim River. *Journal of Geographical Sciences*, 19(1), 25-35. DOI: 10.1007/s11442-009-0025-0.
- Xu, Z., Y. Chen., & J. Li. (2004). Impact of climate change on water resources in the Tarim River basin. *Water Resources Management*, 18(5), 439-458. DOI:10.1023/B:WARM.0000049142.95583.98.
- Yang, T., X. Wang., Z. Yu., V. Krysanova., X. Chen., F. W. Schwartz., & E. A. Sudicky. (2014). Climate change and probabilistic scenario of streamflow extremes in an alpine region. *Journal of Geophysical Research: Atmospheres*, 119, 8535–8551. doi:10.1002/2014JD021824.
- Yang, Y., Y. Chen., W. Li., M. Wang., & G. Sun. (2010). Impacts of climatic change on river runoff in northern Xinjiang of China over last fifty years. *Chinese Geographical Science*, 20(3), 193-201. doi:10.1007/s11769-010-0193-y.
- Yao, J. Q., Q. Yang., W. Y. Mao., Y. Zhao., & X. B. Xu. (2016). Precipitation trend-Elevation relationship in arid regions of the China. *Global and Planetary Change*, 143, 1-9. doi:10.1016/j.gloplacha.2016.05.007.
- Yao, T., J. Pu., A. Lu., Y. Wang., & W. Yu. (2007). Recent Glacial Retreat and Its Impact on Hydrological Processes on the Tibetan Plateau, China, and Surrounding Regions. *Arctic, Antarctic and Alpine Research*, 39(4), 642-650.
- Yao, T., Y. Wang., S. Liu., J. Pu., Y. Shen., & A. Lu. (2004). Recent glacial retreat in High Asia in China and its impact on water resource in Northwest China. *Science in China Series D Earth Sciences*, 47(12), 1065-1075. doi:10.1360/03yd0256.
- Yatagai, A., K. Kamiguchi., O. Arakawa., A. Hamada., N. Yasutomi., & A. Kitoh. (2012). APHRODITE: Constructing a Long-Term Daily Gridded Precipitation Dataset for Asia Based on a Dense Network of Rain Gauges. *Bulletin of the American Meteorological Society*, 93(9), 1401-1415. doi:10.1175/BAMS-D-11-00122.1.

- Ye, B., D. Yang., K. Jiao., T. Han., Z. Jin., H. Yang., & Z. Li. (2005). The Urumqi River source Glacier No. 1, Tianshan, China: Changes over the past 45 years. *Geophysical Research Letters*, 32(21), L21504. doi:10.1029/2005GL024178.
- Ye, Z., H. Liu., Y. Chen., S. Shu., Q. Wu., & S. Wang. (2017). Analysis of water level variation of lakes and reservoirs in Xinjiang, China using ICESat laser altimetry data (2003–2009). *PLoS One*, 12(9), e0183800. doi:10.1371/journal.pone.0183800.
- Yin, Z.-Y., H. Wang., & X. Liu. (2014). A Comparative Study on Precipitation Climatology and Interannual Variability in the Lower Midlatitude East Asia and Central Asia. *Journal of Climate*, 27(20), 7830-7848. doi:10.1175/JCLI-D-14-00052.1.
- Yong, Z., L. Shiyin., & D. Yongjian. (2007). Glacier meltwater and runoff modelling, Keqicar Baqi glacier, southwestern Tien Shan, China. *Journal of Glaciology*, 53(180), 91-98. DOI: 10.3189/172756507781833956.
- Yongjian, D. (1998), *Recent degradation of permafrost in China and the response to climatic warming*. In Proceedings of the 7th International Conference of Permafrost. Yellowknife, Canada (pp. 23-27).
- You, Q., J. Min., W. Zhang., N. Pepin., & S. Kang. (2015). Comparison of multiple datasets with gridded precipitation observations over the Tibetan Plateau. *Climate Dynamics*, 45(3), 791-806. doi:10.1007/s00382-014-2310-6.
- You, Q., K. Fraedrich., G. Ren., N. Pepin., & S. Kang. (2013). Variability of temperature in the Tibetan Plateau based on homogenized surface stations and reanalysis data. *International Journal of Climatology*, 33(6), 1337-1347. doi:10.1002/joc.3512.
- You, Q., S. Kang., E. Aguilar., N. Pepin., W.-A. Flügel., Y. Yan., Y. Xu., Y. Zhang., & J. Huang. (2011). Changes in daily climate extremes in China and their connection to the large scale atmospheric circulation during 1961–2003. *Climate Dynamics*, 36(11-12), 2399-2417.
- Zhai, P., & X. Pan. (2003). Trends in temperature extremes during 1951–1999 in China. *Geophysical Research Letters*, 30(17), 1913. doi:10.1029/2003GL018004.
- Zhai, P., X. Zhang., H. Wan., & X. Pan. (2005). Trends in Total Precipitation and Frequency of Daily Precipitation Extremes over China. *Journal of Climate*, 18(7), 1096-1108. doi:10.1175/JCLI-3318.1.
- Zhang S., B Ye., S Liu., X Zhang., & S Hagemann. (2012). A modified monthly degree-day model for evaluating glacier runoff changes in China. Part I: model development. *Hydrological Processes*, 26: 1686-1696. DOI:10.1002/hyp.8286.
- Zhang, F., H. Zhang., S. C. Hagen., M. Ye., D. Wang., D. Gui., C. Zeng., L. Tian., & J. Liu (2015). Snow cover and runoff modelling in a high mountain catchment with scarce data: effects of temperature and precipitation parameters. *Hydrological Processes*, 29(1), 52-65. doi:10.1002/hyp.10125.
- Zhang, F., S. Ahmad., H. Zhang., X. Zhao., X. Feng., & L. Li. (2016). Simulating low and high streamflow driven by snowmelt in an insufficiently gauged alpine basin. *Stochastic Environmental Research and Risk Assessment*, 30(1), 59-75. doi:10.1007/s00477-015-1028-2.

- Zhang, Q., C.-Y. Xu., H. Tao., T. Jiang., & Y. D. Chen. (2010). Climate changes and their impacts on water resources in the arid regions: a case study of the Tarim River basin, China. *Stochastic Environmental Research and Risk Assessment*, 24(3), 349-358. doi:10.1007/s00477-009-0324-0.
- Zhang, Q., X. Gu., V. P. Singh., P. Sun., X. Chen., & D. Kong. (2016a). Magnitude, frequency and timing of floods in the Tarim River basin, China: Changes, causes and implications. *Global and Planetary Change*, 139, 44-55. doi:10.1016/j.gloplacha.2015.10.005.
- Zhang, S., B. Ye., S. Liu., X. Zhang., & S. Hagemann. (2012a). A modified monthly degree-day model for evaluating glacier runoff changes in China. Part I: model development. *Hydrological Processes*, 26(11), 1686-1696. doi:10.1002/hyp.8286.
- Zhang, X., L. Alexander., G. C. Hegerl., P. Jones., A. K. Tank., T. C. Peterson., B. Trewin., & F. W. Zwiers. (2011). Indices for monitoring changes in extremes based on daily temperature and precipitation data. *Wiley Interdisciplinary Reviews: Climate Change*, 2(6), 851-870, doi:10.1002/wcc.147.
- Zhang, Y., B. Li., A. Bao., C. Zhou., X. Chen., & X. Zhang. (2007). Study on snowmelt runoff simulation in the Kaidu River basin. *Science in China Series D Earth Sciences*, 50(1), 26-35. doi:10.1007/s11430-007-5007-4.
- Zhang, Y., L. Fu., J. Pan., & Y. Xu. (2017). Projected Changes in Temperature Extremes in China Using PRECIS. *Atmosphere*, 8(1), doi:10.3390/atmos8010015.
- Zhang, Y., W. wie., F. Jiang., M. Liu., W. Wang., L. Bai., & K. Li. (2012b). Brief communication "Assessment of change in temperature and precipitation over Xinjiang, China", *Natural hazards and earth system sciences. Discuss.* doi:10.5194/nhess-12-1327-2012.
- Zhang, Y., Y. Luo., L. Sun., S. Liu., X. Chen., & X. Wang. (2016b). Using glacier area ratio to quantify effects of melt water on runoff. *Journal of Hydrology*, 538, 269-277, doi: 10.1016/j.jhydrol.2016.04.026.
- Zhang, Y., Y. Xu., W. Dong., L. Cao., & M. Sparrow. (2006). A future climate scenario of regional changes in extreme climate events over China using the PRECIS climate model. *Geophysical Research Letters*, 33(24), L24702. doi:10.1029/2006GL027229.
- Zhao, H. Y., Jun-Qin, G., Cun-Jie, Z., Lan-Dong, S., Xu-Dong, Z., Jing-Jing, L., ... & Yan-Chun, L. (2014). Climate Change Impacts and Adaptation Strategies in Northwest China. *Advances in Climate Change Research*, 5(1), 7-16. doi: 10.3724/SP.J.1248.2014.007.
- Zhao, J., S Zhou., Y He., Y Ye., & S Liu. (2006). ESR dating of glacial tills and glaciations in the Urumqi River headwaters, Tianshan Mountains, China. *Quaternary International*, 144(1), 61-67. doi:10.1016/j.quaint.2005.05.013.
- Zhao, L., Q. Wu., S. S. Marchenko., & N. Sharkhuu. (2010). Thermal state of permafrost and active layer in Central Asia during the International Polar Year. *Permafrost and Periglacial Processes*, 21(2), 198-207. DOI: 10.1002/ppp.688.
- Zhou, H., Li, W., Wang, Y., & Ye, Z. (2016). Characteristics of Stable Isotopes in an Inland Lake and Their Implications for Water Management in Northwestern China. *Journal of Water Resource and Protection*, 8(06): 631. DOI: 10.4236/jwarp.2016.86052.

Zhuang, X.W., Li, Y.P., Huang, G.H., & Liu, J. (2015). Assessment of climate change impacts on watershed in cold-arid region: an integrated multi-GCM-based stochastic weather generator and stepwise cluster analysis method. *Climate Dynamics*, 1-19. DOI:10.1007/s00382-015-2831-7.

Appendices

Supporting information for chapter 2

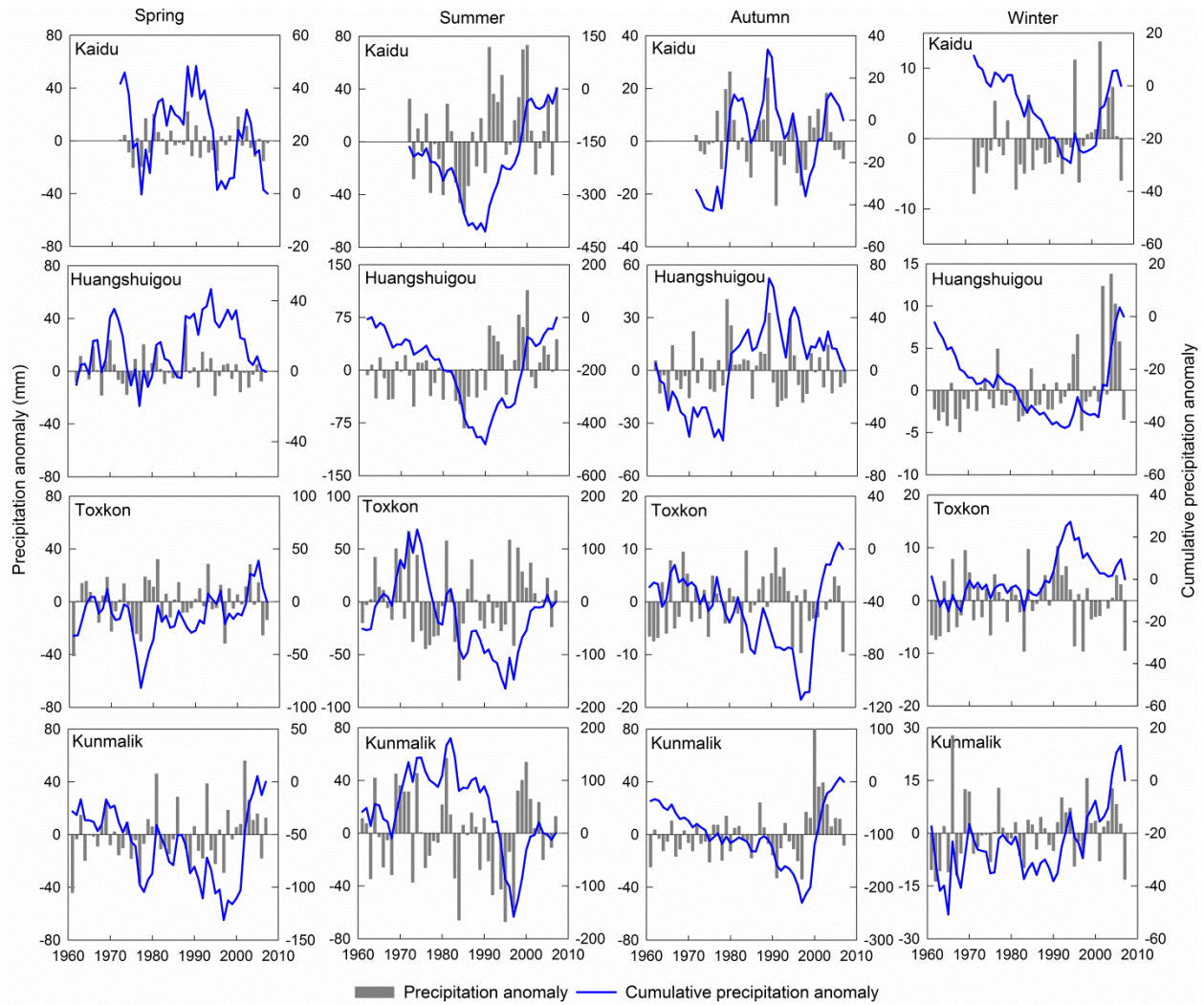


Figure s2.1. Seasonal and cumulative anomalies of precipitation in the Kaidu (1972-2008), Huangshuigou (1962-2008), Toxkon (1961-2007) and Kunmalik (1961-2007) basins.

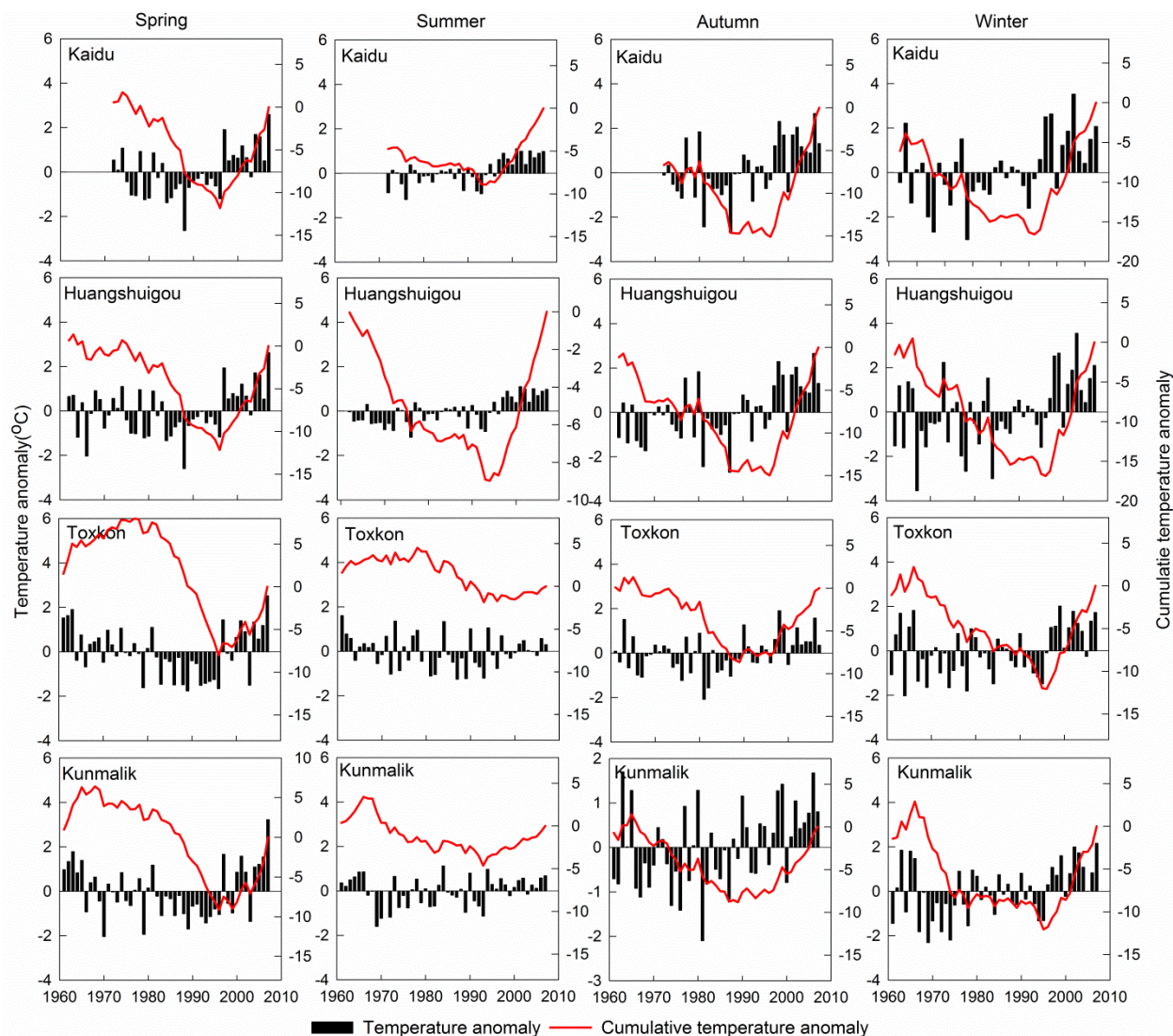


Figure s2.2. Seasonal and cumulative anomalies of temperature in the Kaidu (1972-2008), Huangshuigou (1962-2008), Toxkon (1961-2007) and Kunmalik (1961-2007) basins.

Supporting information for chapter 3

Figure S3.1 provides the spatial variation of annual mean precipitation on the Northern and Southern slopes over Tianshan Mountains, which combine with the distribution of temperature data (Figure 3.2) together illustrate that the Tianshan Mountains can be divided into different subregions based on the topography and climatic conditions.

Figure S3.2 is used to validate the reliability of HOBO-logger data. Due to the different data availability, the HOBO-logger data (2014.09-2015.08) was compared with long-term average (1961-2011) Bayinbuluke(BYBLK) station (2458 m a.s.l) data inside Kaidu Basin. The station H2

was chosen from HOBO-logger data due to the close range of altitude (2470 m a.s.l) and geographical location near the BYBLK station. Generally, temperature data (Tmax, Tmean and Tmin) from station H2 is correlated with the station-observed data (BYBLK). Figure S3.2 suggests that the HOBO data-loggers generally represent the monthly average temperature pattern in the Tianshan Mountains.

Figure S3.3 and Figure S3.4 are implied to verify whether the single station (elevation: 1739 m) on the south slope play a great role in the lapse rate calculation. Linear regressions were examined separately with and without the single Baluntai (BLT) station. The fit didn't improve when the single station was removed and we failed to reject the null hypothesis at 95% for Tmin both with and without the single high station ($P = 0.38$ and 0.55 , respectively; Figure S3.3 ab). For Tmean, the linear regression is significant with the single station (Figure S3.4, $P < 0.05$), while rejects the null hypothesis without the station (Figure S3.4 b, $P = 0.18$). The findings indicated that the Tmin is less related to elevation. Since Tmean was calculated with Tmax and Tmin, thus, the uncertainties from Tmin will obviously change the regression slope of Tmean. In addition, a possible drawback to perform the regression analysis with the annual mean data sets is that the winter temperature inversion will also bias the slope and intercept, especially for Tmin. This is one of the only high elevation stations in the southern slopes of Tianshan Mountains, and we have no evidence to believe that the measurement data should be regarded as an outlier. Thus, the best model in this case may still be linear regression, which can be used to describe the relationship between elevation and temperature on the annual scale.

For compare purpose, Figure S3.5 reveals the winter temperature inversion in monthly scales in the Kaidu Basin.

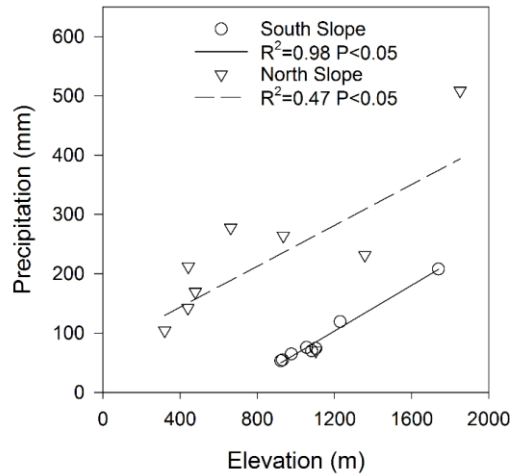


Figure S3.1. Linear fit for the relationship between annual mean precipitation and elevation (1961-2011).

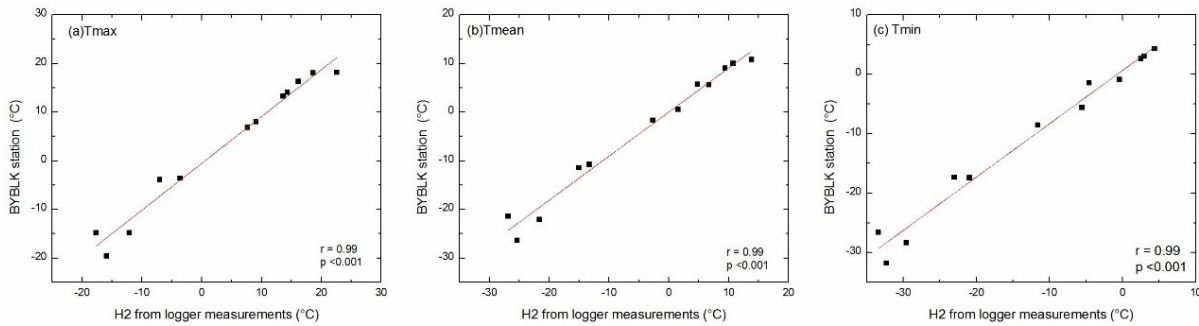


Figure S3.2. Comparison of monthly Tmax(a), Tmean(a) and Tmin(a) between logger measurements with BYBLK station. Red lines are linear regression.

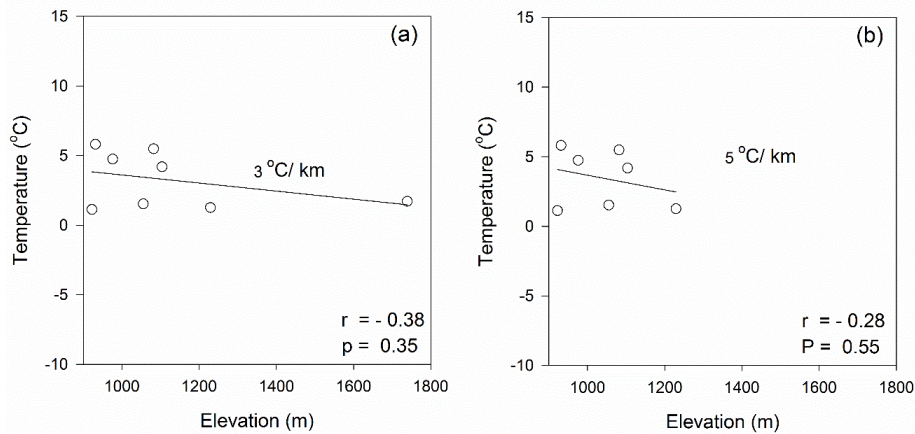


Figure S3.3. Altitudinal variation in the minimum annual temperature (Tmin) with its linear fit and γ_{local} for the Southern slopes of the Tianshan Mountains, with (a) and without (b) the highest mountain station.

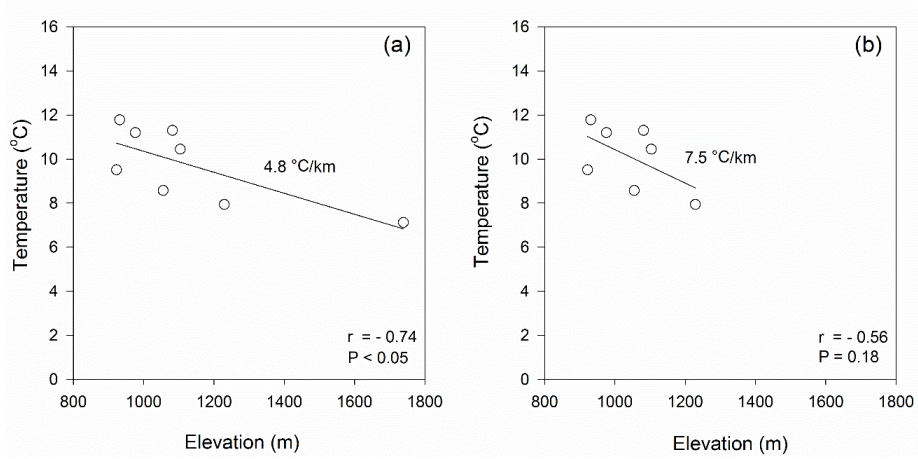


Figure S3.4. Altitudinal variation in the mean annual temperature (T_{mean}) with its linear fit and γ_{local} for the Southern slopes of the Tianshan Mountains, with (a) and without (b) the highest mountain station.

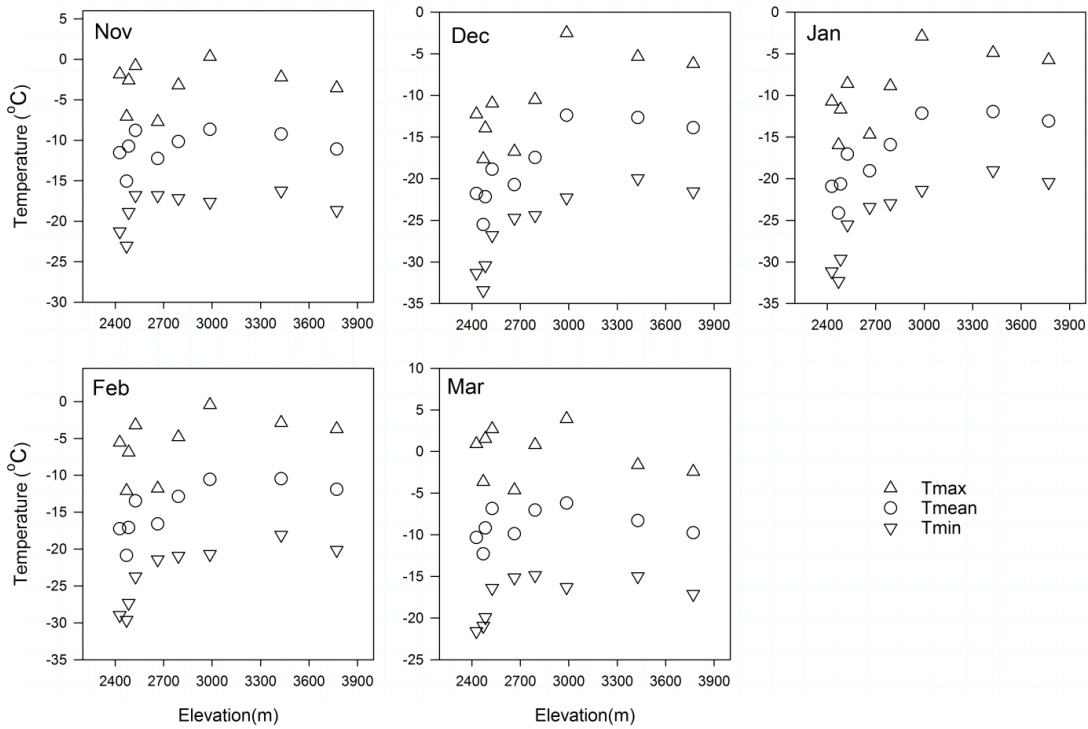


Figure S3.5. Relationship between elevation with temperature (T_{max} , T_{mean} and T_{min}) in winter time in Kaidu Basin.

Supporting information for chapter 4

Figure S4.1 shows spatial resolution of APHRODITE, CRU, CFSR, ERA-Interim, MERRA-2 and TRMM products and the corresponding gridded points in the Kaidu Basin. APHRODITE and TRMM data have the same gridded box $0.25^\circ \times 0.25^\circ$. The resolution of CRU and CFSR gridded datasets are $0.5^\circ \times 0.5^\circ$ and $0.3125^\circ \times 0.3125^\circ$, respectively. The resolution of MERRA-2 is $0.625^\circ \times 0.5^\circ$ while the resolution of ERA-interim is $0.125^\circ \times 0.125^\circ$.

Figure S4.2 illustrates the relationship between annual precipitation and elevations on the southern slopes over the Tianshan Mountains. The linear regression showed that precipitation gradient in this study can be obtained based on the stations on the southern slopes of the Tianshan Mountains.

Figure S4.3 shows the HRUs which were delineated by overlaying different geospatial datasets. The HRUs are even distributed in the Kaidu Basin which can generally represent the local relief and geographical units.

Figure S4 gives the information of the known reservoirs before the outlet of the Kaidu Basin. We don't have too much information about the reservoirs, especially the operation information. Given the evident impacts of the reservoirs, post-reservoir period was provided only for information in the manuscript. Detailed information on the reservoirs are not directly relevant to our study. However, the basic information might be useful for other studies in this basin. There are two reservoirs before the outlet. The Dashankou reservoir is the main reservoir in the Kaidu Basin which was commissioned in December 1992. The design storage and regulation storage are $0.29^8 \times 10^8 \text{ m}^3$ and $6 \times 10^6 \text{ m}^3$, respectively. The Chahanwusu reservoir started construction in 2004 and came to operation in 2007. The design storage and regulation storage of Chahanwusu reservoir are $1.76 \times 10^8 \text{ m}^3$ and $1.15 \times 10^8 \text{ m}^3$, respectively. More reservoirs were planned in the past decades.

Figure S4.5-S4.8. Taylor diagrams show seasonal comparisons of gridded precipitation products compared with the corresponding observation stations. Seasonally, most gridded products have dissatisfactory performance (Figures S4.5-S4.8). CFSR and ERA-Interim had higher SD and RMS than the other datasets, and the correlations with the station data were below 0.5 in nearly all the seasons, except for the Bayinbuluke station. CRU and MERRA-2 performed inconsistent in different seasons and at different stations. For the mountainous Bayinbuluke station, the RMS of MERRA-2 is higher than CRU in all the seasons. CRU has lower correlation coefficients with the

observation than MERRA-2. However, the highest correlation coefficients and smallest RMS were found in APHRODITE in all the seasons.

Figure S4.9 shows mean monthly difference between elevation corrected ERA-Interim gridded data and nine HOBO weather stations. The largest bias in winter may be due to temperature inversion in the Kaidu Basin, which was well captured by the HOBO stations but not the ERA-Interim temperature data.

Figure S4.10. Simulated and observed monthly streamflow during the (a) calibration (1982–1986) and (b) validation period (1987–1991). And scatter plots of simulated and observed monthly streamflow during the (c) calibration (1982–1986) and (d) validation period (1987–1991). The simulated streamflow from April to June are lower than the observed streamflow in the calibration period (Figure S10a). Simulated streamflow from July to September are generally higher than the observed streamflow (Figure S10ab). The correlation coefficients (r^2) of simulated and observed streamflow in the calibration and validation periods are 0.83 and 0.86, respectively. Generally, monthly comparison of observed and simulated streamflow demonstrated that the performance of the J2000 model is generally acceptable.

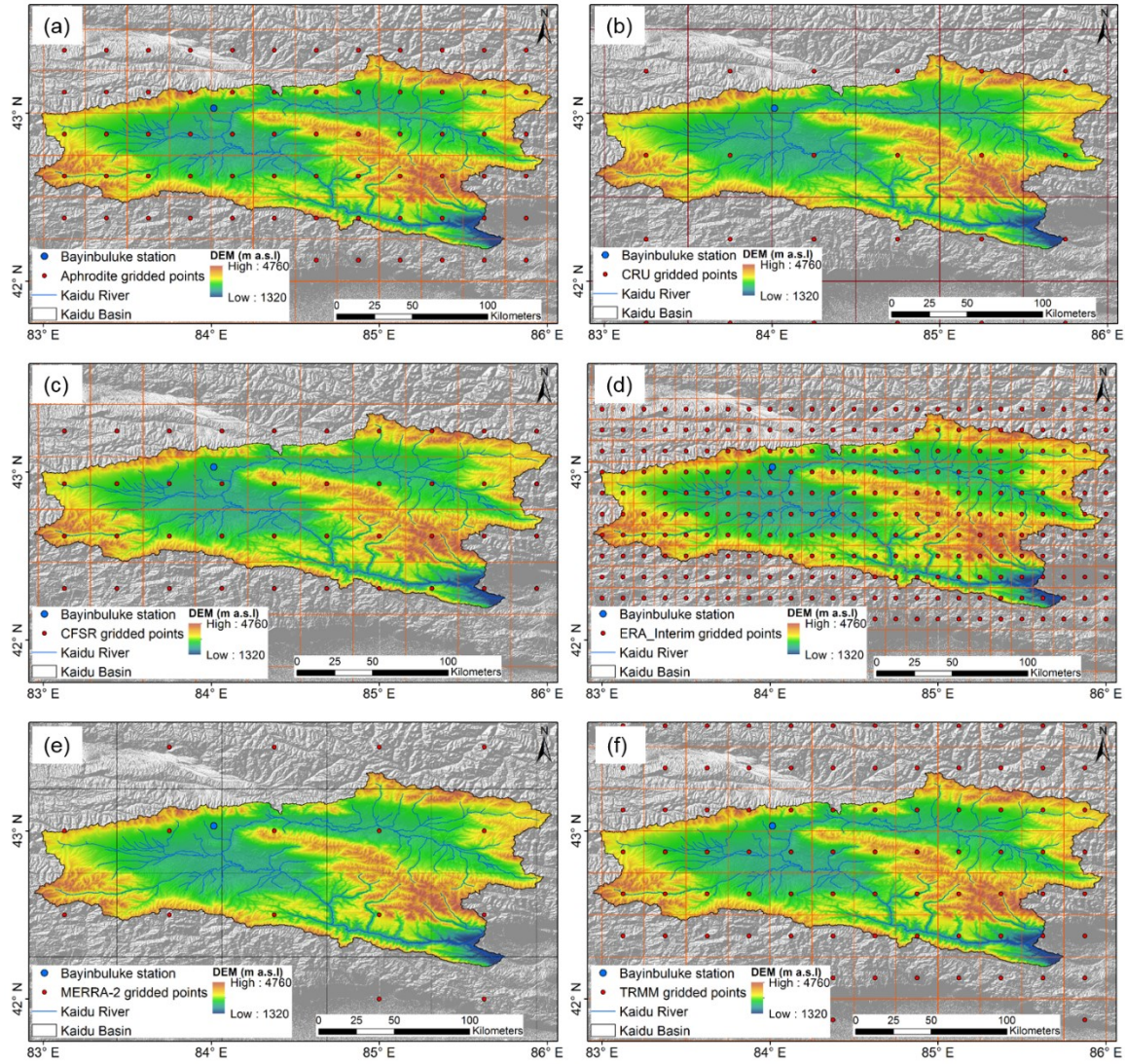


Figure S4.1. Spatial resolution of different gridded products: (a) APHRODITE, (b) CRU, (c) CFSR, (d) ERA_Interim, (e) MERRA-2 and (f) TRMM.

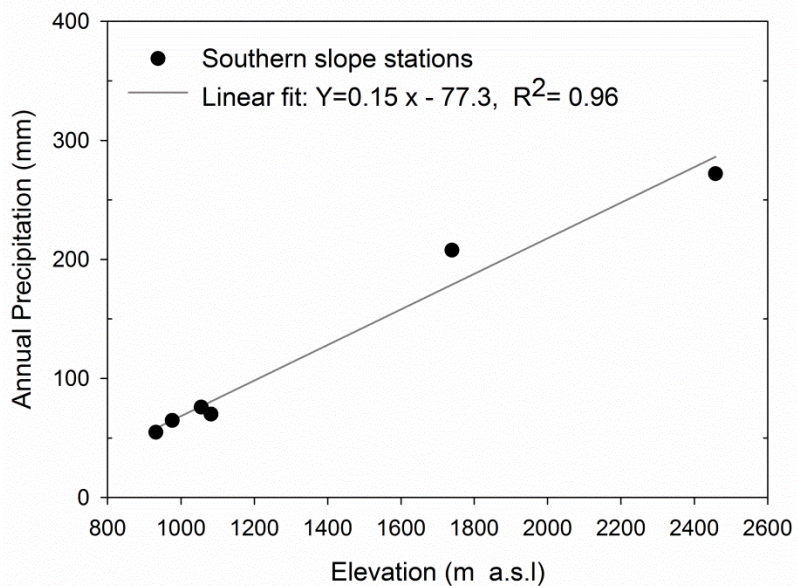


Figure S4.2. Linear regression of annual precipitation and elevations on the southern slopes of Tianshan Mountains (1961-2011).

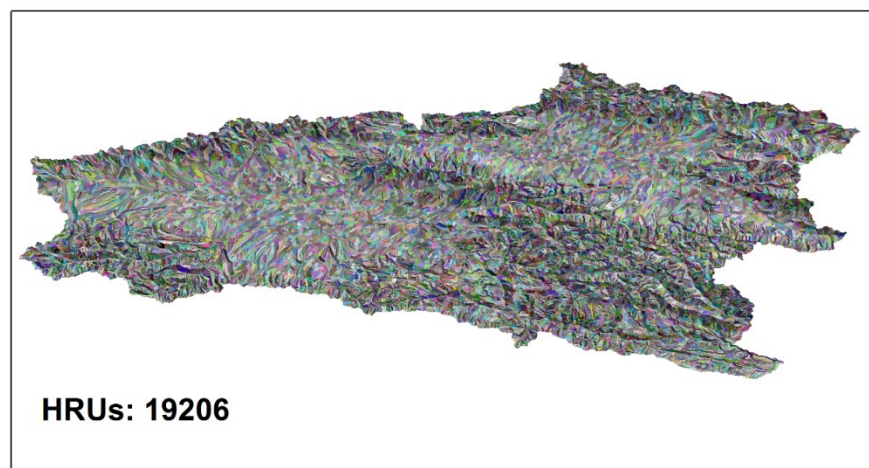


Figure S4.3. 19,206 HRUs were delineated based on DEM, lithology, Land use/Land cover and soil datasets.

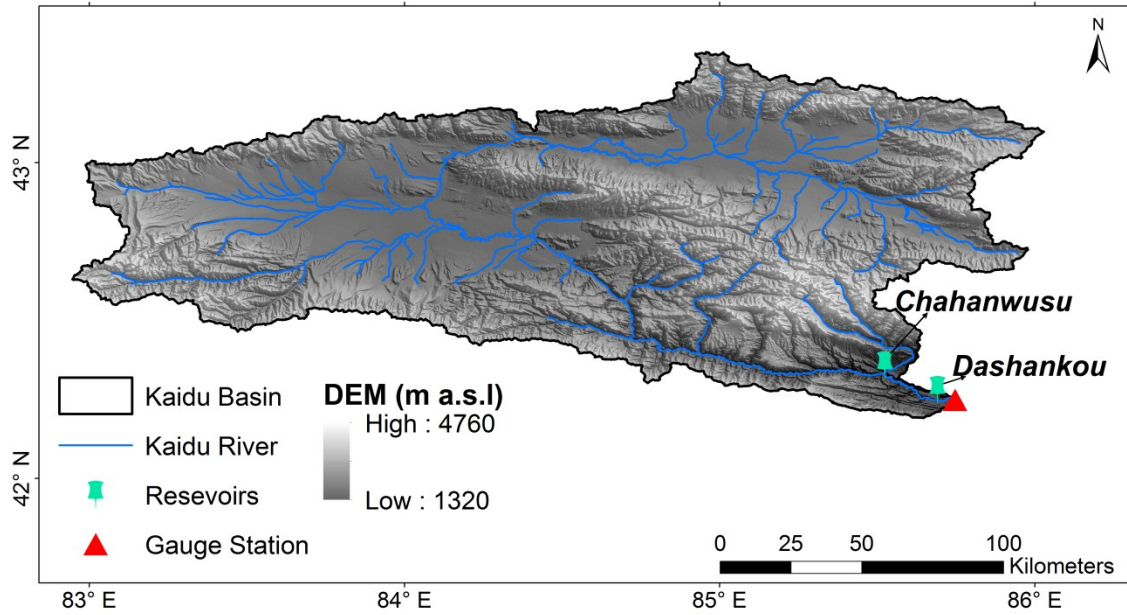


Figure S4.4. Known reservoirs before the outlet in the Kaidu Basin.

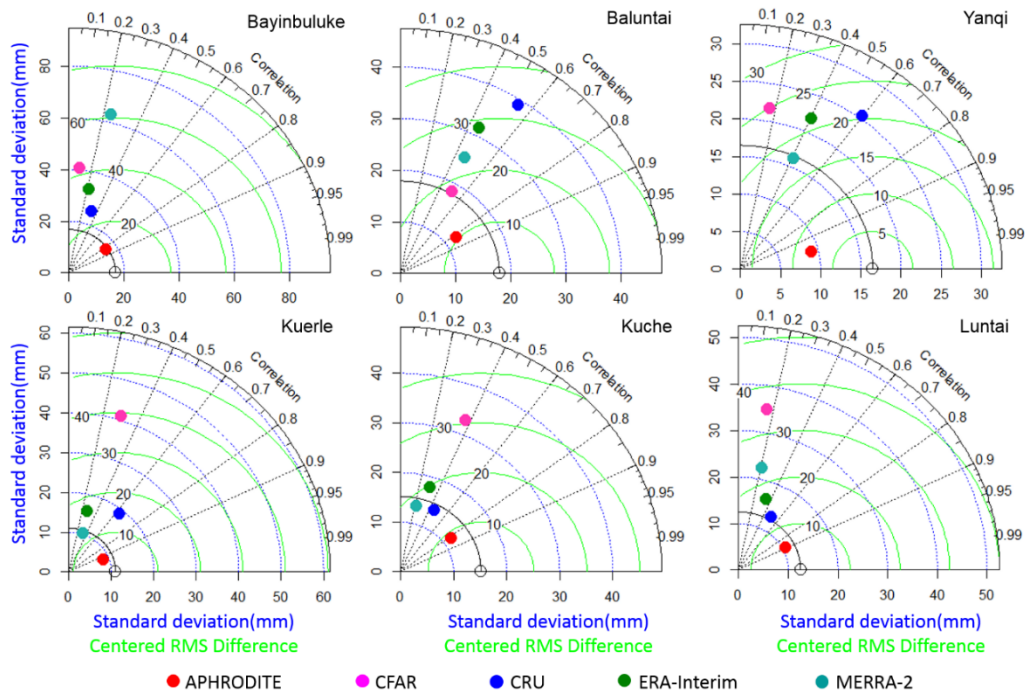


Figure S4.5. Taylor diagrams for displaying correlation coefficient, SD and RMS of mean spring precipitation from observational stations and different gridded products based on the overlapping period 1979–2007. The azimuthal position gives correlation coefficient. The blue radial coordinates and the green concentric semi-circles indicate SD and RMS values, respectively.

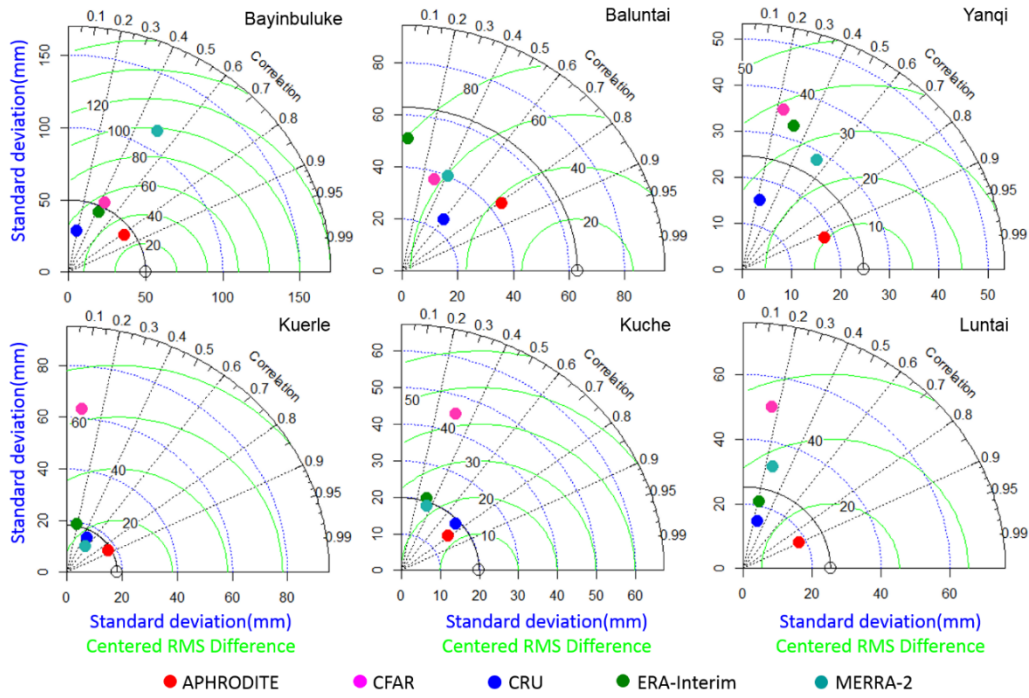


Figure S4.6. Same as Figure S4.5 but for summer precipitation.

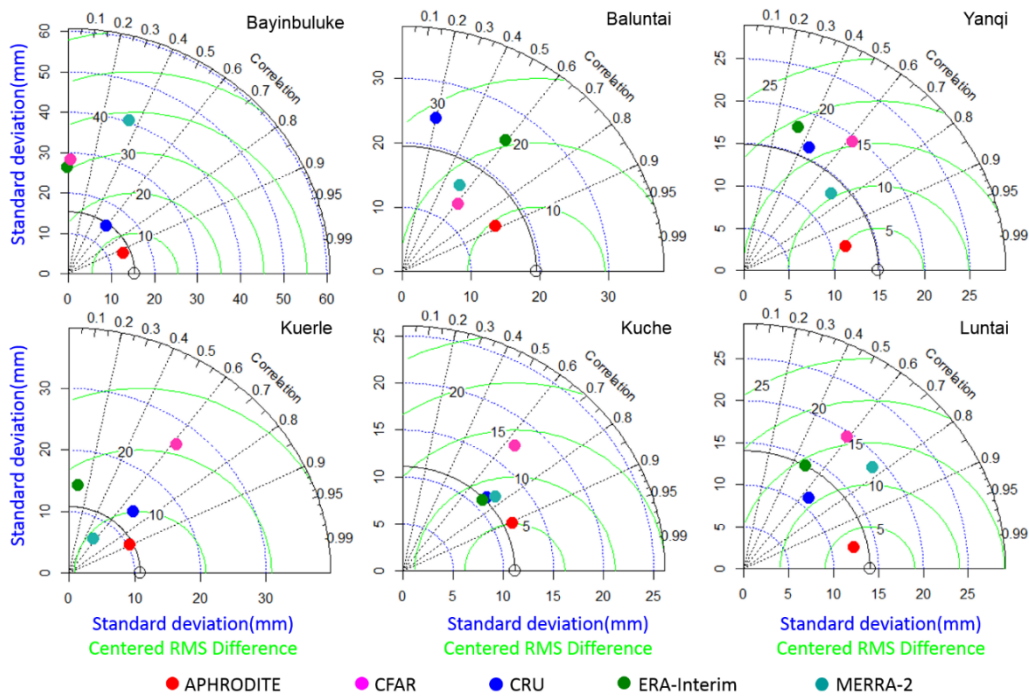


Figure S4.7. Same as Figure S4.5 but for autumn precipitation.

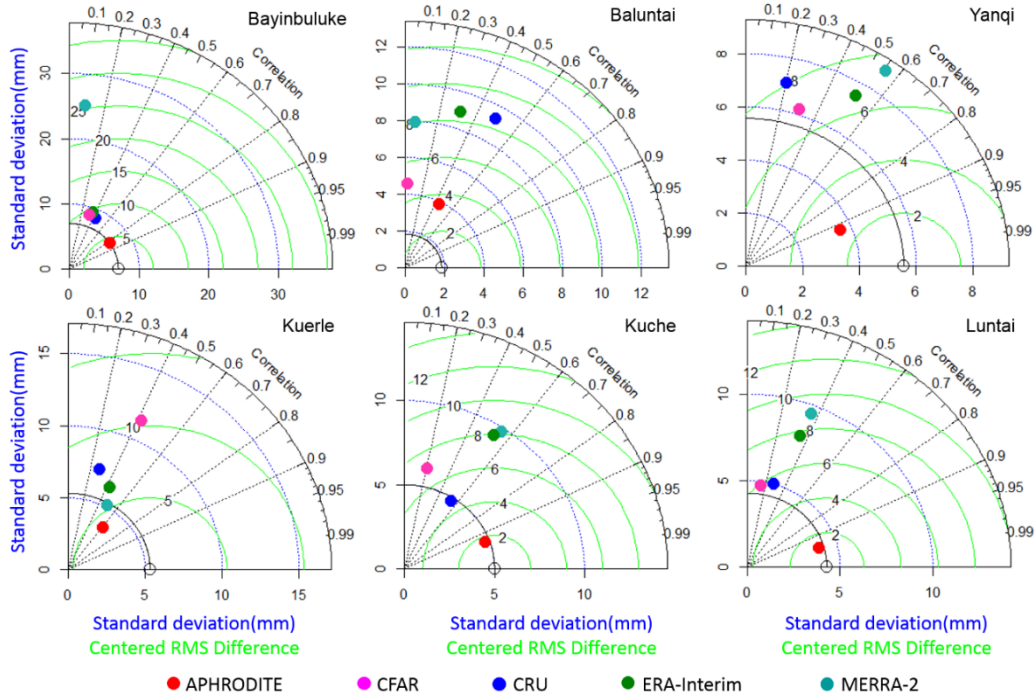


Figure S4.8. Same as Figure S4.5 but for winter precipitation.

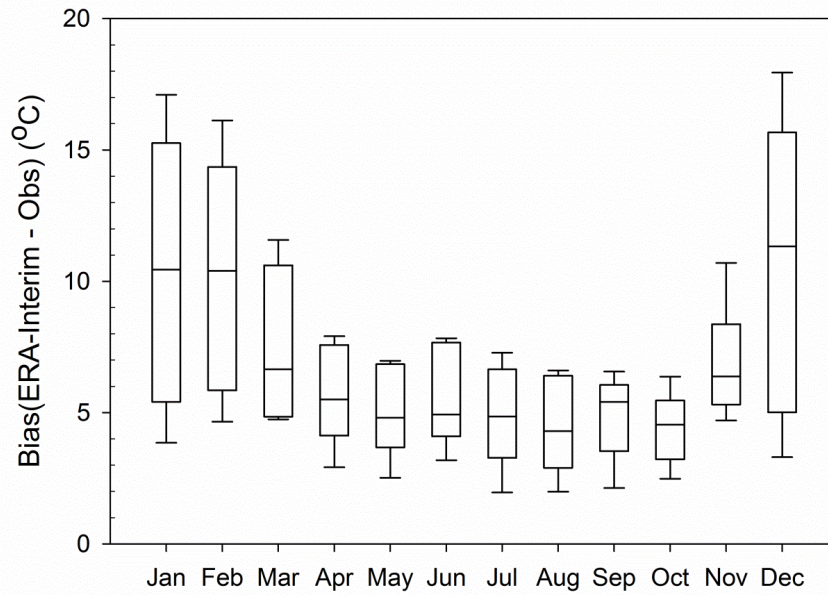


Figure S4.9. Boxplot of monthly bias (ERA-Interim minus observed) for nine HOBO sites (2014.09–2015.08).

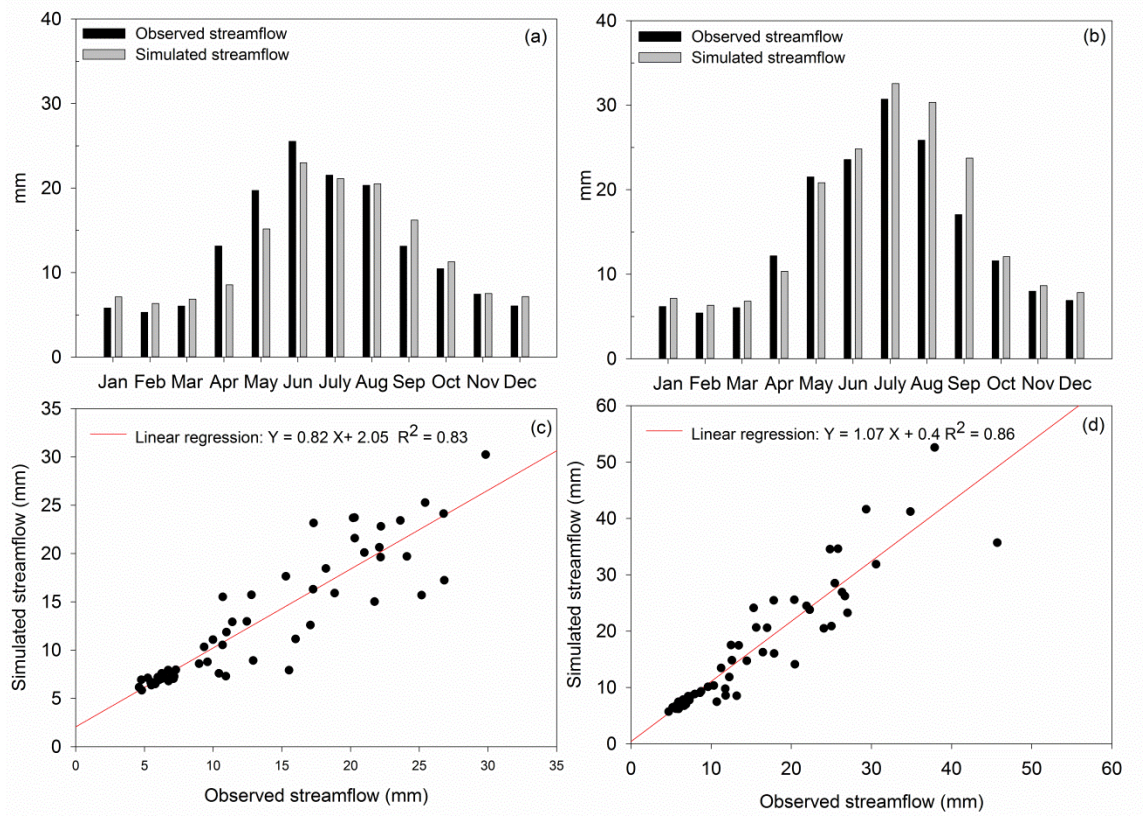


Figure S4.10. Simulated and observed monthly streamflow during the (a) calibration (1982–1986) and (b) validation period (1987–1991) and scatter plots between simulated and observed monthly streamflow during the (c) calibration (1982–1986) and (d) validation period (1987–1991).

Selbständigkeitserklärung

Ich erkläre, dass ich die vorliegende Arbeit selbständig und unter Verwendung der angegebenen Hilfsmittel, persönlichen Mitteilungen und Quellen angefertigt habe.

Jena, Mar 2018

(Yanjun Shen)

Curriculum Vitae

Personal information:

Name: Yanjun Shen

M/F: Male

Date of Birth: 05/17/1986

Nationality: Chinese

Education:

Oct 2013 – Feb 2018 Ph.D. Candidate in Geoinformatik

Friedrich-Schiller-Universität Jena, Jena, Germany,

Sep 2010 - Jun 2013 M.Sc. in Ecology

Center for Agricultural Resources Research, Institute of Genetics and
Developmental Biology, Chinese Academy of Sciences, China,

Sep 2006 - Jun 2010 B.Sc in Geographical Science

College of Resources and Environmental Sciences, Hebei Normal
University, China

Publications:

Shen, Y.-J., Y. Shen, M. Fink, S. Kralisch, & A. Brenning. (2018), Unraveling the hydrology of the glacierized Kaidu Basin by integrating multi-source data in the Tianshan Mountains, northwestern China. *Water Resources Research*, 54, 557–580. Doi:10.1002/2017WR021806.

Shen, Y.-J., Y. Shen, M. Fink, S. Kralisch, Y. Chen., & A. Brenning. (2018), Trends and variability in streamflow and snowmelt runoff timing in the southern Tianshan Mountains, *Journal of Hydrology*, 557, 173-181. doi:10.1016/j.jhydrol.2017.12.035.

Shen, Y.-J., Y. Shen., J. Goetz., & A. Brenning. (2016), Spatial-temporal variation of near-surface temperature lapse rates over the Tianshan Mountains, central Asia, *Journal of geographical research atmospheres.*, 121, 14,006–14,017. doi: 10.1002/2016JD025711.

Shen Y.-J., LI Hong-Jun, LEI Yu-Ping, Analysis of drought during the growth season of winter wheat in the piedmont region of Mt. Taihang—A case study at Baoding area, *Agriculture Research in the Arid Areas*, 2013,03:222-226 (in Chinese with English abstract).

Shen Y.-J., LI Hong-Jun, LEI Yu-Ping, Application and research progress of drought indices, *South-to-North Water Transfers and Water Science & Technology*. 2013, (4):128-133 (in Chinese with English abstract).

PEI Hong-Wei, CHANG Chun-Ping, HE Wen-Hui, **Shen Yan-Jun**, Depopulation of rural areas under the backdrop of urbanization—A case study of Kangbao County, Northwest of HeBei Province, *Chinese Journal of Eco-Agriculture*, 2009, 17(1): 169–173 (in Chinese with English abstract)

Jena, March 2018